

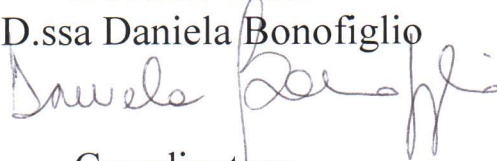
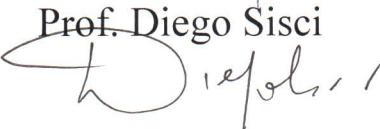
*Università della Calabria*

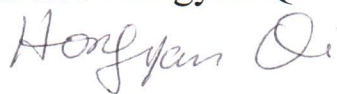
*Facoltà di Farmacia e Scienze della Nutrizione e della Salute  
Dipartimento Farmaco-Biologico (MED/05 PATOLOGIA CLINICA)*

---

*Dottorato di Ricerca in “Biochimica Cellulare ed  
Attività dei Farmaci in Oncologia” (XXI ciclo)*

## **Molecular mechanism of PPAR $\gamma$ -mediated apoptosis in different cancer cells**

Docente Tutor  
D.ssa Daniela Bonofiglio  
  
Coordinatore  
Prof. Diego Sisci  


Dottoranda  
D.ssa Hongyan Qi  




---

Anno Accademico 2007-2008

*To my Parents  
and my Fiancé*

# INDEX

<b>Introduction</b> .....	1
<b>Materials and Methods</b> .....	7
➤ Reagents.....	7
➤ Cell cultures.....	7
➤ Plasmids.....	8
➤ Immunoblotting.....	9
➤ Reverse Transcription-Polymerase Chain Reaction (RT-PCR) assay .....	9
➤ Transfection assay.....	10
➤ RNA interference (RNAi).....	11
➤ DNA Fragmentation.....	12
➤ MTT assay.....	12
➤ Electrophoretic Mobility Shift Assay (EMSA).....	12
➤ Chromatin Immunoprecipitation (ChIP) assays.....	14
➤ JC-1 Mitochondrial Membrane Potential Detection Assay.....	16
➤ Cytochrome <i>C</i> Detection.....	17
➤ Flow Cytometry Assay.....	18
➤ [3H]Thymidine incorporation.....	18
➤ Antisense Oligodeoxynucleotide Experiments.....	19

➤ Statistical analysis.....	19
<b>Results.....</b>	<b>20</b>
➤ BRL triggers intrinsic apoptotic events through p53-activated pathway in MCF7 cells.....	20
➤ PPAR $\gamma$ activates the Fas/FasL apoptotic pathway in MCF7 cells.....	23
➤ PPAR $\gamma$ -mediated apoptosis is a common mechanism in breast cancer cells.....	26
➤ Low doses of the combined BRL and 9RA treatment induce intrinsic apoptosis in breast cancer cells.....	27
➤ Combined treatment of BRL and 9RA, as a common mechanism, leads to the p53-mediated DNA fragmentation in breast cancer cells.....	34
➤ BRL induces growth inhibition of thyroid cancer cells by upregulating p21 <sup>Cip1/WAF1</sup> gene expression.....	35
<b>Discussion.....</b>	<b>43</b>
<b>References.....</b>	<b>50</b>

### **Scientific Publication**

1. Bonofiglio D., Cione E., **Qi H.**, Pingitore A., Perri M., Catalano S., Panno M. L., Genchi G., Fuqua S. AW., Andò S. Combined low doses of PPAR $\gamma$  and RXR ligands trigger intrinsic apoptotic pathway in human breast cancer cells. Submitted in American Journal of Pathology Cellular and Molecular Biology of Disease 2008 Nov
2. Bonofiglio D., **Qi H.**, Gabriele S., Belmonte M., Catalano S., Aquila S., Andò S. “PPAR $\gamma$  inhibits follicular and anaplastic thyroid carcinoma cells growth by up-regulating p21Cip1/WAF1 gene in a Sp1-dependent manner.” Endocrine-Related Cancer 2008 Jun 15(2):545-57

3. Bonofiglio D., Gabriele S., Aquila S., **Qi H.**, Belmonte M., Catalano S., Andò S. "Peroxisome proliferator-activated receptor gamma activates fas ligand gene promoter inducing apoptosis in human breast cancer cells." *Breast Cancer Res Treat.* 2008 Feb 22
4. Bonofiglio D., Aquila S., Catalano S., Gabriele S., Belmonte M., Middea E., **Qi H.**, Morelli C., Gentile M., Maggiolini M., Andò S. "Peroxisome Proliferator-Activated Receptor (PPAR) gamma activates p53 gene promoter binding to the NFkB sequence in human MCF7 breast cancer cells." *Mol Endocrinol.* 2006 20(12) 3083-92
5. Bonofiglio D., Cione E., **Qi H.**, Pingitore A., Perri M., Catalano S., Panno M. L., Genchi G., Andò S. The apoptotic effects of rosiglitazone and 9-cis-retinoic acid at low dose on human breast carcinoma cells as markers of benefit in neoadjuvant therapy of mammary cancer. XXIV Congress International SIP/ASIP 2008, Cosenza, Sep 10-13 2008
6. Catalano S., Barone I., Giordano P., Rizza P., **Qi H.**, Gu G., Bonofiglio D., Andò S. First evidence of non-genomic estradiol induced up-regulation of aromatase enzymatic activity in MCF-7 breast cancer cells. XXIV Congress International SIP/ASIP 2008, Cosenza, Sep 10-13 2008
7. Cione E., Bonofiglio D., **Qi H.**, Perri M., Pingitore A., Catalano S., Panno M.L., Genchi G. and Andò S. Activated pathway through which Rosiglitazone and 9 cis Retinoic Acid, when combined at low doses, induce apoptosis in human breast cancer cells. FASEB Summer Research Conferences, Jun 15-20, 2008
8. **Qi H.**, Bonofiglio D., Cione E., Pingitore A., Perri M., Catalano S., Panno M.L., Giordano F., Genchi G. and Andò S. Evidences that BRL in combination with 9 cis RA at low doses inhibits cell growth and induces apoptosis in MCF-7 human breast cancer cells. BIT Life Sciences' 1<sup>st</sup> Annual WORLD CANCER CONGRESS-2008, Jun 12-15 2008
9. **Qi H.**, Bonofiglio D., Gabriele S., Catalano S., Aquila S., Andò S. PPAR  $\gamma$  inhibits follicular and anaplastic thyroid carcinoma cells growth by up-regulating p21Cip1/WAF1 gene in a Sp1-dependent manner. Contributo a IV Convegno Nazionale Fondazione Lilli, Feb 22-23 2008
10. **Qi H.**, Gabriele S., Belmonte M., Bonofiglio D., Andò S. Peroxisome Proliferator-Activated Receptor gamma activates Fas Ligand gene promoter through Sp1 site in human MCF7 breast cancer cells. Contributo a III Convegno Nazionale Fondazione Lilli, Feb 23-24 2007
11. Gabriele S., Bonofiglio D., Aquila S., Belmonte M., **Qi H.**, Catalano S., Middea E., Andò S. Peroxisome Proliferator-Activated Receptor (PPAR) gamma activates FAS ligand gene promoter through Sp1 site in human MCF7 breast

cancer cells. Contributo a XXVIII Congresso Nazionale SIP 2006, Pavia, Sep 19-22 2006

12. Bonofiglio D., Catalano S., Gabriele S., Belmonte M., **Qi H.**, Maggiolini M., Andò S. The peroxisome proliferator-activated receptor gamma ligand rosiglitazone up-regulates p21 gene expression in human thyroid carcinoma cells. Congresso nazionale carcinomi tiroidei dal laboratorio al letto del malato e ritorno. Assisi, Feb 2-4 2006
13. Bonofiglio D., Aquila S., Gabriele S., Gentile M., Belmonte M., Morelli C., **Qi H.**, Fusaro S., Andò S. Up-regulation of p53 gene expression by PPAR gamma in human MCF-7 breast cancer cells. “ 3rd International symposium on PPARs efficacy and safety from basiscience to clinical applications” Monte Carlo, Monaco, Mar 19-23, 2005

---

 INTRODUCTION

Peroxisome Proliferator-Activated Receptor gamma (PPAR $\gamma$ ), a prototypical member of the nuclear receptor superfamily, plays key roles in energy homeostasis by modulating glucose and lipid metabolism and transport. Moreover, PPAR $\gamma$  can regulate cell proliferation, differentiation and survival (Lemberger et al. 1996; Lefebvre et al. 2006), immune and inflammatory responses (Fig. 1), involved in several diseases including obesity, diabetes, cardiovascular disease, and cancer (Lehrke and Lazar 2005).

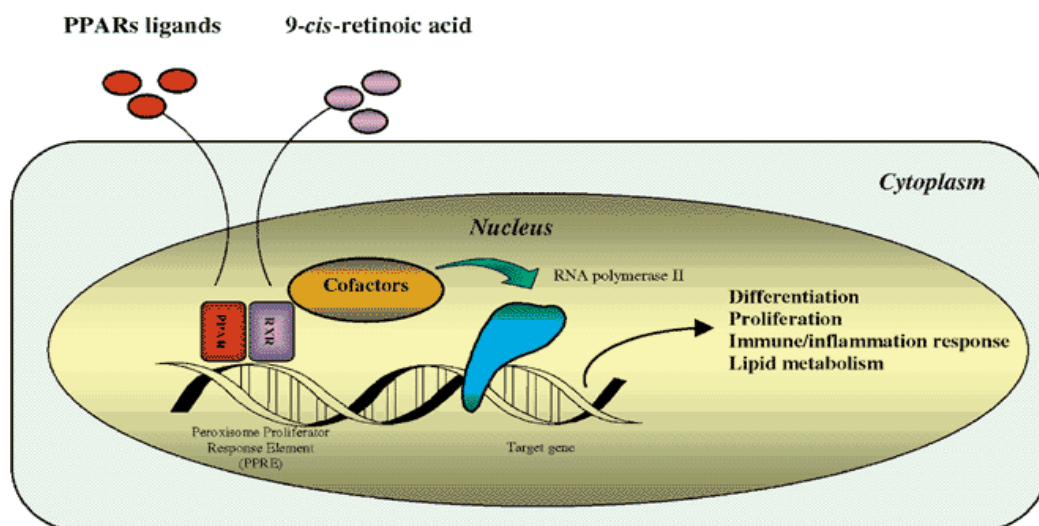


**Fig. 1** General mechanisms of gene transcription modulation by PPARs

It is located on chromosome 3 at position 3p25, (Greene et al. 1995), ubiquitously expressed in different tissues and particularly in adipose tissues and enterocytes (Kersten et al. 2000). There are four PPAR $\gamma$  isoforms derived from the alternative promoters, PPAR $\gamma$ 1, $\gamma$ 2, $\gamma$ 3 and  $\gamma$ 4 (Mueller et al. 2002), with the intrinsic ability to stimulate adipogenesis by induction of the similar changes in the pre-adipocyte expression profile.

Such as all the nuclear receptors, PPAR $\gamma$  is characterized from a common organization of the translated region in six coding exons with the following distribution: one exon for the N-terminal A/B domain, two exons for the DNA-binding domain (DBD), one for each of the two zinc-fingers, one exon for the hinge region, and two exons for the ligand-binding domain (LBD) (Fig. 2).

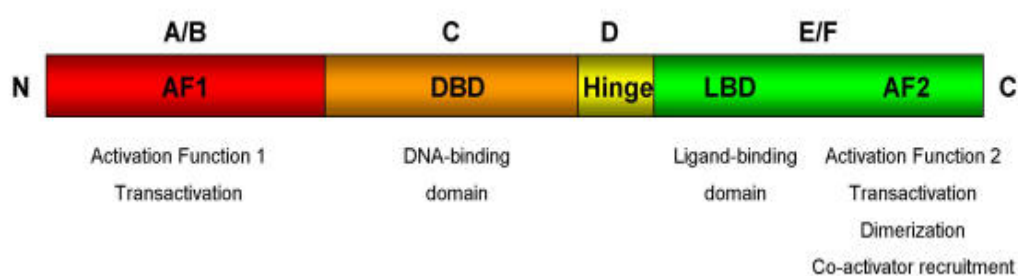


**Fig. 2** A schematic illustration of the domain structure of PPAR $\gamma$ .

PPAR $\gamma$  functions as a transcription factor by heterodimerizing with the retinoid X receptor (RXR), after which this complex binds to specific DNA sequence elements called Peroxisome Proliferator Response Elements (PPREs). PPREs are direct repeats of the consensus sequence with a spacing of one nucleotide (AGGTCA-N-AGGTCA) (Palmer et al. 1995) The heterodimer PPAR/RXR activated with their ligands can bind to PPREs in promoter regions of target genes, coactivators or corepressors are recruited to this complex to modulate gene transcription (DiRenzo et al. 1997; McInerney et al. 1998; Yuan et al. 1998) (Fig. 3).



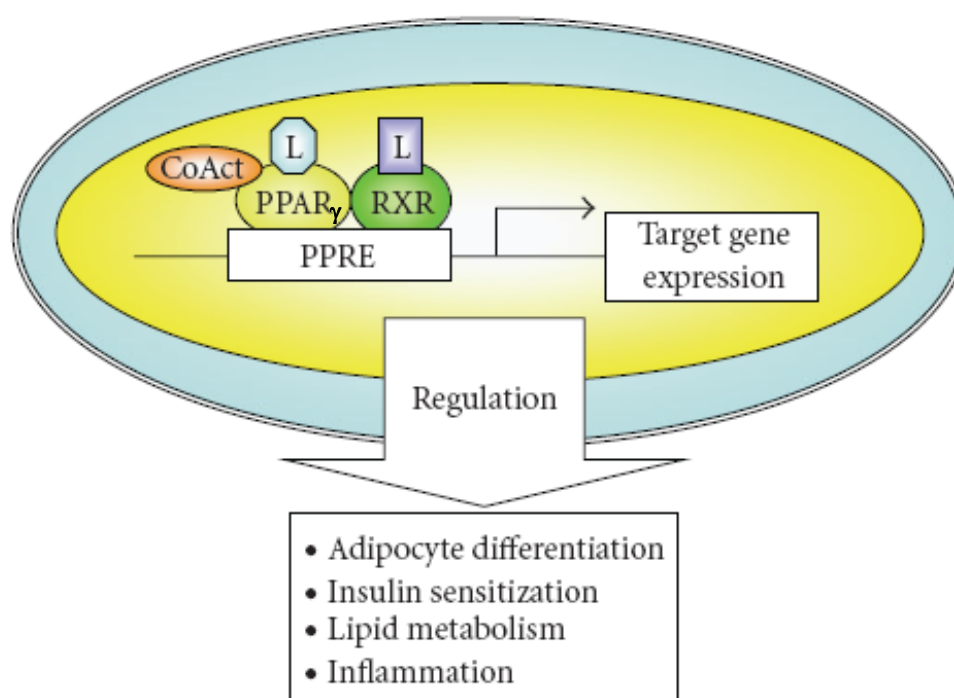


**Fig. 3** Mechanism of activation by heterodimer of PPAR $\gamma$  and RXR.

Synthetic and endogenous PPAR $\gamma$  ligands have been used to elucidate the role of PPAR $\gamma$ . Specifically, thiazolidinediones (TZDs) including pioglitazone, ciglitazone, troglitazone and rosiglitazone (BRL) are synthetic PPAR $\gamma$  ligands which are insulin-sensitizing agents developed to treat diabetes mellitus (Sertznig et al. 2007). The naturally occurring prostaglandin, 15-deoxy- $\Delta$ 12,14-prostaglandin J<sub>2</sub>(15d-PGJ<sub>2</sub>), is generally considered to be an endogenous PPAR $\gamma$  ligand (Forman et al. 1995; Kliewer et al. 1995). The promiscuous nature of PPAR $\gamma$  may lead to the binding of multiple ligands resulting in the activation of many cellular pathways including induction of apoptosis.

Apoptosis or programmed cell death is a highly regulated process critical for normal development and tissue homeostasis, induced from signals inside or outside the cell including radiation, viral infection, growth factors, and hormones (Steller et al.

1995). The induction of apoptosis can occur through two pathways: the intrinsic apoptotic pathway which involves signaling through the mitochondria and the extrinsic apoptotic pathway which is initiated through activation of cell surface death receptors (Debatin and Kramer 2004). Apoptotic signaling through the intrinsic pathway involves the activation of the proapoptotic Bcl-2 family members Bax and Bak, which facilitate the release of cytochrome *C* from the mitochondria and subsequent caspase-9 activation. Moreover, it has been reported that the p53 tumor suppressor gene regulates the transcription of effectors that are also responsible for growth arrest and intrinsic apoptosis in certain cell types in a transcription-dependent manner (Caelles et al. 1994; Vousden and Lu 2002). The function of p53 is finely tuned through an interaction with other transduction pathways regulating the cell network (Appella 2001; Woods and Vousden 2002; Haupt 2003; O'Brate and Giannakakou 2003; Yu and Zhang 2005). For instance, striking evidence has recently emerged for a cross talk between p53 and relevant transcription factors, such as the glucocorticoid, androgen and estrogen receptors (Sengupta and Wasylyk 2004). It was therefore proved that these nuclear receptors are able to induce a cytosolic accumulation of p53, altering its stability and, consequently, its function (Sengupta and Wasylyk 2004). Among the p53 target genes, the p21<sup>Cip1/WAF1</sup> has been recognized to exert an essential role in mediating cell cycle arrest at both G1 and G2-M checkpoints (Harper et al. 1993; Liu and Lozano 2005). p21<sup>Cip1/WAF1</sup> inhibits cyclin D1 or E/cyclin-dependent kinase in G1 and cyclin B/cdc2 in G2-M arrest, eliciting regulatory effects on DNA replication and repair (Tom et al. 2001).

Apoptotic signaling through the extrinsic pathway is initiated by ligands binding to death receptors or by induction of trimerization of these receptors (Ashkenazi and Dixit 1998). The death receptors belong to the tumor necrosis factor (TNF) receptor superfamily, which includes Fas, TNFR1, DR3, DR4 (TRAIL-R1), DR5 (TRAIL-R2), and DR6. Upon ligand binding and trimerization of death receptors, the intracellular death domain of the death receptors recruits adapter proteins such as Fas-associated death domain (FADD), forming a death-inducing signaling complex (DISC) which helps recruitment of procaspase-8 to the DISC. Caspase-8 is then activated, leading to activation of the downstream effector caspases such as caspase-3 and -7. It has also been suggested that FasL functions as an autocrine/paracrine mediator of apoptosis induced by DNA-damaging anticancer chemotherapeutic agents (Kasibhatla et al. 1998; Mo and Beck 1999) (Fig. 4).

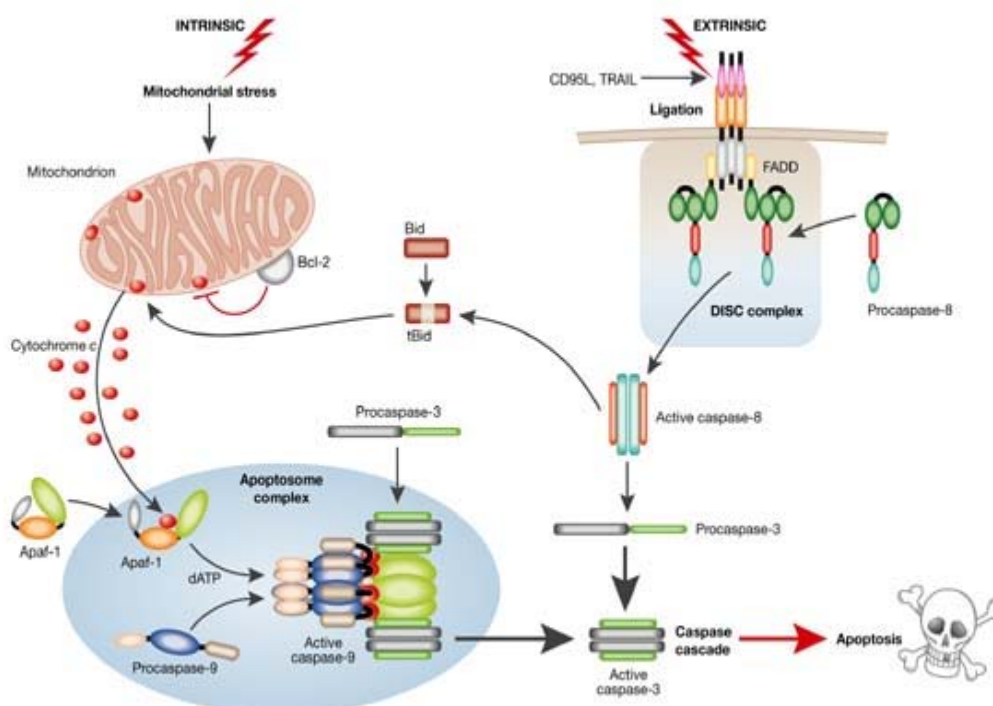


**Fig. 4** Intrinsic and extrinsic death pathways.

In the past few years, we have investigated different molecular mechanisms through which PPAR $\gamma$  ligand BRL induces antiproliferative effects and apoptosis in human breast and thyroid cancer cells.

Recently, we have demonstrated the ability of combined treatment with BRL and specific ligand of RXR 9-*cis* retinoic acid (9RA), at low doses, in inducing apoptotic events in breast cancer cells.

Altogether, our data suggest that PPAR $\gamma$  ligands represent pharmacologic tools to be exploited in the novel therapeutic adjuvant strategies for treatment of patients affected by breast and thyroid carcinoma.

## MATERIALS AND METHODS

### **Reagents**

Rosiglitazone (BRL49653, BRL) was from Alexis (San Diego, CA USA). The irreversible PPAR $\gamma$ -antagonist GW9662 (GW), specific inhibitor of GC binding, mithramycin (M) 9-*cis*-retinoic acid (9RA) were purchased from Sigma (Milan, Italy). All compounds were solubilized in DMSO or in ethanol (Sigma).

### **Cell cultures**

Wild-type human breast cancer MCF7 cells (a gift from Ewa Surmacz, Sbarro Institute for Cancer Research and Molecular Medicine, Philadelphia, PA) and MDA-MB231 (MDA) breast cancer cells were grown in DMEM plus glutamax containing 10% fetal calf serum (FCS) (Invitrogen, Milan, Italy) and 1mg/ml penicillin-streptomycin (P/S). BT20 breast cancer cells were grown in MEM added as DMEM. MCF7 tamoxifen resistant (MCF7-TR1) breast cancer cells (a gift from Dr. Susan Fuqua, Breast Center, Baylor College of Medicine, Houston, TX, USA) were grown in MEM with glutamax containing 10% FBS, 1% amino acid essential, 1 $\mu$ M 4-hydroxytamoxifen and 1mg/ml penicillin-streptomycin. SKBR-3 breast cancer cells were grown in DMEM without red phenol, plus glutamax containing 10% fetal bovine serum (Invitrogen) and 1mg/ml penicillin-streptomycin. T-47D breast cancer cells were grown in RPMI 1640 with glutamax containing 10% fetal bovine serum (FBS), 1mM sodium pyruvate, 10mM HEPES, 2,5g/l glucose, 0,2U/ml insulin and 1mg/ml penicillin-streptomycin. Normal breast epithelial MCF10 cells were grown in DMEM-F12 plus glutamax

containing 5% horse serum (Sigma), 1mg/ml P/S, 0,5µg/ml hydrocortisone and 10µg/ml insulin.

Human follicular WRO and anaplastic FRO thyroid cancer cells (a gift from Dr. F. Arturi, University of Magna Grecia, Catanzaro, Italy) were grown in DMEM plus glutamax containing 10% FBS (Invitrogen) and 1mg/ml P/S.

### **Plasmids**

The p53 promoter-luciferase reporters, constructed using pGL2 for cloning of p53-1 and -6, and TpGL2 for p53-13 and-14 were kindly provided by Dr. Stephen H. Safe (Texas A & M University, College Station, TX). The constructs used were generated by Safe (Qin et al. 2002) from the human p53 gene promoter as follows: p53-1 (containing the -1800 to +12 region), p53-6 (containing the -106 to +12 region), p53-13 (containing the -106 to -40 region) and p53-14 (containing the -106 to -49 region). The p53 antisense plasmid (AS/p53) were gifts from Dr. Moshe Oren (Weizmann Institute of Science, Rehovot, Israel). The human wild type p21<sup>Cip1/WAF1</sup> promoter-luciferase (luc) reporter (p21<sup>Cip1/WAF1</sup> wt) and its deletion construct which lacks the two p53-binding sites (p21<sup>Cip1/WAF1</sup> Δp53) were kind gifts from Dr. T. Sakai (Kyoto Prefectural University of Medicine, Kyoto, Japan). As an internal transfection control, we cotransfected the plasmid pRL-CMV (Promega Corp., Milan, Italy) that expresses Renilla luciferase enzymatically distinguishable from firefly luciferase by the strong cytomegalovirus enhancer/promoter.

### **Immunoblotting**

Cells were grown in 10cm dishes to 70–80% confluence and exposed to treatments in a serum-free medium (SFM) as indicated. Cells were then harvested in cold PBS and resuspended in lysis buffer containing 20mM HEPES (pH 8), 0.1mM EDTA, 5mM MgCl<sub>2</sub>, 0.5M NaCl, 20% glycerol, 1% Nonidet P-40, and inhibitors (0.1mM Na<sub>3</sub>VO<sub>4</sub>, 1% PMSF, 20mg/ml aprotinin). Protein concentration was determined by Bio-Rad Protein Assay (Bio-Rad Laboratories, Hercules, CA). A 50µg portion of protein lysates was used for Western blotting, resolved on a 10% SDS-polyacrylamide gel, transferred to a nitrocellulose membrane, and probed with an antibody directed against the p53, p21<sup>Cip1/WAF1</sup>, caspases 9, FasL, PPAR $\gamma$  and Sp1 (Santa Cruz Biotechnology, CA USA), caspase 8 (Biomol International, Butler PikePlymouth, PA USA). As internal control, all membranes were subsequently stripped (0.2M glycine, pH 2.6, for 30 min at room temperature) of the first antibody and reprobed with anti- $\beta$  actin or anti-GAPDH antibodies. The antigen-antibody complex was detected by incubation of the membranes for 1 hour at room temperature with peroxidase-coupled goat antimouse or antirabbit IgG and revealed using the enhanced chemiluminescence system (Amersham Pharmacia Buckinghamshire, UK). Blots were then exposed to film (Kodak film, Sigma). The intensity of bands representing relevant proteins was measured by Scion Image laser densitometry scanning program.

### **Reverse Transcription-Polymerase Chain Reaction (RT-PCR) assay**

Cells were grown in 10cm dishes to 70–80% confluence, and exposed to treatments in SFM as indicated. Total cellular RNA was extracted using TRIZOL

reagent (Invitrogen) as suggested by the manufacturer. The purity and integrity were checked spectroscopically and by gel electrophoresis before carrying out the analytical procedures. The evaluation of gene expression was performed by a semiquantitative RT-PCR method as previously described (Maggiolini et al. 1999). For p53, p21<sup>Cip1/WAF1</sup>, FasL and the internal control gene 36B4, the primers were: 5'-GTGGAAGGAAATTTGCGTGT-3' (p53 forward) and 5'-CCAGTGTGATGATGGTGAGG-3' (p53 reverse), 5'-GCTTCATGCCAGCTACTTCC-3' (p21 forward) and 5'-CTGTGCTCACTTCAGGGTCA-3' (p21 reverse), 5'-GGA ATG GGA AGA CAC CTA TGG A-3' (FasL forward) and 5'-AGAGAGAGCTCAGATACGTTGAC-3' (FasL reverse), 5'-CTCAACATCTCCCCCTTCTC-3' (36B4 forward) and 5'-CAAATCCCATATCCTCGTCC-3' (36B4 reverse) to yield, respectively, products of 190 bp with 18 cycles, 270 bp with 18 cycles, 299 bp with 25 cycles and 408 bp with 12 cycles. The results obtained as optical density arbitrary values were transformed to percentage of the control (percent control) taking the samples from untreated cells as 100%.

### **Transfection assay**

Cells were transferred into 24-well plates with 500 $\mu$ L of regular growth medium/well the day before transfection. The medium was replaced with lacking phenol red and serum on the day of transfection, which was done using Fugene 6 reagent as recommended by the manufacturer (Roche Diagnostics, Mannheim, Germany) with a mixture containing 0.5 $\mu$ g of promoter-luciferase reporter



plasmid, and 5ng of pRL-CMV. After transfection for 24 hours, treatments were added in SFM as indicated and cells were incubated for an additional 24 hours, cells were pre-treated for 2 hours with M or GW where applicable. Firefly and Renilla luciferase activities were measured using the Dual Luciferase Kit (Promega). The firefly luciferase values of each sample were normalized by Renilla luciferase activity and data were reported as relative light units.

To abrogate p53 expression MCF7 cells plated into 10cm dishes were transfected with 5 $\mu$ g of AS/p53 using Fugene 6 reagent as recommended by the manufacturer (Roche Diagnostics).

#### **RNA interference (RNAi)**

Cells were plated in 6 well dishes with regular growth medium the day before transfection to 60–70% confluence. On the second day the medium was changed with SFM without P/S and cells were transfected with 25 bp RNA duplex of stealth RNAi targeted human FasL mRNA sequence 5'-GCC CAU UUA ACA GGC AAG UCC AAC U-3' (Invitrogen), with 25 bp RNA duplex of validate RNAi targeted human PPAR $\gamma$  mRNA sequence 5'-GCC UGC AUC UCC ACC UUA UUA UUC U-3' or with a stealth RNAi control (Invitrogen) to a final concentration of 100 nM using Lipofectamine 2000 (Invitrogen) as recommended by the manufacturer. After 5 hours the transfection medium was changed with SFM in order to avoid Lipofectamine 2000 toxicity and cells were exposed to 1 $\mu$ M BRL for the next 48 hours and then lysed as described for WB analysis or treated for 72 hours and then collected as described for the DNA fragmentation.

### **DNA Fragmentation**

DNA fragmentation was determined by gel electrophoresis. Cells were grown in 10cm dishes to 70 % confluence, and then treated with BRL and/or GW for 72 hours. In another sets of experiments, cells were treated with 100nM BRL alone or in combination of 50nM 9RA for 56 hours. After the treatments cells were collected and washed with PBS and pelleted at 1800 rpm for 5 minutes. The samples were resuspended in 0.5ml of extraction buffer (50mM, Tris-HCl, pH 8; 10mM EDTA, 0.5% SDS) fo The DNA pellet was resuspended in 15µl of H<sub>2</sub>O treated with RNAse A for 30 minutes at 37°C. The absorbance of the DNA solution at 260 and 280nm was determined by spectrophotometry. The extracted DNA (40µg/lane) was subjected to electrophoresis on 1.5% agly significant.

**MTT assay** (Mosmann 1983). Cells (2x10<sup>5</sup> cells/ml) were grown in 6 well plates and exposed to BRL 100nM, 9RA 50nM alone or in combination for 48 hours in serum free medium (SFM). 100µl of MTT (5mg/ml) were added to each well, and the plates were incubated for 4 hours at 37°C. Then, 1ml 0.04N HCl in isopropanol was added to solubilise the cells. The absorbance was measured with the Ultrospec 2100 Pro spectrophotometer (Amersham-Biosciences) at a test wavelength of 570nm with a reference wavelength of 690nm. The optical density (O.D.) was calculated as the difference between the two absorbencies. Percent viability was calculated as O.D. of drug-treated sample/control O.D.

### **Electrophoretic Mobility Shift Assay (EMSA)**

Nuclear extracts from MCF7, WRO and FRO cells were prepared as previously described (Andrews and Faller 1991). Briefly, MCF7 cells plated into 10cm

dishes were grown to 70-80% confluence shifted to SFM for 24 h and then treated with BRL or/and 9RA for 6 hours. Thereafter, cells were scraped into 1.5ml of cold PBS. Cells were pelleted for 10 seconds and resuspended in 400  $\mu$ l cold buffer A (10mM HEPES-KOH pH 7.9 at 4°C, 1.5mM MgCl<sub>2</sub>, 10mM KCl, 0.5mM dithiothreitol, 0.2mM PMSF, 1mM leupeptin) by flicking the tube. The cells were allowed to swell on ice for 10 minutes and then vortexed for 10 seconds. Samples were centrifuged for 10 seconds and the supernatant fraction discarded. The pellet was resuspended in 50 $\mu$ l of cold Buffer B (20mM HEPES-KOH pH 7.9, 25% glycerol, 1.5mM MgCl<sub>2</sub>, 420mM NaCl, 0.2mM EDTA, 0.5mM dithiothreitol, 0.2mM PMSF, 1mM leupeptin) and incubated in ice for 20 minutes for high-salt extraction. Cellular debris were removed by centrifugation for 2 minutes at 4°C and the supernatant fraction (containing DNA binding proteins) was stored at -70°C. The probe was generated by annealing single stranded oligonucleotides and labeled with [ $\gamma$ 32P] ATP (Amersham Pharmacia) and T4 polynucleotide kinase (Promega) and then purified using Sephadex G50 spin columns (Amersham Pharmacia).

The DNA sequence of the NF $\kappa$ B used as probe or as cold competitor is the following: NF $\kappa$ B, 5'-AGTTGAGGGGACTTTCCCAGGC-3' and the sequence, obtained from the p53 promoter gene. Sp1 sequence, present in the native human p21<sup>Cip1/WAF1</sup> promoter gene used as probe or as cold competitor is the following: Sp1, 5'-GGG GGT CCC GCC TCC TTG A-3' (Sigma). The protein binding reactions were carried out in 20 $\mu$ l of buffer [20mM Hepes pH 8, 1mM EDTA, 50mM KCl, 10mM DTT, 10% glicerol, 1mg/ml BSA, 50 $\mu$ g/ml poly dI/dC] with

50,000 cpm of labeled probe, 5 $\mu$ g of MCF7 nuclear protein and 5 $\mu$ g of poly (dI-dC). The mixtures were incubated at room temperature for 20 minutes in the presence or absence of unlabeled competitors oligonucleotides.

For the experiments involving anti-PPAR $\gamma$ , anti-RXR $\alpha$  and anti-Sp1 antibodies and IgG (Santa Cruz Biotechnology, Inc., Santa Cruz, CA), and the treatment of 100nM M in vitro, the reaction mixture was incubated with these antibodies and this treatment at 4°C for 30 minutes before addition of labelled probe. The entire reaction mixture was electrophoresed through a 6% polyacrylamide gel in 0.25X Tris borate-EDTA for 3 hours at 150 V. Gel was dried and subjected to autoradiography at -70°C.

#### **Chromatin Immunoprecipitation (ChIP) assays**

For ChIP assay, MCF7, WRO and FRO cells were grown in 10cm dishes to 50-60% confluence, shifted to SFM for 24 hours and then treated with 1 $\mu$ M BRL and 100nM M for 1 hour or pre-incubated with M where required. In another sets of experiments, cells were treated with 100nM BRL alone or in combination of 50nM 9RA. Thereafter, cells were washed twice with PBS and cross-linked with 1% formaldehyde at 37°C for 10 minutes. Next, cells were washed twice with PBS at 4°C, collected and resuspended in 200 $\mu$ l of lysis buffer (1% SDS, 10mM EDTA, 50mM Tris-HCl pH 8.1) and left on ice for 10 minutes. Then, cells were sonicated four times for 10 seconds at 30 % of maximal power (Sonics, Vibra Cell 500 W Sonics and Materials, Inc., Newtown, CT)) and collected by centrifugation at 4°C for 10 minutes at 14,000 rpm. The supernatants were diluted in 1.3ml of IP buffer (0.01% SDS, 1.1% Triton X-100, 1.2mM EDTA, 16.7mM Tris-HCl pH 8.1,

16.7mM NaCl) followed by immunoclearing with 80µl of sonicated salmon sperm DNA/protein A agarose (UBI, DBA Srl, Milan - Italy) for 1 hour at 4°C.

The precleared chromatin was immunoprecipitated with anti-PPAR $\gamma$ , anti-Sp1, anti-RXR $\alpha$  and anti-RNA pol II antibodies (Santa Cruz Biotechnology). A agarose were added and precipitation was further continued for 2 hours at 4°C. After pelleting, the precipitates were washed sequentially for 5 minutes with the following buffers: wash A (0.1% SDS, 1% Triton X-100, 2mM EDTA, 20mM Tris-HCl (pH 8.1), 150mM NaCl); wash B (0.1% SDS, 1% Triton X-100, 2mM EDTA, 20mM Tris-HCl (pH 8.1), 500mM NaCl); and wash C (0.25M LiCl, 1% NP-40, 1% sodium deoxycholate, 1mM EDTA, 10mM Tris-HCl (pH 8.1)), and then twice with TE buffer (10mM Tris, 1mM EDTA). The immunocomplexes were eluted with the elution buffer (1% SDS, 0.1M NaHCO<sub>3</sub>). The eluates were reverse cross-linked by heating at 65°C and digested with proteinase K (0.5mg/ml) at 45°C for overnight. DNA was obtained by phenol/chloroform/isoamyl alcohol extraction. To each sample, 2ml of 10mg/ml yeast tRNA (Sigma) were added and DNA was precipitated with 70% ethanol for 24 hours at -20°C, and then washed with 95% ethanol and resuspended in 20ml TE buffer.

A 5µl volume of each sample was used for PCR with primers flanking a sequence present in the p53 promoter: 5'-CTGAGAGCAAACGCAAAG-3' (forward) and 5'-CAGCCCGAACGCAAAGTGTC-3' (reverse) containing the  $\kappa$ B site from -254 to -242 region. In another set of experiments we used for PCR the following sequence of p21<sup>Cip1/WAF1</sup> promoter: 5'-GATTTGTGGCTCACTTCGTGGG-3' (forward) and 5'-GCAGCTGCTCACACCTCAGCT-3' (reverse) (Gene Bank,

accession number: U24170). The PCR conditions for the p53 promoter 45 sec at 94°C, were while for the p21<sup>Cip1/WAF1</sup> promoter fragments were, respectively, 40 sec at 57°C, 90 sec at 72°C; 1 minute at 95°C, 1 minute at 60°C, and 1 minute at 72°C. The amplification products obtained with 30 cycles were analyzed in a 2% agarose gel and visualized by ethidium bromide staining. The negative control was provided by PCR amplification without a DNA sample. The specificity of reactions was ensured using normal mouse and rabbit IgG (Santa Cruz Biotechnology).

#### **JC-1 Mitochondrial Membrane Potential Detection Assay**

The loss of mitochondrial membrane potential ( $\Delta\Psi_m$ ) was monitored with the dye 5,5',6,6'-tetra-chloro-1,1',3,3'-tetraethylbenzimidazolyl-carbocyanine iodide (JC-1) (Biotium, Hayward, USA). JC-1 is capable of selectively entering mitochondria, where it forms monomers and emits green fluorescence when  $\Delta\Psi_m$  is relatively low. At a high  $\Delta\Psi_m$ , JC-1 aggregates and gives red fluorescence (Cossarizza et al 1993). MCF7 cells were grown in 10cm dishes and treated with 100nM BRL plus 50nM 9RA for 48 hours, then Cell were trypsinized, washed in ice-cold PBS, and incubated with 10mM JC-1 at 37°C in a 5% CO<sub>2</sub> incubator for 20 minutes in darkness. Subsequently, cells were washed twice with PBS and analyzed by fluorescence microscopy. The aggregate red form has absorption/emission maxima of 585/590nm. The green monomeric form has absorption/emission maxima of 510/527nm. Both apoptotic and healthy cells can be visualized by fluorescence microscopy using a wide band-pass filter suitable for detection of fluorescein and rhodamine emission spectra.

### **Cytochrome C Detection**

Cytochrome *C* was detected by western blotting in mitochondrial and cytoplasmic fractions. Cells were harvested by centrifugation at 2,500 rpm for 10 minutes at 4°C. The pellets were suspended in 36µl RIPA buffer plus 10µg/ml aprotinin, 50mM phenylmethylsulfonylfluoride and 50mM sodium orthovanadate and then 4µl of 0.1% digitonine were added. Cells were incubated for 15 minutes at 4°C and centrifuged at 12,000 rpm for 30 minutes at 4°C. The resulting mitochondrial pellet was resuspended in 3% Triton X-100, 20mM Na<sub>2</sub>SO<sub>4</sub>, 10mM PIPES and 1mM EDTA, pH 7.2, and centrifuged at 12,000 rpm for 10 minutes at 4°C. Proteins of the mitochondrial and cytosolic fractions were determined by Lowry method (Lowry et al. 1951). Equal amounts of protein (40µg) were resolved by 15% SDS-PAGE and electrotransferred to nitrocellulose membranes. The membranes were incubated in blocking buffer over night at 4°C, followed by incubation with 1:1000 sheep polyclonal antihuman cytochrome *C* antibody (2 hours, room temperature) and then with HRP-conjugated (horse radish peroxidase-conjugated) secondary antibody (1:2000) for 2 hours at 4°C. As internal control, membrane was subsequently stripped (0.2 M glycine, pH 2.6, for 30 minutes at room temperature) of the first antibody and reprobed with anti-GAPDH antibody (Santa Cruz Biotechnology). The antigen-antibody complex was detected by incubation of the membranes for 1 hour at room temperature with peroxidase-coupled goat anti-mouse or antirabbit IgG and revealed using the enhanced chemiluminescence system (Amersham Pharmacia). Blots were then

exposed to film (Kodak film). The intensity of bands representing relevant proteins was measured by Scion Image laser densitometry scanning program.

#### **Flow Cytometry Assay**

MCF7 cells ( $1 \times 10^6$  cells/well) in a six wells plate were shifted to SFM for 24 hours and then treatments were added in SFM for 48 hours. Thereafter, cells were trypsinized, centrifuged at 3,000 rpm for 3 minutes, washed with PBS. Addition of 0.5 $\mu$ l of FITC antibodies anti-caspase 9 and anti-caspase 8 in all samples was performed and then incubated for 45 minutes in at 37°C. Consequently cells was centrifuged at 3,000 rpm for 5 minutes. The pellets were washed with 300 $\mu$ l of wash buffer and centrifuged. The last passage was repeated twice, the supernatant removed, and cells dissolved in 300 $\mu$ l of wash buffer. Finally, cells were analyzed with the FACScan (Becton Dickinson and Co., Franklin Lakes, NJ).

#### **[<sup>3</sup>H]Thymidine incorporation**

WRO and FRO cells were seeded in six-well plates in regular growth medium. On the second day, cells were incubated in DMEM supplemented with 1% charcoal stripped FCS (CS-FCS) for the indicated times in the presence of increasing BRL concentrations or GW. The medium was renewed every 2 days together with the appropriate treatments. [<sup>3</sup>H]Thymidine (1mCi/mL; New England Nuclear, Newton, MA) was added to the medium for the last 6 hours. After rinsing with PBS, the cells were washed once with 10% and thrice with 5% trichloroacetic acid. Cells were lysed by adding 0.1N NaOH and then incubated 30 minutes at 37°C. Thymidine incorporation was determined by scintillation counting.



### **Antisense Oligodeoxynucleotide Experiments**

The oligonucleotides used were: 5'-GACATCACCAGGATCGGACAT-3' for p21<sup>Cip1/WAF1</sup>, and 5'-GATCTCAGCACGGCAAAT-3' for the scrambled control (cs). For antisense experiments, a concentration of 200nM of the indicated oligonucleotides (ODN) was transfected using Fugene 6 reagent as recommended by the manufacturer for 4 hours, before treatment with vehicle or BRL. The transfection was re-newed every 2 days together with the appropriate treatments.

### **Statistical analysis**

Statistical analysis was performed using ANOVA followed by Newman-Keuls testing to determine differences in means.  $p < 0.05$  was considered as statistically significant.

## RESULTS

### **BRL triggers intrinsic apoptotic events through p53-activated pathway in MCF7 cells**

On the basis of our (Bonofiglio et al. 2005) and other (Clay et al. 1999; Patel et al. 2001) studies, demonstrating the inhibition of the PPAR $\gamma$  ligands on proliferation of breast cancer cells, we aimed to investigate the molecular mechanisms underlying these effects. Considering that the tumor suppressor gene p53 is mainly involved in the growth arrest and in the intrinsic apoptotic process promoted by different factors, we examined the potential ability of PPAR $\gamma$  to modulate the expression of p53 along with its natural target gene p21<sup>Cip1/WAF1</sup>. The mRNA (Fig. 1A) and protein levels (Fig. 1B) of both p53 and p21<sup>Cip1/WAF1</sup> were up-regulated in a time- and dose-dependent manner in MCF7 cells treated with BRL. These stimulations were abrogated by GW (Fig. 1) suggesting a direct involvement of PPAR $\gamma$ .

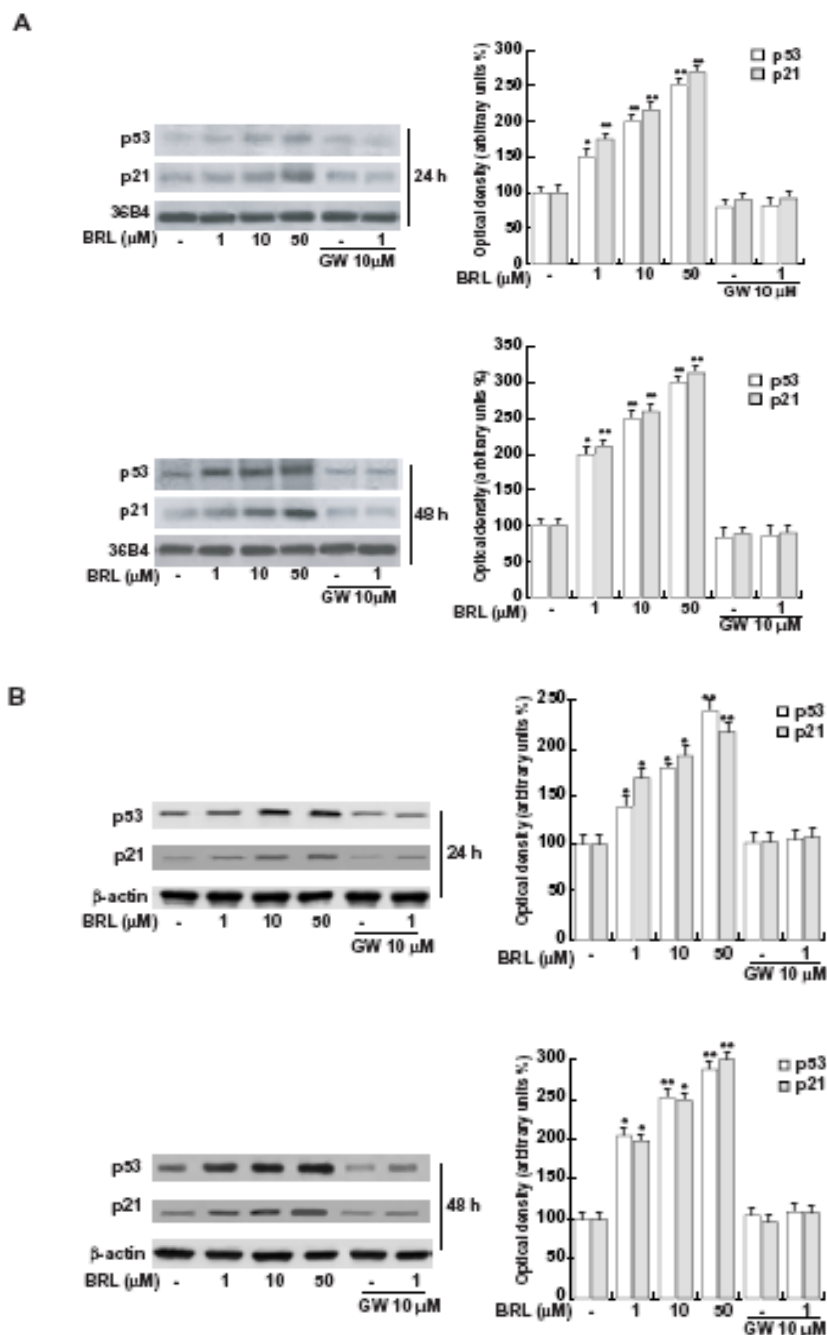


**Fig. 1** Semiquantitative RT-PCR evaluation (A) and immunoblots (B) of p53 and p21<sup>Cip1/WAF1</sup> expression. MCF7 cells were treated for 24 and 48 hours with increasing concentrations of BRL as indicated, 10 μM GW alone or in combination with 1 μM BRL. 36B4 mRNA levels were determined as control. β-actin was used as loading control. The side panels show the quantitative representations of data (mean±S.D.) of three independent experiments performed for each condition. \*p<0.05 and \*\*p<0.01 BRL-treated vs untreated cells.

Having demonstrated that PPAR $\gamma$  mediates p53 expression induced by BRL, we investigated the cleavage of caspase 9, which is an important component of the intrinsic apoptotic process (Cohen 1997). Notably, the treatment of MCF7 cells with BRL for 48 h promoted the caspase-9 activation, which was prevented by GW and in presence of an expression vector encoding p53 antisense (AS/p53) (Fig. 2A), which abolished p53 expression (Fig. 2B). As evidenced in DNA fragmentation assay, PPAR $\gamma$  was also involved in the apoptosis triggered by BRL because this effect was completely and partially reversed by GW and by the AS/p53, respectively (Fig. 2C). Taken together, these results indicate that, at least in part, a cross talk between PPAR $\gamma$  and p53 may be responsible for the growth arrest and apoptosis induced by BRL in MCF7 cells.

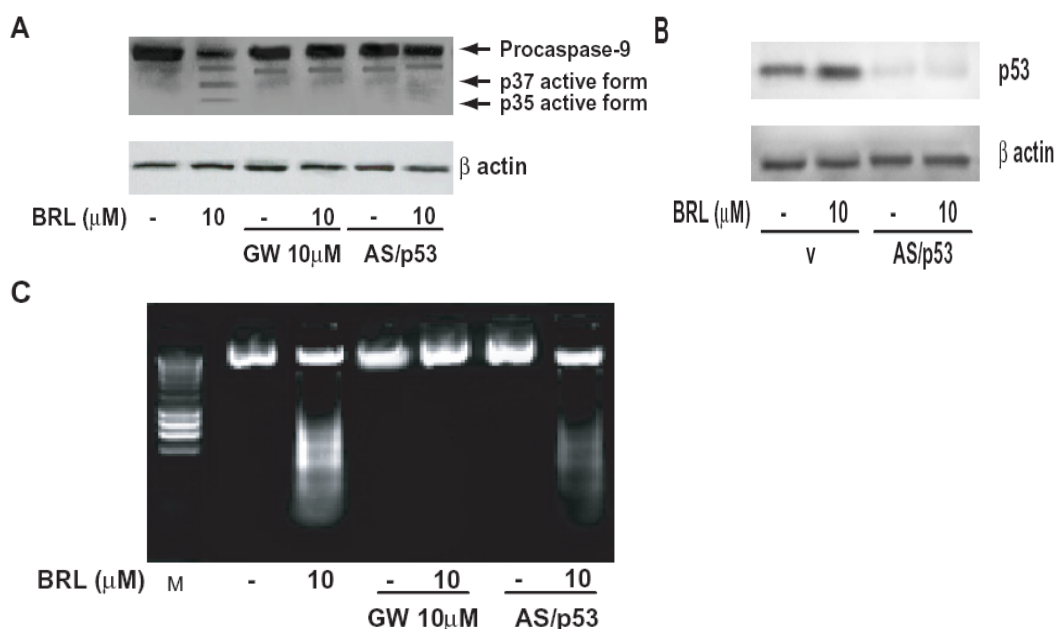


**Fig. 2** A) MCF7 cells were treated with BRL alone or in combination with GW for 48 hours as indicated, or transfected with an expression plasmid encoding for p53 antisense (AS/p53). Positions of procaspase-9 and its cleavage products are indicated by arrowheads to the right. One of three similar experiments is presented.  $\beta$ -actin was used as loading control on the same stripped blot. B) p53 protein expression (evaluated by WB) in MCF7 cells transfected with an empty vector

(v) or a AS/p53 and treated as indicated.  $\beta$ -actin was used as loading control. C) DNA laddering was performed in MCF7 cells treated for 72 hours as indicated, or transfected with AS/p53.

### PPAR $\gamma$ activates the Fas/FasL apoptotic pathway in MCF7 cells

In order to understand whether PPAR $\gamma$  triggers cell death also activating extrinsic apoptotic events such as Fas/FasL signalling, we first evaluated the ability of PPAR $\gamma$  agonist BRL to modulate FasL expression in MCF7 cells.

A BRL dose-dependent increase in FasL content was observed by WB analysis after 24 hours of treatment (Fig. 3A). Furthermore, by a semiquantitative Reverse RT-PCR method, after 24 hours upon increasing BRL concentration, we showed that BRL was able to upregulate FasL gene expression in a dose-dependent manner (Fig. 3 B). The upregulation of FasL expression induced by BRL was reversed when we used GW, (Fig. 3A and B) implying a PPAR $\gamma$ -dependent action in MCF7 cells.

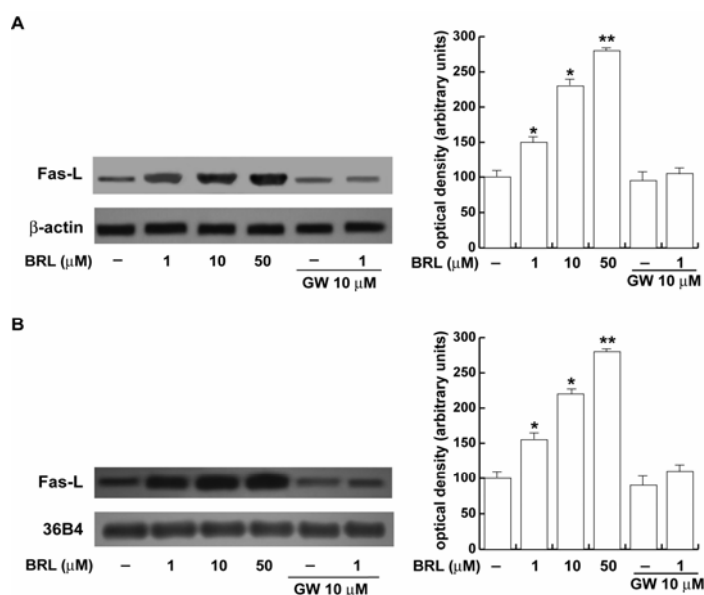


**Fig. 3** A) Immunoblots of FasL from MCF7 cells treated for 24 hours with vehicle (-), increasing BRL concentrations, 10 $\mu$ M GW alone or in combination with 1 $\mu$ M BRL.  $\beta$ -actin was used as

loading control. The side panel shows the quantitative representation of data (mean±S.D.) of three independent experiments including that of B after densitometry and correction for  $\beta$ -actin expression. B) Semiquantitative RT-PCR evaluation of FasL mRNA expression. MCF7 cells were treated as in A. 36B4 mRNA levels were determined as control. The side panel shows the quantitative representation of data (mean±S.D.) of three independent experiments including that of C after densitometry and correction for 36B4 expression. \* $p < 0.05$  BRL-treated vs untreated cells \*\* $p < 0.01$  BRL-treated vs untreated cells.

Fas/FasL signalling when activated recruits adapter proteins and cysteine proteases such as caspase 8 leading to apoptosis (Green 1998 and references therein). To better define the action of PPAR $\gamma$  on Fas/FasL pathway, we used GW as well as both PPAR $\gamma$  and FasL RNA interferences (i) to evaluate the activation of caspase 8, key component of the extrinsic apoptotic process. By WB analysis our data showed that untreated MCF7 cells expressed the pro-form of caspase 8, while only after BRL exposure caspase 8 was activated as evidenced by the presence of its 11 kDa cleavage product (Fig. 4C). The active caspase 8 cleavage was absent in cells treated with GW alone or combined with BRL, or inhibiting both the expression of PPAR $\gamma$  and FasL by the respective RNAis (Fig. 4C). As shown in Figs 4A and 4B, PPAR $\gamma$  and FasL RNAi were able to inhibit the two proteins expression, respectively. The apoptotic process is associated with morphological changes and biochemical events such as nuclear condensation and fragmentation, the fragments correspond to strands of DNA that were cleaved at internucleosomal regions and create a 'ladder pattern' when electrophoresed on an agarose gel (Montague and Cidlowski 1996). Because of its near universality, internucleosomal DNA degradation is considered a diagnostic hallmark of cells

undergoing apoptosis. Therefore, we studied DNA fragmentation assay under BRL treatment in MCF7 cells evidencing that the induced apoptosis is PPAR $\gamma$ -dependent as it was reversed by the PPAR $\gamma$  RNAi (Fig. 4D). These results indicate a positive crosstalk between PPAR $\gamma$  and FasL that is responsible for BRL-induced extrinsic apoptosis in MCF7 cells.

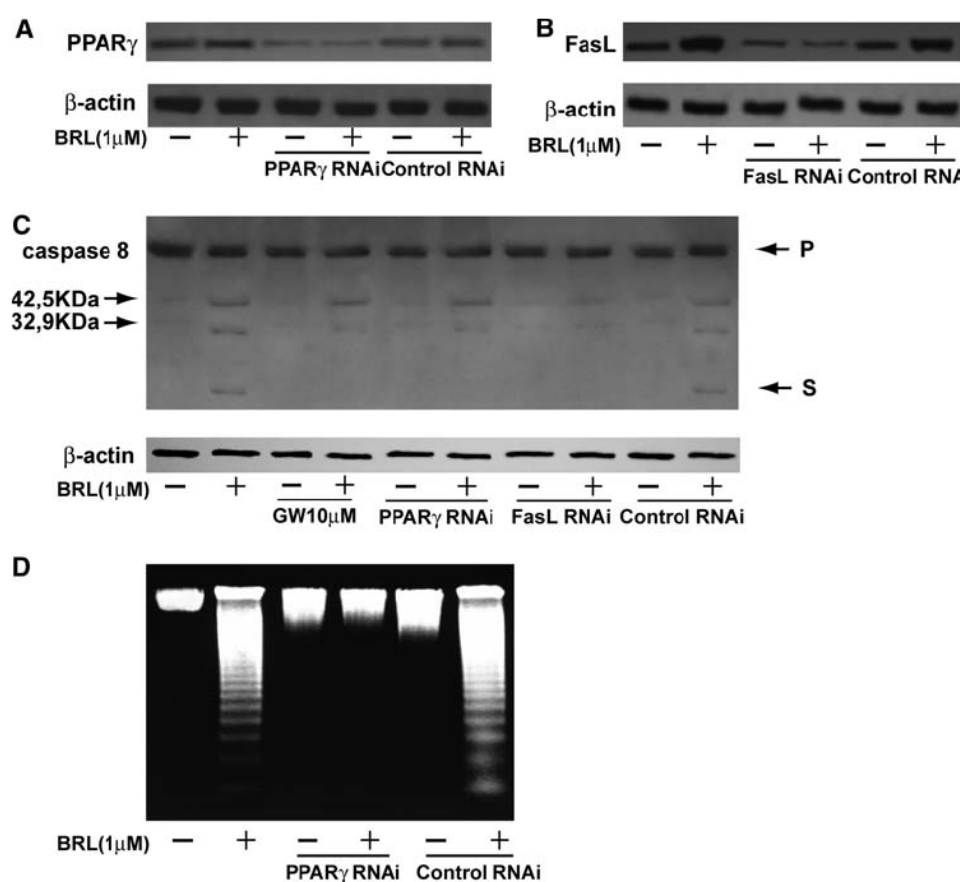


**Fig. 4** PPAR $\gamma$  (A) and FasL (B) protein expression (evaluated by WB) in MCF7 cells transfected with a 25-nucleotide of RNA interference (RNAi) targeted human PPAR $\gamma$  or FasL mRNA sequence respectively, or with control RNAi as reported in Materials and Methods and treated for 48 hours as indicated.  $\beta$ -actin was used as loading control. C) MCF7 cells were treated for 48 hours as indicated, or transfected with PPAR $\gamma$ , FasL or control RNAi. Positions of procaspase 8 (P) and its active cleavage product (S) are indicated by arrowheads on the right. One of three similar experiments is presented.  $\beta$ -actin was used as loading control on the same stripped blot. D) DNA laddering was performed in MCF7 cells treated for 72 hours as indicated, or transfected with PPAR $\gamma$  or control RNAi.

### PPAR $\gamma$ -mediated apoptosis is a common mechanism in breast cancer cells

Additionally, we examined other human breast cancer cell lines to determine whether the involvement of FasL is unique to MCF7 cells or it is a common mechanism by which PPAR $\gamma$  mediates apoptosis in breast cancer. MDA and BT20 cells, both expressing Fas and FasL (Fig. 5A), showed a FasL upregulation upon BRL treatment, which was reduced by PPAR $\gamma$  RNAi (Fig. 5B). DNA fragmentation assay under BRL treatment in MDA and BT20 cells confirmed that the PPAR $\gamma$ - induced apoptosis (Fig. 5C) addresses a general mechanism in breast cancer cells.

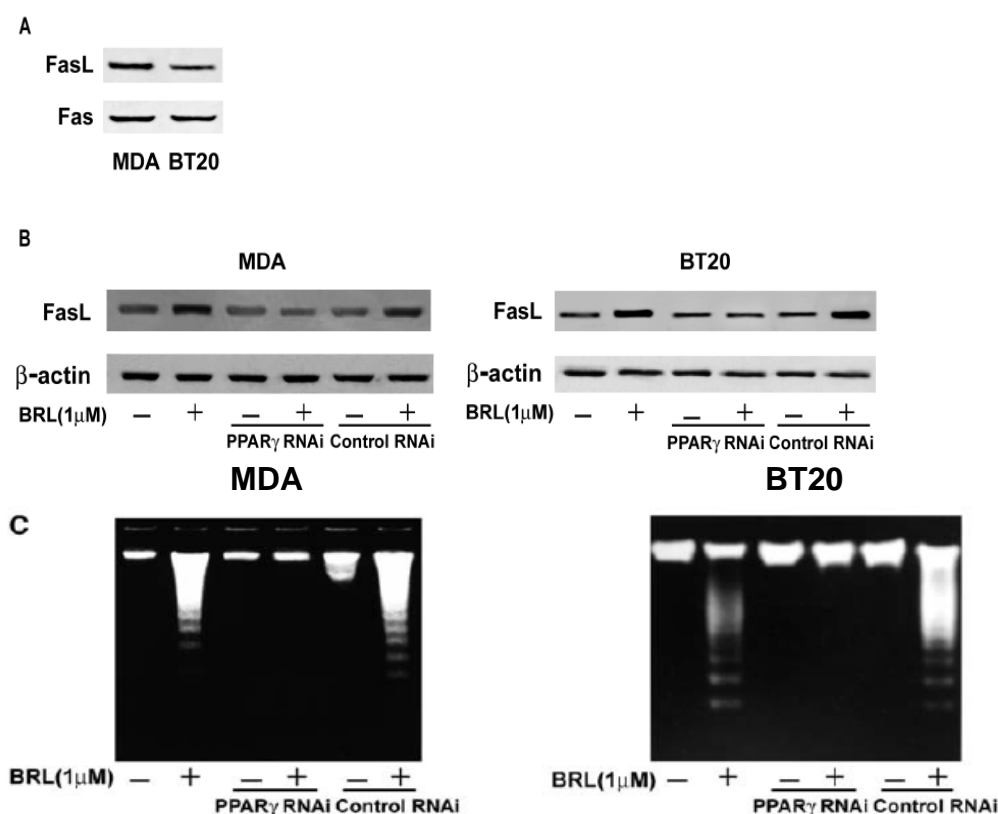


**Fig. 5** A) FasL and Fas protein expression (evaluated by WB) in MDA and BT20 breast cancer cells. B) MDA and BT-20 cells were treated for 48 hours as indicated, or transfected with a 25-nucleotide of RNA interference (RNAi) targeted human PPAR $\gamma$  mRNA sequence or with control RNAi as reported in Materials and Methods.  $\beta$ -actin was used as loading control. One of three



similar experiments is presented. C) DNA laddering was performed in MDA and BT20 cells treated for 72 hours as indicated, or transfected with PPAR $\gamma$  or control RNAi.

### Low doses of the combined BRL and 9RA treatment induce intrinsic apoptosis in breast cancer cells

To investigate whether low doses of combined agents are able to inhibit cell growth, we first assessed the effects of BRL 100nM and 9RA 50nM on a normal epithelial breast cells MCF10 and on a panel of breast cancer cell lines: MCF7, MCF7-TR1, SKBR3 and T47D. We observed that the separate treatment with BRL does not elicit any significant effect on cell viability in all breast cell lines tested, while 9RA reduces cell vitality only in T47D cells (Table 1), in the presence of both ligands cell viability is strongly reduced in all breast cancer cells, but not MCF10 cells (Table 1).

% OF VITALITY RESPECT TO CONTROL			
Breast cell lines	BRL100nM	9RA50nM	BRL+9RA
MCF-10	90,4 $\pm$ 0,867	96,7 $\pm$ 0,927	98,7 $\pm$ 1,067
MCF-7	86,5 $\pm$ 0,505	87,9 $\pm$ 1,205	51,8* $\pm$ 0,905
MCF-7 TR1	89,9 $\pm$ 1,535	115 $\pm$ 1,375	68,7* $\pm$ 1,145
SKBR-3	96,8 $\pm$ 0,875	90,5 $\pm$ 0,657	58,9* $\pm$ 0,932
T-47D	78,4 $\pm$ 1,110	60,7* $\pm$ 1,763	34,5** $\pm$ 0,730

**Table 1** Breast cells were treated for 48 hours in the presence of BRL 100nM or/and 9RA 50nM. Cell viability was measured by MTT assay. Data were presented as mean $\pm$ S.D. of three independent experiments done in triplicate and expressed as percentage of vitality respect to control. \*p<0.05 treated vs untreated cells, \*\*p<0.01 treated vs untreated cells.

On the basis of our recent work demonstrating that micromolar doses of BRL activate PPAR $\gamma$ , which in turn triggers apoptotic events through an upregulation of p53 expression in MCF7 cells (Bonofiglio et al. 2006), we aim to evaluate the ability of nanomolar doses of BRL and 9RA alone or in combination to modulate

p53 expression along with its natural target gene p21<sup>Cip1/WAF1</sup> in MCF7 cells. A significant increase in p53 and p21<sup>Cip1/WAF1</sup> content was observed by WB only upon combined treatment after 24 and 36 hours (Fig. 6A). Furthermore, we showed an upregulation of p53 and p21<sup>Cip1/WAF1</sup> mRNA levels induced by BRL plus 9RA after 12 and 24 hours (Fig. 6B).

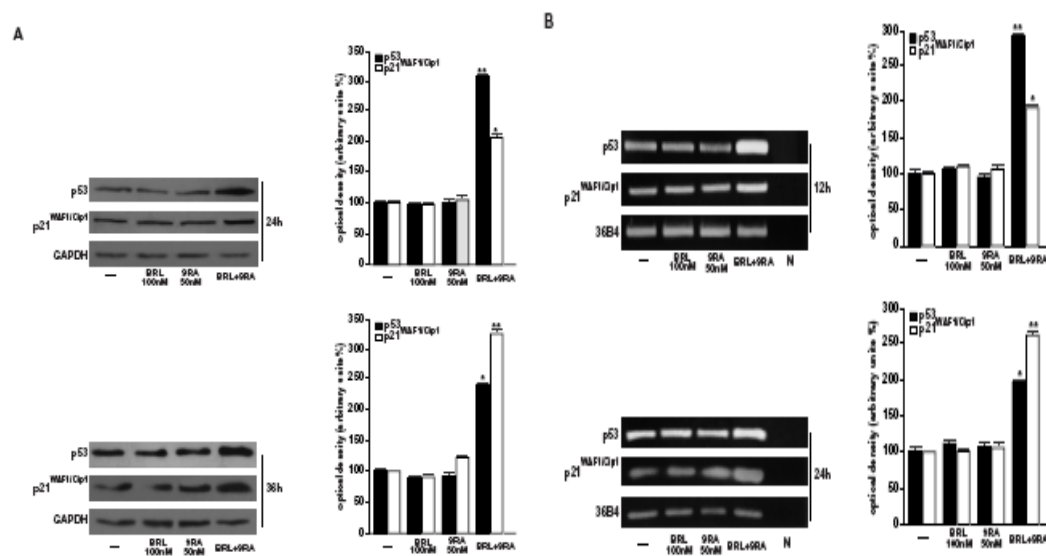


**Fig. 6** A) Immunoblots of p53 and p21<sup>Cip1/WAF1</sup> from extracts of MCF7 cells treated with BRL 100nM and 9RA 50nM alone or in combination for 24 and 36 hours. GAPDH was used as loading control. The side panels show the quantitative representation of data (mean±S.D.) of three independent experiments after densitometry. B) p53 and p21<sup>Cip1/WAF1</sup> mRNA expression in MCF7 cells treated as in A for 12 and 24 hours. The side panels show the quantitative representation of data (mean±S.D.) of three independent experiments after densitometry and correction for 36B4 expression. \*p<0.05 combined-treated vs untreated cells. \*\*p<0.01 combined-treated vs untreated cells. N: RNA sample without the addition of reverse transcriptase (negative control).

To investigate whether low doses of BRL and 9RA are able to transactivate the p53 promoter gene, we transiently transfected MCF-7 cells with a luciferase reporter construct (named p53-1) containing the upstream region of the p53 gene spanning from -1800 to +12 (Fig. 7A). Treatment for 24 hours with BRL 100nM or 9RA 50nM did not induce luciferase expression, while an increase in the

transactivation of p53-1 promoter was observed in the presence of both ligands (Fig. 7B). To identify the region within the p53 promoter responsible for its transactivation, we used deleted constructs expressing different binding sites such as CTF-1/YY1, nuclear factor-Y (NF-Y), NFκB and GC sites (Fig. 7A). In transfection experiments performed using the mutants p53-6 and p53-13 encoding the regions from -106 to +12 and from -106 to -40, respectively, the responsiveness to BRL plus 9RA was still observed (Fig. 7A). In contrast, using deleted construct in NFκB domain (p53-14) encoding the sequence from -106 to -49, the transactivation of p53 by both ligands was absent (Fig. 7B), suggesting that NFκB site is required for p53 transcriptional activity.

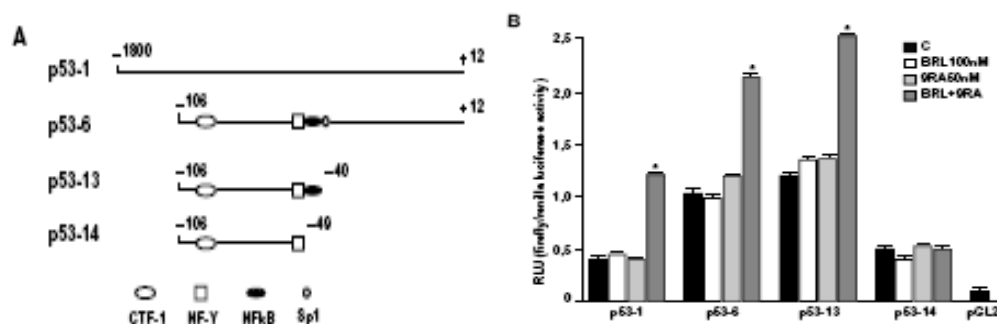


**Fig. 7** A) Schematic map of the p53 promoter fragments used in this study. B) MCF-7 cells were transiently transfected with p53 gene promoter-luc reporter constructs (p53-1, p53-6, p53-13, p53-14) and treated for 24 hours with BRL 100nM and 9RA 50nM alone or in combination. The luciferase activities were normalized to the renilla luciferase as internal transfection control and data were reported as RLU values. Columns are mean  $\pm$  S.D. of three independent experiments performed in triplicate. \* $p < 0.05$  combined-treated vs untreated cells. pGL2: basal activity measured in cells transfected with pGL2 basal vector; RLU, Relative Light Units. CTF-1, CCAAT-binding transcription factor-1; NF-Y, nuclear factor-Y; NFκB, nuclear factor κB.

To gain further insight into the involvement of NFκB site in the p53 transcriptional response to BRL plus 9RA, we performed EMSA experiments using synthetic oligodeoxynucleotides corresponding to the NFκB sequence.

As shown in Figure 8A, we evidenced the formation of a specific DNA binding complex in nuclear extracts from MCF7 cells (lane 1), since it was abrogated by 100-fold molar excess of unlabeled probe (lane 2). Of note, BRL treatment induced a slight increase in the specific band (lane 3), while no changes were observed upon 9RA exposure (lane 4). The combined treatment increased the DNA binding complex (lane 5), which was immunodepleted and supershifted using anti-PPAR $\gamma$  (lane 6) or anti-RXR $\alpha$  (lane 7) antibodies. These data indicate that heterodimer PPAR $\gamma$ /RXR $\alpha$  binds to NF $\kappa$ B site located in the promoter of p53 *in vitro*.

Next, the interaction of both nuclear receptors with the p53 promoter was further elucidated by ChIP assays. Using anti-PPAR $\gamma$  and anti-RXR $\alpha$  antibodies, formaldehyde cross-linked protein-chromatin complexes were immunoprecipitated from MCF7 cells treated with BRL 100nM and/or 9RA 50nM. PCR was used to determine the recruitment of either PPAR $\gamma$  or RXR $\alpha$  to the p53 region containing the NF $\kappa$ B site. The results indicate that either PPAR $\gamma$  or RXR $\alpha$  recruitment was increased upon BRL plus 9RA exposure (Fig. 8B). In the same conditions, an augmented RNA-Pol II recruitment was obtained by immunoprecipitating cells with an anti-RNA-Pol II antibody, indicating that a positive regulation of p53 transcription activity was induced by combined treatment (Fig. 8B).

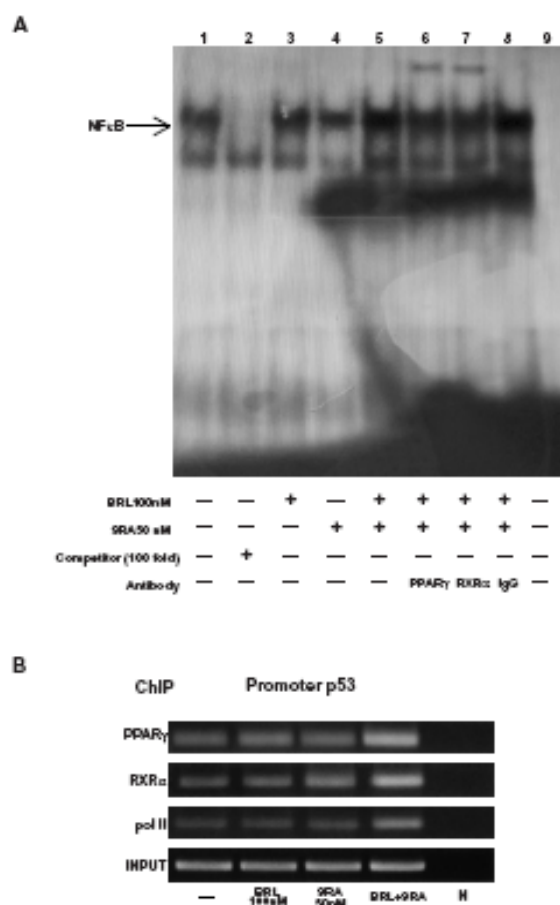


**Fig. 8** A) Nuclear extracts from MCF7 cells (lane 1) were incubated with a double-stranded NF $\kappa$ B consensus sequence probe labeled with [ $^{32}$ P] and subjected to electrophoresis in a 6% polyacrylamide gel. Competition experiments were done, adding as competitor a 100-fold molar excess of unlabeled probe (lanes 2). Nuclear extracts from MCF7 cells were treated with 100nM BRL (lane 3) and 50nM 9RA (lane 4), and in combination (lane 5). Anti-PPAR $\gamma$  (lane 6), anti-RXR $\alpha$  (lane 7) and IgG (lane 8) antibodies were incubated. Lane 9 contains probe alone. B) MCF7 cells were treated for 1 hour with 100nM BRL and/or 50nM 9RA as indicated, and then cross-linked with formaldehyde and lysed. The soluble chromatin was immunoprecipitated with anti-PPAR $\gamma$ , anti-RXR $\alpha$  and anti-RNA Pol II antibodies. The immunocomplexes were reverse cross-linked, and DNA was recovered by phenol/chloroform extraction and ethanol precipitation. The p53 promoter sequence containing NF $\kappa$ B was detected by PCR with specific primers. To control input DNA, p53 promoter was amplified from 30  $\mu$ l of initial preparations of soluble chromatin (before immunoprecipitations). N: negative control provided by PCR amplification without DNA sample.

Since disruption of mitochondrial integrity is one of the early events leading to apoptosis, we want to assess whether BRL plus 9RA affect the function of mitochondria by analyzing membrane potential with a mitochondria fluorescent dye JC-1 (Smiley et al.1991; Cossarizza et al. 1993). As shown in Fig. 9A, in non-

apoptotic cells (control), the intact mitochondrial membrane potential allows the lipophilic dye, accumulation of in aggregated form in mitochondria which display red fluorescence. In MCF7 cells, treatment with BRL 100nM or 9RA 50nM did not change the red fluorescence (data not shown), whereas cells treated with both ligands stain green fluorescent, since JC-1 cannot accumulate within the mitochondria and it remains as a monomeric form in the cytoplasm (Fig. 9A). Concomitantly, cytochrome *C* release from mitochondria into the cytosol, a critical step in the apoptotic cascade, was demonstrated after combined treatment (Fig. 9B).

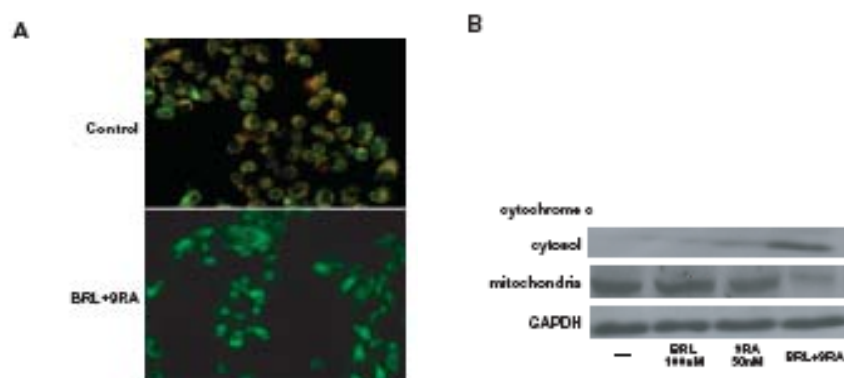


**Fig. 9** A) MCF7 cells were treated with 100nM BRL plus 50nM 9RA for 48 hours and then we used fluorescent microscopy to analyze the results of JC-1 (5,5',6,6'-tetrachloro-1,1',3,3'-tetraethylbenzimidazolylcarbocyanine iodide) kit. In control non-apoptotic cells, the dye stains the mitochondria red. In treated apoptotic cells, JC-1 remains in the cytoplasm in a green fluorescent form. B) MCF7 cells were treated for 48 hours with BRL 100nM and/or 9RA 50nM in combination. GAPDH was used as loading control.

To identify the major contributor of the activated intrinsic apoptotic process, we evaluated the cleavage of caspases. Notably, the treatment of MCF7 cells with BRL plus 9RA for 48 hours promoted only the caspase 9 activation (Table 2A). No change in caspase 8 activation was observed, suggesting that

heterodimerization of PPAR $\gamma$ /RXR $\alpha$  triggers only the intrinsic apoptotic pathway (Table 2B).

A

Caspase 9	% of Activation	SD
control	14,16	$\pm 2,565$
BRL100nM	17,23	$\pm 1,678$
9RA50nM	18,14	$\pm 0,986$
BRL+9RA	33,88 *	$\pm 5,216$

B

Caspase 8	% of Activation	SD
control	9,20	$\pm 1,430$
BRL100nM	8,12	$\pm 1,583$
9RA50nM	7,90	$\pm 0,886$
BRL+9RA	10,56	$\pm 2,160$

**Table 2** Cells were stimulated for 48 hours in presence of BRL 100nM, 9RA 50nM alone or in combination. The activation of caspase 9 (A) and caspase 8 (B) was analyzed by Flow cytometry assay. Data were presented as (mean $\pm$ S.D.) of triplicate experiments. \* $p < 0.05$  combined-treated vs untreated cells.

We also demonstrated DNA fragmentation under BRL plus 9RA treatment in MCF7 cells, which was prevented by GW and in presence of AS/p53 (Fig. 10B), able to abolish p53 expression (Fig. 10A).

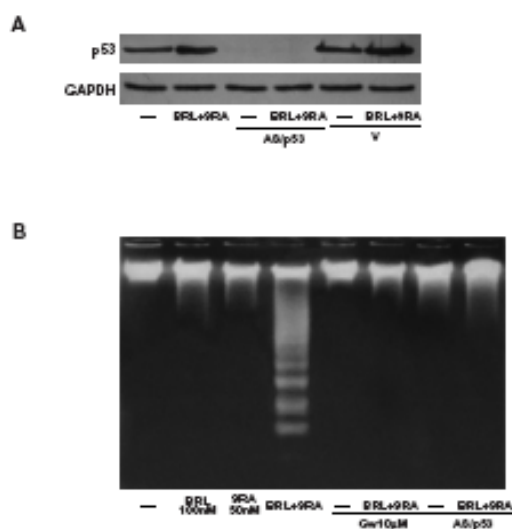


**Fig. 10** A) Immunoblot of p53 from MCF7 cells transfected with an expression plasmid encoding for p53 antisense (AS/p53) or an empty vector (v) and treated for 56 hours as indicated. GAPDH was used as loading control. B) DNA laddering was performed in MCF7 cells transfected and treated as indicated. One of three similar experiments is presented.

---

### Combined treatment of BRL and 9RA, as a common mechanism, leads to the p53-mediated DNA fragmentation in breast cancer cells

Finally, we examined in three additional human breast malignant cell lines: MCF7-TR1, SKBR3 and T47D the capability of low doses of PPAR $\gamma$  and RXR ligands to activate apoptosis. DNA fragmentation assay showed that only in the presence of combined treatment cells underwent apoptosis in a p53-mediated manner (Fig. 11), implicating a general mechanism in breast carcinoma.

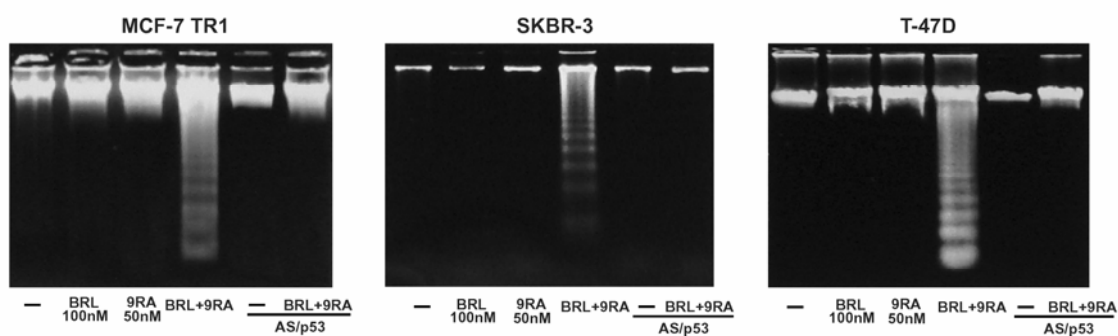


**Fig. 11** DNA laddering was performed in MCF7 TR1, SKBR3 and T47D treated for 56 hours as indicated, or transfected with AS/p53 plasmid. One of three similar experiments is presented.



### BRL induces growth inhibition of thyroid cancer cells by upregulating p21<sup>Cif1/WAF1</sup> gene expression

It has been reported that the PPAR $\gamma$  agonists exert antiproliferative effects on thyroid carcinoma cells (Kuboto et al. 1998; Clay et al. 1999; Ohta et al. 2001). In order to analyse the molecular mechanism underlying the growth inhibitory effects exerted by PPAR $\gamma$  ligands, we first treated human follicular WRO and anaplastic FRO thyroid cancer cells with increasing BRL concentrations for 5 days. BRL inhibited the growth of both thyroid cancer cells in a dose- and PPAR $\gamma$ -dependent manner, since this effect was no longer notable in the presence of GW (Fig. 12).

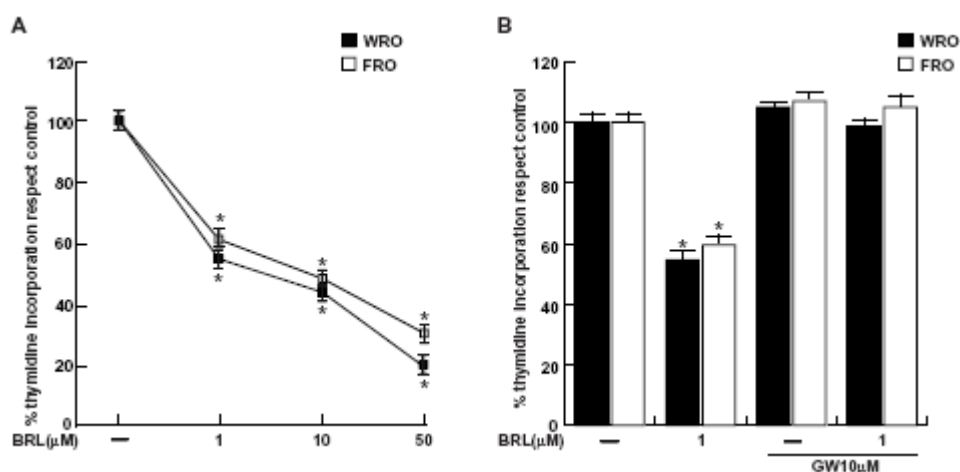


**Fig. 12** A) WRO and FRO cells were treated for 5 days with vehicle (-) or with increasing BRL concentrations. B) Both thyroid cancer cells were treated for 5 days with vehicle (-), 1  $\mu$ M BRL, 10  $\mu$ M GW alone or in combination with BRL. On day 6, [<sup>3</sup>H] thymidine incorporation was determined by scintillation counting. Data are expressed as mean  $\pm$  S.D. of three independent experiments performed in triplicate. \*P < 0.05 BRL-treated vs untreated cells.

Therefore, we aimed to examine the potential ability of the PPAR $\gamma$  agonist BRL to modulate p53 along with its natural target gene p21<sup>Cip1/WAF1</sup> in both thyroid cancer cells. Interestingly, BRL upregulated the protein expression of p21<sup>Cip1/WAF1</sup> in a dose-dependent manner in the WRO and FRO cells, while did not modify the p53 protein content (Fig. 13).

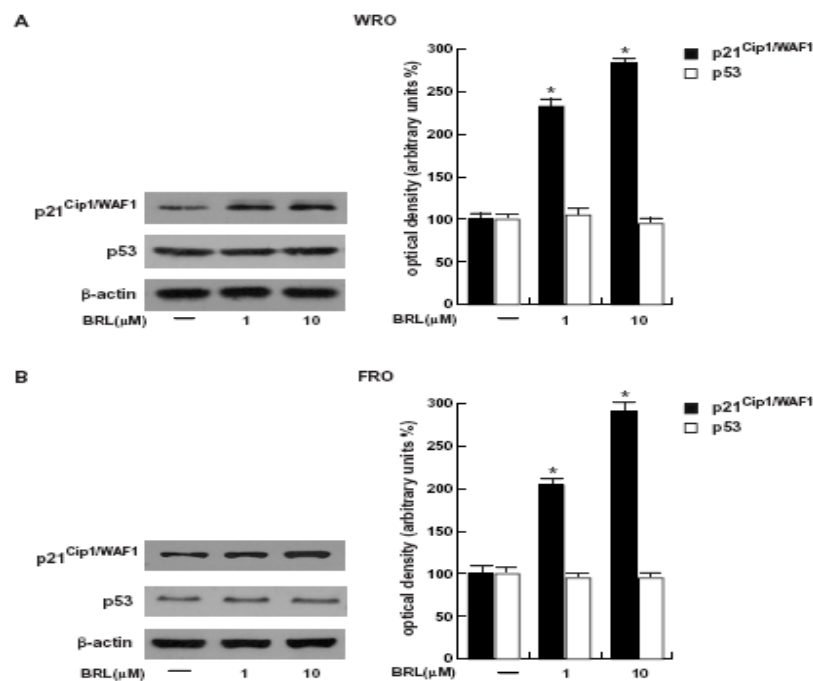


**Fig. 13** Immunoblots of p21<sup>Cip1/WAF1</sup> and p53 from (A) WRO and (B) FRO cells treated for 24 hours with vehicle (-) and with increasing BRL concentrations. b-Actin was used as the loading control. The side panels show the quantitative representation of data (mean $\pm$ S.D.) of three independent experiments included that presented in A and B respectively. \*P<0.05 BRL-treated versus untreated cells.

Next, we investigated the mRNA expression of p21<sup>Cip1/WAF1</sup>, which was induced by BRL at an increasing concentration in both thyroid cancer cells. We observed that BRL upregulated mRNA expression of p21<sup>Cip1/WAF1</sup> is also in a dose-dependent manner in the WRO and FRO cells. Using GW, BRL action was

abrogated, suggesting a direct involvement of PPAR $\gamma$  in mediating this effect (Fig. 14).

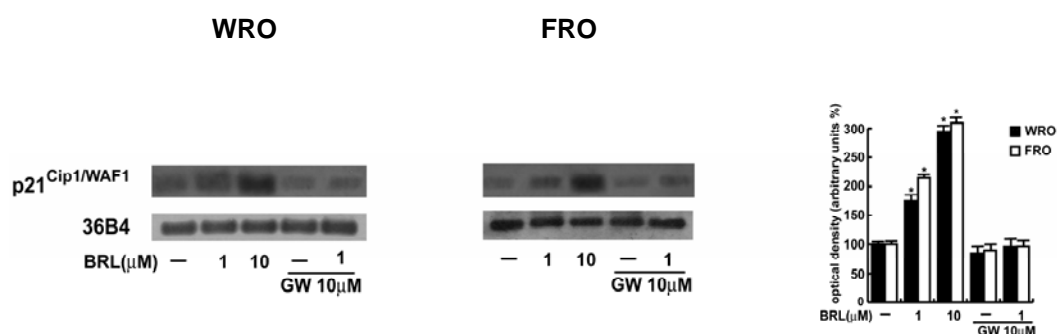


**Fig. 14** Semiquantitative RT-PCR evaluation of p21<sup>Cip1/WAF1</sup> mRNA expression in WRO and FRO cells. 36B4 mRNA levels were determined as control. The side panel shows the quantitative representation of data (mean $\pm$ S.D.) of three independent experiments after densitometry and correction for 36B4 expression. \*p<0.05 BRL-treated vs untreated cells.

The aforementioned observations prompted us to investigate whether BRL is able to transactivate the p21<sup>Cip1/WAF1</sup> promoter gene, which contains two p53-response elements (Li et al. 1994; Wu and Schonthal 1997). Thus, WRO and FRO cells were transiently transfected with the human wild-type p21<sup>Cip1/WAF1</sup> promoter-luciferase fusion plasmid (p21<sup>Cip1/WAF1</sup> wt) or with a promoter construct that lacks the two p53-binding sites (p21<sup>Cip1/WAF1</sup>  $\Delta$ p53; Fig. 15A). BRL was able to transactivate both constructs, defining the minimal region of p21<sup>Cip1/WAF1</sup> promoter responsible for its induction independently of p53 (Fig. 15B). Such effects were reversed by GW, suggesting that the transactivation of p21<sup>Cip1/WAF1</sup> by BRL occurs in a PPAR $\gamma$ -dependent manner (Fig. 15B). Since the deleted mutant p21<sup>Cip1/WAF1</sup>  $\Delta$ p53 encoding the region from -124 to +11 expresses multiple Sp1 sites, we performed transfection experiments using mithramycin, a

specific inhibitor of GC binding (Blume et al. 1991). The transactivation of this construct induced by BRL was abrogated by mithramycin, indicating an involvement of Sp1 transcription factor in the PPAR $\gamma$  action observed in WRO and FRO cells (Fig. 15B).

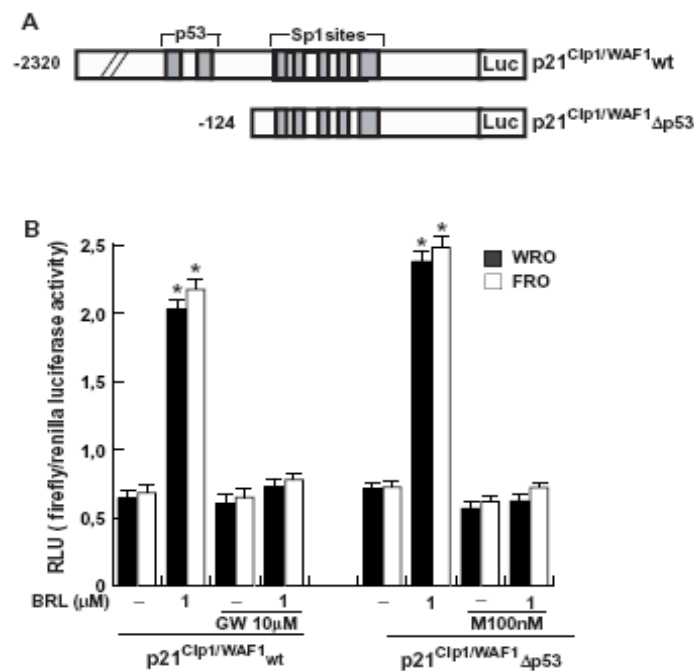


**Fig. 15** A) Schematic map of the p21<sup>Cip1/WAF1</sup> promoter plasmids used in this study. B) WRO and FRO cells were transiently transfected with the wild-type p21 promoter luciferase (p21<sup>Cip1/WAF1</sup><sub>wt</sub>) and then treated with vehicle (-), BRL, GW alone or in combination with BRL. Both thyroid cancer cells were transiently transfected with deleted construct (p21<sup>Cip1/WAF1</sup><sub>Δp53</sub>) and then treated as above. The luciferase activities were normalized to the Renilla luciferase as internal transfection control and data were reported as RLU values. Columns are mean ± S.D. of three independent experiments performed in triplicate. \*p < 0.05 BRL-treated vs untreated cells. RLU, relative light units; M, mithramycin.

In order to further support whether Sp1 sites mediate the BRL-induced upregulation of p21<sup>Cip1/WAF1</sup>, we performed EMSA using synthetic oligodeoxyribonucleotides corresponding to the Sp1 site located in the human p21<sup>Cip1/WAF1</sup> gene promoter, as probe. In nuclear extracts from WRO cells (Fig. 16A) we obtained the formation of specific bands (lane 1), which were strongly

increased in cells treated with BRL (lane 2). Competition binding studies demonstrated that a 100-fold molar excess of unlabeled probe inhibited the formation of these complexes (lane 3). The addition of mithramycin, which binds to GC boxes and prevents sequential Sp1 binding, decreased the intensity of the bands to Sp1 DNA sequence (lane 4). Of note, the anti-PPAR $\gamma$  and anti-Sp1 antibodies (lanes 5 and 6 respectively) were able to supershift the specific bands. Different controls were used to assess the specificity of the binding; IgG that did not generate supershifted bands (lane 7), human Sp1 recombinant protein alone (lane 8), and Sp1 in combination with either cold competitor (lane 9) or the anti-Sp1 antibody (lane 10). As shown in Fig. 16B, similar results, such as an increased DNA-binding complex under BRL (lane 2), a reduction of the band intensity by using mithramycin (lane 4), and supershifted bands in the presence of the anti-PPAR $\gamma$  and anti-Sp1 antibodies (lanes 5 and 6) were obtained in FRO cells.

The interaction of PPAR $\gamma$  with the p21<sup>Cip1/WAF1</sup> gene promoter was *in vivo* investigated by CHIP assay. WRO and FRO chromatin were immunoprecipitated with the anti-PPAR $\gamma$ , the anti-Sp1, the anti-RNA Pol II antibodies. PCR was used to determine the recruitment of PPAR $\gamma$  to the p21<sup>Cip1/WAF1</sup> region containing the Sp1 site. As shown in Fig. 16C and D, the results indicated that PPAR $\gamma$  was weakly and constitutively bound to the p21<sup>Cip1/WAF1</sup> promoter in untreated cells

and this recruitment was increased upon BRL treatment, while in the presence of mithramycin the BRL effect was reversed in both thyroid cancer cells. In addition, the positive regulation of the p21<sup>Cip1/WAF1</sup> transcription activity through Sp1 induced by BRL was demonstrated by the increased recruitment of RNA Pol II, which was reversed in the presence of mithramycin. Altogether, the data indicate that PPAR $\gamma$  binding to the Sp1 transcription factor exerts stimulatory effects on p21<sup>Cip1/WAF1</sup> gene expression.

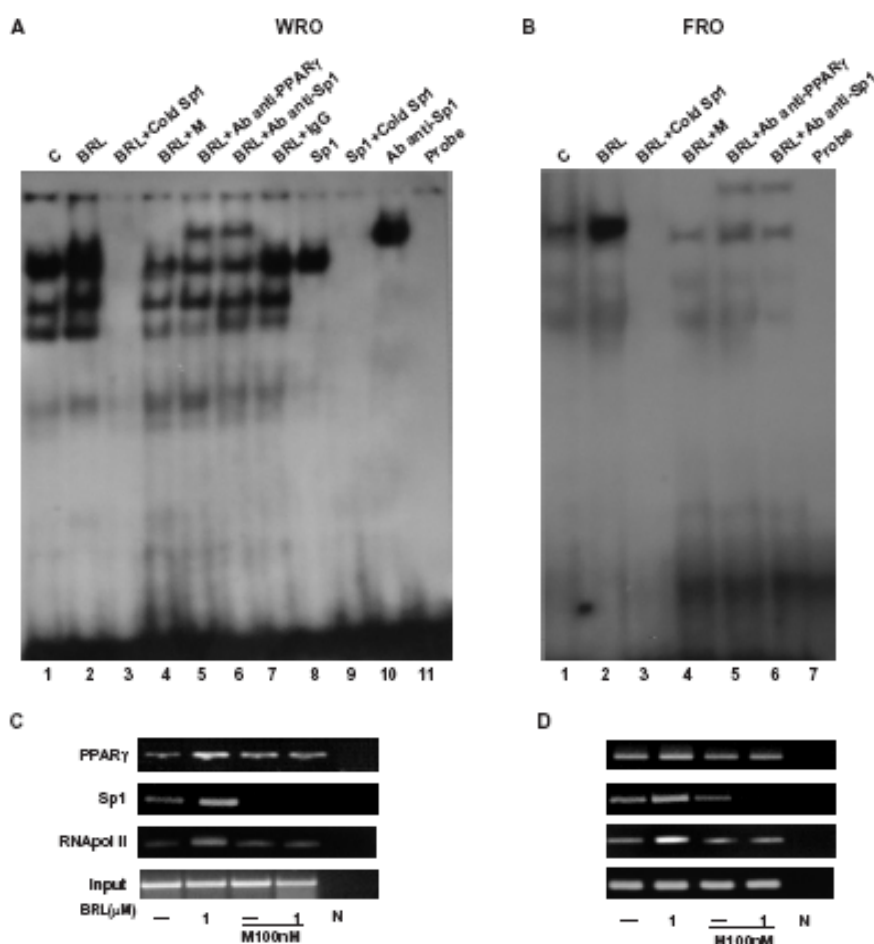


**Fig. 16** A) Nuclear extracts from WRO cells (lane 1) were incubated with a double-stranded Sp1 sequence probe labeled with [ $\gamma$ 32P] and subjected to electrophoresis in a 6% polyacrylamide gel. In lane 2, nuclear extracts were treated with 1 $\mu$ M BRL. Competition experiments were performed adding as competitor a 100-fold molar excess of unlabeled Sp1 probe (lane 3) or 100 nM mithramycin (M) (lane 4). Anti-PPAR $\gamma$  and anti-Sp1 antibodies and IgG were incubated with

---

nuclear extracts treated with BRL (lanes 5, 6, and 7). One microliter of human Sp1 recombinant protein (lane 8) was incubated with a double-stranded Sp1 sequence probe. A 100-fold molar excess of unlabeled Sp1 probe (lane 9) or anti-Sp1 antibody (lane 10) was added to Sp1 protein. Lane 11 contains probe alone. B) Nuclear extracts from FRO cells were incubated with a double-stranded Sp1 sequence probe labeled with [ $\gamma$ 32P] and subjected to electrophoresis in a 6% polyacrylamide gel. In lane 2, nuclear extracts were treated with 1  $\mu$ M BRL. Competition experiments were performed adding as competitor a 100-fold molar excess of unlabeled Sp1 probe (lane 3) or 100 nM mithramycin (M) (lane 4). Anti-PPAR $\gamma$  and anti-Sp1 antibodies were incubated with nuclear extracts treated with BRL (lanes 5 and 6 respectively). Lane 7 contains probe alone. C) WRO and D) FRO cells were treated as indicated, then cross-linked with formaldehyde, and lysed. The soluble chromatin was immunoprecipitated with the anti-PPAR $\gamma$ , anti-Sp1, anti-RNA Pol II antibodies. The p21<sup>Cip1/WAF1</sup> promoter sequence containing Sp1 was detected by PCR with specific primers, as described in Materials and Methods. To control input DNA, the p21<sup>Cip1/WAF1</sup> promoter was amplified from 30 $\mu$ l initial preparations of soluble chromatin (before immunoprecipitations). N, negative control provided by PCR amplification without DNA sample; M, mithramycin.

To confirm the BRL-induced growth inhibition of thyroid cancer cells through p21<sup>Cip1/WAF1</sup>, WRO and FRO cells were transfected with the p21<sup>Cip1/WAF1</sup> antisense (AS)-ODN or control scrambled (cs)-ODN in the proliferation assay. Noteworthy, the inhibitory effect exerted by BRL on cell proliferation was reversed by p21<sup>Cip1/WAF1</sup> AS-ODN but not by cs-ODN in both thyroid cancer cells (Fig. 17A) in which the p21<sup>Cip1/WAF1</sup> protein levels under these experimental conditions were assessed by WB (Fig. 17B). Taken together, these results indicate that the antiproliferative effect exerted by BRL in thyroid cancer cells involves a positive crosstalk between PPAR $\gamma$  and p21<sup>Cip1/WAF1</sup>-signaling pathway.

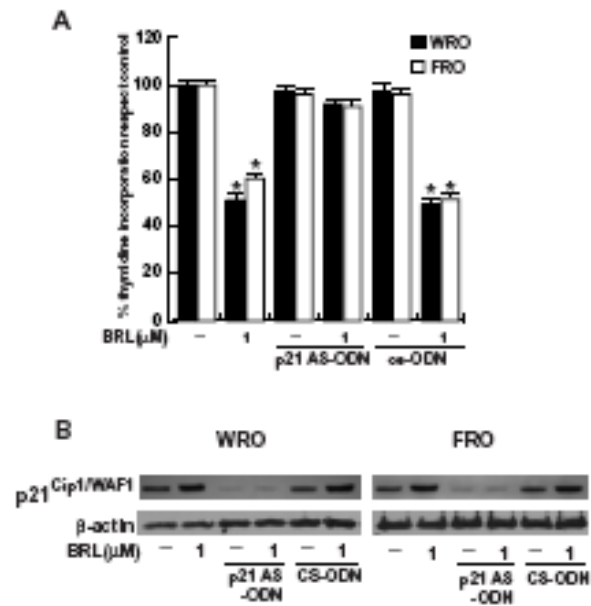


**Fig. 17** A) WRO and FRO cells were treated in the presence of vehicle (-) or with BRL, transfected using p21<sup>Cip1/WAF1</sup> antisense (p21 AS) or control scrambled (cs) oligonucleotides (ODN) as indicated. On day 6, [<sup>3</sup>H]thymidine incorporation was determined by scintillation counting. Data are expressed as mean±S.D. of three independent experiments performed in triplicate. \*p<0.05 BRL-treated vs untreated cells. B) Immunoblots of p21<sup>Cip1/WAF1</sup> from thyroid carcinoma cells treated as in A. β-Actin was used as the loading control.



## DISCUSSION

In the present study we have showed the molecular mechanisms of the inhibitory action exerted by the cognate PPAR $\gamma$ -ligand BRL in breast cancer and thyroid carcinoma cells.

Considering the key role elicited by p53 tumor suppressor gene in the growth inhibition and apoptosis (Yu and Zhang 2005; Haupt et al. 2003), we have evaluated whether PPAR $\gamma$  signaling converges on p53 transduction pathway in MCF7 cells. Of interest, we found that BRL exposure up-regulates both p53 mRNA and protein levels with a concomitant increase of p21<sup>Cip1/WAF1</sup> expression. These effects were abrogated in the presence of the specific antagonist GW, addressing a PPAR $\gamma$ -mediated mechanism. A large body of evidence has suggested the straightforward role of p53 signaling in the apoptotic cascades that include the activation of caspases, a family of cytoplasmic cysteine proteases (Schuler and Green 2001). The intrinsic apoptotic pathway involves a mitochondria-dependent process, which results in cytochrome c release and, thereafter, activation of caspase-9 (Cohen 1997). Furthermore, apoptosis is characterized by distinct morphological changes including the internucleosomal cleavage of DNA, which is recognized as a DNA ladder (Cohen 1997 and references therein). Notably, we evidenced that in a consecutive series of events, BRL at micromolar concentration: 1) up-regulates the expression of p53 and 2) its effector p21<sup>Cip1/WAF1</sup>, 3) triggers the cleavage of caspase 9, and 4) induces DNA fragmentation in a PPAR $\gamma$ -mediated manner.

Since the PPAR $\gamma$ -mediated apoptosis is not completely blocked by using the p53 antisense, we suggest that final PPAR $\gamma$  action in this concern is complex and it may require a multifactorial coordination of different signalling cascades. From there, we investigated the potential of PPAR $\gamma$  in inducing apoptotic events through a direct involvement of the Fas/FasL extrinsic apoptotic pathway in breast cancer cells. The Fas/FasL signalling system plays an important role in chemotherapy-induced apoptosis in several different cell types (Kasibhatla et al. 1998; Mo and Beck, 1999). In our MCF7 cells, positive to Fas and FasL, we found that BRL through PPAR $\gamma$  activation upregulates FasL at both protein and mRNA levels. Despite the FasL relevance, its cell and tissue distribution, and the apparent differences of its expression in a cell-specific manner, little knowledge is available how FasL expression is regulated. Engagement of the FasL homotrimer to three Fas molecules induces apoptosis by clustering of the receptor's death domains (Nagata 1997; Green 1998). This leads to the binding of FADD and caspase 8 to the receptor (Green 1998). In the present study, we obtained the active cleavage of caspase 8 under BRL treatment at micromolar doses, that is no longer detectable in the presence of GW as well as inhibiting both the expression of FasL and PPAR $\gamma$  by the respective RNAis. Of note, PPAR $\gamma$ -induced apoptosis appears to be a general mechanism in breast cancer cells since it occurs in MCF7, MDA and BT20 cells.

In the second part of our investigation, we evidenced that the combined treatment with low doses of PPAR $\gamma$  and RXR ligands may target selectively breast carcinoma cells inhibiting cell proliferation and inducing apoptosis. It is well

known that PPAR $\gamma$ , through heterodimerization with RXR, potentiates its own binding to DNA and its transactivation (Kliwer et al. 1992; Zhang et al. 1992). The potential additive antitumoral effects of PPAR $\gamma$  and RXR agonists, both at elevated doses, has also been shown in human breast cancer cells, (Grommes et al. 2004 and references therein). However, previous reports documented remarkable side effects of PPAR $\gamma$  and RXR ligands consisting with weight gain and plasma volume expansion (Arakawa et al., 2004; Rangwala and Lazar 2004; Staels 2005) and hypertriglyceridemia and suppression of the thyroid hormone axis (Pinaire and Reifel-Miller 2007), respectively. In the present study we demonstrated that nanomolar concentrations of PPAR $\gamma$  agonist BRL and RXR ligand 9RA alone or in combination do not elicit any substantial change in cell vitality on normal breast epithelial cells. In contrast, the combined treatment with both agents exerts a significant effect on cell viability of different breast cancer cells. Functional assays with deleted constructs of the p53 promoter showed that the NF $\kappa$ B binding site is required for the transcriptional response to low doses of BRL plus 9RA in MCF7 cells. NF $\kappa$ B was shown to physically interact with PPAR $\gamma$  (Chung et al. 2000), which in some circumstances binds to DNA cooperatively with NF $\kappa$ B (Couturier et al. 1999; Sun et al. 2002), further enhancing the NF $\kappa$ B-DNA binding (Ikawa et al. 2001). Our EMSA and ChIP assay demonstrated that these agents at nanomolar concentration only when in combination appeared to be effective in the binding and in the recruitment of both PPAR $\gamma$  and RXR $\alpha$  on the p53 promoter sequence. BRL plus 9RA treatment at the doses tested also increases the binding of RNA-Pol II to p53 promoter gene addressing a positive transcriptional

regulation able to produce a consecutive series of events featuring intrinsic apoptotic pathway. The specific involvement of intrinsic apoptotic pathway was confirmed by the activation of caspase 9, while we do not observe any modification of caspase 8, a key component of the extrinsic apoptotic process. The crucial role of p53 in mediating apoptosis raised by the evidence that the described event is abrogated in the presence of AS/p53.

In the last part of our study, we demonstrated that PPAR $\gamma$  acts as a tumor suppressor gene against two different human thyroid carcinoma cell lines. In both WRO, a well-differentiated thyroid follicular carcinoma and FRO, an undifferentiated/anaplastic thyroid carcinoma, PPAR $\gamma$  inhibits cell growth by stimulating the expression of the cyclin-dependent kinase inhibitor p21<sup>Cip1/WAF1</sup> in a p53 independent manner. Previous studies have reported that BRL and other thiazolidinediones inhibit thyroid carcinoma cell proliferation in a PPAR $\gamma$ -dependent fashion (Chung et al. 2002; Martelli et al. 2002; Klopper et al. 2004; Aiello et al. 2006; Chen et al. 2006; Copland et al. 2006), PPAR $\gamma$  mediates the upregulation of p21<sup>Cip1/WAF1</sup> (Chung et al. 2002; Han et al. 2004; Hong et al. 2004), p21<sup>Cip1/WAF1</sup> mediates PPAR $\gamma$ -induced growth arrest in cancer cells including thyroid (Han et al. 2004; Copland et al. 2006), and PPAR $\gamma$  mediates p21<sup>Cip1/WAF1</sup> mRNA induction via Sp1-enhanced binding to the p21<sup>Cip1/WAF1</sup>, KDR, and hormonesensitive lipase promoters (Han et al. 2004; Hong et al. 2004; Sassa et al. 2004; Deng et al. 2006). From our study, the specific role of PPAR $\gamma$  in upregulating p21<sup>Cip1/WAF1</sup> raised by the evidence that this effect is completely abrogated either in the presence of specific siRNA of PPAR $\gamma$  or by the

pretreatment with GW. The molecular events responsible for the induction of p21<sup>Cip1/WAF1</sup> by PPAR $\gamma$  ligands are consistent with the enhanced transcriptional activation of this gene as it raised by the capability of the ligand to activate the promoter of p21<sup>Cip1/WAF1</sup>. p21<sup>Cip1/WAF1</sup>, a classic p53 responsive gene, was first identified as a p53-inducible gene, more recently its induction was shown to occur via p53-independent mechanisms in various cell lines stimulated for differentiation and growth arrest, including thyroid carcinoma cells (Park et al. 2001). In both thyroid cancer cell lines, p21<sup>Cip1/WAF1</sup> BRL transactivation occurs independent of p53 since the deletion of the two p53 response elements of the promoter maintains promoter activity. Moreover, since p53 levels do not respond to BRL treatment it is reasonable that the mechanism is p53-independent because our thyroid cancer cell lines have either mutated nonfunctional p53 (WRO cells) or scantily expressed p53 wild-type form (FRO cells), as reported previously (Fagin et al. 1993). Multiple transcription factor binding sites within the human p21<sup>Cip1/WAF1</sup> promoter have been described to be able to interact with Sp1 including regulatory elements for Sp1 that play important roles in cell cycle arrest and apoptosis in carcinoma cells (Moon et al. 2006; Tvrdí'k et al. 2006; Fang et al. 2007). Sp1 has been considered traditionally as a ubiquitous factor associated closely with core promoter activities; it has recently been observed that it participates in several cases of regulated gene transcription triggered by multiple signaling pathways and metabolic or differentiation conditions. Recently, it has been showed that NRs can form ternary complexes with Sp1 and GC-rich DNA and in this complex NRs could also serve as auxiliary factors for Sp1 bound to

GC-rich DNA (Husmann et al. 2000). Our data sustain this functional model of a tripartite complex of Sp1, PPAR $\gamma$ , and GC-rich DNA. For instance, in our study, EMSA and ChIP assays demonstrated the coexistence of the two proteins in the DNA-binding complexes, addressing that the functional interaction between PPAR $\gamma$  and Sp1 could modulate the activity of the human p21<sup>Cip1/WAF1</sup> promoter under basal other than BRL-inducible conditions in WRO and FRO cell lines. Our data show a discrepancy with those of previous publication in which Sp1 interacts with the consensus GC-rich sequence in p21<sup>Cip1/WAF1</sup> promoter gene and this band was not directly associated with PPAR $\gamma$  under the conditions used for the gel mobility shift assay (Hong et al. 2004). Besides, it has also been reported in another cell system that PPAR $\gamma$  ligands enhanced nuclear protein-binding activities of Sp1 and C/EBP sites in p21<sup>Cip1/WAF1</sup> promoter (Han et al. 2004). Our data show that treatment with mithramycin, a specific inhibitor of Sp1, completely reversed the activation of p21<sup>Cip1/WAF1</sup> promoter by BRL, suggesting furthermore that the interaction between PPAR $\gamma$  and Sp1 is essential for such activation.

The crucial role of p21<sup>Cip1/WAF1</sup> in mediating the inhibitory effect of PPAR $\gamma$  in cell proliferation has been definitively demonstrated in thyroid cells transfected with p21 AS-ODN and with increasing PPAR $\gamma$  plasmid amounts in the cell growth assay.

In conclusion, the data presented in our studies focused on a variety of anticancer activities mediated by PPAR $\gamma$  and further candidate PPAR $\gamma$  ligands in the treatment of patients affected by breast carcinoma as well as by follicular and particularly anaplastic thyroid cancer.

Additionally, our last results suggest that multidrug regimens with low doses of PPAR $\gamma$  and RXR ligands may perspectivevely represent a novel therapeutic tool also for those breast cancer patients , who developed resistance to antiestrogen therapy.

## REFERENCES

- Aiello A, Pandini G, Frasca F, Conte E, Murabito A, Sacco A, Genua M, Vigneri R & Belfiore A** 2006 Peroxisomal proliferator-activated receptor-gamma agonists induce partial reversion of epithelial-mesenchymal transition in anaplastic thyroid cancer cells. *Endocrinology* 147 4463–4475.
- Andrews NC & Faller DV** 1991 A rapid micropreparation technique for extraction of DNA-binding proteins from limiting numbers of mammalian cells. *Nucleic Acids Res* 19 2499.
- Appella E** 2001 Modulation of p53 function in cellular regulation. *Eur J Biochem* 268 2763.
- Arakawa K, Ishihara T, Aoto M, Inamasu M, Kitamura K & Saito A** 2004 An antidiabetic thiazolidinedione induces eccentric cardiac hypertrophy by cardiac volume overload in rats. *Clin Exp Pharmacol Physiol* 31 8–13.
- Ashkenazi A & Dixit VM** 1998 Death receptors: signaling and modulation. *Science* 281 1305–1308.
- Blume SW, Snyder RC, Ray R, Thomas S, Koller CA & Miller DM** 1991 Mithramycin inhibits SP1 binding and selectively inhibits transcriptional activity of the dihydrofolate reductase gene in vitro and in vivo. *Journal of Clinical Investigations* 88 1613–1621.
- Bonofiglio D, Aquila S, Catalano S, Gabriele S, Belmonte M, Middea E, Qi H, Morelli C, Gentile M, Maggiolini M & Andò S** 2006 Peroxisome proliferator-activated receptor-gamma activates p53 gene promoter binding to the nuclear factor-kappaB sequence in human MCF7 breast cancer cells. *Molecular Endocrinology* 20 3083–3092.
- Bonofiglio D, Gabriele S, Aquila S, Catalano S, Gentile M, Middea E, Giordano F & Andò S** 2005 Estrogen receptor alpha binds to peroxisome proliferator-activated receptor response element and negatively interferes with peroxisome proliferator-activated receptor gamma signaling in breast cancer cells. *Clinical Cancer Research* 11 6139–6147.
- Caelles C, Helmborg A & Karin M** 1994 p53-Dependent apoptosis in the absence of transcriptional activation of p53-target genes. *Nature* 370 220–223.
- Chen Y, Wang SM, Wu JC & Huang SH** 2006 Effects of PPARgamma agonists on cell survival and focal adhesions in a Chinese thyroid carcinoma cell line. *Journal of Cellular Biochemistry* 98 1021–1035.
- Chung SH, Onoda N, Ishikawa T, Ogisawa K, Takenaka C, Yano Y, Hato F & Hirakawa K** 2002 Peroxisome proliferator-activated receptor gamma activation induce cell cycle arrest via p53-independent pathway in human anaplastic thyroid cancer cells. *Japanese Journal of Cancer Research* 93 1358–1365.
- Chung SW, Kang BY, Kim SH, Pak YK, Cho D, Trinchieri G & Kim TS** 2000 Oxidized low density lipoprotein inhibits interleukin-12 production in lipopolysaccharide-activated mouse macrophages via direct interactions between peroxisome proliferator-activated receptor- $\gamma$  and nuclear factor- $\kappa$ B. *J Biol Chem* 275 32681–32687.



- Clay CE, Namen AM, Atsumi G, Willingham MC, High KP, Kute TE, Trimboli AJ, Fonteh AN, Dawson PA & Chilton FH** 1999 Influence of J series prostaglandins on apoptosis and tumorigenesis of breast cancer cells. *Carcinogenesis* 20 1905–1911.
- Cohen GM** 1997 Caspases: the executioners of apoptosis. *Biochem J* 326 1–16.
- Copland JA, Marlow LA, Kurakata S, Fujiwara K, Wong AK, Kreinest PA, Williams SF, Haugen BR, Klopper JP & Smallridge RC** 2006 Novel high-affinity PPAR $\gamma$  agonist alone and in combination with paclitaxel inhibits human anaplastic thyroid carcinoma tumor growth via p21WAF1/CIP1. *Oncogene* 25 2304–2317.
- Cossarizza A, Baccarani-Contri M, Kalashnikova G & Franceschi C** 1993 A new method for the cytofluorimetric analysis of mitochondrial membrane potential using the J-aggregate forming lipophilic cation 5,5',6,6'-tetrachloro-1,1',3,3' tetraethylbenzimidazolylcarbocyanine iodide (JC-1). *Biochem. Biophys. Res. Commun.* 197 40-45.
- Couturier C, Brouillet A, Couriaud C, Koumanov K, Bereziat G & Andreani M** 1999 Interleukin 1 $\beta$  induces type II-secreted phospholipase A2 gene in vascular smooth muscle cells by a nuclear factor  $\kappa$ B and peroxisome proliferator-activated receptor-mediated process. *J Biol Chem* 274 23085–23093.
- Debatin KM & Krammer PH** 2004 Death receptors in chemotherapy and cancer. *Oncogene* 23 2950–2966.
- Deng T, Shan S, Li PP, Shen ZF, Lu XP, Cheng J & Ning ZQ** 2006 Peroxisome proliferator-activated receptor- $\gamma$  transcriptionally up-regulates hormone-sensitive lipase via the involvement of specificity protein-1. *Endocrinology* 147 875–884.
- DiRenzo J, Soderstrom M & Kurokawa R** 1997 Peroxisome proliferator-activated receptors and retinoic acid receptors differentially control the interactions of retinoid X receptor heterodimers with ligands, coactivators, and corepressors. *Molecular and Cellular Biology* 17 2166–2176.
- Fagin JA, Matsuo K, Karmakar A, Chen DL, Tang SH & Koeffler HP** 1993 High prevalence of mutations of the p53 gene in poorly differentiated human thyroid carcinomas. *Journal of Clinical Investigations* 91 179–184.
- Fang Z, Fu Y, Liang Y, Li Z, Zhang W, Jin J, Yang Y & Zha X** 2007 Increased expression of integrin  $\beta$ 1 subunit enhances p21WAF1/Cip1 transcription through the Sp1 sites and p300-mediated histone acetylation in human hepatocellular carcinoma cells. *Journal of Cellular Biochemistry* 101 654–664.
- Forman BM, Tontonoz P, Chen T, Brun RP, Spiegelman BM & Evans RM** 1995 15-deoxy- $\Delta$  12,14-prostaglandin J2 is a ligand for the adipocyte determination factor PPAR $\gamma$ . *Cell* 83 803–812.
- Green DR.** 1998 Apoptotic pathways: the roads to ruin. *Cell* 94 695-698.
- Greene ME, Blumberg B, McBride OW, Yi HF, Kronquist K, Kwan K, Hsieh L, Greene G & Nimer SD** 1995 Isolation of the human peroxisome proliferator activated receptor  $\gamma$  cDNA: expression in hematopoietic cells and chromosomal mapping. *Gene* 4 281–299.

- Grommes C, Landreth GE & Heneka MT** 2004 Antineoplastic effects of peroxisome proliferator-activated receptor gamma agonists. *Lancet Oncol.* 5 419-429.
- Han S, Sidell N, Fisher BP & Roman J** 2004 Up-regulation of p21 gene expression by peroxisome proliferator-activated receptor gamma in human lung carcinoma cells. *Clinical Cancer Research* 10 1911–1919.
- Harper JW, Adami GR, Wei N, Keyomarsi K & Elledge SJ** 1993 The p21 Cdk-interacting protein Cip1 is a potent inhibitor of G1 cyclin-dependent kinases. *Cell* 75 805–816.
- Haupt S, Berger M, Goldberg Z & Haupt Y** 2003 Apoptosis- the p53 network. *J Cell Sci* 116 4077–4085.
- Hong J, Samudio I, Liu S, Abdelrahim M & Safe S** 2004 Peroxisome proliferator-activated receptor gamma-dependent activation of p21 in panc-28 pancreatic cancer cells involves Sp1 and Sp4 proteins. *Endocrinology* 145 5774–5785.
- Husmann M, Dragneva Y, Romahn E & Jehnichen P** 2000 Nuclear receptors modulate the interaction of Sp1 and GC-rich DNA via ternary complex formation. *Biochemical Journal* 352 763–772.
- Ikawa H, Kameda H, Kamitani H, Baek SJ, Nixon JB, His LC & Eling TE** 2001 Effect of PPAR activators on cytokine stimulated cyclooxygenase-2 expression in human colorectal carcinoma cells. *Exp Cell Res* 267 73–80.
- Kasibhatla S, Brunner T, Genestier L, Echeverri F, Mahboubi A & Green DR** 1998 DNA damaging agents induce expression of Fas ligand and subsequent apoptosis in T lymphocytes via the activation of NF-kappa B and AP-1. *Mol Cell* 4 543-551.
- Kersten S, Desvergne B & Wahali W** 2000 Roles of PPARs in health and disease. *Nature* 25 421-424.
- Kliwer SA, Lenhard JM, Willson TM, Patel I, Morris DC & Lehmann JM** 1995 A prostaglandin J2 metabolite binds peroxisome proliferator-activated receptor gamma and promotes adipocyte differentiation. *Cell* 83 813–819.
- Kliwer SA, Umesono K, Mangelsdorf DJ & Evans RM** 1992 Retinoid X receptor interacts with nuclear receptors in retinoic acid, thyroid hormone, and vitamin D3 signaling. *Nature* 355 446-449.
- Klopper JP, Hays WR, Sharma V, Baumbusch MA, Hershman JM & Haugen BR** 2004 Retinoid X receptor-gamma and peroxisome proliferator-activated receptor-gamma expression predicts thyroid carcinoma cell response to retinoid and thiazolidinedione treatment. *Molecular Cancer Therapeutics* 3 1011–1020.
- Kuboto T, Koshizuka K, Williamson IA, Asou H, Said JW, Holden S, Miyoshi I & Koeffler HP** 1998 Ligand of peroxisome proliferator-activated receptor gamma (rosiglitazone) has potent anti-tumor effects agonist human prostate cancer both in vitro and in vivo. *Cancer Research* 58 3344–3352.
- Lefebvre P, Chinetti G, Fruchart JC & Staels B** 2006 Sorting out the roles of PPARalpha in energy metabolism and vascular homeostasis. *Journal of Clinical Investigation* 116 571–580.
- Lehrke M & Lazar MA** 2005 The many faces of PPARgamma. *Cell* 123 993–999.

- Lemberger T, Desvergne B & Wahli W** 1996 Peroxisome proliferator-activated receptors: a nuclear receptor signaling pathway in lipid physiology. *Annual Review of Cell and Developmental Biology* 12 335–363.
- Li Y, Jenkins CW, Nichols MA & Xiong Y** 1994 Cell cycle expression and p53 regulation of cyclin-dependent kinase inhibitor p21. *Oncogene* 9 2261–2268.
- Liu G & Lozano G** 2005 p21 Stability: linking chaperones to a cell cycle checkpoint. *Cancer Cell* 7 113–114.
- Lowry OH, Rosebrough NJ & Randall RJ** 1951 Protein measurement with the Folin phenol reagent. *J Biol Chem.* 193 265-275.
- Maggiolini M, Donze O & Picard DA** 1999 A non-radioactive method for inexpensive quantitative RT-PCR. *Biol Chem* 380 695-697.
- Martelli ML, Iuliano R, Le Pera I, Sama` I, Monaco C, Cammarota S, Kroll T, Chiariotti L, SantoroM& Fusco A** 2002 Inhibitory effects of peroxisome proliferatoractivated receptor gamma on thyroid carcinoma cell growth. *Journal of Clinical Endocrinology and Metabolism* 87 4728–4735.
- McInerney EM, Rose DW & Flynn SE** 1998 Determinants of coactivator LXXLL motif specificity in nuclear receptor transcriptional activation. *Genes & Development* 12 3357–3368.
- Mo YY & Beck WT** 1999 DNA damage signals induction of fas ligand in tumor cells. *Mol Pharmacol* 55 216-222.
- Montague JW & Cidlowski JA** 1996 Cellular catabolism in apoptosis: DNA degradation and endonuclease activation. *Experientia* 52 957-962.
- Moon SK, Choi YH, Kim CH & Choi WS** 2006 p38MAPK mediates benzyl isothiocyanate-induced p21WAF1 expression in vascular smooth muscle cells via the regulation of Sp1. *Biochemical and Biophysical Research Communications* 350 662–668.
- Mosmann T** 1983 Rapid colorimetric assay for cellular growth and survival: application to proliferation and cytotoxicity assays. *J Immunol Methods* 65 55-63.
- Mueller E, Drori S, Aiyer A, Yie J, Sarraf P, Chen H, Hauser S, Rosen ED, Ge K, Roeder RG & Spiegelman BM** 2002 Genetic analysis of adipogenesis through peroxisome proliferator-activated receptor-gamma isoforms. *J Biol Chem* 277 41925–41930.
- Nagata S** 1997 Apoptosis by death factor. *Cell* 88 355-365.
- O'Brate A & Giannakakou P** 2003 The importance of p53 location: nuclear or cytoplasmic zip code? *Drug Resistance Update* 6 313–322.
- Ohta K, Endo T, Haraguchi K, Hershman JM & Onaya T** 2001 Ligands for peroxisome proliferator-activated receptor gamma inhibit growth and induce apoptosis of human papillary thyroid carcinoma cells. *Journal of Clinical Endocrinology and Metabolism* 86 2170–2177.
- Palmer CNA, Hsu MH, Griffin KJ & Johnson EF** 1995 Novel sequence determinants in peroxisome proliferators signalling. *Journal of Biological Chemistry* 270 16114–16121.
- Park JW, Jang MA, Lee YH, Passaniti A & Kwon TK** 2001 p53-independent elevation of p21 expression by PMA results from PKC-mediated mRNA stabilization. *Biochemical and Biophysical Research Communications* 280 244–248.

- Patel L, Pass I, Coxon P, Downes CP, Smith SA & Macphee CH** 2001 Tumor suppressor and anti-inflammatory actions of PPAR $\gamma$  agonist are mediated via upregulation of PTEN. *Curr Biol* 11 764–768.
- Pinaire JA & Reifel-Miller A** 2007 Therapeutic potential of retinoid x receptor modulators for the treatment of the metabolic syndrome. *PPAR Res.* 2007 94156.
- Qin C, Nguyen T, Stewart J, Samudio I, Burghardt R & Safe S** 2002 Estrogen up-regulation of p53 gene expression in MCF-7 breast cancer cells is mediated by calmodulin kinase IV-dependent activation of a nuclear factor- $\kappa$ B/CCAAT-binding transcription factor-1 complex. *Mol Endocrinol* 16 1793–1809.
- Rangwala SM & Lazar MA** 2004 Peroxisome proliferator-activated receptor gamma in diabetes and metabolism. *Trends Pharmacol Sci* 25 331–336.
- Sassa Y, Hata Y, Aiello LP, Taniguchi Y, Kohno K & Ishibashi T** 2004 Bifunctional properties of peroxisome proliferator-activated receptor gamma1 in KDR gene regulation mediated via interaction with both Sp1 and Sp3. *Diabetes* 53 1222–1229.
- Schuler M & Green DR** 2001 Mechanisms of p53-dependent apoptosis. *Biochem Soc Trans* 29 684–688.
- Sengupta S & Wasylyk B** 2004 Physiological and pathological consequences of the interactions of the p53 tumor suppressor with the glucocorticoid, androgen, and estrogen receptors. *Ann NY Acad Sci* 1024 54–71.
- Sertznig P, Seifert M, Tilgen W & Reichrath J** 2007 Present concepts and future outlook: function of peroxisome proliferator-activated receptors (PPARs) for pathogenesis, progression, and therapy of cancer. *Journal of Cellular Physiology* 212 1–12.
- Smiley ST, Reers M, Mottola-Hartshorn C, Lin M, Chen A, Smith TW, Steele GD & Chen LB** 1991 Intracellular heterogeneity in mitochondrial membrane potentials revealed by a J-aggregate forming lipophilic cation JC-1. *Proc. Natl. Acad. Sci. USA* 88 3671–3675.
- Staals B** 2005 Fluid retention mediated by renal PPARgamma. *Cell Metab* 2 77–78.
- Steller H** 1995 Mechanisms and genes of cellular suicide. *Science* 267 1445–1449.
- Sun YX, Wright HT & Janciasukiene S** 2002 Alpha1-Antichymotrypsin/Alzheimer's peptide A $\beta$  (1–42) complex perturbs lipid metabolism and activates transcription factors PPAR and NF $\kappa$ B in human neuroblastoma (Kelly) cells. *J Neurosci Res* 67 511–522.
- Tom S, Ranalli TA, Podust VN & Bambara RA** 2001 Regulatory roles of p21 and apurinic/apyrimidinic endonuclease 1 in base excision repair. *J Biol Chem* 276 48781–48789.
- Tvrđi'k D, Dundr P, Pový'sil C, Pytl'ík R & Plankova' M** 2006 Up-regulation of p21/WAF1 expression is mediated by Sp1/Sp3 transcription factors in TGF $\beta$ 1-arrested malignant B cells. *Medical Science Monitor* 12 227–234.
- Vousden KH & Lu X** 2002 Live or let die: the cell's response to p53. *Nature Reviews. Cancer* 2 594–604.
- Woods DB & Vousden KH** 2001 Regulation of p53 function. *Exp Cell Res* 264 56–66.

**Wu RC & Schonthal AH** 1997 Activation of p53-p21waf1 pathway in response to disruption of cell-matrix interactions. *Journal of Biological Chemistry* 272 29091–29098.

**Yu J & Zhang L** 2005 The transcriptional targets of p53 in apoptosis control. *Biochem Biophys Res Commun* 331 851–858.

**Yu J & Zhang L** 2005 The transcriptional targets of p53 in apoptosis control. *Biochem Biophys Res Commun* 331 851–858.

**Yuan CX, Ito M, Fondell JD, Fu ZY & Roeder RG** 1998 The TRAP220 component of a thyroid hormone receptor-associated protein (TRAP) coactivator complex interacts directly with nuclear receptors in a ligand-dependent fashion. *Proceedings of the National Academy of Sciences of the United States of America* 95 7939–7944.

**Zhang XK, Hoffmann B, Tran PBV, Graupner G & Pfahl M** 1992 Retinoid X receptor is an auxiliary protein for thyroid hormone and retinoic acid receptors. *Nature* 355 441–445.

## TITLE PAGE

**Combined low doses of PPAR $\gamma$  and RXR ligands trigger intrinsic apoptotic pathway in human breast cancer cells.**

<sup>1</sup>Daniela Bonofiglio, <sup>1</sup>Erika Cione, <sup>1</sup>Hongyan Qi, <sup>1</sup>Attilio Pingitore, <sup>1</sup>Mariarita Perri, <sup>1</sup>Stefania Catalano, <sup>2</sup>Maria Luisa Panno, <sup>1</sup>Giuseppe Genchi, <sup>3</sup>Suzanne AW Fuqua and <sup>2,4,5</sup>Sebastiano Andò

<sup>1</sup>Dept. Pharmaco-Biology, University of Calabria 87036 Arcavacata di Rende (Cosenza) Italy, <sup>2</sup>Dept. Cellular Biology, University of Calabria 87036 Arcavacata di Rende (Cosenza) Italy <sup>3</sup>Baylor College of Medicine, Lester and Sue Smith Breast Center and the Dept. of Medicine, One Baylor Plaza, Houston, TX 77030, USA

<sup>4</sup>Centro Sanitario, University of Calabria 87036 Arcavacata di Rende (Cosenza) Italy

<sup>5</sup>Faculty of Pharmacy, University of Calabria 87036 Arcavacata di Rende (Cosenza) Italy.

**Running title:** Low doses of PPAR $\gamma$  and RXR ligands in breast cancer cells

Corresponding Author: Prof. Sebastiano Andò, Faculty of Pharmacy, University of Calabria, 87036 Arcavacata - Rende (Cosenza), ITALY; Tel: +39 0984 496201; Fax +39 0984 496203;

E-mail: [sebastiano.ando@unical.it](mailto:sebastiano.ando@unical.it)

Footnotes: This work was supported by AIRC, MURST and Ex 60%.

Key words: PPAR $\gamma$ , RXR, apoptosis, caspase 9, breast cancer.

## **Abstract**

Ligand activation of PPAR $\gamma$  and RXR induces antitumoral effects in different types of cancer. In our study, we evaluated the ability of combined PPAR $\gamma$  ligand Rosiglitazone (BRL) and RXR ligand 9-*cis*-retinoic acid (9RA), both at nanomolar levels, to promote antiproliferative effects in breast cancer cells. Low doses of both compounds only in combination exert a strong inhibition of cell viability in MCF-7, MCF-7TR1, SKBR-3 and T-47D breast cancer cells, while MCF-10 normal breast epithelial cells are completely unaffected. In MCF-7 cells combined ligands are able to up-regulate mRNA and protein levels of tumor suppressor gene p53 and its effector p21<sup>WAF1/Cip1</sup>. Functional experiments indicated that NF $\kappa$ B site in p53 promoter is required for the transcriptional response to BRL plus 9RA. Next, focusing on intrinsic apoptotic process, we observed that MCF-7 cells displayed the ordained sequence of events: a disruption of mitochondrial membrane potential, a release of cytochrome *c*, a strong caspase 9 activation and, finally, a DNA fragmentation. Given the ability of an expression vector for p53 antisense to abrogate the biological effect of both ligands, an involvement of p53 in PPAR $\gamma$ /RXR-dependent activity may be argued in all human breast malignant cell lines tested. Taken together, our results address that multidrug regimens consisting of combination with PPAR $\gamma$  and RXR ligands may provide a therapeutic advantage in breast cancer treatment.

## INTRODUCTION

Breast cancer is the leading cause of death among women in the world. The principal effective endocrine therapy for advanced treatment on this type of cancer is anti-estrogens but therapeutic choices are limited for ER $\alpha$ -negative tumors, which are often aggressive. Besides, the development of cancer cells that are resistant to chemotherapeutic agents is a major clinical obstacle to the successful treatment of breast cancer which provides the strong stimulus for exploring new approaches *in vitro*. Using ligands of nuclear hormone receptors (NHRs) to inhibit tumor growth and progression is a novel strategy for cancer therapy. An example of this is the treatment of acute promyelocytic leukemia (APL) using all-*trans*-retinoic-acid (ATRA) the specific ligand for retinoic acid receptors (RARs) (1-3). A further paradigm for the use of retinoids in cancer therapy is for early lesions of head and neck cancer (4) and squamous cell carcinoma of the cervix (5).

RAR, retinoid X receptor (RXR) and peroxisome proliferator receptor  $\gamma$  (PPAR $\gamma$ ) are ligand-activated transcription factors belonging to the NHRs super-family having the capability to modulate gene networks involved in controlling growth and cellular differentiation (6). Particularly, heterodimerization of PPAR $\gamma$  with RXR by own ligands greatly enhances DNA binding to a direct repeated consensus sequence AGGTCA and transcriptional activation (7). Previous data have shown that PPAR $\gamma$ , poorly expressed in normal breast epithelial cells (8), is present at higher levels in breast cancer cells (9) and its synthetic ligands, such as thiazolidinediones (TZDs) were discovered to induce growth arrest and differentiation in breast carcinoma cells *in vitro* and in animal models (10-11). Recently, in human cultured breast cancer cells the TZD Rosiglitazone (BRL) promotes antiproliferative effects and activates different molecular pathways leading to distinct apoptotic processes (12-14).

Apoptosis, the genetically controlled and programmed death leading to cellular self-elimination, can be initiated by two major routes: the intrinsic and extrinsic pathways. The intrinsic pathway is triggered in response to a variety of apoptotic stimuli that produce damage within the cell, including anticancer agents, oxidative damage and UV irradiation, and is mediated through the mitochondria. The extrinsic pathway is activated by extracellular ligands able to induce oligomerization of death



receptors, such as Fas, followed by the formation of the death-inducing signaling complex, after which the caspases cascade can be activated.

Previous data showed that the combination of PPAR $\gamma$  ligand with either ATRA or 9-*cis*-retinoic acid (9RA) can induce apoptosis in some breast cancer cells (15). Furthermore, Elstner et al. demonstrated that the combination of these drugs at micromolar concentrations reduced tumor mass without any toxic effects in mice (8). However, in humans PPAR $\gamma$  agonists at high doses exert many side effects including weight gain due to increased adiposity, edema, hemodilution, and plasma-volume expansion, which preclude their clinical application in patients with heart failure (16-18). The undesirable effects of RXR-specific ligands on hypertriglyceridemia and suppression of the thyroid hormone axis have been also reported (19). Thus, in the present study we have elucidated the molecular mechanism by which combined treatment with BRL and 9RA at nanomolar doses triggers apoptotic events in breast cancer cells, suggesting potential therapeutical uses for these compounds.

## **MATERIALS AND METHODS**

**Reagents** - BRL49653 (BRL) was from Alexis (San Diego, CA USA), the irreversible PPAR $\gamma$ -antagonist GW9662 (GW) and 9-*cis*-retinoic acid (9RA) were purchased from Sigma (Milan, Italy).

**Plasmids** - The p53 promoter-luciferase plasmids, kindly provided by Dr. Stephen H. Safe (Texas A&M University, College Station, TX, USA), were generated from the human p53 gene promoter as follows: p53-1 (containing the -1800 to +12 region), p53-6 (containing the -106 to +12 region), p53-13 (containing the -106 to -40 region) and p53-14 (containing the -106 to -49 region) (20). As an internal transfection control, we cotransfected the plasmid pRL-CMV (Promega Corp., Milan, Italy) that expresses Renilla luciferase enzymatically distinguishable from firefly luciferase by the strong cytomegalovirus enhancer promoter. The pGL3 vector containing three copies of a PPRE sequence upstream of the minimal thymidine kinase promoter ligated to a luciferase reporter gene (3XPPRE-TK-pGL3) was a gift from Dr. R.

Evans (The Salk Institute, San Diego, CA, USA). The p53 antisense plasmid (AS/p53) was kindly provided from Dr. Moshe Oren (Weizmann Institute of Science, Rehovot, Israel).

**Cell Cultures** - Wild-type human breast cancer MCF-7 cells were grown in DMEM-F12 plus glutamax containing 5% new-born calf serum (Invitrogen, Milan, Italy) and 1 mg/ml penicillin-streptomycin. MCF-7 tamoxifen resistant (MCF-7TR1) breast cancer cells were generated in Dr. Fuqua's laboratory similar to that described by Herman (21) maintaining cells in MEM with 10% foetal bovine serum (FBS) (Invitrogen), 6 ng/ml insulin, penicillin (100 units/ml), streptomycin (100 µg/ml) and adding 4-hydroxytamoxifen in 10-fold increasing concentrations every weeks (from  $10^{-9}$  to  $10^{-6}$  final). Cells were thereafter routinely maintained with 1µM 4-hydroxytamoxifen. SKBR-3 breast cancer cells were grown in DMEM without red phenol, plus glutamax containing 10% FBS and 1 mg/ml penicillin-streptomycin. T-47D breast cancer cells were grown in RPMI 1640 with glutamax containing 10% FBS, 1mM sodium pyruvate, 10mM HEPES, 2,5g/L glucose, 0,2 U/ml insulin and 1 mg/ml penicillin-streptomycin. MCF-10 normal breast epithelial cells were grown in DMEM-F12 plus glutamax containing 5% horse serum (Sigma), 1 mg/ml penicillin-streptomycin, 0,5 µg/ml hydrocortisone and 10 µg/ml insulin.

**MTT Assay** - Cell viability was determined with the MTT assay (22). Cells ( $2 \times 10^5$  cells/ml) were grown in 6 well plates and exposed to BRL 100nM, 9RA 50nM alone or in combination for 48 h in serum free medium (SFM). 100 µl of MTT (5mg/ml) were added to each well, and the plates were incubated for 4 h at 37 °C. Then, 1 ml 0.04N HCl in isopropanol was added to solubilise the cells. The absorbance was measured with the Ultrospec 2100 Pro-spectrophotometer (Amersham-Biosciences, Milan, Italy) at a test wavelength of 570 nm with a reference wavelength of 690 nm. The optical density (O.D.) was calculated as the difference between the two absorbencies.

**Immunoblotting** - Cells were grown in 10cm dishes to 70–80% confluence and exposed to treatments in SFM as indicated. Cells were then harvested in cold phosphate-buffered saline (PBS) and resuspended in lysis buffer containing 20mM HEPES (pH 8), 0.1mM EGTA, 5mM MgCl<sub>2</sub>, 0.5M NaCl, 20% glycerol, 1% Triton,

and inhibitors (0.1mM sodium orthovanadate, 1% phenylmethylsulfonylfluoride (PMSF), 20mg/ml aprotinin). Protein concentration was determined by Bio-Rad Protein Assay (Bio-Rad Laboratories, Hercules, CA USA). A 40µg portion of protein lysates was used for Western blotting (WB), resolved on a 10% SDS-polyacrylamide gel, transferred to a nitrocellulose membrane, and probed with an antibody directed against the p53, p21<sup>WAF1/Cip1</sup> (Santa Cruz Biotechnology, CA USA). As internal control, all membranes were subsequently stripped (0.2 M glycine, pH 2.6, for 30 min at room temperature) of the first antibody and reprobbed with anti-GAPDH antibody (Santa Cruz Biotechnology). The antigen-antibody complex was detected by incubation of the membranes for 1 h at room temperature with peroxidase-coupled goat antimouse or antirabbit IgG and revealed using the enhanced chemiluminescence system (Amersham Pharmacia, Buckinghamshire UK). Blots were then exposed to film (Kodak film, Sigma). The intensity of bands representing relevant proteins was measured by Scion Image laser densitometry scanning program.

**RT-PCR Assay** - MCF-7 cells were grown in 10cm dishes to 70–80% confluence and exposed to treatments in SFM as indicated. Total cellular RNA was extracted using TRIZOL reagent (Invitrogen) as suggested by the manufacturer. The purity and integrity were checked spectroscopically and by gel electrophoresis before carrying out the analytical procedures. Two micrograms of total RNA were reverse transcribed in a final volume of 20 µl using a RETROscript kit as suggested by the manufacturer (Promega). The cDNAs obtained were amplified by PCR using the following primers: 5'-GTGGAAGGAAATTTGCGTGT-3' (p53 forward) and 5'-CCAGTGTGATGATGGTGAGG-3' (p53 reverse), 5'-GCTTCATGCCAGCTACTTCC-3' (p21 forward) and 5'-CTGTGCTCACTTCAGGGTCA-3' (p21 reverse), 5'-CTCAACATCTCCCCCTTCTC-3' (36B4 forward) and 5'-CAAATCCCATATCCTCGTCC-3' (36B4 reverse) to yield, respectively, products of 190 bp with 18 cycles, 270 bp with 18 cycles, and 408 bp with 12 cycles. To check for the presence of DNA contamination, a reverse transcription PCR was performed on 2 µg of total RNA without Monoley murine leukemia virus reverse transcriptase (the negative control). The results obtained as optical density arbitrary values were transformed to percentage of the control taking the samples from untreated cells as 100%.

**Transfection Assay** - MCF-7 cells were transferred into 24 well plates with 500 $\mu$ l of regular growth medium/well the day before transfection. The medium was replaced with SFM on the day of transfection, which was performed using Fugene 6 reagent as recommended by the manufacturer (Roche Diagnostics, Mannheim, Germany) with a mixture containing 0.5 $\mu$ g of promoter-luc or reporter-luc plasmid and 5ng of pRL-CMV. After transfection for 24 h, treatments were added in SFM as indicated, and cells were incubated for an additional 24 h. Firefly and Renilla luciferase activities were measured using the Dual Luciferase Kit (Promega). The firefly luciferase values of each sample were normalized by Renilla luciferase activity, and data were reported as Relative Light Units.

MCF-7 cells plated into 10cm dishes were transfected with 5 $\mu$ g of AS/p53 using Fugene 6 reagent as recommended by the manufacturer (Roche Diagnostics). The activity of AS/p53 was verified using Western blot to detect changes in p53 protein levels. Empty vector was used to ensure that DNA concentrations were constant in each transfection.

**EMSA** - Nuclear extracts from MCF-7 cells were prepared as previously described (23). Briefly, MCF-7 cells plated into 10cm dishes were grown to 70–80% confluence, shifted to SFM for 24 h, and then treated with 100nM BRL, 50nM 9RA alone and in combination for 6 h. Thereafter, cells were scraped into 1.5ml of cold PBS, pelleted for 10 sec and resuspended in 400 $\mu$ l cold buffer A (10mM HEPES-KOH, pH 7.9, at 4 °C, 1.5mM MgCl<sub>2</sub>, 10mM KCl, 0.5mM dithiothreitol, 0.2mM PMSF, 1mM leupeptin) by flicking the tube. Cells were allowed to swell on ice for 10 min and then vortexed for 10 sec. Samples were then centrifuged for 10 sec and the supernatant fraction was discarded. The pellet was resuspended in 50 $\mu$ l of cold Buffer B (20mM HEPES-KOH, pH 7.9; 25% glycerol; 1.5mM MgCl<sub>2</sub>; 420mM NaCl; 0.2mM EDTA; 0.5mM dithiothreitol; 0.2mM PMSF; 1mM leupeptin) and incubated in ice for 20 min for high-salt extraction. Cellular debris was removed by centrifugation for 2 min at 4 °C, and the supernatant fraction (containing DNA-binding proteins) was stored at -70 °C. The probe was generated by annealing single-stranded oligonucleotides and labeled with [<sup>32</sup>P]ATP (Amersham Pharmacia) and T4 polynucleotide kinase (Promega) and then purified using Sephadex G50 spin columns (Amersham Pharmacia). The DNA sequence of the NF $\kappa$ B located within p53 promoter as probe is 5'-AGT TGA GGG GAC TTT CCC AGG C-3' (Sigma

Genosys, Cambridge, UK). The protein-binding reactions were carried out in 20µl of buffer [20mM HEPES (pH 8), 1mM EDTA, 50mM KCl, 10mM dithiothreitol, 10% glycerol, 1mg/ml BSA, 50µg/ml polydeoxyinosinic deoxycytidylic acid] with 50,000 cpm of labeled probe, 20µg of MCF7 nuclear protein, and 5µg of polydeoxyinosinic deoxycytidylic acid. The mixtures were incubated at room temperature for 20 min in the presence or absence of unlabeled competitor oligonucleotides. For the experiments involving anti-PPAR $\gamma$  and anti-RXR $\alpha$  antibodies (Santa Cruz Biotechnology), the reaction mixture was incubated with these antibodies at 4 °C for 30 min before addition of labeled probe. The entire reaction mixture was electrophoresed through a 6% polyacrylamide gel in 0.25X Tris borate-EDTA for 3 h at 150 V. Gel was dried and subjected to autoradiography at -70 °C.

**ChIP Assay** - MCF-7 cells were grown in 10cm dishes to 50–60% confluence, shifted to SFM for 24 h, and then treated for 1 h as indicated. Thereafter, cells were washed twice with PBS and cross-linked with 1% formaldehyde at 37 °C for 10 min. Next, cells were washed twice with PBS at 4 °C, collected and resuspended in 200µl of lysis buffer (1% SDS; 10mM EDTA; 50 mM Tris-HCl, pH 8.1), and left on ice for 10 min. Then, cells were sonicated four times for 10 sec at 30% of maximal power (Vibra Cell 500 W; Sonics and Materials, Inc., Newtown, CT) and collected by centrifugation at 4 °C for 10 min at 14,000 rpm. The supernatants were diluted in 1.3 ml of immunoprecipitation buffer (0.01% SDS; 1.1% Triton X-100; 1.2mM EDTA; 16.7mM Tris-HCl, pH 8.1; 16.7mM NaCl) followed by immunoclearing with 60µl of sonicated salmon sperm DNA/protein A agarose (DBA Srl, Milan, Italy) for 1 h at 4 °C. The precleared chromatin was immunoprecipitated with anti-PPAR $\gamma$ , anti-RXR $\alpha$  or anti-RNA Pol II antibodies (Santa Cruz Biotechnology). At this point, 60µl salmon sperm DNA/protein A agarose was added, and precipitation was further continued for 2 h at 4 °C. After pelleting, precipitates were washed sequentially for 5 min with the following buffers: Wash A [0.1% SDS, 1% Triton X-100, 2mM EDTA, 20mM Tris-HCl (pH 8.1), 150mM NaCl], Wash B [0.1% SDS, 1% Triton X-100, 2mM EDTA, 20mM Tris-HCl (pH 8.1), 500mM NaCl], and Wash C [0.25M LiCl, 1% NP-40, 1% sodium deoxycholate, 1mM EDTA, 10mM Tris-HCl (pH 8.1)], and then twice with TE buffer (10mM Tris, 1mM EDTA). The immunocomplexes were eluted with elution buffer (1% SDS, 0.1 M NaHCO<sub>3</sub>). The eluates were reverse cross-linked by heating at 65 °C and digested with proteinase K (0.5mg/ml) at 45 °C

for 1 h. DNA was obtained by phenol-chloroform-isoamyl alcohol extraction. Two microliters of 10mg/ml yeast tRNA (Sigma) were added to each sample, and DNA was precipitated with 95% ethanol for 24 h at -20 °C and then washed with 70% ethanol and resuspended in 20µl of TE buffer. A 5µl volume of each sample was used for PCR with primers flanking a sequence present in the p53 promoter: 5'-CTGAGAGCAAACGCAAAAG-3' (forward) and 5'-CAGCCCGAACGCAAAGTGTC-3' (reverse) containing the κB site from -254 to -42 region. The PCR conditions for the p53 promoter fragments were, 45 sec at 94 °C, 40 sec at 57 °C, 90 sec at 72 °C. The amplification products obtained in 30 cycles were analyzed in a 2% agarose gel and visualized by ethidium bromide staining. The negative control was provided by PCR amplification without a DNA sample. The specificity of reactions was ensured using normal mouse and rabbit IgG (Santa Cruz Biotechnology).

**JC-1 Mitochondrial Membrane Potential Detection Assay** - The loss of mitochondrial membrane potential was monitored with the dye 5,5',6,6'-tetra-chloro-1,1',3,3'-tetraethylbenzimidazolyl-carbocyanine iodide (JC-1) (Biotium, Hayward, USA). In healthy cells, the dye stains the mitochondria bright red. The negative charge established by the intact mitochondrial membrane potential allows the lipophilic dye, bearing a delocalized positive charge, to enter the mitochondrial matrix where it aggregates and gives red fluorescence. In apoptotic cells, the mitochondrial membrane potential collapses, and the JC-1 cannot accumulate within the mitochondria, it remains in the cytoplasm in a green fluorescent monomeric form (24). MCF-7 cells were grown in 10cm dishes and treated with 100 nM BRL and/or 50 nM 9RA for 48 hours, then cells were trypsinized, washed in ice-cold PBS, and incubated with 10mM JC-1 at 37 °C in a 5% CO<sub>2</sub> incubator for 20 min in darkness. Subsequently, cells were washed twice with PBS and analyzed by fluorescence microscopy. The red form has absorption/emission maxima of 585/590 nm. The green monomeric form has absorption/ emission maxima of 510/527 nm. Both healthy and apoptotic cells can be visualized by fluorescence microscopy using a wide band-pass filter suitable for detection of fluorescein and rhodamine emission spectra.

**Cytochrome C Detection** - Cytochrome C was detected by western blotting in mitochondrial and cytoplasmic fractions. Cells were harvested by centrifugation at

2,500 rpm for 10 min at 4 °C. The pellets were suspended in 36µl RIPA buffer plus 10µg/ml aprotinin, 50mM PMSF and 50mM sodium orthovanadate and then 4µl of 0.1% digitonine were added. Cells were incubated for 15 min at 4 °C and centrifuged at 12,000 rpm for 30 min at 4 °C. The resulting mitochondrial pellet was resuspended in 3% Triton X-100, 20mM Na<sub>2</sub>SO<sub>4</sub>, 10mM PIPES and 1mM EDTA, pH 7.2, and centrifuged at 12,000 rpm for 10 min at 4 °C. Proteins of the mitochondrial and cytosolic fractions were determined by Bio-Rad Protein Assay (Bio-Rad Laboratories). Equal amounts of protein (40 µg) were resolved by 15% SDS-PAGE and electrotransferred to nitrocellulose membranes and probed with an antibody directed against the cytochrome *C* (Santa Cruz Biotechnology). Then, membranes were subjected to the same procedures described for immunoblotting.

**Flow Cytometry Assay** - MCF-7 cells ( $1 \times 10^6$  cells/well) were grown in 6 well plates and shifted to SFM for 24 h before adding treatments for 48 h. Thereafter, cells were trypsinized, centrifuged at 3,000 rpm for 3 min, washed with PBS. Addition of 0.5µl of FITC antibodies anti-caspase 9 and anti-caspase 8 (Calbiochem, Milan, Italy) in all samples was performed and then incubated for 45 min in at 37 °C. Cells were centrifuged at 3,000 rpm for 5 min, the pellets were washed with 300µl of wash buffer and centrifuged. The last passage was repeated twice, the supernatant removed, and cells dissolved in 300µl of wash buffer. Finally, cells were analyzed with the FACScan (Becton Dickinson and Co., Franklin Lakes, NJ).

**DNA Fragmentation** - DNA fragmentation was determined by gel electrophoresis. MCF-7 cells were grown in 10cm dishes to 70% confluence and exposed to treatments. After 56 h cells were collected and washed with PBS and pelleted at 1,800 rpm for 5 min. The samples were resuspended in 0.5ml of extraction buffer (50mM Tris-HCl, pH 8; 10mM EDTA, 0.5% SDS) for 20 min in rotation at 4 °C. DNA was extracted with phenol-chloroform three times and once with chloroform. The aqueous phase was used to precipitate nucleic acids with 0.1 volumes of 3M sodium acetate and 2.5 volumes cold ethanol overnight at -20 °C. The DNA pellet was resuspended in 15µl of H<sub>2</sub>O treated with RNase A for 30 min at 37 °C. The absorbance of the DNA solution at 260 and 280 nm was determined by spectrophotometry. The extracted DNA (40µg/lane) was subjected to electrophoresis on 1.5% agarose gels. The gels were stained with ethidium bromide and then photographed.

**Statistical Analysis** - Statistical analysis was performed using ANOVA followed by Newman-Keuls testing to determine differences in means.  $P < 0.05$  was considered as statistically significant.

## RESULTS

### **Nanomolar concentrations of the combined BRL and 9RA treatment affect cell viability in breast cancer cells.**

Previous studies demonstrated that micromolar doses of PPAR $\gamma$  ligand BRL and RXR ligand 9RA exert antiproliferative effects on breast cancer cells (13, 15, 25-26). Thus, to investigate whether low doses of combined agents are able to inhibit cell growth, we first assessed the effects of BRL 100 nM and 9RA 50 nM on normal and malignant breast cell lines. We observed that treatment with BRL does not elicit any significant effect on cell viability in all breast cell lines tested, while 9RA reduces cell vitality only in T47-D cells (Table 1). Notably, in the presence of both ligands cell viability is strongly reduced in all breast cancer cells: MCF-7, its variant MCF-7TR1, SKBR-3 and T-47D, while MCF-10 normal breast epithelial cells are completely unaffected (Table 1).

### **BRL and 9RA upregulate p53 and p21<sup>WAF1/Cip1</sup> expression in MCF-7 cells**

Our recent work demonstrated that micromolar doses of BRL activate PPAR $\gamma$  which in turn triggers apoptotic events through an upregulation of p53 expression (12). On the basis of these results, we aim to evaluate the ability of nanomolar doses of BRL and 9RA alone or in combination to modulate p53 expression along with its natural target gene p21<sup>WAF1/Cip1</sup> in MCF-7 cells. A significant increase in p53 and p21<sup>WAF1/Cip1</sup> content was observed by WB only upon combined treatment after 24 and 36 h (Fig. 1A). Furthermore, we showed an upregulation of p53 and p21<sup>WAF1/Cip1</sup> mRNA levels induced by BRL plus 9RA after 12 and 24 h (Fig. 1B).

### **Low doses of PPAR $\gamma$ and RXR ligands transactivate p53 gene promoter**

To investigate whether low doses of BRL and 9RA are able to transactivate the p53 promoter gene, we transiently transfected MCF-7 cells with a luciferase reporter construct (named p53-1) containing the upstream region of the p53 gene spanning



from -1800 to +12 (Fig. 2A). Treatment for 24 h with BRL 100 nM or 9RA 50 nM did not induce luciferase expression, while an increase in the transactivation of p53-1 promoter was observed in the presence of both ligands (Fig. 2B). To identify the region within the p53 promoter responsible for its transactivation, we used deleted constructs expressing different binding sites such as CTF-1, nuclear factor-Y (NF-Y), NF $\kappa$ B and GC sites (Fig. 2A). In transfection experiments performed using the mutants p53-6 and p53-13 encoding the regions from -106 to +12 and from -106 to -40, respectively, the responsiveness to BRL plus 9RA was still observed (Fig. 2B). In contrast, using deleted construct in NF $\kappa$ B domain (p53-14) encoding the sequence from -106 to -49, the transactivation of p53 by both ligands was absent (Fig. 2B), suggesting that NF $\kappa$ B site is required for p53 transcriptional activity.

#### **Heterodimer PPAR $\gamma$ /RXR $\alpha$ binds to NF $\kappa$ B sequence in EMSA and in ChIP Assay**

To gain further insight into the involvement of NF $\kappa$ B site in the p53 transcriptional response to BRL plus 9RA, we performed EMSA experiments using synthetic oligodeoxyribonucleotides corresponding to the NF $\kappa$ B sequence within p53 promoter. As shown in Figure 3A, we evidenced the formation of a specific DNA binding complex in nuclear extracts from MCF-7 cells (lane 1), since it was abrogated by 100-fold molar excess of unlabeled probe (lane 2). BRL treatment induced a slight increase in the specific band (lane 3), while no changes were observed upon 9RA exposure (lane 4). The combined treatment increased the DNA binding complex (lane 5), which was immunodepleted and supershifted using anti-PPAR $\gamma$  (lane 6) or anti-RXR $\alpha$  (lane 7) antibodies. These data indicate that heterodimer PPAR $\gamma$ /RXR $\alpha$  binds to NF $\kappa$ B site located in the promoter of p53 *in vitro*.

Next, the interaction of both nuclear receptors with the p53 promoter was further elucidated by ChIP assays. Using anti-PPAR $\gamma$  and anti-RXR $\alpha$  antibodies, protein-chromatin complexes were immunoprecipitated from MCF-7 cells treated with BRL 100 nM and 9RA 50 nM. PCR was used to determine the recruitment of PPAR $\gamma$  and RXR $\alpha$  to the p53 region containing the NF $\kappa$ B site. The results indicate that either PPAR $\gamma$  or RXR $\alpha$  recruitment was increased upon BRL plus 9RA exposure (Fig. 3B). In same condition, an augmented RNA-Pol II recruitment was obtained by immunoprecipitating cells with an anti-RNA-Pol II antibody, indicating

that a positive regulation of p53 transcription activity was induced by combined treatment (Fig. 3B).

#### **BRL and 9RA induce mitochondrial membrane potential disruption and release of cytochrome C from mitochondria into the cytosol in MCF-7 cells**

It is well known that the straightforward role of p53 signaling in the intrinsic apoptotic cascades involves a mitochondria-dependent process, which results in cytochrome C release and activation of caspase-9. Since disruption of mitochondrial integrity is one of the early events leading to apoptosis, we want to assess whether BRL plus 9RA affect the function of mitochondria by analyzing membrane potential with a mitochondria fluorescent dye JC-1 (24, 27). As shown in Fig. 4A, in non-apoptotic cells (control) the intact mitochondrial membrane potential allows the accumulation of lipophilic dye in aggregated form in mitochondria which display red fluorescence. In MCF-7 cells, treatment with BRL 100 nM or 9RA 50 nM did not change the red fluorescence (data not shown), whereas cells treated with both ligands stain green fluorescent, since JC-1 cannot accumulate within the mitochondria and it remains as a monomeric form in the cytoplasm (Fig. 4A). Concomitantly, cytochrome C release from mitochondria into the cytosol, a critical step in the apoptotic cascade, was demonstrated after combined treatment (Fig. 4B).

#### **Caspase-9 cleavage and DNA fragmentation induced by BRL plus 9RA in MCF-7 cells**

BRL and 9RA at nanomolar concentration separately did not induce any effects on caspase-9, which on the contrary appears activated in the presence of both compounds (Table 2A). No effects were elicited by either the combined or the separate treatment on caspase-8 activation, a marker of extrinsic apoptotic pathway (Table 2B). Since internucleosomal DNA degradation is considered a diagnostic hallmark of cells undergoing apoptosis, we studied DNA fragmentation under BRL plus 9RA treatment in MCF-7 cells, evidencing that the induced apoptosis was prevented by either the specific antagonist of PPAR $\gamma$  GW9662 (GW) or in the presence of AS/p53, which is able to abolish p53 expression (Fig. 5A).

To also test the ability of low doses of both BRL and 9RA to induce transcriptional activity of PPAR $\gamma$ , we transiently transfected PPRE reporter gene in MCF-7 cells and we observed an enhanced luciferase activity, which was reversed by

GW treatment (Fig. 1 Supplemental data). These data are in agreement with previous observations demonstrating that PPAR $\gamma$ /RXR heterodimerization greatly enhances DNA binding and transcriptional activation (28-29).

Finally, we examined in three additional human breast malignant cell lines: MCF-7 TR1, SKBR-3 and T-47D the capability of low doses of PPAR $\gamma$  and RXR ligands to trigger apoptosis. DNA fragmentation assay showed that only in the presence of combined treatment cells underwent apoptosis in a p53-mediated manner (Fig. 5B), implicating a general mechanism in breast carcinoma.

## DISCUSSION

The key finding of this study is that the combined treatment with low doses of PPAR $\gamma$  and RXR ligands can selectively affect breast cancer cells through cell growth inhibition and apoptosis.

The ability of PPAR $\gamma$  ligands to induce differentiation and apoptosis in a variety of cancer cell types, as in human lung (30), colon (31) and breast (10) has been exploited in experimental cancer therapies (32). Besides, PPAR $\gamma$  agonists administration in liposarcoma patients resulted in histologic and biochemical differentiation markers *in vivo* (33). However, a pilot study of short-term therapy with PPAR $\gamma$  ligand Rosiglitazone in early-stage breast cancer patients does not elicit significant effects on tumor cell proliferation, although the changes observed in PPAR $\gamma$  expression may be relevant to breast cancer progression (34). On the other hand, the natural ligand for RXR 9RA (35) has been effective *in vitro* against many types of cancer, including breast tumor (36-40). Recently, RXR-selective ligands were discovered to inhibit proliferation of ATRA-resistant breast cancer cells *in vitro* and caused regression of the disease in animal models (41). The additive antitumoral effects of PPAR $\gamma$  and RXR agonists, both at elevated doses, have been shown in human breast cancer cells (15, 42 and references therein). However, it should be take into account that high doses of both ligands have in humans remarkable side effects like weight gain and plasma volume expansion for PPAR $\gamma$  ligands (16-18) and hypertriglyceridemia and suppression of the thyroid hormone axis for RXR ligands (19).

In the present study we demonstrated that nanomolar concentrations of BRL and 9RA in combination do no induce noticeable influences in cell vitality on normal

breast epithelial cells, while they exert significant antiproliferative effects on breast cancer cells. The molecular mechanism underlying these effects has been elucidated in MCF-7 cells in which an upregulation of tumor suppressor gene p53 has been evidenced. Functional assays with deleted constructs of the p53 promoter showed that the NF $\kappa$ B site is required for the transcriptional response to BRL plus 9RA treatment. NF $\kappa$ B was shown to physically interact with PPAR $\gamma$  (43), which in some circumstances binds to DNA cooperatively with NF $\kappa$ B (44-46). It has been previously reported that micromolar doses of both PPAR $\gamma$  and RXR agonists synergized to generate an increased level of NF $\kappa$ B-DNA binding able to trigger apoptosis in Pre-B cells (47). Our EMSA and CHIP assay demonstrated that these agents at nanomolar concentration only when in combination appeared to be effective in the binding and in the recruitment of either PPAR $\gamma$  or RXR $\alpha$  on the NF $\kappa$ B site located in the p53 promoter sequence. BRL plus 9RA at the doses tested also increase the recruitment of RNA-Pol II to p53 promoter gene addressing a positive transcriptional regulation able to produce a consecutive series of events featuring apoptotic pathway. It is well known that the changes in mitochondrial membrane permeability, an important step in the induction of cellular apoptosis, is concomitant with collapse of the electrochemical gradient across the mitochondrial membrane through the formation of pores in the mitochondria leading to the release of cytochrome *C* into the cytoplasm, and subsequently with cleavage of procaspase-9. This cascade of events, featuring the mitochondria-mediated death pathway, were detected in BRL plus 9RA-treated MCF-7 cells. Besides, the activation of caspase 9, in the presence of no changes in the biological activity of caspase 8, addresses how in our experimental model only the intrinsic apoptotic pathway is the effector of the combined treatment with the two ligands. The crucial role of p53 gene in mediating apoptosis raised by the evidence that the described apoptotic cascade was abrogated in the presence of AS/p53 in all breast cancer cell lines tested, including tamoxifen resistant breast cancer cells, where other authors evidenced EGFR, IGF-1R and c-Src signaling constitutively activated and responsible for a more aggressive phenotype consistent with an increased motility and invasiveness (48-50). This gives emphasis to the potential use of the combined therapy with low doses of both BRL and 9RA as novel therapeutic tool particularly for breast cancer patients who developed resistance to antiestrogen therapy.

## REFERENCES

1. Warrell Jr RP, Frankel SR, Miller Jr WH, Scheinberg DA, Itri LM, Hittelman WN, Vyas R, Andreeff M, Tafuri A, Jakubowski A: Differentiation therapy of acute promyelocytic leukemia with tretinoin (all-trans-retinoic acid). *N Engl J Med* 1991, 324:1385–1393
2. Chen ZX, Xue YQ, Zhang R, Tao RF, Xia XM, Li C, Wang W, Zu WY, Yao XZ, Ling BJ: A clinical and experimental study on all-*trans* retinoic acid-treated acute promyelocytic leukemia patients. *Blood* 1991, 78:1413–1419
3. Degos L, Chomienne C, Daniel MT, Berger R, Dombret H, Fenaux P, Castaigne S: Treatment of first relapse of acute promyelocytic leukemia with all-*trans* retinoic acid. *Lancet* 1990, 336:1440–1441
4. Hong WK, Lippman SM, Itri LM, Karp DD, Lee JS, Byers RM, Schantz SP, Kramer AM, Lotan R, Peters LJ: Prevention of second primary tumors with isotretinoin in squamous-cell carcinoma of the head and neck. *N Engl J Med* 1990, 323:795–801
5. Lippman SM, Kavanagh JJ, Paredes-Espinoza M, Delgadillo-Madrueno F, Paredes-Casillas P, Hong WK, Holdener E, Krakoff I: 13-cis-retinoic acid plus interferon alpha-2a: highly active systemic therapy for squamous cell carcinoma of the cervix. *J Natl Cancer Inst* 1992, 84:241-245
6. Mangelsdorf DJ, Thummel C, Beato M, Herrlich P, Schütz G, Umesono K, Blumberg B, Kastner P, Mark M, Chambon P, Evans RM: The nuclear receptor superfamily: the second decade. *Cell* 1995, 83:835-839
7. Heyman RA, Mangelsdorf DJ, Dyck JA, Stein RB, Eichele G, Evans RM, Thaller C: 9-cis retinoic acid is a high affinity ligand for the retinoid X receptor. *Cell* 1992, 68:397–406
8. Elstner E, Müller C, Koshizuka K, Williamson EA, Park D, Asou H, Shintaku P, Said JW, Heber D, Koefler HP: Ligands for peroxisome proliferator-activated receptor  $\gamma$  and retinoic acid receptor inhibit growth and induce

- apoptosis of human breast cancer cells *in vitro* and in BNX mice. Proc Natl Acad Sci USA 1998, 95:8806–8811
9. Tontonoz P, Hu E, Spiegelman BM: Stimulation of adipogenesis in fibroblasts by PPAR gamma 2, a lipid-activated transcription factor. Cell 1994, 79:1147–1156
  10. Mueller E, Sarraf P, Tontonoz P, Evans RM, Martin KJ, Zhang M, Fletcher C, Singer S, Spiegelman BM: Terminal differentiation of human breast cancer through PPAR $\gamma$ . Mol Cell 1998, 1:465-470
  11. Suh N, Wang Y, Williams CR, Risingsong R, Gilmer T, Willson TM, Sporn MB: A new ligand for the peroxisome proliferator-activated receptor-gamma (PPAR-gamma), GW7845, inhibits rat mammary carcinogenesis. Cancer Res 1999, 59:5671-5673
  12. Bonofiglio D, Aquila S, Catalano S, Gabriele S, Belmonte M, Middea E, Qi H, Morelli C, Gentile M, Maggiolini M, Andò S: Peroxisome proliferator-activated receptor-gamma activates p53 gene promoter binding to the nuclear factor-kappaB sequence in human MCF7 breast cancer cells. Mol Endocrinol 2006, 20:3083-3092
  13. Bonofiglio D, Gabriele S, Aquila S, Catalano S, Gentile M, Middea E, Giordano F, Andò S: Estrogen Receptor alpha binds to Peroxisome Proliferator-Activated Receptor (PPAR) Response Element and negatively interferes with PPAR gamma signalling in breast cancer cells. Clin Cancer Res 2005, 11:6139-6147
  14. Bonofiglio D, Gabriele S, Aquila S, Qi H, Belmonte M, Catalano S, Andò S: Peroxisome proliferator-activated receptor gamma activates fas ligand gene promoter inducing apoptosis in human breast cancer cells. Breast Cancer Res Treat 2008, Feb 22 [Epub ahead of print]
  15. Elstner E, Williamson EA, Zang C, Fritz J, Heber D, Fenner M, Possinger K, Koeffler HP: Novel therapeutic approach: ligands for PPAR $\gamma$  and retinoid

- receptors induce apoptosis in bcl-2-positive human breast cancer cells. *Breast Cancer Res Treat* 2002, 74:155–165
16. Arakawa K, Ishihara T, Aoto M, Inamasu M, Kitamura K, and Saito A: An antidiabetic thiazolidinedione induces eccentric cardiac hypertrophy by cardiac volume overload in rats. *Clin Exp Pharmacol Physiol* 2004, 31:8–13
  17. Rangwala SM and Lazar MA: Peroxisome proliferator-activated receptor gamma in diabetes and metabolism. *Trends Pharmacol Sci* 2004, 25:331–336
  18. Staels B: Fluid retention mediated by renal PPARgamma. *Cell Metab* 2005, 2:77–78
  19. Pinaire JA, Reifel-Miller A: Therapeutic potential of retinoid x receptor modulators for the treatment of the metabolic syndrome. *PPAR Res.* 2007, 2007:94156. Mar 28 [Epub 2007]
  20. Qin C, Nguyen T, Stewart J, Samudio I, Burghardt R, Safe S: Estrogen up-regulation of p53 gene expression in MCF-7 breast cancer cells is mediated by calmodulin kinase IV-dependent activation of a nuclear factor *k*B/CCAAT-binding transcription factor-1 complex. *Mol Endocrinol* 2002, 16:1793–1809
  21. Herman ME, Katzenellenbogen BS: Response-specific antiestrogen resistance in a newly characterized MCF-7 human breast cancer cell line resulting from long-term exposure to trans-hydroxytamoxifen. *J Steroid Biochem Mol Biol* 1996, 59:121-134
  22. Mosmann T: Rapid colorimetric assay for cellular growth and survival: application to proliferation and cytotoxicity assays. *J Immunol Methods* 1983, 65:55-63
  23. Andrews NC, Faller DV: A rapid micropreparation technique for extraction of DNA-binding proteins from limiting numbers of mammalian cells. *Nucleic Acids Res* 1991, 19:2499

24. Cossarizza A, Baccarani-Contri M, Kalashnikova G, Franceschi C: A new method for the cytofluorimetric analysis of mitochondrial membrane potential using the J-aggregate forming lipophilic cation 5,5',6,6'-tetrachloro-1,1',3,3' tetraethylbenzimidazolylcarbo-cyanine iodide (JC-1). *Biochem Biophys Res Commun* 1993, 197: 40-45
25. Mehta RG, Williamson E, Patel MK, Koeffler HP: A ligand of peroxisome proliferator-activated receptor gamma, retinoids, and prevention of preneoplastic mammary lesions. *J Natl Cancer Inst* 2000, 92:418-423
26. Crowe DL, Chandraratna RA: A retinoid X receptor (RXR)-selective retinoid reveals that RXR-alpha is potentially a therapeutic target in breast cancer cell lines, and that it potentiates antiproliferative and apoptotic responses to peroxisome proliferator-activated receptor ligands. *Breast Cancer Res* 2004, 6:R546-55
27. Smiley ST, Reers M, Mottola-Hartshorn C, Lin M, Chen A, Smith TW, Steele GD, Chen LB: Intracellular heterogeneity in mitochondrial membrane potentials revealed by a J-aggregate forming lipophilic cation JC-1. *Proc Natl Acad Sci USA* 1991, 88:3671-3675
28. Kliewer SA, Umesono K, Mangelsdorf DJ, Evans RM: Retinoid X receptor interacts with nuclear receptors in retinoic acid, thyroid hormone, and vitamin D3 signaling. *Nature* 1992, 355:446-449
29. Zhang XK, Hoffmann B, Tran PBV, Graupner G, Pfahl M: Retinoid X receptor is an auxiliary protein for thyroid hormone and retinoic acid receptors. *Nature* 1992, 355:441-445
30. Tsubouchi Y, Sano H, Kawahito Y, Mukai S, Yamada R, Kohno M, Inoue K, Hla T, Kondo M: Inhibition of human lung cancer cell growth by the peroxisome proliferator activated receptor  $\gamma$  agonists through induction of apoptosis. *Biochem Biophys Res Commun* 2000, 270:400-405
31. Kitamura S, Miyazaki Y, Shinomura Y, Kondo S, Kanayama S, Matsuzawa Y: Peroxisome proliferator activated receptor  $\gamma$  induces growth arrest and



- differentiation markers of human colon cancer cells. *Jpn J Cancer Res* 1999, 90:75-80
32. Roberts-Thomson SJ: Peroxisome proliferator activated receptors in tumorigenesis: targets of tumor promotion and treatment. *Immunol Cell Biol* 2000, 78:436-441
  33. Demetri GD, Fletcher CDM, Mueller E, Sarraf P, Naujoks R, Campbell N, Spiegelman BM, Singer S: Induction of solid tumor differentiation by the peroxisome proliferator activated receptor  $\gamma$  ligand troglitazone in patients with liposarcoma. *Proc Natl Acad Sci USA* 1999, 96:3951-3956
  34. Yee LD, Williams N, Wen P, Young DC, Lester J, Johnson MV, Farrar WB, Walker MJ, Povoski SP, Suster S, Eng C: Pilot study of rosiglitazone therapy in women with breast cancer: effects of short-term therapy on tumor tissue and serum markers. *Clin Cancer Res* 2007, 13:246-252
  35. Leblanc BP, Stunnenberg HG: 9-cis retinoic acid signaling: changing partners causes some excitement. *Genes Dev* 1995, 9:1811-1816
  36. Crouch GD, Helman LJ: All trans retinoic acid inhibits the growth of human rhabdomyosarcoma cell lines. *Cancer Res* 1991, 51:4882-4887
  37. Delia D, Aiello A, Lombardi L, Pelicci PG, Grignani F, Formelli F, Menard S, Costa A, Veronesi U, Pierotti MA: N-(4-hydroxyphenyl) retinamide induces apoptosis of malignant hemopoietic cell lines including those unresponsive to retinoic acid. *Cancer Res* 1993, 53:6036-6041
  38. Rubin M, Fenig E, Rosenauer A, Menendez-Botet C, Achkar C, Bentel JM, Yahalom J, Mendelsohn J, Miller WH: 9-cis retinoic acid inhibits growth of breast cancer cells and downregulates estrogen receptor mRNA and protein. *Cancer Res* 1994, 54:6549-6556
  39. Sun SY, Yue P, Dawson MI, Shroot B, Michel S, Lamph WW, Heyman RA, Teng M, Chandraratna RAS, Shudo K, Hong WK, Lotan R: Differential effects of synthetic nuclear retinoid receptor selective retinoids on the growth

- of human non-small cell lung carcinoma cells. *Cancer Res* 1997, 57:4931-4939
40. Wu Q, Dawson MI, Zheng Y, Hobbs PD, Agadir A, Jong L, Li Y, Liu R, Lin BZ, Zhang XK: Inhibition of trans retinoic acid resistant human breast cancer cell growth by retinoid X receptor selective retinoids. *Mol Cell Biol* 1997, 17:6598-6608
  41. Bischoff ED, Gottardis MM, Moon TE, Heyman RA, Lamph WW: Beyond tamoxifen: the retinoid X receptor selective ligand LGD1069 (TARGRETIN) causes complete regression of mammary carcinoma. *Cancer Res* 1998, 58:479-484
  42. Grommes C, Landreth GE, Heneka MT: Antineoplastic effects of peroxisome proliferator-activated receptor gamma agonists. *Lancet Oncol.* 2004, 5:419-429
  43. Chung SW, Kang BY, Kim SH, Pak YK, Cho D, Trinchieri G, Kim TS: Oxidized low density lipoprotein inhibits interleukin-12 production in lipopolysaccharide-activated mouse macrophages via direct interactions between peroxisome proliferator-activated receptor- $\gamma$  and nuclear factor  $\kappa$ B. *J Biol Chem* 2000, 275:32681–32687
  44. Couturier C, Brouillet A, Couriaud C, Koumanov K, Bereziat G, Andreani M: Interleukin 1beta induces type II-secreted phospholipase A2 gene in vascular smooth muscle cells by a nuclear factor  $\kappa$ B and peroxisome proliferator-activated receptor-mediated process. *J Biol Chem* 1999, 274:23085–23093
  45. Sun YX, Wright HT, Janciasukiene S: Alpha1-Antichymotrypsin/Alzheimer's peptide A $\beta$ (1–42) complex perturbs lipid metabolism and activates transcription factors PPAR $\gamma$  and NF $\kappa$ B in human neuroblastoma (Kelly) cells. *J Neurosci Res* 2002, 67:511–522
  46. Ikawa H, Kameda H, Kamitani H, Baek SJ, Nixon JB, His LC, Eling TE: Effect of PPAR activators on cytokine stimulated cyclooxygenase-2

expression in human colorectal carcinoma cells. *Exp Cell Res* 2001, 267:73–80

47. Schlezinger JJ, Jensen BA, Mann KK, Ryu HY, Sherr DH: Peroxisome proliferator-activated receptor  $\gamma$ -mediated NF $\kappa$ B activation and apoptosis in pre-B cells. *J Immunol* 2002, 169:6831–6841
48. Knowlden JM, Hutcheson IR, Jones HE, Madden T, Gee JMW, Harper ME, Barrow D, Wakeling AE, Nicholson RI: Elevated levels of EGFR/c-erbB2 heterodimers mediate an autocrine growth regulatory pathway in Tamoxifen-resistant MCF-7 cells. *Endocrinology* 2003, 144:1032-1044
49. Jones HE, Goddard L, Gee JMW, Hiscox S, Rubini M, Barrow D, Knowlden JM., Williams S, Wakeling AE, Nicholson RI: Insulin-like growth factor-I receptor signaling and acquired resistance to gefitinib (ZD1839, Iressa) in human breast and prostate cancer cells. *Endocr Relat Cancer* 2004, 11:793-814
50. Hiscox S, Morgan L, Green TP, Barrow D, Gee J, Nicholson RI: Elevated Src activity promotes cellular invasion and motility in tamoxifen resistant breast cancer cells. *Breast Cancer Res Treat* 2005, 7:1-12

## FIGURE LEGENDS

**Figure 1 Upregulation of p53 and p21<sup>WAF1/Cip1</sup> expression induced by BRL plus 9RA in MCF-7 cells.** (A) Immunoblots of p53 and p21<sup>WAF1/Cip1</sup> from extracts of MCF-7 cell treated with BRL 100nM and 9RA 50nM alone or in combination for 24 and 36 h. GAPDH was used as loading control. The side panels show the quantitative representation of data (mean  $\pm$  S.D.) of three independent experiments after densitometry. (B) p53 and p21<sup>WAF1/Cip1</sup> mRNA expression in MCF-7 cells treated as in A for 12 and 24 h. The side panels show the quantitative representation of data (mean  $\pm$  S.D.) of three independent experiments after densitometry and correction for 36B4 expression. \*p<0.05 and \*\*p<0.01 combined-treated vs untreated cells. N: RNA sample without the addition of reverse transcriptase (negative control).

**Figure 2 BRL and 9RA transactivate p53 promoter gene in MCF-7 cells.** (A) Schematic map of the p53 promoter fragments used in this study. (B) MCF-7 cells were transiently transfected with p53 gene promoter-luc reporter constructs (p53-1, p53-6, p53-13, p53-14) and treated for 24 h with BRL 100nM and 9RA 50nM alone or in combination. The luciferase activities were normalized to the Renilla luciferase as internal transfection control and data were reported as RLU values. Columns are mean  $\pm$  S.D. of three independent experiments performed in triplicate. \*p<0.05 combined-treated vs untreated cells. pGL2: basal activity measured in cells transfected with pGL2 basal vector; RLU, Relative Light Units. CTF-1, CCAAT-binding transcription factor-1; NF-Y, nuclear factor-Y; NF $\kappa$ B, nuclear factor  $\kappa$ B.

**Figure 3 PPAR $\gamma$ /RXR $\alpha$  binds to NF $\kappa$ B sequence in EMSA and in ChIP Assay.** (A) Nuclear extracts from MCF-7 cells (lane 1) were incubated with a double-stranded NF $\kappa$ B consensus sequence probe labeled with [<sup>32</sup>P] and subjected to electrophoresis in a 6% polyacrylamide gel. Competition experiments were done, adding as competitor a 100-fold molar excess of unlabeled probe (lane 2). Nuclear extracts from MCF-7 were treated with 100nM BRL (lane 3), 50nM 9RA (lane 4) and in combination (lane5). Anti-PPAR $\gamma$  (lane 6), anti-RXR $\alpha$  (lane 7) and IgG (lane 8) antibodies were

incubated. Lane 9 contains probe alone. (B) MCF-7 cells were treated for 1 h with 100nM BRL and/or 50nM 9RA as indicated, and then cross-linked with formaldehyde and lysed. The soluble chromatin was immunoprecipitated with anti-PPAR $\gamma$ , anti-RXR $\alpha$  and anti-RNA Pol II antibodies. The immunocomplexes were reverse cross-linked, and DNA was recovered by phenol/chloroform extraction and ethanol precipitation. The p53 promoter sequence containing NF $\kappa$ B was detected by PCR with specific primers. To control input DNA, p53 promoter was amplified from 30  $\mu$ l of initial preparations of soluble chromatin (before immunoprecipitations). N: negative control provided by PCR amplification without DNA sample.

**Figure 4 Mitochondrial membrane potential disruption and release of cytochrome C induced by BRL and 9RA in MCF-7 cells.** (A) MCF-7 cells were treated with 100nM BRL plus 50nM 9RA for 48 h and then used fluorescent microscopy to analyze the results of JC-1 (5,5',6,6'-tetrachloro-1,1',3,3'- tetraethylbenzimidazolylcarbocyanine iodide) kit. In control non-apoptotic cells, the dye stains the mitochondria red. In treated apoptotic cells, JC-1 remains in the cytoplasm in a green fluorescent form. (B) MCF-7 cells were treated for 48 h with BRL 100nM and/or 9RA50nM. GAPDH was used as loading control.

**Figure 5 Combined treatment of BRL and 9RA trigger apoptosis in breast cancer cells.** (A) DNA laddering was performed in MCF-7 cells transfected and treated as indicated for 56 h. One of three similar experiments is presented. The side panel shows the immunoblot of p53 from MCF-7 cells transfected with an expression plasmid encoding for p53 antisense (AS/p53) or empty vector (v) and treated with 100nM BRL plus 50nM 9RA for 56 h. GAPDH was used as loading control. (B) DNA laddering was performed in MCF-7 TR1, SKBR-3, T47-D cells transfected with AS/p53 or empty vector (v) and treated as indicated. One of three similar experiments is presented.

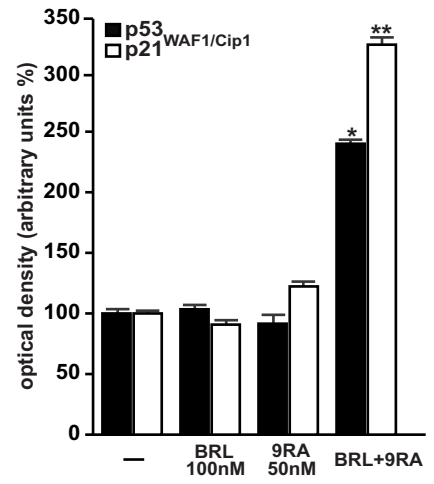
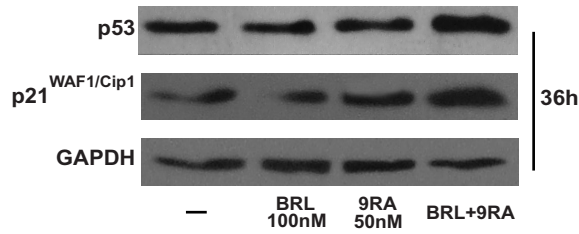
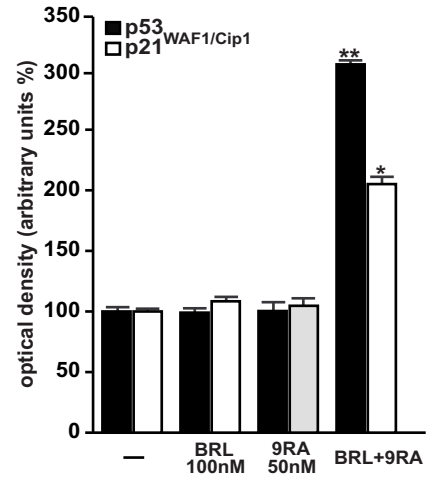
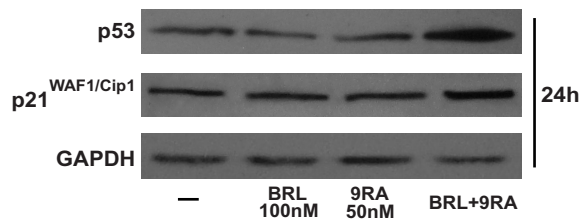
**Table 1 Cell vitality in breast cell lines.** Breast cells were treated for 48 h in the presence of BRL 100nM or/and 9RA 50nM. Cell vitality was measured by MTT assay. Data were presented as mean  $\pm$  S.D. of three independent

experiments done in triplicate and expressed as percentage of vitality respect to control. \*p<0.05 and \*\*p<0.01 treated vs untreated cells.

**Table 2 Activation of caspases in MCF-7 cells.** Cells were stimulated for 48 h in presence of BRL 100nM, 9RA 50nM alone or in combination. The activation of caspase 9 (A) and caspase 8 (B) was analysed by Flow Cytometry Assay. Data were presented as mean  $\pm$  S.D. of triplicate experiments. \*p<0.05 combined-treated vs untreated cells.

**Supplemental data: Figure 1 BRL and 9RA transactivate PPRE reported gene in MCF-7 cells.** MCF-7 cells were transfected with a PPRE reporter gene and treated with BRL, 9RA and GW as indicated. The luciferase activity was normalized to the Renilla luciferase as internal transfection control and data were reported as RLU values. Columns are mean  $\pm$  S.D. of three independent experiments performed in triplicate. \*p<0.05 combined-treated vs untreated cells. RLU, Relative Light Units.

**A**



**B**

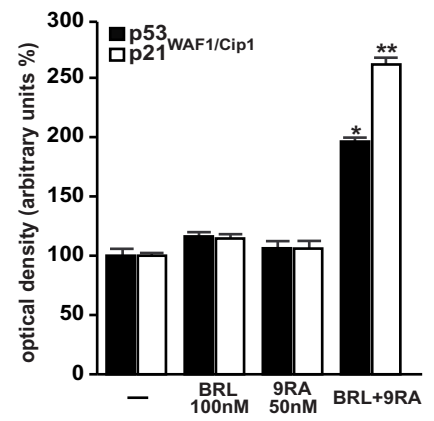
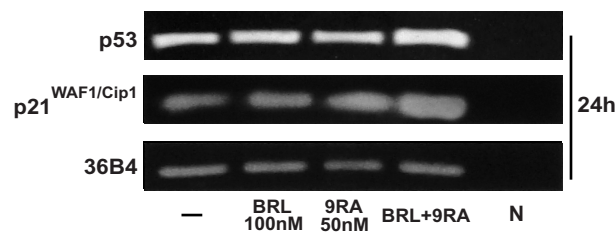
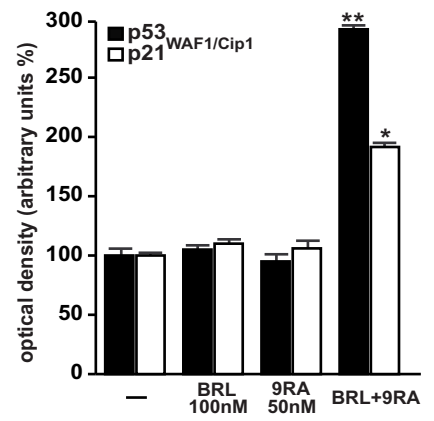
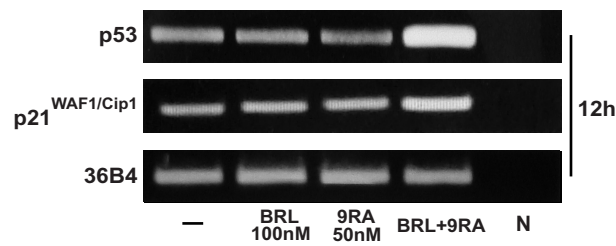


**Fig. 1**

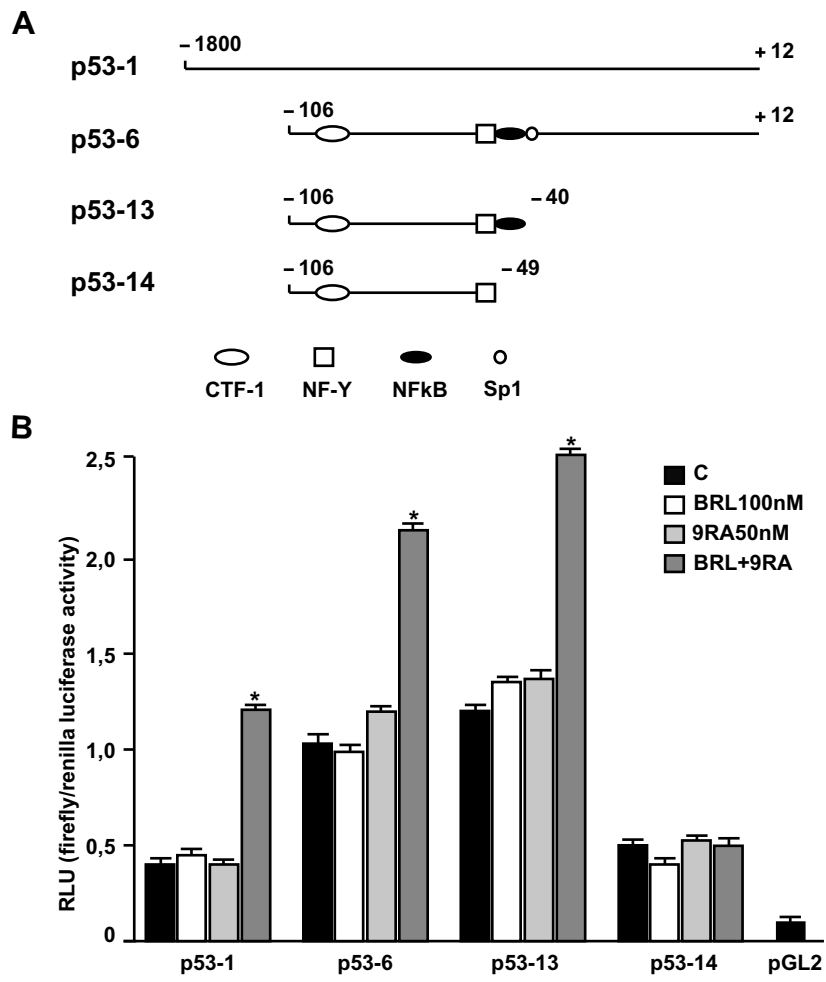


Fig. 2

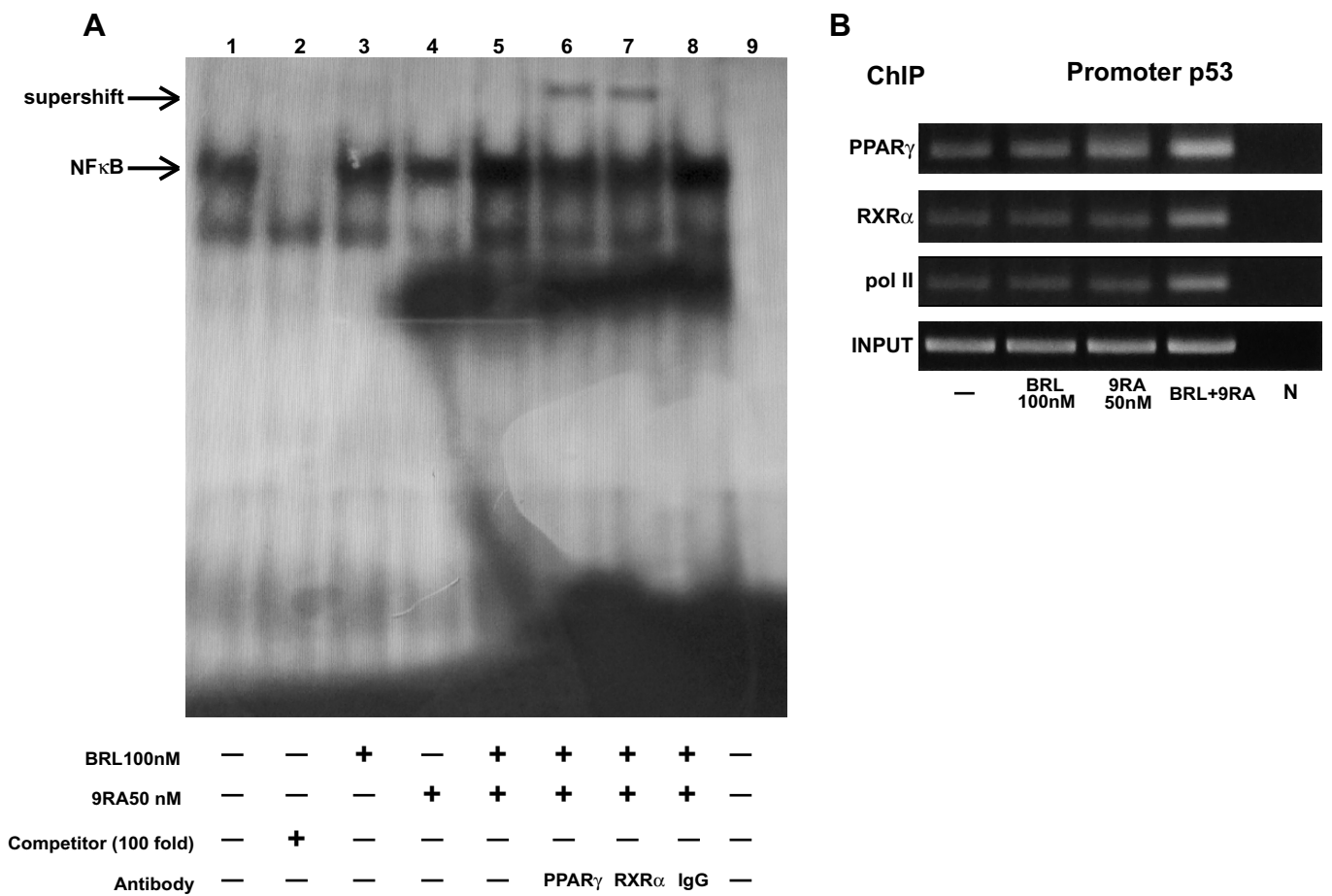
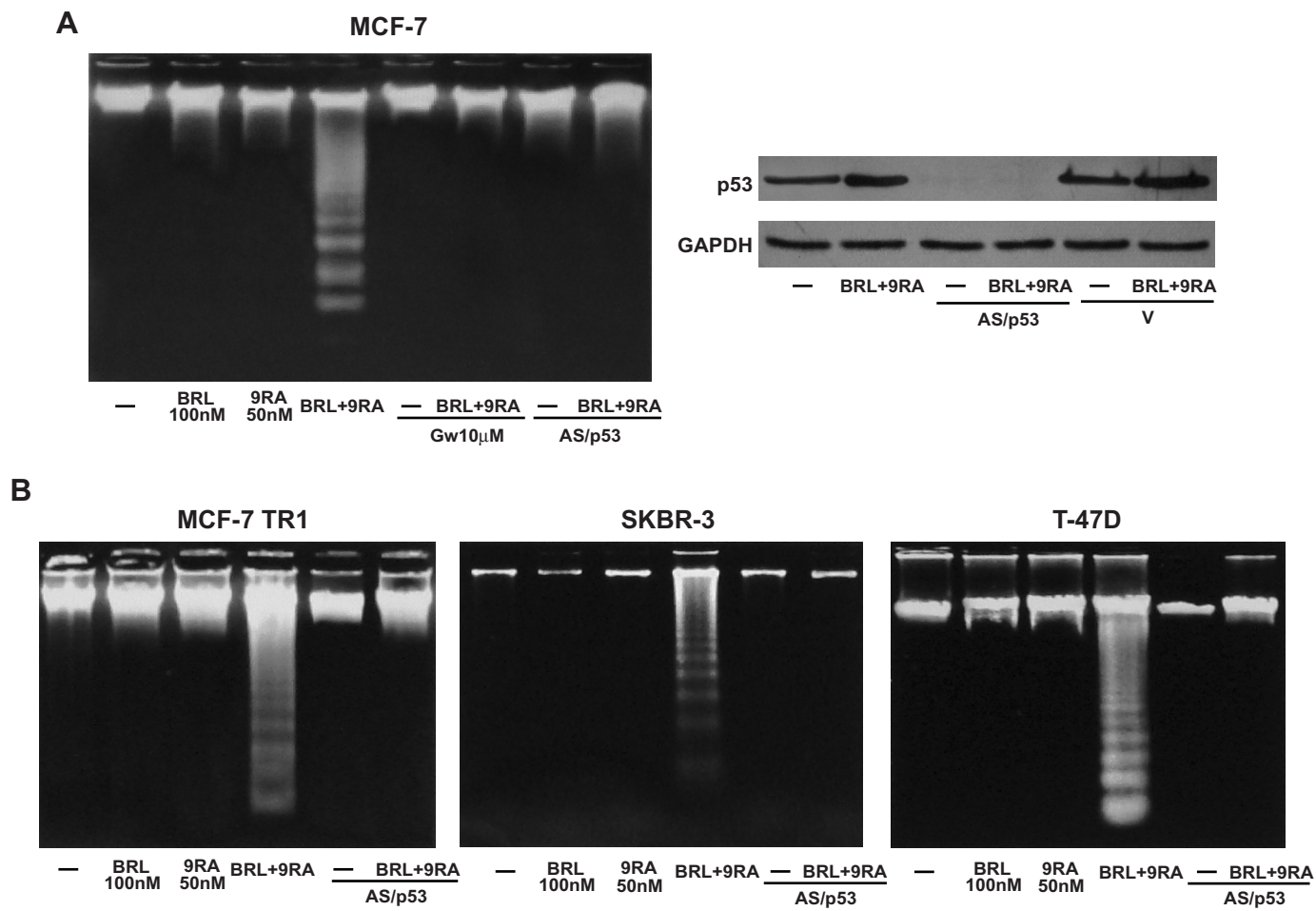
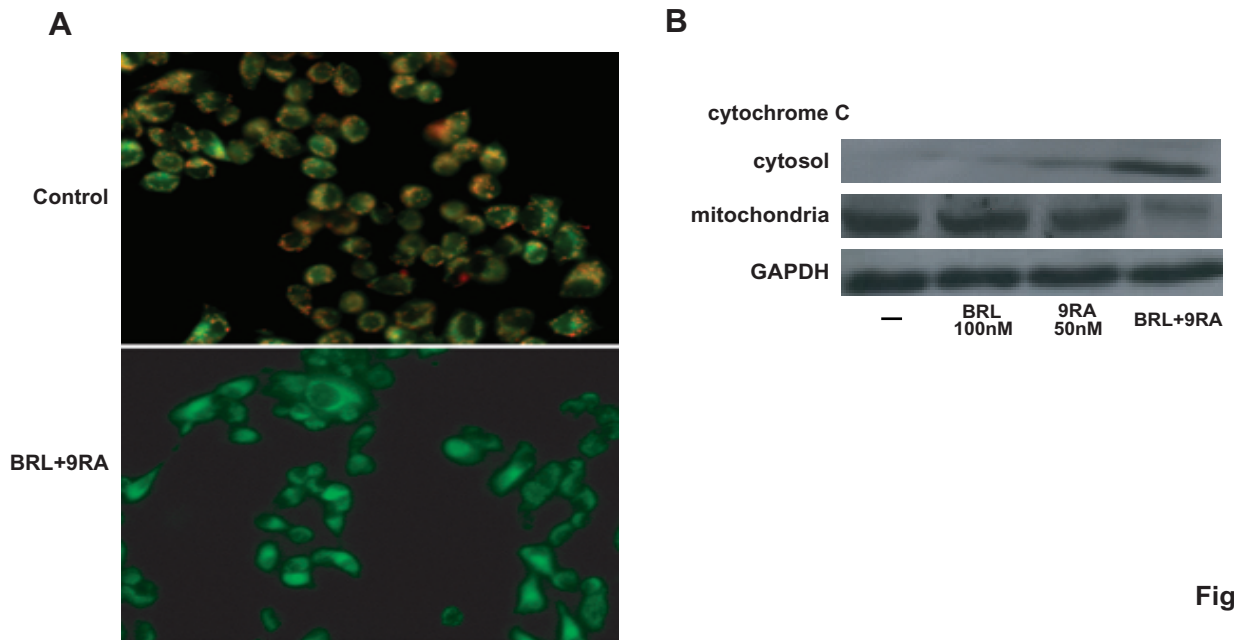


Fig. 3





% OF VITALITY RESPECT TO CONTROL			
Breast cell lines	BRL100nM	9RA50nM	BRL+9RA
MCF-10	90,4±0,867	96,7±0,927	98,7±1,067
MCF-7	86,5±0,505	87,9±1,205	51,8*±0,905
MCF-7 TR1	89,9±1,535	115±1,375	68,7*±1,145
SKBR-3	96,8±0,875	90,5±0,657	58,9*±0,932
T-47D	78,4±1,110	60,7*±1,763	34,5**±0,730

Table 1

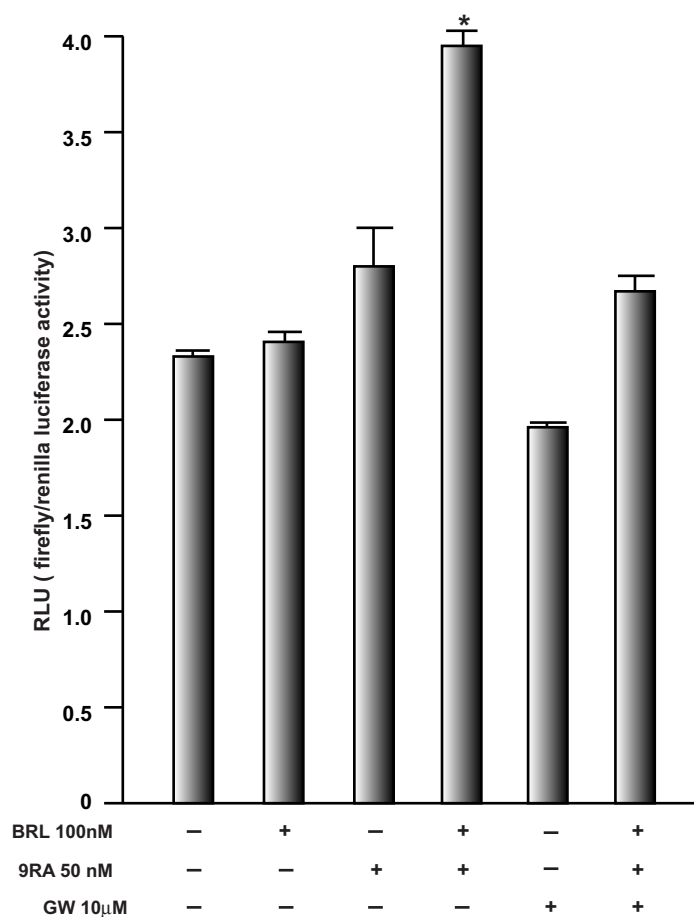
A

Caspase 9	% of Activation	SD
control	14,16	±2,565
BRL100nM	17,23	±1,678
9RA50nM	18,14	±0,986
BRL+9RA	33,88 *	±5,216

B

Caspase 8	% of Activation	SD
control	9,20	±1,430
BRL100nM	8,12	±1,583
9RA50nM	7,90	±0,886
BRL+9RA	10,56	±2,160

Table 2



Suppl. Fig. 1

# Peroxisome proliferator-activated receptor $\gamma$ inhibits follicular and anaplastic thyroid carcinoma cells growth by upregulating p21<sup>Cip1/WAF1</sup> gene in a Sp1-dependent manner

D Bonfiglio<sup>1,2\*</sup>, H Qi<sup>1\*</sup>, S Gabriele<sup>1</sup>, S Catalano<sup>1,2</sup>, S Aquila<sup>1,2</sup>, M Belmonte<sup>1</sup> and S Andò<sup>2,3,4</sup>

<sup>1</sup>Department of Pharmaco-Biology, <sup>2</sup>Centro Sanitario, <sup>3</sup>Department of Cellular Biology and <sup>4</sup>Faculty of Pharmacy, University of Calabria, 87036 Arcavacata di Rende (Cosenza), Italy

(Correspondence should be addressed to S Andò; Email: sebastiano.ando@unical.it)

\*D Bonfiglio and H Qi contributed equally to this work

## Abstract

Peroxisome proliferator-activated receptor  $\gamma$  (PPAR $\gamma$ ) has been demonstrated to be anti-neoplastic against various human tumors. The aim of this study was to delineate the molecular mechanism underlying PPAR $\gamma$  ligand rosiglitazone (BRL) antiproliferative effects in follicular WRO and anaplastic FRO human thyroid carcinoma cells. BRL upregulated the p21<sup>Cip1/WAF1</sup> levels in the two thyroid cancer cells, while did not modify the p53 protein content. Different evidences indicate that the p21<sup>Cip1/WAF1</sup> upregulation by BRL requires a functional PPAR $\gamma$ , since it was reversed by silencing PPAR $\gamma$  and pretreatment with GW9662, an irreversible PPAR $\gamma$  antagonist. Transient transfection assays showed that BRL triggered the transcriptional activity of p21<sup>Cip1/WAF1</sup> promoter gene in a p53-independent way, being a p21<sup>Cip1/WAF1</sup> promoter construct deleted in the p53 sites still activated by BRL. The Sp1 inhibitor mithramycin silenced the p21<sup>Cip1/WAF1</sup> promoter activity suggesting an important role of Sp1 in mediating BRL activation. The electrophoretic mobility shift and chromatin immunoprecipitation (ChIP) assays evidenced a functional interaction between PPAR $\gamma$  and Sp1 in regulating p21<sup>Cip1/WAF1</sup>. Intriguingly, ChIP analysis revealed in the p21<sup>Cip1/WAF1</sup> gene promoter an increased recruitment of the RNA Pol II associated with an increased histone H3 acetylation and a reduced H3 methylation. The biological event, consistent with PPAR $\gamma$ -induced WRO and FRO cell growth inhibition, was reversed by p21<sup>Cip1/WAF1</sup> antisense oligonucleotides and was confirmed by increasing the PPAR $\gamma$  expression, suggesting a crucial role exerted by p21<sup>Cip1/WAF1</sup> in PPAR $\gamma$  action. Our results further candidate BRL as a potential agent able to inhibit tumor progression of follicular and anaplastic thyroid carcinoma.

*Endocrine-Related Cancer* (2008) 15 545–557

## Introduction

Peroxisome proliferator-activated receptor  $\gamma$  (PPAR $\gamma$ ) is a member of the nuclear receptor (NR) family of ligand-induced transcription factors, which is best known for its differentiating effects on adipocytes and insulin-mediated metabolic functions (Desvergne & Wahli 1999). However, PPAR $\gamma$  is also involved in cell cycle

control, inflammation, atherosclerosis, apoptosis, and carcinogenesis (Auwerx 1999). Consistently, PPAR $\gamma$  agonists decrease the growth rate of various malignant cell lines and induce differentiation and apoptosis in diverse carcinoma, including thyroid cancer cells (Tontonoz *et al.* 1997, Elstner *et al.* 1998, Kuboto *et al.* 1998, Mueller *et al.* 1998, Chung *et al.* 2002,

Martelli et al. 2002, Klopper et al. 2004, Aiello et al. 2006, Chen et al. 2006, Copland et al. 2006).

Thyroid cancers are the most common malignancy of endocrine organs (Parkin et al. 2005), with an incidence rate that steadily increased over the past few decades (Liu et al. 2001). More than 95% of thyroid carcinomas are derived from follicular epithelial cells, while a minority of tumors (2%) is referred as undifferentiated or anaplastic carcinoma, one of the most aggressive human malignancies (Kondo et al. 2006). A majority of well-differentiated thyroid cancers can be effectively managed by surgical resection with or without radioactive iodine ablation and only a subset of these tumors can behave aggressively. By contrast, there is no effective form of treatment presently available for patients affected by anaplastic neoplasia and hence they have an extremely poor prognosis (Ain 1998).

The growth activity of well-differentiated compared with undifferentiated thyroid carcinoma is low and this difference is governed by altered cell cycle regulators (Kondo et al. 2006 and references therein). Among a family of negative cell cycle regulators, the p21<sup>Cip1/WAF1</sup> member of the cyclin-dependent-kinase interacting protein/kinase inhibitory protein (CIP/KIP) family plays a crucial role in the growth arrest mediated by either p53-dependent (el-Diery et al. 1993) or p53-independent mechanism (Jiang et al. 1994). The p21<sup>Cip1/WAF1</sup> was shown to be involved in PPAR $\gamma$ -mediated growth regulation in different cancer cells, including thyroid (Han et al. 2004, Hong et al. 2004, Bonfiglio et al. 2006, Copland et al. 2006). Particularly, PPAR $\gamma$  mediates the upregulation of p21<sup>Cip1/WAF1</sup> (Chung et al. 2002, Han et al. 2004, Hong et al. 2004) and a mechanism through which PPAR $\gamma$  mediates p21<sup>Cip1/WAF1</sup> mRNA induction was shown to be via Sp1-enhanced binding to the p21<sup>Cip1/WAF1</sup>, KDR and hormone-sensitive lipase promoters (Han et al. 2004, Hong et al. 2004, Sassa et al. 2004, Deng et al. 2006).

In this study, we have investigated the way through which the PPAR $\gamma$  ligand rosiglitazone (BRL49653, BRL) induces growth inhibition in follicular WRO and anaplastic FRO thyroid cancer cells. Independent of the p53 pathway, the underlying molecular mechanism involves a functional interaction between PPAR $\gamma$  and Sp1 to Sp1 sites of the p21<sup>Cip1/WAF1</sup> promoter gene.

## Materials and methods

### Reagents

BRL was purchased from Alexis (San Diego, CA, USA); the irreversible PPAR $\gamma$ -antagonist GW9662

(GW) and the Sp1-specific inhibitor, mithramycin, were from Sigma. All compounds were solubilized in dimethyl sulfoxide (Sigma) also used as the vehicle.

### Cell cultures

Human follicular WRO and anaplastic FRO thyroid cancer cells (a gift from Dr F Arturi, University of Magna Grecia, Catanzaro, Italy) were grown in Dulbecco's Modified Eagle's Medium (DMEM) plus glutamax containing 10% fetal bovine serum (FBS; Invitrogen) and 1 mg/ml penicillin–streptomycin (P/S).

### Plasmids

The human wild-type p21<sup>Cip1/WAF1</sup> promoter-luciferase (luc) reporter (p21<sup>Cip1/WAF1</sup> wt) and its deletion construct that lacks the two p53-binding sites (p21<sup>Cip1/WAF1</sup>  $\Delta$ p53) were kind gifts from Dr T Sakai (Kyoto Prefectural University of Medicine, Kyoto, Japan). The PPAR $\gamma$  expression plasmid was a gift from Dr R Evans (The Salk Institute, San Diego, CA, USA). As an internal transfection control we co-transfected the plasmid pRL-CMV (Promega), which expresses *Renilla luciferase* enzymatically distinguishable from firefly *luciferase* by the strong cytomegalovirus enhancer/promoter.

### [<sup>3</sup>H]thymidine incorporation

WRO and FRO cells were seeded in 12-well plates in a regular growth medium. On the second day, the cells were incubated in DMEM supplemented with 1% charcoal-stripped-FBS in the presence of vehicle or with treatments. The medium was renewed every 2 days together with the appropriate treatments. [<sup>3</sup>H]thymidine (1  $\mu$ Ci/ml; New England Nuclear, Newton, MA, USA) was added to the medium for the last 6 h of the sixth day. After rinsing with PBS, the cells were washed once with 10% and thrice with 5% trichloroacetic acid. The cells were lysed by adding 0.1 M NaOH and then incubated for 30 min at 37 °C. Thymidine incorporation was determined by scintillation counting.

### Immunoblotting

The cells were grown in 10 cm dishes to 70–80% confluence and exposed to treatments for 24 h in a serum-free medium (SFM), as indicated. They were then harvested in cold PBS and resuspended in a lysis buffer containing 20 mM HEPES (pH 8), 0.1 mM EDTA, 5 mM MgCl<sub>2</sub>, 0.5 M NaCl, 20% glycerol, 1% NP-40, and inhibitors (0.1 mM Na<sub>3</sub>VO<sub>4</sub>, 1% phenylmethylsulphonyl fluoride (PMSF), 20 mg/ml

aprotinin). The protein concentration was determined using Bio-Rad Protein Assay (Bio-Rad Laboratories). A 50 µg portion of protein lysates was used for western blotting (WB), resolved on a 10% SDS-polyacrylamide gel, transferred to a nitrocellulose membrane and probed with an antibody directed against the p21<sup>Cip1/WAF1</sup>, p53, PPAR $\gamma$  and Sp1 (Santa Cruz Biotechnology, Santa Cruz, CA, USA). As the internal control, all membranes were subsequently stripped (0.2 M glycine (pH 2.6) for 30 min at room temperature) of the first antibody and reprobed with anti- $\beta$ -actin antibody (Santa Cruz Biotechnology). The antigen–antibody complex was detected by incubation of the membranes for 1 h at room temperature with peroxidase-coupled goat anti-mouse or anti-rabbit IgG and revealed using the enhanced chemiluminescence system (ECL system, Amersham Pharmacia). The blots were then exposed to Kodak film (Sigma). The intensity of bands representing relevant proteins was measured using the Scion Image laser densitometry scanning program.

#### Reverse transcription-PCR (RT-PCR) assay

Cells were grown in 10 cm dishes to 60–70% confluence and exposed to treatments for 24 h in SFM. The total cellular RNA was extracted using TRIZOL reagent (Invitrogen) as suggested by the manufacturer. The purity and integrity were checked spectroscopically and by gel electrophoresis before carrying out the analytical procedures. The evaluation of gene expression was performed by the semiquantitative RT-PCR method as described previously (Maggiolini *et al.* 1999). For p21<sup>Cip1/WAF1</sup> and the internal control gene 36B4, the primers were: 5'-GCTTCATGCCAGCTACTTCC-3' (p21<sup>Cip1/WAF1</sup> forward) and 5'-CTGTGCTCACTTCAGGGTCA-3' (p21<sup>Cip1/WAF1</sup> reverse), and 5'-CTCAACATCTCCC CTTCTC-3' (36B4 forward) and 5'-CAAATCCCA TATCCTCGTCC-3' (36B4 reverse) to yield respectively the products of 270 bp with 20 cycles and 408 bp with 12 cycles. The results obtained as optical density arbitrary values were transformed to percentage of the control (percent control) taking the samples from untreated cells as 100%.

#### Transfection assay

The cells were transferred into 24-well plates with 500 µl regular growth medium/well the day before transfection. The medium was replaced with SFM on the day of transfection, which was performed using Fugene 6 reagent as recommended by the manufacturer (Roche) with a mixture containing 0.5 µg promoter-luc

reporter plasmids and 5 ng pRL-CMV. After 24 h transfection, SFM was treated as indicated and the cells were incubated for a further 24 h. Firefly and *R. luciferase* activities were measured using the Dual Luciferase Kit (Promega).

#### Electrophoretic mobility shift assay (EMSA)

Nuclear extracts from thyroid cancer cells were prepared as described previously for EMSA (Andrews & Fallor 1991). Briefly, both cell lines plated into 10 cm dishes were grown to 70–80% confluence, shifted to SFM for 24 h, and then treated with 1 µM BRL for 6 h. Thereafter, the cells were scraped into 1.5 ml cold PBS. They were pelleted for 10 s and resuspended in 400 µl cold buffer A (10 mM HEPES–KOH (pH 7.9) at 4 °C, 1.5 mM MgCl<sub>2</sub>, 10 mM KCl, 0.5 mM dithiothreitol, 0.2 mM PMSF, 1 mM leupeptin) by flicking the tube. The cells were then allowed to swell on ice for 10 min and then vortexed for 10 s. The samples were then centrifuged for 10 s and the supernatant fraction discarded. The pellet was resuspended in 50 µl cold Buffer B (20 mM HEPES–KOH (pH 7.9), 25% glycerol, 1.5 mM MgCl<sub>2</sub>, 420 mM NaCl, 0.2 mM EDTA, 0.5 mM dithiothreitol, 0.2 mM PMSF, 1 mM leupeptin) and incubated in ice for 20 min for high-salt extraction. Cellular debris was removed by centrifugation for 2 min at 4 °C and the supernatant fraction (containing DNA-binding proteins) was stored at –70 °C. The probe was generated by annealing single-stranded oligonucleotides and labeled with [ $\gamma$ -<sup>32</sup>P] ATP (Amersham Pharmacia) and T4 polynucleotide kinase (Promega), and then purified using Sephadex G50 spin columns (Amersham Pharmacia). The DNA sequence of Sp1, present in the native human p21<sup>Cip1/WAF1</sup> promoter gene, used as the probe or the cold competitor is the following: Sp1, 5'-GGGGGT CCCGCCTCCTTGA-3' (Sigma). The protein-binding reactions were carried out in 20 µl buffer (20 mM HEPES (pH 8), 1 mM EDTA, 50 mM KCl, 10 mM DTT, 10% glycerol, 1 mg/ml BSA, 50 µg/ml poly dI/dC) with 50 000 c.p.m. labeled probe, 5 µg nuclear protein or 1 µl human Sp1 recombinant protein (Promega), and 5 µg poly(dI-dC). The mixtures were incubated at room temperature for 20 min in the presence or absence of unlabeled competitor oligonucleotides. For the experiments involving the anti-PPAR $\gamma$  and anti-Sp1 antibodies and IgG (Santa Cruz Biotechnology), the reaction mixture was incubated with these antibodies at 4 °C for 30 min before the addition of labeled probe. Mithramycin (100 nM) was incubated with the labeled probe for 30 min at 4 °C before the addition of nuclear extracts. The entire

reaction mixture was electrophoresed through a 6% polyacrylamide gel in 0.25 $\times$  Tris borate–EDTA for 3 h at 150 V. The gel was dried and subjected to autoradiography at  $-70^{\circ}\text{C}$ .

### **Chromatin immunoprecipitation and re-immunoprecipitation (ChIP and reChIP) assay**

For ChIP assay, thyroid carcinoma cells were grown in 10 cm dishes to 50–60% confluence, shifted to SFM for 24 h, and then treated with 1  $\mu\text{M}$  BRL for 1 h or pre-incubated with mithramycin for 1 h where required. Thereafter, the cells were washed twice with PBS and cross-linked with 1% formaldehyde at  $37^{\circ}\text{C}$  for 10 min. Next, the cells were washed twice with PBS at  $4^{\circ}\text{C}$ , collected, and resuspended in 200  $\mu\text{l}$  lysis buffer (1% SDS, 10 mM EDTA, 50 mM Tris–HCl (pH 8.1)) and left on ice for 10 min. Then, the cells were sonicated four times for 10 s at 30% of maximal power (Sonics and Materials Inc., Vibra Cell 500 W) and collected by centrifugation at 11 000  $g$  for 10 min, at  $4^{\circ}\text{C}$ . The supernatants were diluted in 1.3 ml IP buffer (0.01% SDS, 1.1% Triton X-100, 1.2 mM EDTA, 16.7 mM Tris–HCl (pH 8.1), 16.7 mM NaCl) followed by immunoclearing with 80  $\mu\text{l}$  sonicated salmon sperm DNA/protein A agarose (UBI, DBA Srl, Milan, Italy) for 1 h at  $4^{\circ}\text{C}$ . The precleared chromatin was immunoprecipitated with anti-PPAR $\gamma$ , anti-Sp1, anti-RNA Pol II (Santa Cruz Biotechnology), anti-acetyl histone H3, and anti-trimethyl histone H3 antibodies (Upstate, Milan, Italy). The chromatin immunoprecipitated with anti-PPAR $\gamma$  was re-immunoprecipitated with the anti-Sp1 antibody. At this point, 60  $\mu\text{l}$  salmon sperm DNA/protein A agarose were added and precipitation was further continued for 2 h at  $4^{\circ}\text{C}$ . After pelleting, the precipitates were washed sequentially for 5 min with the following buffers: wash A (0.1% SDS, 1% Triton X-100, 2 mM EDTA, 20 mM Tris–HCl (pH 8.1), 150 mM NaCl); wash B (0.1% SDS, 1% Triton X-100, 2 mM EDTA, 20 mM Tris–HCl (pH 8.1), 500 mM NaCl); and wash C (0.25 M LiCl, 1% NP-40, 1% sodium deoxycholate, 1 mM EDTA, 10 mM Tris–HCl (pH 8.1)), and then twice with TE buffer (10 mM Tris, 1 mM EDTA). The immunocomplexes were eluted with the elution buffer (1% SDS, 0.1 M NaHCO<sub>3</sub>). The eluates were reverse cross-linked by heating at  $65^{\circ}\text{C}$  and digested with proteinase K (0.5 mg/ml) at  $45^{\circ}\text{C}$  for overnight. DNA was obtained by phenol/chloroform/isoamyl alcohol extraction. To each sample, 2  $\mu\text{l}$  of 10 mg/ml yeast tRNA (Sigma) were added and DNA was precipitated with 70% ethanol for 24 h at  $-20^{\circ}\text{C}$ , and then washed with 95% ethanol and resuspended in 20  $\mu\text{l}$  TE buffer.

A 5  $\mu\text{l}$  volume of each sample was used for PCR amplification with the following primers flanking a sequence of p21<sup>Cip1/WAF1</sup> promoter: 5'-GATTTGT GGCTCACTTCGTGGG-3' (forward) and 5'-GCA GCTGCTCACACCTCAGCT-3' (reverse) (Gene Bank, accession number U24170). The PCR conditions were 1 min at  $95^{\circ}\text{C}$ , 1 min at  $60^{\circ}\text{C}$ , and 1 min at  $72^{\circ}\text{C}$ . The amplification products obtained in 30 cycles were analyzed in a 2% agarose gel and visualized by ethidium bromide staining. The negative control was provided by PCR amplification without the DNA sample. The specificity of the reactions was ensured using normal mouse and rabbit IgG (Santa Cruz Biotechnology).

### **ChIP/immunoblot assay**

For the ChIP/immunoblot assay, thyroid carcinoma cells were subjected to the procedure of ChIP assay, as described above, until we obtained the immunocomplexes. At this time, we added the Laemmli buffer to the immunocomplexes and performed the WB analysis, as described by the Upstate protocol.

### **Antisense oligodeoxynucleotide experiments**

The oligonucleotides used were: 5'-GACATCACC AGGATCGGACAT-3' for p21, and 5'-GATCTCAG CACGGCAAAT-3' for the scrambled control (cs). For antisense experiments, a concentration of 200 nM of the indicated oligonucleotides (ODN) was transfected using Fugene 6 reagent as recommended by the manufacturer for 4 h, before treatment with vehicle or BRL. The transfection was renewed every 2 days together with the appropriate treatments.

### **RNA interference (RNAi)**

Cells were plated in six-well dishes in the regular growth medium the day before transfection to 60–70% confluence. On the second day, the medium was changed with SFM without P/S and the cells were transfected with 25 bp RNA duplex of validated RNAi-targeted human PPAR $\gamma$  mRNA sequence 5'-AGA AUAUAAGGUGGAGAUGCAGGC-3' sequence (Invitrogen) or with a stealth RNAi-negative control low GC (Invitrogen) to a final concentration of 100 nM using Lipofectamine 2000 (Invitrogen), as recommended by the manufacturer. After 5 h, the transfection medium was changed with SFM in order to avoid Lipofectamine 2000 toxicity and the cells were exposed to vehicle or BRL for the next 24 h and then lysed as described for WB analysis.

## Statistical analysis

Statistical analysis was performed using ANOVA followed by Newman–Keuls testing to determine the differences in means.  $P < 0.05$  was considered statistically significant.

## Results

### BRL induces growth inhibitory effects in WRO and FRO cells

On the basis of other (Kuboto *et al.* 1998, Clay *et al.* 1999, Ohta *et al.* 2001) and our (Bonfiglio *et al.* 2005, 2006) studies demonstrating the inhibitory effects of the PPAR $\gamma$  agonists on the proliferation of different cancer cells, we first treated human follicular WRO and anaplastic FRO thyroid cancer cells with increasing BRL concentrations for 5 days. BRL inhibited the growth of both thyroid cancer cells in a dose- and PPAR $\gamma$ -dependent manner, since this effect was no longer notable in the presence of its specific antagonist GW9662 (GW; Fig. 1A and B).

### BRL upregulates p21<sup>Cip1/WAF1</sup> expression in thyroid cancer cells

The p53 tumor suppressor gene plays an undisputed role as a major mediator of cell cycle arrest and/or apoptosis in the response of mammalian cells to stress stimuli and p21<sup>Cip1/WAF1</sup>, a known p53-downstream gene, has been suggested to mediate p53-induced growth arrest triggered by DNA damage (Vousden & Lu 2002). Therefore, we aimed to examine the potential ability of the PPAR $\gamma$  agonist BRL to modulate p53 along with its natural target gene p21<sup>Cip1/WAF1</sup> in both thyroid cancer cells. Interestingly, BRL upregulated the protein expression of p21<sup>Cip1/WAF1</sup> in a dose-dependent manner in the WRO and FRO cells, while did not modify the p53 protein content (Fig. 2A and B). Next, we investigated the mRNA expression of p21<sup>Cip1/WAF1</sup>, which was induced by BRL at an increasing concentration in both thyroid cancer cells (Fig. 3A). Using GW, BRL action was abrogated, suggesting a direct involvement of PPAR $\gamma$  in mediating this effect (Fig. 3A). To definitively confirm the mechanism by which BRL upregulates p21<sup>Cip1/WAF1</sup> levels, we inhibited PPAR $\gamma$  expression by RNAi (Fig. 3B). The effect of BRL on p21<sup>Cip1/WAF1</sup> expression was prevented in the presence of PPAR $\gamma$  RNAi, while it was still notable using a control RNAi (Fig. 3C), demonstrating the crucial role of PPAR $\gamma$  in BRL-induced upregulation of p21<sup>Cip1/WAF1</sup>.

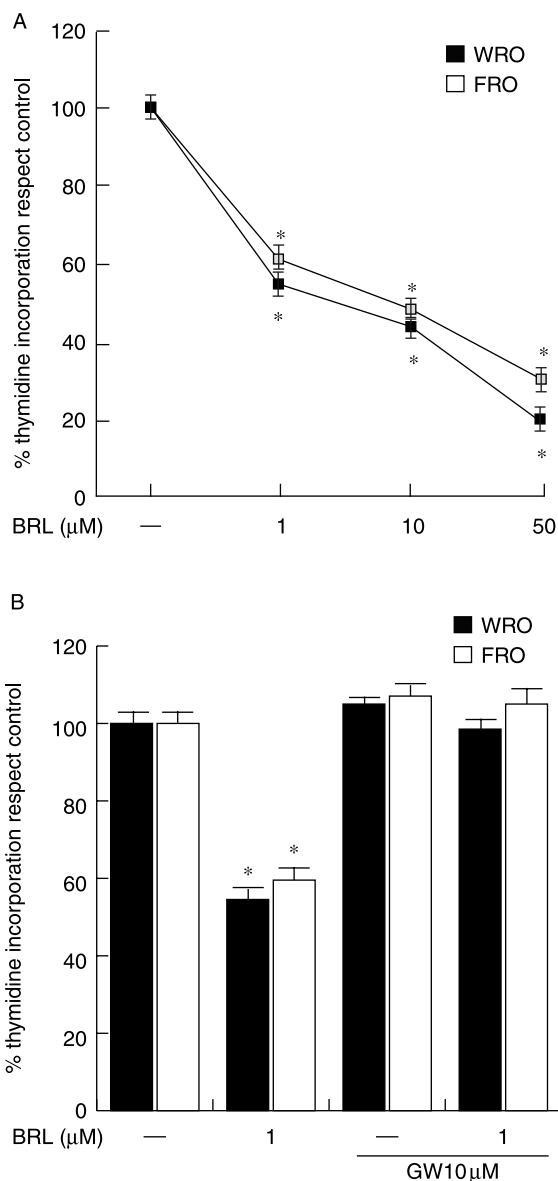


**Figure 1** Antiproliferative effects exerted by PPAR $\gamma$  agonist BRL in follicular WRO and anaplastic FRO thyroid cancer cells. (A) WRO and FRO cells were treated for 5 days with vehicle (—) or with increasing BRL concentrations. (B) Both thyroid cancer cells were treated for 5 days with vehicle (—), 1  $\mu$ M BRL, 10  $\mu$ M GW alone or in combination with BRL. On day 6, [ $^3$ H] thymidine incorporation was determined by scintillation counting. Data are expressed as mean  $\pm$  s.d. of three independent experiments performed in triplicate. \* $P < 0.05$  BRL-treated versus untreated cells.

### BRL transactivates p21<sup>Cip1/WAF1</sup> gene promoter

The aforementioned observations prompted us to investigate whether the PPAR $\gamma$  ligand is able to transactivate the p21<sup>Cip1/WAF1</sup> promoter gene, which contains two p53-response elements (Li *et al.* 1994,

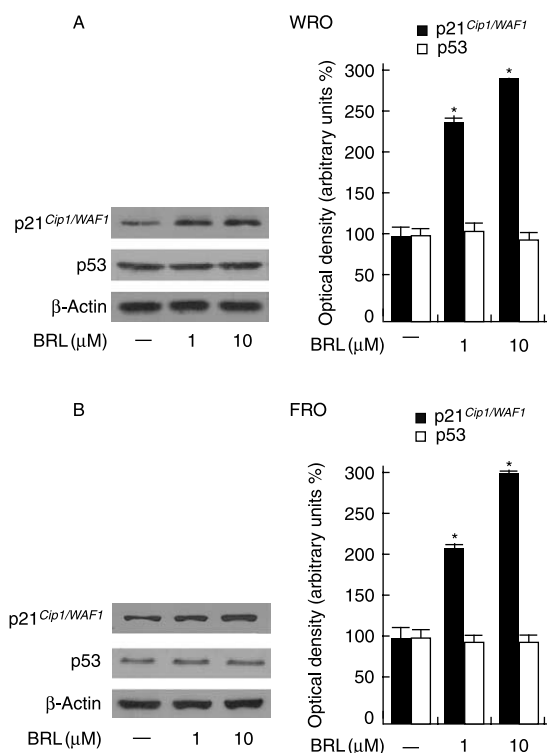


**Figure 2** Modulation of p21<sup>Cip1/WAF1</sup> protein level by BRL. Immunoblots of p21<sup>Cip1/WAF1</sup> and p53 from (A) WRO and (B) FRO cells treated for 24 h with vehicle (–) and with increasing BRL concentrations.  $\beta$ -Actin was used as the loading control. The side panels show the quantitative representation of data (mean  $\pm$  s.d.) of three independent experiments included that presented in A and B respectively. \* $P < 0.05$  BRL-treated versus untreated cells.

Wu & Schonthal 1997). Thus, WRO and FRO cells were transiently transfected with the human wild-type p21<sup>Cip1/WAF1</sup> promoter–luciferase fusion plasmid (p21<sup>Cip1/WAF1</sup> wt) or with a promoter construct that lacks the two p53-binding sites (p21<sup>Cip1/WAF1</sup>  $\Delta$ p53; Fig. 4A). BRL was able to transactivate both constructs, defining the minimal region of p21<sup>Cip1/WAF1</sup> promoter responsible for its induction independently of p53 (Fig. 4B). Such effects were reversed by GW, suggesting that the transactivation of p21<sup>Cip1/WAF1</sup> by BRL occurs in a PPAR $\gamma$ -dependent manner (Fig. 4B). Since the deleted mutant p21<sup>Cip1/WAF1</sup>  $\Delta$ p53 encoding the region from –124 to +11 expresses multiple Sp1 sites, we performed transfection experiments using mithramycin, a specific inhibitor of GC binding (Blume *et al.* 1991). The transactivation of this construct induced by BRL was abrogated by mithramycin, indicating an involvement of Sp1 transcription factor in the PPAR $\gamma$  action observed in WRO and FRO cells (Fig. 4B).

### BRL binds to Sp1 sites of the p21<sup>Cip1/WAF1</sup> promoter gene in EMSA

In order to further support whether Sp1 sites mediate the BRL-induced upregulation of p21<sup>Cip1/WAF1</sup>, we performed EMSA using synthetic oligodeoxyribonucleotides corresponding to the Sp1 site located in the human p21<sup>Cip1/WAF1</sup> gene promoter, as probe. In nuclear extracts from WRO cells (Fig. 5A) we obtained the formation of specific bands (lane 1), which were strongly increased in cells treated with BRL (lane 2). Competition binding studies demonstrated that a 100-fold molar excess of unlabeled probe inhibited the formation of these complexes (lane 3). The addition of mithramycin, which binds to GC boxes and prevents sequential Sp1 binding, decreased the intensity of the bands to Sp1 DNA sequence (lane 4). Of note, the anti-PPAR $\gamma$  and anti-Sp1 antibodies (lanes 5 and 6 respectively) were able to supershift the specific bands. Different controls were used to assess the specificity of the binding; IgG that did not generate supershifted bands (lane 7), human Sp1 recombinant protein alone (lane 8), and Sp1 in combination with either cold competitor (lane 9) or the anti-Sp1 antibody (lane 10). As shown in Fig. 5B, similar results, such as an increased DNA-binding complex under BRL (lane 2), a reduction of the band intensity by using mithramycin (lane 4), and supershifted bands in the presence of the anti-PPAR $\gamma$  and anti-Sp1 antibodies (lanes 5 and 6) were obtained in FRO cells.

### Functional interaction of PPAR $\gamma$ with p21<sup>Cip1/WAF1</sup> by ChIP and reChIP assays

The interaction of PPAR $\gamma$  with the p21<sup>Cip1/WAF1</sup> gene promoter was further investigated by ChIP assay. WRO and FRO chromatin were immunoprecipitated with the anti-PPAR $\gamma$ , the anti-Sp1, the anti-RNA Pol II, the anti-acetyl histone H3, and the anti-trimethyl histone H3 antibodies. The PPAR $\gamma$  immunoprecipitated chromatin was re-immunoprecipitated with the anti-Sp1 antibody. PCR was used to determine the recruitment of PPAR $\gamma$  to the p21<sup>Cip1/WAF1</sup> region containing the Sp1 site. As shown in Fig. 6A, the results indicated that PPAR $\gamma$  was weakly and constitutively bound to the p21<sup>Cip1/WAF1</sup> promoter in untreated cells and this recruitment was increased upon BRL treatment, while in the presence of mithramycin the BRL effect was reversed in both thyroid cancer cells. Histone modification plays an important role in controlling gene expression (He & Lehming 2003). For example, acetylation of histone H3 at lysine 9 and methylation of histone H3 at lysine 9 are associated



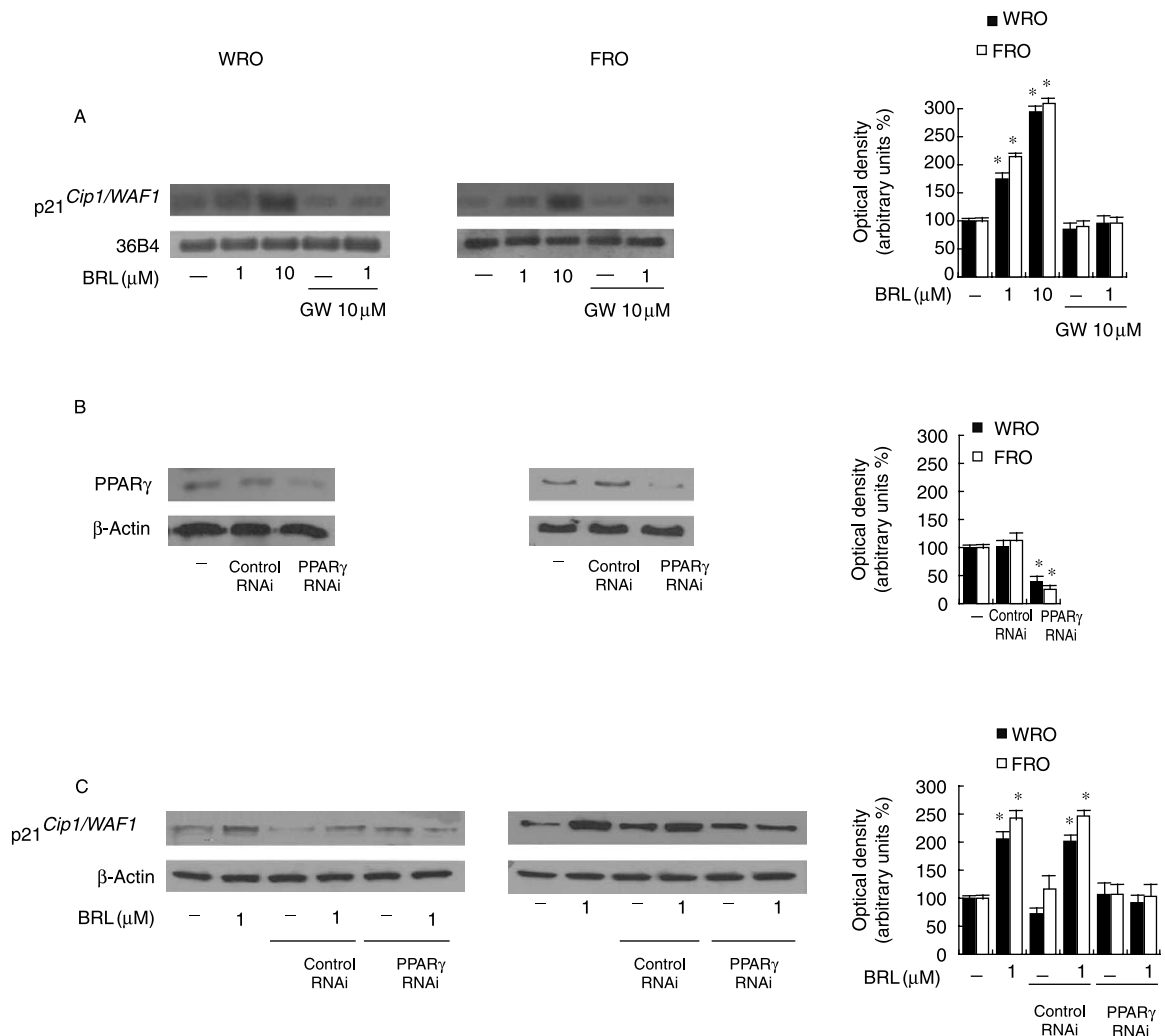


**Figure 3** BRL upregulates p21<sup>Cip1/WAF1</sup> mRNA expression. (A) Semiquantitative RT-PCR evaluation of p21<sup>Cip1/WAF1</sup> mRNA expression in WRO and FRO cells treated for 24 h in the presence of vehicle (–) or with treatments as indicated. 36B4 mRNA levels were determined as control. In the side panel is shown the quantitative representation of data (mean ± s.d.) of three independent experiments included that presented in A after densitometry and correction for 36B4 expression. \**P* < 0.05 BRL-treated versus untreated cells. (B) PPAR<sub>γ</sub> protein expression (evaluated by WB) in WRO and FRO cells not transfected (–) or transfected with 25 nucleotide of validated RNA interference (RNAi) targeted human PPAR<sub>γ</sub> mRNA sequence (PPAR<sub>γ</sub> RNAi) or with stealth RNAi negative control (control RNAi), as reported in Materials and methods. β-Actin was used as loading control. The side panel shows the quantitative representation of data (mean ± s.d.) of three independent experiments included that presented in B. (C) Immunoblots of p21<sup>Cip1/WAF1</sup> in thyroid cancer cells treated in the presence of vehicle (–) or with BRL 1 μM, transfected using PPAR<sub>γ</sub> RNAi or control RNAi. β-Actin was used as loading control. The side panel shows the quantitative representation of data (mean ± s.d.) of three independent experiments included that presented in C.

with transcriptional activation and repression respectively. Besides, since it was speculated that increased degrees of H3 Lys9 methylation are associated with an increased stability of silencing (Rice *et al.* 2003; mono- versus di- versus tri-), we used a specific anti-H3 trimethylated at lysine 9 antibody. Noteworthy, an increased recruitment of H3 acetylated at lysine 9 and a reduction of H3 trimethylated at lysine 9 upon BRL treatment was observed. In addition, the positive

regulation of the p21<sup>Cip1/WAF1</sup> transcription activity through Sp1 induced by BRL was demonstrated by the increased recruitment of RNA Pol II, which was reversed in the presence of mithramycin. Altogether, the data indicate that PPAR<sub>γ</sub> binding to the Sp1 transcription factor exerts stimulatory effects on p21<sup>Cip1/WAF1</sup> gene expression. The physical interaction between the PPAR<sub>γ</sub> and Sp1 proteins was strengthened by the ChIP/immunoblot assay (Fig. 6B).

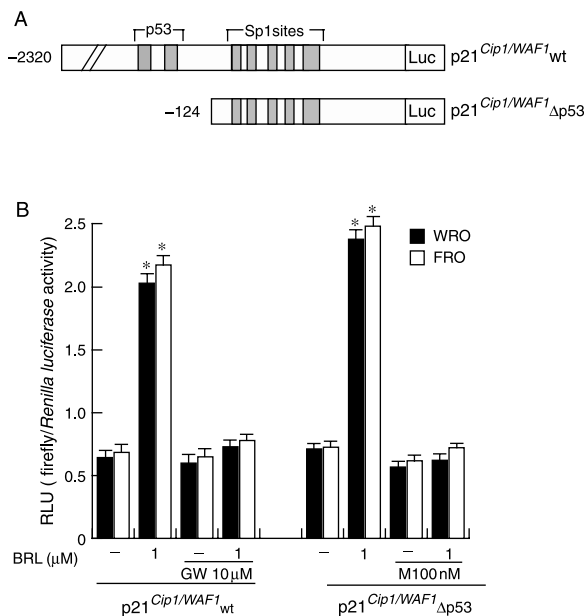


**Figure 4** BRL induces the transcriptional activity of p21<sup>Cip1/WAF1</sup> promoter gene. (A) Schematic map of the p21<sup>Cip1/WAF1</sup> promoter plasmids used in this study. (B) WRO and FRO cells were transiently transfected with the wild-type p21 promoter-luciferase (p21<sup>Cip1/WAF1</sup> wt) and then treated with vehicle (-), 1 μM BRL, 10 μM GW alone or in combination with BRL. Both thyroid cancer cells were transiently transfected with deleted construct (p21<sup>Cip1/WAF1</sup> Δp53) and then treated with vehicle (-), 1 μM BRL, 100 nM M alone or in combination with BRL. The luciferase activities were normalized to the *Renilla luciferase* as internal transfection control and data were reported as RLU values. Columns are mean ± s.d. of three independent experiments performed in triplicate. \*P < 0.05 BRL-treated versus untreated cells. RLU, relative light units; M, mithramycin.

### p21<sup>Cip1/WAF1</sup> antisense oligodeoxynucleotides prevent the BRL-induced growth inhibition in thyroid cancer cells

To confirm the BRL-induced growth inhibition of thyroid cancer cells through p21<sup>Cip1/WAF1</sup>, WRO and FRO cells were transfected with the p21<sup>Cip1/WAF1</sup> antisense (AS)-ODN or control scrambled (cs)-ODN in the proliferation assay. In previous studies, the utilization of AS-ODN of p21<sup>Cip1/WAF1</sup> *in vivo* and *in vitro* has been shown to be a sensitive way to examine its role in the inhibition of cell proliferation, angiogenesis, matrix protein production, and induction of apoptosis (Tian *et al.* 2000, Weiss *et al.* 2003). Noteworthy, the inhibitory effect exerted by BRL on cell proliferation was reversed by p21<sup>Cip1/WAF1</sup> AS-ODN but not by cs-ODN in both thyroid cancer cells (Fig. 7A) in which the p21<sup>Cip1/WAF1</sup> protein levels under these experimental conditions were assessed by WB (Fig. 7B). To support our data we evaluated a dose-dependence of the growth inhibition (Fig. 7C)

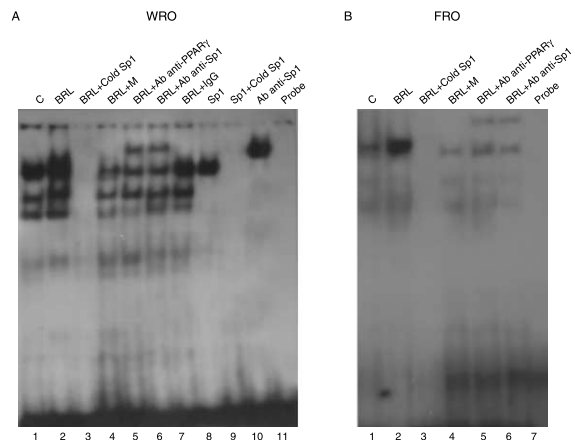


**Figure 5** BRL increases the binding to Sp1 sites located within the p21<sup>Cip1/WAF1</sup> promoter region in EMSA. (A) Nuclear extracts from WRO cells (lane 1) were incubated with a double-stranded Sp1 sequence probe labeled with [ $\gamma$ -<sup>32</sup>P] and subjected to electrophoresis in a 6% polyacrylamide gel. In lane 2, nuclear extracts were treated with 1 μM BRL. Competition experiments were performed adding as competitor a 100-fold molar excess of unlabeled Sp1 probe (lane 3) or 100 nM mithramycin (M) (lane 4). Anti-PPAR $\gamma$  and anti-Sp1 antibodies and IgG were incubated with nuclear extracts treated with BRL (lanes 5, 6, and 7). One microliter of human Sp1 recombinant protein (lane 8) was incubated with a double-stranded Sp1 sequence probe. A 100-fold molar excess of unlabeled Sp1 probe (lane 9) or anti-Sp1 antibody (lane 10) was added to Sp1 protein. Lane 11 contains probe alone. (B) Nuclear extracts from FRO cells were incubated with a double-stranded Sp1 sequence probe labeled with [ $\gamma$ -<sup>32</sup>P] and subjected to electrophoresis in a 6% polyacrylamide gel. In lane 2, nuclear extracts were treated with 1 μM BRL. Competition experiments were performed adding as competitor a 100-fold molar excess of unlabeled Sp1 probe (lane 3) or 100 nM mithramycin (M) (lane 4). Anti-PPAR $\gamma$  and anti-Sp1 antibodies were incubated with nuclear extracts treated with BRL (lanes 5 and 6 respectively). Lane 7 contains probe alone.

and the p21<sup>Cip1/WAF1</sup> induction (Fig. 7D) by PPAR $\gamma$ , transfecting in both thyroid cancer cell lines increasing doses of PPAR $\gamma$ -expressing vector (0.5, 1, and 2 μg). Taken together, these results indicate that the anti-proliferative effect exerted by BRL in thyroid cancer cells involves a positive crosstalk between PPAR $\gamma$ - and p21<sup>Cip1/WAF1</sup>-signaling pathway.

## Discussion

An inhibitory action of PPAR $\gamma$  in the thyroid tumors growth and progression was documented (Ohta *et al.* 2001, Martelli *et al.* 2002, Klopper *et al.* 2004, Aiello *et al.* 2006). Particularly, BRL and other thiazolidinediones inhibit thyroid carcinoma cell proliferation in a PPAR $\gamma$ -dependent fashion (Chung *et al.* 2002, Martelli *et al.* 2002, Klopper *et al.* 2004, Aiello *et al.* 2006, Chen *et al.* 2006, Copland *et al.* 2006), PPAR $\gamma$  mediates the upregulation of p21<sup>Cip1/WAF1</sup>

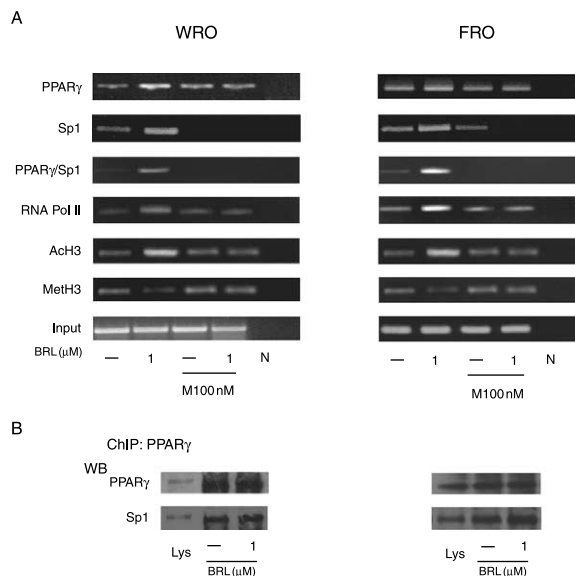


**Figure 6** Functional interaction between PPAR $\gamma$  and p21<sup>Cip1/WAF1</sup> promoter in ChIP and ReChIP assays. (A) WRO and FRO cells were treated as indicated, then cross-linked with formaldehyde, and lysed. The soluble chromatin was immunoprecipitated with the anti-PPAR $\gamma$ , anti-Sp1, anti-RNA Pol II, anti-acetyl histone H3 (AcH3), and anti-trimethyl histone H3 (MethH3) antibodies. Chromatin immunoprecipitated with the anti-PPAR $\gamma$  antibody was re-immunoprecipitated with the anti-Sp1 antibody. The p21<sup>Cip1/WAF1</sup> promoter sequence containing Sp1 was detected by PCR with specific primers, as described in Materials and methods. To control input DNA, the p21<sup>Cip1/WAF1</sup> promoter was amplified from 30  $\mu$ l initial preparations of soluble chromatin (before immunoprecipitations). N, negative control provided by PCR amplification without DNA sample; M, mithramycin. (B) Immunoblots of PPAR $\gamma$  and Sp1 from WRO and FRO cells treated with BRL 1  $\mu$ M in which chromatin was immunoprecipitated with the anti-PPAR $\gamma$  antibody. Lys, cell lysates.

(Chung *et al.* 2002, Han *et al.* 2004, Hong *et al.* 2004), p21<sup>Cip1/WAF1</sup> mediates PPAR $\gamma$ -induced growth arrest in cancer cells including thyroid (Han *et al.* 2004, Copland *et al.* 2006), and PPAR $\gamma$  mediates p21<sup>Cip1/WAF1</sup> mRNA induction via Sp1-enhanced binding to the p21<sup>Cip1/WAF1</sup>, KDR, and hormone-sensitive lipase promoters (Han *et al.* 2004, Hong *et al.* 2004, Sassa *et al.* 2004, Deng *et al.* 2006). In this report, we demonstrated that PPAR $\gamma$  acts as a tumor suppressor gene against two different human thyroid carcinoma cell lines. In both WRO, a well-differentiated thyroid follicular carcinoma and FRO, an undifferentiated/anaplastic thyroid carcinoma, PPAR $\gamma$  inhibits cell growth by stimulating the expression of the cyclin-dependent kinase inhibitor p21<sup>Cip1/WAF1</sup>.

From our study, the specific role of PPAR $\gamma$  in upregulating p21<sup>Cip1/WAF1</sup> raised by the evidence that this effect was completely abrogated either in the presence of specific siRNA to PPAR $\gamma$  or by the

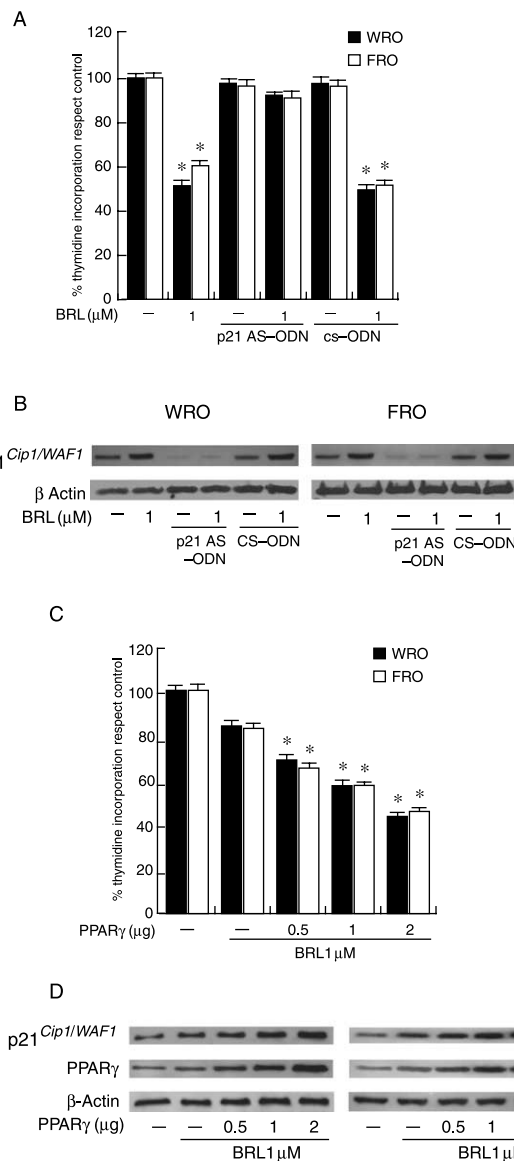


**Figure 7** The antiproliferative effects exerted by BRL in thyroid cancer cells are p21<sup>Cip1/WAF1</sup>-mediated. (A) WRO and FRO cells were treated in the presence of vehicle (-) or with BRL 1  $\mu$ M, transfected using p21<sup>Cip1/WAF1</sup> antisense (p21 AS) or control scrambled (cs) oligonucleotides (ODN) as indicated. On day 6, [<sup>3</sup>H]thymidine incorporation was determined by scintillation counting. Data are expressed as mean  $\pm$  s.d. of three independent experiments performed in triplicate. \**P* < 0.05 BRL-treated versus untreated cells. (B) Immunoblots of p21<sup>Cip1/WAF1</sup> from thyroid carcinoma cells treated as in A.  $\beta$ -Actin was used as the loading control. (C) WRO and FRO cells were treated in the presence of vehicle (-) or with BRL 1  $\mu$ M and transfected with increasing doses of PPAR $\gamma$  expression plasmid. After 48 h, [<sup>3</sup>H]thymidine incorporation was determined by scintillation counting. Data are expressed as mean  $\pm$  s.d. of three independent experiments performed in triplicate. \**P* < 0.05 BRL-treated versus untreated cells. (D) Immunoblots of p21<sup>Cip1/WAF1</sup> and PPAR $\gamma$  from thyroid carcinoma cells treated as in C.  $\beta$ -Actin was used as loading control.

pretreatment with GW, a potent and selective antagonist of PPAR $\gamma$  that causes specific and irreversible loss of binding. The molecular events responsible for the induction of p21<sup>Cip1/WAF1</sup> by PPAR $\gamma$  ligands are consistent with the enhanced transcriptional activation of this gene as it raised by the capability of the ligand to activate the promoter of p21<sup>Cip1/WAF1</sup>. Then, we asked whether the above reported activation was direct or mediated by p53, being p21<sup>Cip1/WAF1</sup> a classic p53 responsive gene. Although, the p21<sup>Cip1/WAF1</sup> gene was first identified as a p53-inducible gene, more recently its induction was shown to occur via p53-independent mechanisms in various cell lines stimulated for differentiation and growth arrest, including thyroid carcinoma cells (Park et al. 2001). The p53 tumor suppressor gene is mutated in about half of most types of cancer arising from a wide spectrum of tissues (Bourdon 2007). As it is concerned with thyroid carcinoma, p53 mutations have rarely been detected in follicular carcinomas, while are more frequent (25–85%) in the anaplastic type (Ito et al. 1992, Nakamura et al. 1992, Donghi et al. 1993). In both thyroid cancer cell lines, p21<sup>Cip1/WAF1</sup> BRL transactivation occurred independent of p53 since the deletion of the two p53 response elements of the promoter maintains promoter activity. Moreover, since p53 levels do not respond to BRL treatment it is reasonable that the mechanism is p53-independent because our thyroid cancer cell lines have either mutated nonfunctional p53 (WRO cells) or scantily expressed p53 wild-type form (FRO cells), as reported previously (Fagin et al. 1993).

Multiple transcription factor binding sites within the human p21<sup>Cip1/WAF1</sup> promoter have been described to be able to interact with Sp1 including regulatory elements for Sp1 that play important roles in cell cycle arrest and apoptosis in carcinoma cells (Moon et al. 2006, Tvrdík et al. 2006, Fang et al. 2007). Sp1 has also been shown to interact directly with proteins of the basal transcription machinery such as TFIID components (Hilton & Wang 2003). On the other hand, Sp1 interacts physically and cooperates functionally with several sequence-specific activators including NF- $\kappa$ B, GATA, YY1, E2F1, Rb, and SREBP-1 (Noé et al. 1998, Rotheneder et al. 1999, Flück & Miller 2004, Zhang et al. 2005, Teferedegne et al. 2006). Sp1 has been considered traditionally as a ubiquitous factor associated closely with core promoter activities; it has recently been observed that it participates in several cases of regulated gene transcription triggered by multiple signaling pathways and metabolic or differentiation conditions. Different members of the nuclear hormone receptors, preferentially activate Sp1 and

other Sp family proteins binding to GC-rich sites that in turn regulate a large number of constitutive and induced mammalian genes (Scarpulla 2002).

Physical interaction of Sp1 with the progesterone receptor (Tseng et al. 2003), estrogen receptor (Panno et al. 2006, Li et al. 2007), and with the orphan receptor chicken ovalbumin upstream promoter transcription factor (Pipaón et al. 1999) has already been demonstrated. Recently, it has been showed that NRs can form ternary complexes with Sp1 and GC-rich DNA and in this complex NRs could also serve as auxiliary factors for Sp1 bound to GC-rich DNA (Husmann et al. 2000). Our data sustain this functional model of a tripartite complex of Sp1, PPAR $\gamma$ , and GC-rich DNA. For instance, in our study, EMSA and ChIP assays demonstrated the coexistence of the two proteins in the DNA-binding complexes, addressing that the functional interaction between PPAR $\gamma$  and Sp1 could modulate the activity of the human p21<sup>Cip1/WAF1</sup> promoter under basal other than BRL-inducible conditions in WRO and FRO cell lines. Our data show a discrepancy with those of previous publication in which Sp1 interacts with the consensus GC-rich sequence in p21<sup>Cip1/WAF1</sup> promoter gene and this band was not directly associated with PPAR $\gamma$  under the conditions used for the gel mobility shift assay (Hong et al. 2004). Besides, it has also been reported in another cell system that PPAR $\gamma$  ligands enhanced nuclear protein-binding activities of Sp1 and C/EBP sites in p21<sup>Cip1/WAF1</sup> promoter (Han et al. 2004). Our data show that treatment with mithramycin, a specific inhibitor of Sp1, completely reversed the activation of p21<sup>Cip1/WAF1</sup> promoter by BRL, suggesting furthermore that the interaction between PPAR $\gamma$  and Sp1 is essential for such activation.

Noteworthy, ChIP analysis also evidenced how the functional interaction between PPAR $\gamma$  and Sp1 in human p21<sup>Cip1/WAF1</sup> promoter is concomitant with an increase in the RNA Pol II recruitment, associated with an enhanced histone H3 acetylation and a reduced H3 methylation. All these events feature an 'open' chromatin conformation and address the coordinated action of the general transcription machinery with chromatin modifying and remodeling enzymes.

The crucial role of p21<sup>Cip1/WAF1</sup> in mediating the inhibitory effect of PPAR $\gamma$  in cell proliferation has been definitively demonstrated in thyroid cells transfected with p21 AS-ODN and with increasing PPAR $\gamma$  plasmid amounts in the cell growth assay. Finally, our findings evidenced how PPAR $\gamma$  inhibits thyroid cancer cell growth circumventing p53 mutation. This supports PPAR $\gamma$  agonists as single agents or as part of combination regimens in the

treatment of patients affected by follicular and particularly anaplastic thyroid cancer.

## Acknowledgements

This work was supported by ‘Epidemiologic Observatory Endemic Goiter and Iodine prophylaxis’, Calabria Region, Centro Sanitario, AIRC and MURST and Ex 60%, 2006. We thank Drs Massimo and Marco D’Erasmus (DBA Italia, Milan, Italy). The authors declare that there is no conflict of interest that would prejudice the impartiality of this scientific work.

## References

- Aiello A, Pandini G, Frasca F, Conte E, Murabito A, Sacco A, Genua M, Vigneri R & Belfiore A 2006 Peroxisomal proliferator-activated receptor-gamma agonists induce partial reversion of epithelial-mesenchymal transition in anaplastic thyroid cancer cells. *Endocrinology* **147** 4463–4475.
- Ain KB 1998 Anaplastic thyroid carcinoma: behaviour, biology, and therapeutic approaches. *Thyroid* **8** 715–726.
- Andrews NC & Faller DV 1991 A rapid micropreparation technique for extraction of DNA-binding proteins from limiting numbers of mammalian cells. *Nucleic Acids Research* **19** 2499.
- Auwerx J 1999 PPAR $\gamma$ , the ultimate thrifty gene. *Diabetologia* **42** 1033–1049.
- Blume SW, Snyder RC, Ray R, Thomas S, Koller CA & Miller DM 1991 Mithramycin inhibits SP1 binding and selectively inhibits transcriptional activity of the dihydrofolate reductase gene *in vitro* and *in vivo*. *Journal of Clinical Investigations* **88** 1613–1621.
- Bonofiglio D, Gabriele S, Aquila S, Catalano S, Gentile M, Middea E, Giordano F & Andò S 2005 Estrogen receptor alpha binds to peroxisome proliferator-activated receptor response element and negatively interferes with peroxisome proliferator-activated receptor gamma signaling in breast cancer cells. *Clinical Cancer Research* **11** 6139–6147.
- Bonofiglio D, Aquila S, Catalano S, Gabriele S, Belmonte M, Middea E, Qi H, Morelli C, Gentile M, Maggiolini M *et al.* 2006 Peroxisome proliferator-activated receptor-gamma activates p53 gene promoter binding to the nuclear factor-kappaB sequence in human MCF7 breast cancer cells. *Molecular Endocrinology* **20** 3083–3092.
- Bourdon JC 2007 p53 and its isoforms in cancer. *British Journal of Cancer* **97** 277–282.
- Chen Y, Wang SM, Wu JC & Huang SH 2006 Effects of PPARgamma agonists on cell survival and focal adhesions in a Chinese thyroid carcinoma cell line. *Journal of Cellular Biochemistry* **98** 1021–1035.
- Chung SH, Onoda N, Ishikawa T, Ogisawa K, Takenaka C, Yano Y, Hato F & Hirakawa K 2002 Peroxisome proliferator-activated receptor gamma activation induce cell cycle arrest via p53-independent pathway in human anaplastic thyroid cancer cells. *Japanese Journal of Cancer Research* **93** 1358–1365.
- Clay CE, Namen AM, Atsumi G, Willingham MC, High KP, Kute TE, Trimboli AJ, Fonteh AN, Dawson PA & Chilton FH 1999 Influence of J series prostaglandins on apoptosis and tumorigenesis of breast cancer cells. *Carcinogenesis* **20** 1905–1911.
- Copland JA, Marlow LA, Kurakata S, Fujiwara K, Wong AK, Kreinest PA, Williams SF, Haugen BR, Klopper JP & Smallridge RC 2006 Novel high-affinity PPAR $\gamma$  agonist alone and in combination with paclitaxel inhibits human anaplastic thyroid carcinoma tumor growth via p21WAF1/CIP1. *Oncogene* **25** 2304–2317.
- Deng T, Shan S, Li PP, Shen ZF, Lu XP, Cheng J & Ning ZQ 2006 Peroxisome proliferator-activated receptor-gamma transcriptionally up-regulates hormone-sensitive lipase via the involvement of specificity protein-1. *Endocrinology* **147** 875–884.
- Desvergne B & Wahli W 1999 Peroxisome proliferator-activated receptors: nuclear control of metabolism. *Endocrine Reviews* **20** 649–688.
- Donghi R, Longoni A, Pilotti S, Michieli P, Della Porta G & Pierotti MA 1993 P53 mutation are restricted to poorly differentiated and undifferentiated carcinomas of the thyroid gland. *Journal of Clinical Investigations* **91** 1753–1760.
- el-Diery WS, Tokino T, Velculescu VE, Levy DB, Parsons R, Trent JM, Lin D, Mercer WE, Kinzler KW & Vogelstein B 1993 WAF1, a potential mediator of p53 tumor suppression. *Cell* **75** 817–825.
- Elstner E, Mueller C, Koshizuka K, Williamson EA, Park D, Asou H, Shintaku P, Said JW, Heber D & Koeffler HP 1998 Ligands for peroxisome proliferator-activated receptor gamma and renoic acid receptor inhibit growth and induce apoptosis of human breast cancer cells *in vitro* and in BNX mice. *PNAS* **95** 8806–8811.
- Fagin JA, Matsuo K, Karmakar A, Chen DL, Tang SH & Koeffler HP 1993 High prevalence of mutations of the p53 gene in poorly differentiated human thyroid carcinomas. *Journal of Clinical Investigations* **91** 179–184.
- Fang Z, Fu Y, Liang Y, Li Z, Zhang W, Jin J, Yang Y & Zha X 2007 Increased expression of integrin beta1 subunit enhances p21WAF1/Cip1 transcription through the Sp1 sites and p300-mediated histone acetylation in human hepatocellular carcinoma cells. *Journal of Cellular Biochemistry* **101** 654–664.
- Flück CE & Miller WL 2004 GATA-4 and GATA-6 modulate tissue-specific transcription of the human gene for P450c17 by direct interaction with Sp1. *Molecular Endocrinology* **18** 1144–1157.
- Han S, Sidell N, Fisher BP & Roman J 2004 Up-regulation of p21 gene expression by peroxisome proliferator-activated receptor  $\gamma$  in human lung carcinoma cells. *Clinical Cancer Research* **10** 1911–1919.

- He H & Lehming N 2003 Global effects of histone modifications. *Briefings in Functional Genomics & Proteomics* **2** 234–243.
- Hilton TL & Wang EH 2003 Transcription factor IID recruitment and Sp1 activation. Dual function of TAF1 in cyclin D1 transcription. *Journal of Biological Chemistry* **278** 12992–13002.
- Hong J, Samudio I, Liu S, Abdelrahim M & Safe S 2004 Peroxisome proliferator-activated receptor  $\gamma$ -dependent activation of p21 in panc-28 pancreatic cancer cells involves Sp1 and Sp4 proteins. *Endocrinology* **145** 5774–5785.
- Husmann M, Dragneva Y, Romahn E & Jehnichen P 2000 Nuclear receptors modulate the interaction of Sp1 and GC-rich DNA via ternary complex formation. *Biochemical Journal* **352** 763–772.
- Ito T, Seyama T, Mizuno T, Tsuyama N, Hayashi T & Hayashi Y 1992 Unique association of p53 mutations with undifferentiated but not with differentiated carcinomas of thyroid gland. *Cancer Research* **52** 1369–1371.
- Jiang H, Lin J, Su ZZ, Collart FR, Huberman E & Fisher PB 1994 Induction of differentiation in human promyelocytic HL-60 leukemia cells activates p21, WAF1/CIP1, expression in absence of p53. *Oncogene* **9** 3397–3406.
- Klopper JP, Hays WR, Sharma V, Baumbusch MA, Hershman JM & Haugen BR 2004 Retinoid X receptor-gamma and peroxisome proliferator-activated receptor-gamma expression predicts thyroid carcinoma cell response to retinoid and thiazolidinedione treatment. *Molecular Cancer Therapeutics* **3** 1011–1020.
- Kondo T, Ezzat S & Asa SL 2006 Pathogenetic mechanisms in thyroid follicular-cell neoplasia. *Nature Reviews. Cancer* **6** 292–306.
- Kuboto T, Koshizuka K, Williamson IA, Asou H, Said JW, Holden S, Miyoshi I & Koeffler HP 1998 Ligand of peroxisome proliferator-activated receptor gamma (rosiglitazone) has potent anti-tumor effects agonist human prostate cancer both *in vitro* and *in vivo*. *Cancer Research* **58** 3344–3352.
- Li Y, Jenkins CW, Nichols MA & Xiong Y 1994 Cell cycle expression and p53 regulation of cyclin-dependent kinase inhibitor p21. *Oncogene* **9** 2261–2268.
- Li D, Mitchell D, Luo J, Yi Z, Cho SG, Guo J, Li X, Ning G, Wu X & Liu M 2007 Estrogen regulates KiSS1 gene expression through estrogen receptor alpha and SP protein complexes. *Endocrinology* **148** 4821–4828.
- Liu S, Semenciw R, Ugnat AM & Mao Y 2001 Increasing thyroid cancer incidence in Canada, 1970–1996: time trends and age-period-cohort effects. *British Journal of Cancer* **85** 1335–1339.
- Maggiolini M, Donzè O & Picard D 1999 A non-radioactive method for inexpensive quantitative RT-PCR. *Biological Chemistry* **380** 695–697.
- Martelli ML, Iuliano R, Le Pera I, Samà I, Monaco C, Cammarota S, Kroll T, Chiariotti L, Santoro M & Fusco A 2002 Inhibitory effects of peroxisome proliferator-activated receptor gamma on thyroid carcinoma cell growth. *Journal of Clinical Endocrinology and Metabolism* **87** 4728–4735.
- Moon SK, Choi YH, Kim CH & Choi WS 2006 p38MAPK mediates benzyl isothiocyanate-induced p21WAF1 expression in vascular smooth muscle cells via the regulation of Sp1. *Biochemical and Biophysical Research Communications* **350** 662–668.
- Mueller E, Sarraf P, Tontonoz P, Evans RM, Martin KJ, Zhang M, Flecher C, Singer S & Spiegelman BM 1998 Terminal differentiation of human breast cancer through PPAR $\gamma$ . *Molecular Cell* **1** 465–470.
- Nakamura T, Yana I, Kobayashi T, Shin E, Karakawa K, Fujita S, Miya A, Mori T, Nishisho I & Takai S 1992 P53 gene mutations associated with anaplastic transformation of human thyroid carcinomas. *Japanese Journal of Cancer Research* **83** 1293–1298.
- Noé V, Alemany C, Chasin LA & Ciudad CJ 1998 Retinoblastoma protein associates with SP1 and activates the hamster dihydrofolate reductase promoter. *Oncogene* **16** 1931–1938.
- Ohta K, Endo T, Haraguchi K, Hershman JM & Onaya T 2001 Ligands for peroxisome proliferator-activated receptor gamma inhibit growth and induce apoptosis of human papillary thyroid carcinoma cells. *Journal of Clinical Endocrinology and Metabolism* **86** 2170–2177.
- Panno ML, Mauro L, Marsico S, Bellizzi D, Rizza P, Morelli C, Salerno M, Giordano F & Andò S 2006 Evidence that the mouse insulin receptor substrate-1 belongs to the gene family on which the promoter is activated by estrogen receptor alpha through its interaction with Sp1. *Journal of Molecular Endocrinology* **36** 91–105.
- Park JW, Jang MA, Lee YH, Passaniti A & Kwon TK 2001 p53-independent elevation of p21 expression by PMA results from PKC-mediated mRNA stabilization. *Biochemical and Biophysical Research Communications* **280** 244–248.
- Parkin DM, Bray F, Ferlay J & Pisani P 2005 Global cancer statistics, 2002. *CA: A Cancer Journal for Clinicians* **55** 74–108.
- Pipaón C, Tsai SY & Tsai MJ 1999 COUP-TF upregulates NGFI-A gene expression through an Sp1 binding site. *Molecular and Cellular Biology* **19** 2734–2745.
- Rice JC, Briggs SD, Ueberheide B, Barber CM, Shabanowitz J, Hunt DF, Shinkai Y & Allis CD 2003 Histone methyltransferases direct different degrees of methylation to define distinct chromatin domains. *Molecular Cell* **12** 1591–1598.
- Rotheneder H, Geymayer S & Haidweger E 1999 Transcription factors of the Sp1 family: interaction with E2F and regulation of the murine thymidine kinase promoter. *Journal of Molecular Biology* **293** 1005–1015.
- Sassa Y, Hata Y, Aiello LP, Taniguchi Y, Kohno K & Ishibashi T 2004 Bifunctional properties of peroxisome proliferator-activated receptor gamma1 in KDR gene regulation mediated via interaction with both Sp1 and Sp3. *Diabetes* **53** 1222–1229.

- Scarpulla RC 2002 Transcriptional activators and coactivators in the nuclear control of mitochondrial function in mammalian cells. *Gene* **286** 81–89.
- Teferedegne B, Green MR, Guo Z & Boss JM 2006 Mechanism of action of a distal NF- $\kappa$ B-dependent enhancer. *Molecular and Cellular Biology* **26** 5759–5770.
- Tian H, Wittmack EK & Jorgensen TJ 2000 p21WAF1/CIP1 antisense therapy radiosensitizes human colon carcinoma by converting growth arrest to apoptosis. *Cancer Research* **60** 679–684.
- Tontonoz P, Singer S, Forman BM, Sarraf P, Fletcher JA, Flechter CD, Brun RP, Mueller E, Altiock S, Oppenheim H *et al.* 1997 Terminal differentiation of human liposarcoma cells induce by ligands for peroxisome proliferator-activated receptor gamma and the retinoid X receptor. *PNAS* **94** 237–241.
- Tseng L, Tang M, Wang Z & Mazella J 2003 Progesterone receptor (hPR) upregulates the fibronectin promoter activity in human decidual fibroblasts. *DNA and Cell Biology* **22** 633–640.
- Tvrđík D, Dunder P, Povýsil C, Pytlík R & Planková M 2006 Up-regulation of p21WAF1 expression is mediated by Sp1/Sp3 transcription factors in TGF $\beta$ 1-arrested malignant B cells. *Medical Science Monitor* **12** 227–234.
- Vousden KH & Lu X 2002 Live or let die: the cell's response to p53. *Nature Reviews. Cancer* **2** 594–604.
- Weiss RH, Marshall D, Howard L, Corbacho AM, Cheung AT & Sawai ET 2003 Suppression of breast carcinoma growth and angiogenesis by an antisense oligodeoxynucleotide to p21 (WAF1/CIP1). *Cancer Letters* **189** 39–48.
- Wu RC & Schonthal AH 1997 Activation of p53-p21waf1 pathway in response to disruption of cell–matrix interactions. *Journal of Biological Chemistry* **272** 29091–29098.
- Zhang C, Shin DJ & Osborne TF 2005 A simple promoter containing two Sp1 sites controls the expression of sterol-regulatory-element-binding protein 1a (SREBP-1a). *Biochemical Journal* **386** 161–168.

# Peroxisome proliferator-activated receptor gamma activates fas ligand gene promoter inducing apoptosis in human breast cancer cells

Daniela Bonofiglio · Sabrina Gabriele · Saveria Aquila ·  
Hongyan Qi · Maria Belmonte · Stefania Catalano ·  
Sebastiano Andò

Received: 12 February 2008 / Accepted: 12 February 2008  
© Springer Science+Business Media, LLC. 2008

**Abstract** In just over a decade, apart from established metabolic actions, peroxisome proliferator-activated receptor gamma (PPAR $\gamma$ ) has evolved as key therapeutic target in cancer disease. Fas ligand (FasL), a trans-membrane protein, induces apoptosis by crosslinking with the Fas receptor. Despite the FasL relevance, little is available on the regulation of its expression. In the current study, we explored for the first time the potential role of PPAR $\gamma$  in triggering apoptotic events through the Fas/FasL pathway in breast cancer cells. In MCF7 cells, by reverse transcription-polymerase chain reaction and Western blotting, we showed that the synthetic PPAR $\gamma$  ligand rosiglitazone (BRL) enhanced FasL expression, that was abrogated by a specific PPAR $\gamma$  antagonist GW9662. Transient transfection assays demonstrated that BRL transactivated human FasL promoter gene in a PPAR $\gamma$ -dependent manner. Progressive 5' deletion analysis has identified a minimal promoter

fragment spanning nucleotides from -318 to -237 bp, which is still sensitive to BRL treatment. FasL promoter activity was abrogated by mithramycin, suggesting an involvement of Sp1 transcription factor in PPAR $\gamma$  action. Electrophoretic mobility shift and chromatin immunoprecipitation assays demonstrated that BRL increased the binding of PPAR $\gamma$  and Sp1 to the Sp1 sequence located within the FasL gene promoter. The role of PPAR $\gamma$  and Fas/FasL pathways in BRL-induced apoptotic events was assessed by caspase 8 cleavage in the presence of GW as well as PPAR $\gamma$  and FasL RNA interferences. Our results indicate that PPAR $\gamma$  positively regulates the FasL gene expression also in MDA-MB231 and in BT20, revealing a new molecular mechanism by which BRL induces apoptosis in breast cancer cells.

**Keywords** PPAR $\gamma$  · FasL · Apoptosis · Caspase 8 · Breast cancer

## Abbreviations

PPAR $\gamma$	Peroxisome proliferator-activated receptor gamma
BRL	Rosiglitazone
MDA	MDA-MB231
RT-PCR	Reverse transcription-polymerase chain reaction
WB	Western blotting
FasL	Fas ligand
EMSA	Electrophoretic mobility shift assay
ChIP	Chromatin immuno-precipitation

## Introduction

Since its discovery at previous decade, it became clear that peroxisome proliferator-activated receptor gamma (PPAR $\gamma$ )

The authors Daniela Bonofiglio and Sabrina Gabriele equally contributed to this work. This work was supported by AIRC, MURST and Ex 60%.

D. Bonofiglio · S. Gabriele · S. Aquila · H. Qi · M. Belmonte ·  
S. Catalano  
Department of Pharmaco-Biology, University of Calabria,  
Arcavacata di Rende, Cosenza 87036, Italy

S. Aquila · S. Catalano · S. Andò  
Centro Sanitario, University of Calabria, Arcavacata di Rende,  
Cosenza 87036, Italy

S. Andò (✉)  
Faculty of Pharmacy, University of Calabria, Arcavacata di  
Rende, Cosenza 87036, Italy  
e-mail: sebastiano.ando@unical.it

S. Andò  
Department of Cellular Biology, University of Calabria,  
Arcavacata di Rende, Cosenza 87036, Italy



is an important modulator in the regulation of complex pathways of mammalian cells' metabolism and recently implicated in cancer [1–3]. Several antineoplastic effects, such as induction of apoptosis and differentiation, have been described as a result of PPAR $\gamma$ -mediated action both in vitro and in vivo [4–10], although the molecular mechanisms by which PPAR $\gamma$  causes these effects remain to be fully elucidated. PPAR $\gamma$  is able to be activated by ligands of physiological or pharmacological origin [11]. Synthetic PPAR $\gamma$  ligands are the thiazolidinediones (TZDs), a class of oral antidiabetic agents, which exert anti-tumoral effects depending on the experimental and cellular settings and in a PPAR $\gamma$ -dependent or PPAR $\gamma$ -independent fashion [12, 13].

In mammals, apoptosis can be initiated by two major routes: the intrinsic and extrinsic death pathways [14]. The intrinsic pathway is triggered in response to a variety of apoptotic stimuli that produce damage within the cell, including anticancer agents, oxidative damage, UV irradiation, and is mediated through the mitochondria. The extrinsic pathway is activated by extracellular ligands able to induce oligomerization of death receptors, such as Fas (also called CD95 or APO1) or other members of the tumor necrosis factor receptor superfamily leading to apoptosis [15].

Fas ligand (FasL), a type II transmembrane protein expressed on the surface of cells, induces apoptotic cell death by binding to its receptor Fas [16, 17]. This binding results in recruitment of the Fas-associated death domain (FADD) protein and caspase 8 zymogens to the receptor and the formation of the death-inducing signalling complex, after which the caspases cascade can be activated [18]. Defects in the Fas/FasL apoptotic signalling pathway provide a survival advantage to cancer cells and may be implicated in tumorigenesis [19]. Recent evidence has indicated the Fas pathway in the induction of tumor cell death and FasL expression has been observed in different tumors including breast cancer [20–22]. It has also been suggested that FasL functions as an autocrine/paracrine mediator of apoptosis induced by DNA-damaging anticancer chemotherapeutic agents [23, 24].

In the past few years, we have investigated different molecular mechanisms through which PPAR $\gamma$  induces anti-proliferative effects, cell cycle arrest and apoptosis in human MCF7 breast cancer cells [25, 26]. In this study, we reported for the first time that PPAR $\gamma$  directly activates FasL promoter gene inducing apoptotic events in breast cancer cells.

## Materials and methods

### Cell cultures

Human MCF7 (a gift from Dr. Ewa Surmacz, Sbarro Institute for Cancer Research and Molecular Medicine,

Philadelphia, USA) MDA-MB231 (ER $\alpha$ -negative, MDA) breast cancer cells were grown in DMEM plus glutamax containing 10% fetal calf serum (FCS) (Invitrogen, Milan, Italy) and 1 mg/ml penicillin–streptomycin (P/S). BT20 (insulin receptor substrate-1, IRS-1 negative) breast cancer cells were grown in MEM added as DMEM.

### Reagents

Rosiglitazone (BRL49653, BRL) was from Alexis (San Diego, CA USA), the irreversible PPAR $\gamma$ -antagonist GW and the Sp1 specific inhibitor, mithramycin were from Sigma (Milan, Italy).

### Plasmids

The firefly luciferase reporter plasmids containing FasL promoter wild-type (FasL Luc-0) or its deletion mutants (FasL Luc-3 and FasL Luc-4) were kind gifts from Dr. Carlos V. Paya (Mayo Clinic, Rochester, Minnesota, USA). Deletion of Sp1 sequence in FasL gene promoter was generated by PCR using as template FasL Luc-3 (p-318 construct). The resulting plasmid encoding the human FasL gene promoter containing the desired deletion was designed FasL Luc-3  $\Delta$ Sp1 and the sequence was confirmed by nucleotide sequence analysis [27]. As an internal transfection control, we co-transfected the plasmid pRL-CMV (Promega Corp., Milan, Italy) that expresses Renilla luciferase enzymatically distinguishable from firefly luciferase by the strong cytomegalovirus enhancer/promoter.

### Immunoblotting

Cells were grown in 10 cm dishes to 70–80% confluence and exposed to treatments in serum free medium (SFM) as indicated. Cells were then harvested in cold phosphate-buffered saline (PBS) and resuspended in lysis buffer containing 20 mM HEPES pH 8, 0.1 mM EDTA, 5 mM MgCl<sub>2</sub>, 0.5 M NaCl, 20% glycerol, 1% NP-40, inhibitors (0.1 mM Na<sub>3</sub>VO<sub>4</sub>, 1% PMSF, 20 mg/ml aprotinin). Protein concentration was determined by Bio-Rad Protein Assay (Bio-Rad Laboratories, Hercules, CA USA). A 60  $\mu$ g portion of protein lysates was used for WB resolved on a 12% SDS-polyacrylamide gel, transferred to a nitrocellulose membrane and probed with antibodies (Abs) directed against the FAS, FasL and PPAR $\gamma$  (Santa Cruz Biotechnology, CA USA), caspase 8 (Biomol International, Butler Pike Plymouth, PA USA). As internal control, all membranes were subsequently stripped (glycine 0.2 M, pH 2.6 for 30 min at room temperature) of the first antibody and reprobed with anti- $\beta$ -actin Ab (Santa Cruz Biotechnology).

The antigen–antibody complex was detected by incubation of the membranes for 1 h at room temperature with

the appropriated secondary antibodies peroxidase-coupled and revealed using the enhanced chemiluminescence system (ECL system, Amersham Pharmacia, Buckinghamshire, UK). Blots were then exposed to film (Kodak film, Sigma). The intensity of bands representing relevant proteins was measured by Scion Image laser densitometry scanning program.

#### Reverse transcription-polymerase chain reaction (RT-PCR) assay

MCF7 cells were grown in 10 cm dishes to 70–80% confluence and exposed to treatments for 24 h in SFM. Total cellular RNA was extracted using TRIZOL reagent (Invitrogen) as suggested by the manufacturer. The purity and integrity were checked spectroscopically and by gel electrophoresis before carrying out the analytical procedures. The evaluation of gene expression was performed by semiquantitative RT-PCR method as previously described [28]. For FasL and the internal control gene 36B4, the primers were: 5'-GGA ATG GGA AGA CAC CTA TGG A-3' (FasL forward) and 5'-AGA GAG AGC TCA GAT ACG TTG AC-3' (FasL reverse), 5'-CTC AAC ATC TCC CCC TTC TC-3' (36B4 forward) and 5'-CAA ATC CCA TAT CCT CGT CC-3' (36B4 reverse) to yield respectively products of 299 bp with 25 cycles and 408 bp with 12 cycles. The results obtained as optical density arbitrary values were transformed to percentage of the control (percent control) taking the samples from untreated cells as 100%.

#### Transient transfection assay

MCF7 cells were transferred into 24 well plates with 500  $\mu$ l of regular growth medium/well the day before transfection. The medium was replaced with SFM on the day of transfection, which was performed using Fugene 6 reagent as recommended by the manufacturer (Roche Diagnostics, Mannheim, Germany) with a mixture containing 0.5  $\mu$ g of promoter-luciferase reporter plasmid and 5 ng of pRL-CMV. After 24 h transfection, treatments were added in SFM as indicated and cells were incubated for further 24 h, cells were pre-treated for 2 h with mithramycin or GW where necessary. Firefly and Renilla luciferase activities were measured using the Dual Luciferase Kit (Promega). The firefly luciferase values of each sample were normalized by Renilla luciferase activity and data were reported as Relative Light Units (RLU) values.

#### Electrophoretic mobility shift assay (EMSA)

Nuclear extracts from MCF7 cells were prepared as previously described [29]. Briefly, MCF7 cells plated into 10 cm

dishes were grown to 70–80% confluence shifted to SFM for 24 h and then treated with 1  $\mu$ M BRL for 6 h. Thereafter, cells were scraped into 1.5 ml of cold PBS. Cells were pelleted for 10 s and resuspended in 400  $\mu$ l cold buffer A (10 mM HEPES-KOH pH 7.9 at 4°C, 1.5 mM MgCl<sub>2</sub>, 10 mM KCl, 0.5 mM dithiothreitol, 0.2 mM PMSF, 1 mM leupeptin) by flicking the tube. The cells were allowed to swell on ice for 10 min and then vortexed for 10 s. Samples were centrifuged for 10 s and the supernatant fraction discarded. The pellet was resuspended in 50  $\mu$ l of cold Buffer B (20 mM HEPES-OH pH 7.9, 25% glycerol, 1.5 mM MgCl<sub>2</sub>, 420 mM NaCl, 0.2 mM EDTA, 0.5 mM dithiothreitol, 0.2 mM PMSF, 1 mM leupeptin) and incubated in ice for 20 min for high-salt extraction. Cellular debris were removed by centrifugation for 2 min at 4°C and the supernatant fraction (containing DNA binding proteins) was stored at -70°C. The probe was generated by annealing single stranded oligonucleotides and labeled with [ $\gamma$ -<sup>32</sup>P] ATP (Amersham Pharmacia) and T4 polynucleotide kinase (Promega) and then purified using Sephadex G50 spin columns (Amersham Pharmacia). The DNA sequence, containing the Sp1, NFAT and NF $\kappa$ B sites, obtained from the native FasL promoter gene used as probe or as cold competitor is the following: 5'-A AAT TGT GGG CGG AAA CTT CCA GGG-3' (Sigma). As cold competitor we also used  $\Delta$ Sp1 oligonucleotide: 5'-AT TGT GTT CGG AAA CTT CCA GGG-3',  $\Delta$ NFAT oligonucleotide: 5'-A AAT TGT GGG CGG TCA CT TCCA GGG-3' and  $\Delta$ NF $\kappa$ B oligonucleotide: 5'-A AAT TGT GGG CGG AAA CAT ATA GGG-3' (Sigma). The protein binding reactions were carried out in 20  $\mu$ l of buffer [20 mM Hepes pH 8, 1 mM EDTA, 50 mM KCl, 10 mM DTT, 10% glycerol, 1 mg/ml BSA, 50  $\mu$ g/ml poly dI/dC] with 50,000 cpm of labeled probe, 5  $\mu$ g of MCF7 nuclear protein and 5  $\mu$ g of poly (dI-dC). The mixtures were incubated at room temperature for 20 min in the presence or absence of unlabeled competitors oligonucleotides. For in vitro mithramycin treatment, 100 nM mithramycin were incubated with the labelled probe for 30 min at 4°C before the addition of nuclear extract. For the experiments involving the anti-PPAR $\gamma$  and anti-Sp1 Abs (Santa Cruz Biotechnology), the reaction mixture was incubated with Ab at 4°C for 30 min before addition of labeled probe. The entire reaction mixture was electrophoresed through a 6% polyacrylamide gel in 0.25  $\times$  Tris borate-EDTA for 3 h at 150 V. Gel was dried and subjected to autoradiography at -70°C.

#### Chromatin immunoprecipitation (ChIP) and Re-ChIP assays

For ChIP assay, MCF7 cells were grown in 10 cm dishes to 50–60% confluence, shifted to SFM for 24 h and then treated with 1  $\mu$ M BRL for 1 h or pre-incubated with

mithramycin for 1 h where required. Thereafter, cells were washed twice with PBS and crosslinked with 1% formaldehyde at 37°C for 10 min. Next, cells were washed twice with PBS at 4°C, collected and resuspended in 200 µl of lysis buffer (1% SDS, 10 mM EDTA, 50 mM Tris-HCl pH 8.1) and left on ice for 10 min. Then, cells were sonicated four times for 10 s at 30% of maximal power (Sonics, Vibra Cell 500 W) and collected by centrifugation at 4°C for 10 min at 14,000 rpm. The supernatants were diluted in 1.3 ml of IP buffer (0.01% SDS, 1.1% Triton X-100, 1.2 mM EDTA, 16.7 mM Tris-HCl pH 8.1, 16.7 mM NaCl) followed by immunoclearing with 80 µl of sonicated salmon sperm DNA/protein A agarose (UBI, DBA Srl, Milan—taly) for 1 h at 4°C. The precleared chromatin was immunoprecipitated with anti-PPAR $\gamma$  Ab and re-immunoprecipitated with anti-RNA Pol II Ab (Santa Cruz Biotechnology). At this point, 60 µl salmon sperm DNA/protein A agarose were added and precipitation was further continued for 2 h at 4°C. After pelleting, precipitates were washed sequentially for 5 min with the following buffers: Wash A (0.1% SDS, 1% Triton X-100, 2 mM EDTA, 20 mM Tris-HCl pH 8.1, 150 mM NaCl), Wash B (0.1% SDS, 1% Triton X-100, 2 mM EDTA, 20 mM Tris-HCl pH 8.1, 500 mM NaCl), and Wash C (0.25 M LiCl, 1% NP-40, 1% sodium deoxycholate, 1 mM EDTA, 10 mM Tris-HCl pH 8.1), and then twice with TE buffer (10 mM Tris, 1 mM EDTA). The immunocomplexes were eluted with elution buffer (1% SDS, 0.1 M NaHCO<sub>3</sub>). The eluates were reverse crosslinked by heating at 65°C and digested with proteinase K (0.5 mg/ml) at 45°C for 1 h. DNA was obtained by phenol/chloroform/isoamyl alcohol extraction. 2 µl of 10 mg/ml yeast tRNA (Sigma) were added to each sample and DNA was precipitated with 70% ethanol for 24 h at -20°C, and then washed with 95% ethanol and resuspended in 20 µl of TE buffer. A 5 µl volume of each sample was used for PCR amplification with the following primers flanking a sequence of FasL promoter: 5'-TAC CCC CAT GCT GAC CTG CTC-3' (forward) and 5'-ACG GGA CCC TGT TGC TGA CTG-3' (reverse) corresponding to the -396 to -76 region (Gene Bank, accession number: AF027385). The PCR conditions were 45 s at 94°C, 40 s at 58°C, and 90 s at 72°C. The amplification products obtained in 30 cycles were analysed in a 2% agarose gel and visualized by ethidium bromide staining. The negative control was provided by PCR amplification without DNA sample. The specificity of reactions was ensured using normal mouse and rabbit IgG (Santa Cruz Biotechnology).

#### ChIP/immunoblot assay

For ChIP/Immunoblot assay, MCF7 cells were subjected to the procedure of ChIP assay, as above described, until we obtained the immunocomplexes. At this time, we added the

Laemmli buffer to the immunocomplexes and performed the WB analysis, as described by the Upstate protocol. The specificity of reactions was ensured using normal rabbit IgG (Santa Cruz Biotechnology).

#### RNA interference (RNAi)

Cells were plated in 6 well dishes with regular growth medium the day before transfection to 60–70% confluence. On the second day the medium was changed with SFM without P/S and cells were transfected with 25 bp RNA duplex of stealth RNAi targeted human FasL mRNA sequence 5'-GCC CAU UUA ACA GGC AAG UCC AAC U-3' (Invitrogen), with 25 bp RNA duplex of validate RNAi targeted human PPAR $\gamma$  mRNA sequence 5'-GCC UGC AUC UCC ACC UUA UUA UUC U-3' or with a stealth RNAi control (Invitrogen) to a final concentration of 100 nM using Lipofectamine 2000 (Invitrogen) as recommended by the manufacturer. After 5 h the transfection medium was changed with SFM in order to avoid Lipofectamine 2000 toxicity and cells were exposed to 1 µM BRL for the next 48 h and then lysed as described for WB analysis or treated for 72 h and then collected as described for the DNA fragmentation.

#### DNA fragmentation

DNA fragmentation was determined by gel electrophoresis. Cells were grown in 10-cm dishes to 70% confluence, PPAR $\gamma$  or control RNAis and then treated with 1 µM BRL and/or 10 µM GW. After 72 h cells were collected and washed with PBS and pelleted at 1,800 rpm for 5 min. The samples were resuspended in 0.5 ml of extraction buffer (50 mM, Tris-HCl, pH 8; 10 mM EDTA, 0.5% SDS) for 20 min in rotation at 4°C. DNA was extracted with phenol-chloroform three times and once with chloroform. The aqueous phase was used to precipitate acids nucleic with 0.1 volumes or of 3 M sodium acetate and 2.5 volumes cold EtOH overnight at -20°C. The DNA pellet was resuspended in 15 µl of H<sub>2</sub>O treated with RNase A for 30 min at 37°C. The absorbance of the DNA solution at 260 and 280 nm was determined by spectrophotometry. The extracted DNA (40 µg/lane) was subjected to electrophoresis on 1.5% agarose gels. The gels were stained with ethidium bromide and then photographed.

#### Statistical analysis

Statistical analysis was performed using ANOVA followed by Newman-Keuls testing to determine differences in means.  $P < 0.05$  was considered as statistically significant.

## Results

MCF7 breast cancer cells express both Fas and FasL

Previous studies have shown that MCF7 cells coexpress both Fas and FasL, indeed controversial data are reported in this context [30–32]. To evaluate if Fas and FasL are expressed in our MCF7 cells, we did WB analysis of cellular lysates and found that they do indeed express both proteins (Fig. 1a).

BRL up-regulates FasL expression in MCF7 cells

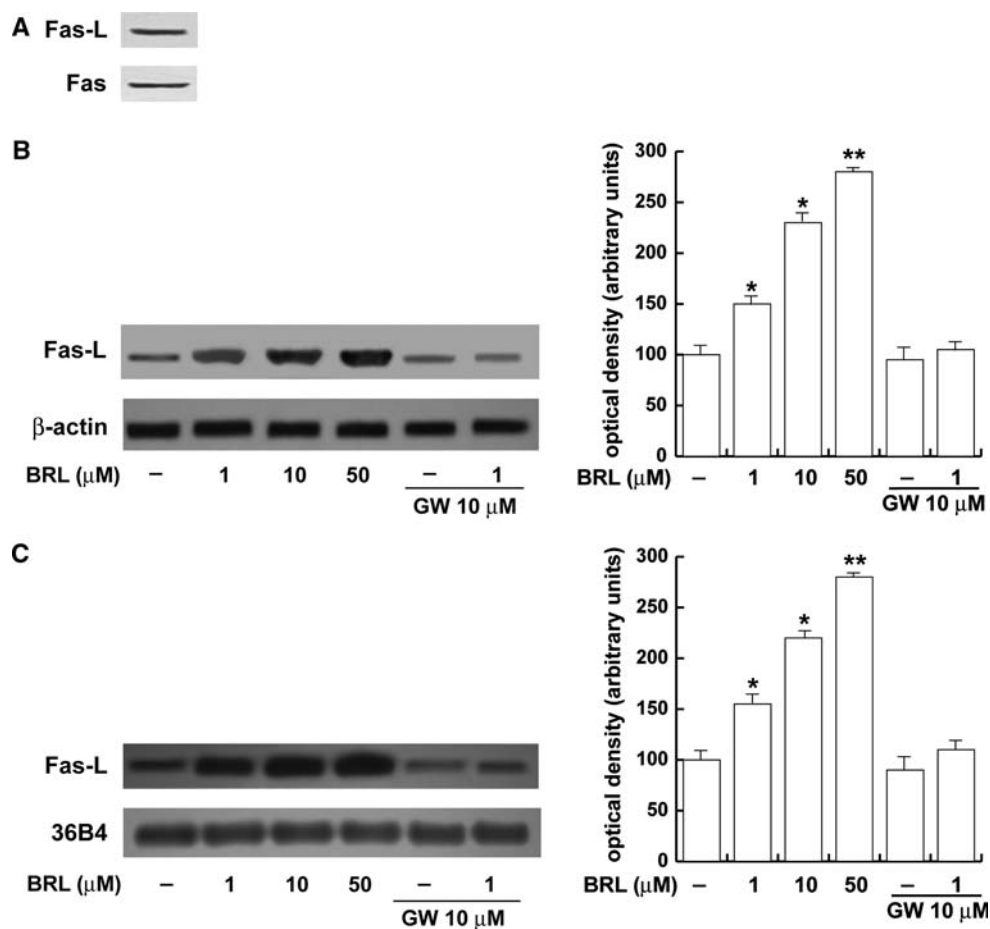
In order to understand whether PPAR $\gamma$  triggers apoptotic events through Fas/FasL signalling, we first evaluated the ability of PPAR $\gamma$  agonist BRL to modulate FasL expression in MCF7 cells. A BRL dose-dependent increase in FasL content was observed by WB after 24 h of treatment (Fig. 1b). Furthermore, by a semiquantitative reverse transcription-polymerase chain reaction (RT-PCR) method, after 24 h upon increasing BRL concentration, we showed that BRL was able to upregulate FasL gene expression in a dose-dependent manner (Fig. 1c). The BRL action on FasL

expression was reversed when we used GW9662 (GW), a specific PPAR $\gamma$  antagonist, (Fig. 1b and c) implying a PPAR $\gamma$ -dependent action in MCF7 cells.

PPAR $\gamma$  transactivates FasL promoter in MCF7 cells

Next, we evaluated whether one of the mechanisms involved in PPAR $\gamma$ -mediated increase of FasL expression could be a direct modulation of the transcriptional activity of its promoter. Transient transfection assays were performed in MCF7 cells using the luciferase reporter constructs containing the region of the human FasL promoter gene spanning from –2365 to –2 bp relative to the translation initiation site (FasL Luc-0) or progressive 5' deletions of the FasL promoter, FasL Luc-3 (from –318 to –2 bp) and FasL Luc-4 (from –237 to –2 bp) (Fig. 2a). Of interest, differences in the basal transcriptional activity were observed among constructs. The results shown in Fig. 2b indicate that transcription from the FasL Luc-0 construct was detectable, but strong and increasing luciferase activity was evidenced with FasL Luc-3 and FasL Luc-4 constructs, suggesting the presence of potential

**Fig. 1** BRL up-regulates FasL protein and mRNA expression in MCF7 cells. **(a)** Immunoblots of FasL and Fas from MCF7 breast cancer cells. **(b)** Immunoblots of FasL from MCF7 cells treated for 24 h with vehicle (-), increasing BRL concentrations, 10  $\mu$ M GW alone or in combination with 1  $\mu$ M BRL.  $\beta$ -actin was used as loading control. The *side panel* shows the quantitative representation of data (mean  $\pm$  S.D.) of three independent experiments including that of **b**. **(c)** Semiquantitative RT-PCR evaluation of FasL mRNA expression. MCF7 cells were treated as in **b**. 36B4 mRNA levels were determined as control. The *side panel* shows the quantitative representation of data (mean  $\pm$  S.D.) of three independent experiments including that of **c** after densitometry and correction for 36B4 expression. \* $P$  < 0.05 BRL-treated vs untreated cells \*\* $P$  < 0.01 BRL-treated vs. untreated cells



negative regulatory regions located within  $-2365$  and  $-318$  bp, consistent with a previous study [33].

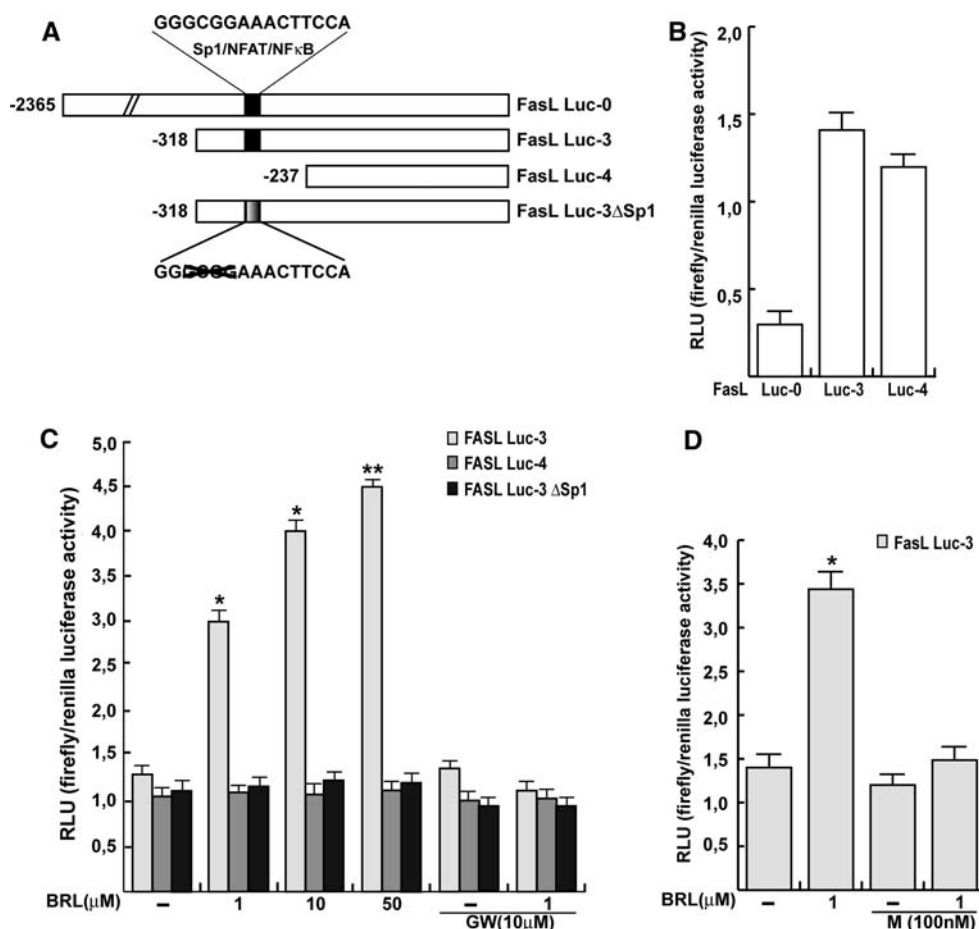
Using the FasL Luc-3 construct, the promoter activity increased upon BRL treatment in a dose-dependent manner, while this effect was abrogated by GW, indicating that FasL promoter activation depends on the presence of a functional PPAR $\gamma$  (Fig. 2c). BRL failed to enhance the transcriptional activity when cells were transfected with FasL Luc-4 construct (Fig. 2c), suggesting that the segment located between  $-318$  and  $-237$  relative to the translation initiation site is crucial for BRL-responsiveness. In particular, this region contains three DNA motifs known to bind the transcription factors Sp1 (named according to the original purification scheme that included Sephacryl and phosphocellulose columns) [34], nuclear factor of activated T cells (NFAT) and nuclear factor- $\kappa$ B (NF $\kappa$ B) (Fig. 2a) [33]. It was reported that Sp1 consensus sequence is necessary for basal transcription from the FasL promoter, and that Sp1 alone is sufficient to drive transcription from the promoter in vivo [33]. We sought to investigate whether Sp1 alone was sufficient to drive FasL transcription or if it required the presence of additional ones. By using a FasL Luc-3 construct deleted in the Sp1 site (Fas Luc-3  $\Delta$ Sp1),

as shown in Fig. 2a, BRL was unable to transactivate FasL promoter (Fig. 2c). Mithramycin is a drug able to bind to GC boxes and then to inhibit Sp1 binding selectively blocking mRNA synthesis from genes that contain functional recognition sites both in vitro and in vivo [35]. Besides, as shown in Fig. 2d, in MCF7 cells transfected with FasL Luc-3 construct and treated with mithramycin, the FasL transactivation upon  $1 \mu\text{M}$  BRL treatment was prevented. Altogether these data strongly suggest that Sp1 plays an important role in regulating FasL transcription also in MCF7 cells.

PPAR $\gamma$  interacts with FasL through Sp1 site in electrophoretic mobility shift assay (EMSA)

To gain further insight into the mechanism involved in the FasL transactivation induced by BRL, we performed EMSA using a synthetic oligodeoxyribonucleotide which contains the Sp1, NFAT and NF $\kappa$ B DNA binding motifs and encompasses the DNA fragment of FasL promoter from  $-288$  to  $-263$  relative to the translation initiation site. We tested for possible interactions of PPAR $\gamma$  with

**Fig. 2** BRL transactivates FasL promoter gene in MCF7 cells. (a) Schematic map of the FasL promoter fragments used in this study. (b) Basal transcriptional activity of the different FasL-luciferase report constructs (Luc-0, Luc-3 and Luc-4). (c) MCF7 cells were treated for 24 h with vehicle (-), increasing BRL concentrations,  $10 \mu\text{M}$  GW alone or in combination with  $1 \mu\text{M}$  BRL. (d) MCF7 cells were treated for 24 h with vehicle (-),  $1 \mu\text{M}$  BRL,  $100 \text{ nM}$  mithramycin (M) alone or in combination with  $1 \mu\text{M}$  BRL. The luciferase activities were normalized to the Renilla luciferase as internal transfection control and data were reported as (RLU values). Columns are mean  $\pm$  S.D. of three independent experiments performed in triplicate. \* $P < 0.05$  BRL-treated vs untreated cells, \*\* $P < 0.01$  BRL-treated vs untreated cells. RLU, Relative Light Units



each of the indicated transcription factors located within the above mentioned FasL promoter region.

In nuclear extracts from MCF7 cells we observed the formation of three specific complexes (Fig. 3, lane 1) which were increased upon BRL treatment (lane 2). The binding was abrogated by 100 fold molar excess of unlabelled probe (lane 3), demonstrating the specificity of the DNA-binding complex. To confirm that FasL transcription induced by BRL in MCF7 cells is regulated by Sp1, nuclear extracts were incubated with three different unlabelled oligonucleotides bearing internal mutations as reported in Materials and Methods.

An excess of unlabeled oligonucleotide containing mutations in the Sp1 site did not compete with the DNA binding of the protein complex (lane 4). In addition,

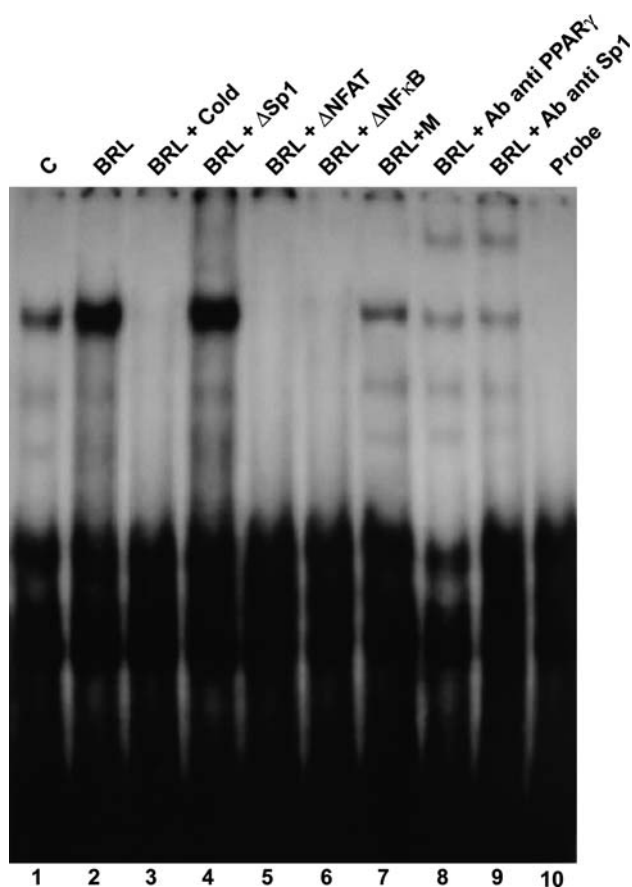


**Fig. 3** PPAR $\gamma$  binds to Sp1 site within FasL promoter region in EMSA. Nuclear extracts from MCF7 cells (lane 1) were incubated with a labeled sequence containing bases  $-288$  to  $-263$  of the wild-type FasL promoter and subjected to electrophoresis in a 6% polyacrylamide gel. In lane 2, nuclear extracts from MCF7 were treated with  $1 \mu\text{M}$  BRL. Competition experiments were performed adding as competitor a 100-fold molar excess of unlabeled FasL probe (lane 3) or  $100 \text{ nM}$  mithramycin (M) (lane 7). An excess of three unlabeled oligonucleotides  $\Delta\text{Sp1}$  (lane 4),  $\Delta\text{NFAT}$  (lane 5) and  $\Delta\text{NF}\kappa\text{B}$  (lane 6), was used. Anti-PPAR $\gamma$  and anti-Sp1 Abs were incubated with nuclear extracts from MCF7 cells treated with  $1 \mu\text{M}$  BRL (lanes 8 and 9, respectively). Lane 10 contains probe alone

incubation with an excess of unlabeled oligonucleotides containing mutations of either NFAT or NF $\kappa\text{B}$  competed both away all DNA-binding activity of the protein complexes bound to the  $^{32}\text{P}$ -labeled wild type  $-288$  to  $-263$  FasL oligonucleotide (lane 5 and 6, respectively). Moreover, the addition of mithramycin in the reaction mixture strongly reduced the intensity of the bands (Fig. 3, lane 7). The involvement of PPAR $\gamma$  and Sp1 in the DNA-binding complexes was confirmed by using the specific anti-PPAR $\gamma$  (lane 8) and anti-Sp1 Abs (lane 9), since both induced supershift and immunodepletion of the bands.

#### Functional interaction of PPAR $\gamma$ with FasL by chromatin immuno-precipitation (ChIP) assay

The interaction of PPAR $\gamma$  with the FasL gene promoter was further investigated by ChIP assay. MCF7 chromatin was immunoprecipitated with the anti-PPAR $\gamma$  Ab and then reprecipitated with the anti-RNA-Pol II or anti-Sp1 Abs. PCR was used to determine the recruitment of PPAR $\gamma$  to the FasL region containing the Sp1 site. The results indicated that PPAR $\gamma$  was weakly constitutively bound to the FasL promoter in untreated cells and this recruitment was increased upon BRL treatment, while mithramycin combined with BRL reversed this effect (Fig. 4a). In addition, by Re-ChIP assays an increased association of Sp1 was obtained and particularly the augmented RNA-Pol II recruitment indicated that a positive regulation of FasL transcription activity was induced by BRL (Fig. 4a). The physical interaction between PPAR $\gamma$  and Sp1 proteins was strengthened by the ChIP/Immunoblot assay (Fig. 4b).

#### PPAR $\gamma$ activates the Fas/FasL apoptotic pathway

Fas/FasL signalling when activated recruits adapter proteins and cysteine proteases such as caspase 8 leading to apoptosis [14]. To better define the action of PPAR $\gamma$  on Fas/FasL pathway, we used GW as well as both PPAR $\gamma$  and FasL RNA interferences (i) to evaluate the activation of caspase 8, key component of the extrinsic apoptotic process. By WB analysis our data showed that untreated MCF7 cells expressed the pro-form of caspase 8, while only after BRL exposure caspase 8 was activated as evidenced by the presence of its  $11 \text{ kDa}$  cleavage product (Fig. 5c). The active caspase 8 cleavage was absent in cells treated with GW alone or combined with BRL, or inhibiting both the expression of PPAR $\gamma$  and FasL by the respective RNAis (Fig. 5c). As shown in Fig. 5a and b, PPAR $\gamma$  and FasL RNAis were able to inhibit the two proteins expression respectively. These data demonstrated for the first time that PPAR $\gamma$  triggers the apoptotic events via Fas/FasL signalling, showing that the extrinsic death

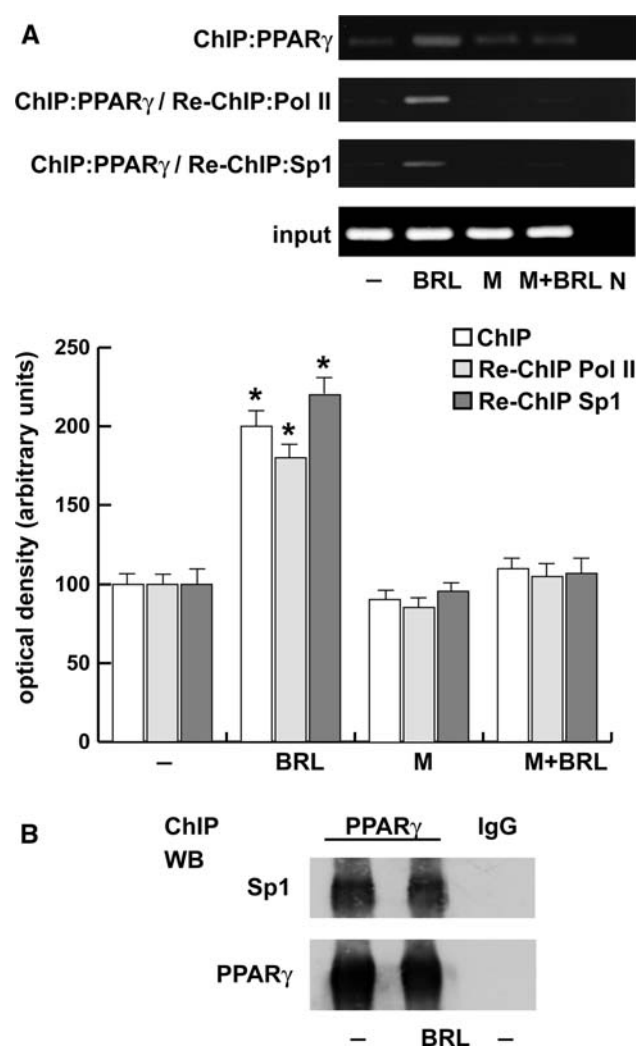


**Fig. 4** Functional interaction between PPAR $\gamma$  and FasL promoter. (a) MCF7 cells were treated as indicated, then cross-linked with formaldehyde and lysed. The soluble chromatin was immunoprecipitated with the anti-PPAR $\gamma$  Ab, (Re-ChIP with the anti-RNA Pol II and anti-Sp1 Abs). The FasL promoter sequence containing Sp1 was detected by PCR with specific primers, as described in Materials and Methods. To control input DNA, FasL promoter was amplified from 30  $\mu$ l of initial preparations of soluble chromatin (before immunoprecipitations). In the bottom of the panel quantitative representation of data of three independent experiments (mean  $\pm$  S.D.) after densitometry. \* $P < 0.05$  BRL-treated vs. untreated cells. M: mithramycin. N, negative control provided by PCR amplification without DNA sample. (b) Immunoblots of Sp1 and PPAR $\gamma$  from MCF7 cells treated with BRL 1  $\mu$ M, in which chromatin was immunoprecipitated with the anti-PPAR $\gamma$  antibody and IgG

pathway is a significant contributor in BRL-induced apoptosis in MCF7 cells.

The apoptotic process is associated with morphological changes and biochemical events such as nuclear condensation and fragmentation, the fragments correspond to strands of DNA that were cleaved at internucleosomal regions and create a 'ladder pattern' when electrophoresed on an agarose gel [36]. Because of its near universality,

internucleosomal DNA degradation is considered a diagnostic hallmark of cells undergoing apoptosis. Therefore, we studied DNA fragmentation assay under BRL treatment in MCF7 cells evidencing that the induced apoptosis is PPAR $\gamma$ -dependent as it was reversed by the PPAR $\gamma$  RNAi (Fig. 5d). These results indicate a positive crosstalk between PPAR $\gamma$  and FasL that is responsible, at least in part, for BRL-induced apoptosis in MCF7 cells.

FasL is a common mechanism by which PPAR $\gamma$  mediates apoptosis in breast cancer cells

Finally, we examined other human breast cancer cell lines to determine whether the involvement of FasL is unique to MCF-7 cells or it is a common mechanism by which PPAR $\gamma$  mediates apoptosis in breast cancer. MDA and BT20 cells, both expressing Fas and FasL (Fig. 6a), showed a FasL upregulation upon BRL treatment, which was reduced by PPAR $\gamma$  RNAi (Fig. 6b). DNA fragmentation assay under BRL treatment in MDA and BT20 cells confirmed that the PPAR $\gamma$ -induced apoptosis involves Fas/FasL signalling (Fig. 6c), addressing a general mechanism in breast cancer cells.

## Discussion

PPAR $\gamma$  ligands are shown to be generally antiproliferative and to induce apoptosis in several malignant cell lineages [4, 6, 7, 9]. Additionally, PPAR $\gamma$  is proved to be a regulator of the expression of many genes relevant to inhibit carcinogenesis [37]. Our previous studies evidenced that PPAR $\gamma$ , through different pathways, is involved in BRL-induced growth arrest and apoptosis in MCF7 breast cancer cells [25, 26]. In the last report, where we explored the involvement of the p53 pathway, it appears that the PPAR $\gamma$ -mediated apoptosis is not completely blocked by using the p53 antisense, suggesting that final PPAR $\gamma$  action in this concern is complex and it may require a multifactorial coordination of different signalling cascades. In this finding, we investigated the potential of PPAR $\gamma$  in inducing apoptotic events through a direct involvement of the Fas/FasL extrinsic apoptotic pathway in breast cancer cells.

The Fas/FasL signalling system plays an important role in chemotherapy-induced apoptosis in several different cell types [23, 24]. FasL is a member of the TNF superfamily that induces apoptosis in susceptible cells upon cross-linking of its own receptor, Fas [15, 16, 38, 39]. FasL is expressed on the cell membrane surface of activated T lymphocytes and cancer cells [40–42]. Significantly, constitutive down-regulation of Fas is involved in drug resistance [43] and associated with a poor prognosis in breast cancer [32].

**Fig. 5** BRL induces the extrinsic apoptotic pathway in MCF7 cells. PPAR $\gamma$  (a) and FasL (b) protein expression (evaluated by WB) in MCF7 cells transfected with a 25-nucleotide of RNA interference (RNAi) targeted human PPAR $\gamma$  or FasL mRNA sequence respectively, or with control RNAi as reported in Materials and Methods or not transfected and treated for 48 h as indicated.  $\beta$ -actin was used as loading control. (c) MCF7 cells were treated for 48 h as indicated, or transfected with PPAR $\gamma$ , FasL or control RNAs. Positions of procaspase 8 (P) and its active cleavage product (S) are indicated by arrowheads on the right. One of three similar experiments is presented.  $\beta$ -actin was used as loading control on the same stripped blot. (d) DNA laddering was performed in MCF7 cells treated for 72-h as indicated, or transfected with PPAR $\gamma$  or control RNAs

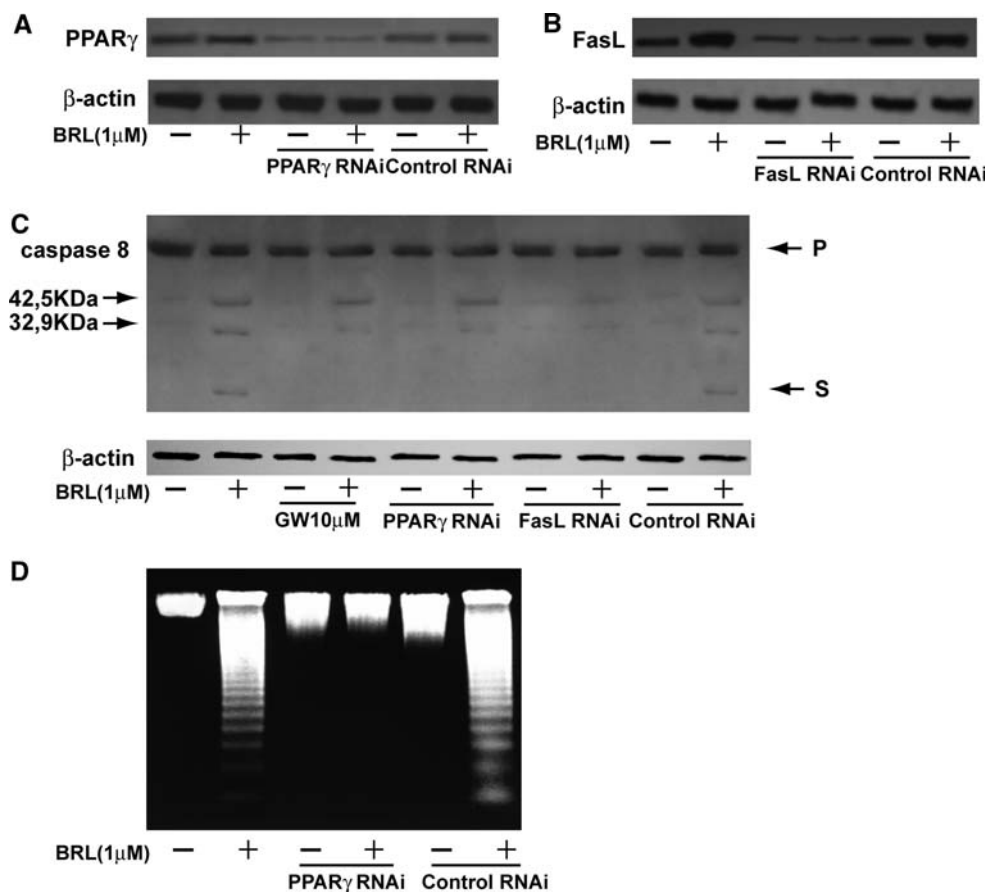
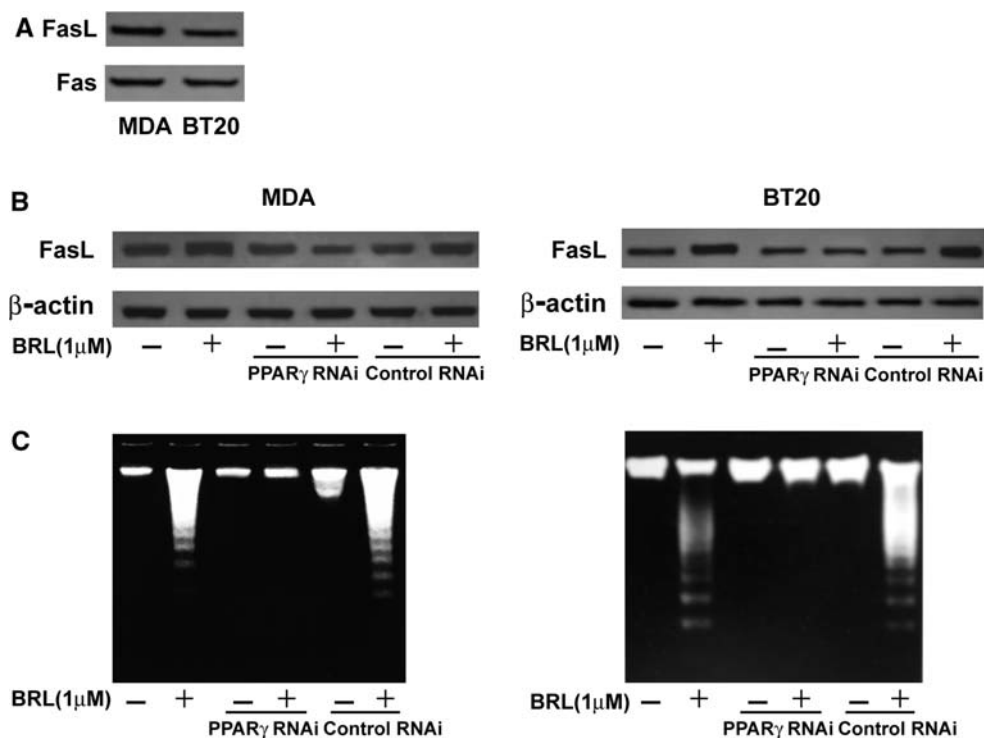


**Fig. 6** BRL induces FasL up-regulation through PPAR $\gamma$  in breast cancer cells. (a) FasL and Fas protein expression (evaluated by WB) in MDA and BT20 breast cancer cells. (b) MDA and BT20 cells were treated for 48 h as indicated, or transfected with a 25-nucleotide of RNA interference (RNAi) targeted human PPAR $\gamma$  mRNA sequence or with control RNAi as reported in Materials and Methods.  $\beta$ -actin was used as loading control. One of three similar experiments is presented. (c) DNA laddering was performed in MDA and BT20 cells treated for 72-h as indicated, or transfected with PPAR $\gamma$  or control RNAs





It has been described that breast cancer cells may be Fas sensitive or Fas insensitive and divergent data are presented on FasL expression in these cells [31, 32]. In our MCF7 cells, positive to Fas and FasL, we found that BRL through PPAR $\gamma$  activation upregulated FasL at both protein and mRNA levels. Despite the FasL relevance, its cell and tissue distribution, and the apparent differences of its expression in a cell-specific manner, little knowledge is available how FasL expression is regulated. Recently, a downregulation of FasL by BRL has been reported in focal cerebral ischemia [44]. It was also showed that prostaglandin 15-deoxy-delta 12,14-prostaglandin J2, a natural PPAR $\gamma$  ligand inhibits FasL gene expression in T lymphocytes *via* a PPAR $\gamma$ -independent mechanisms [45]. Indeed it is quite common for biological signalling pathways to vary depending on tissue type or cell condition.

We demonstrated that BRL increased the transactivation of FasL promoter in a dose-related and in a PPAR $\gamma$ -dependent manner. Promoter deletion analysis of FasL has delineated a minimal promoter fragment spanning nucleotides from -318 to -237 bp, which was responsible for BRL activity. Indeed, the abovementioned region included three DNA motifs known to bind the transcription factors Sp1, NFAT and NF $\kappa$ B [33]. NF $\kappa$ B was reported to physically interact with PPAR $\gamma$  [46], which in some circumstances binds to DNA cooperatively with NF $\kappa$ B [26, 46, 47]. NFAT and Sp1 are critical factors responsible for FasL gene activation [48]. NFAT is a family of related transcription factors that plays a central role in regulating the immune response and it has been demonstrated the involvement of NFAT in FasL transcription [33, 49]. Several studies indicate that many mammalian gene types are controlled by Sp1, including genes for structural proteins, metabolic enzymes, cell cycle regulators, transcription factors, growth factors, surface receptors, and others [50]. PPAR $\gamma$  has been documented to functionally interact with Sp1 to modulate gene expression [51, 52]. These findings are in agreement with our results since the PPAR $\gamma$ -mediated transactivation of FasL promoter was abolished by using mithramycin and a construct deleted of the Sp1 site. By EMSA studies with nuclear extract from MCF7 cells, a binding of PPAR $\gamma$  to the Sp1 sequence located within the FasL promoter was observed, it was enhanced by BRL and immunodepleted by both PPAR $\gamma$  and Sp1 Abs, addressing the coexistence of the two proteins in the DNA binding complexes. In addition, the interaction between PPAR $\gamma$  and FasL promoter was supported by CHIP assay where BRL treatment also increases the binding of RNA-Pol II to this promoter gene addressing a positive transcriptional regulation mediated by PPAR $\gamma$ .

Engagement of the FasL homotrimer to three Fas molecules induces apoptosis by clustering of the receptor's death domains [14, 15]. This leads to the binding of FADD and caspase 8 to the receptor [14]. In the present study, we

obtained the active cleavage of caspase 8 under BRL treatment, that was no longer detectable in the presence of GW as well as inhibiting both the expression of FasL and PPAR $\gamma$  by the respective RNAs. Previous works from our group have identified important pathways underlying the role of PPAR $\gamma$  in cell growth, cycle arrest and apoptosis in MCF7 breast cancer cells [25, 26]. First, we evidenced an opposite effects of estrogen receptor (ER)  $\alpha$  and PPAR $\gamma$  on the regulation of the PI3K/AKT pathway, classically involved in cell survival and proliferation, eliciting divergent responses in presence of the cognate ligands 17 $\beta$ -estradiol and BRL respectively in estrogen-dependent MCF7 cells [25]. Subsequently, we showed that BRL promotes the growth arrest and apoptosis in MCF7 cells through a crosstalk between p53 and PPAR $\gamma$ . Our results indicated that in a consecutive series of events BRL: (1) up-regulates the expression of p53 and (2) its effector p21WAF1/Cip1, (3) triggers the cleavage of caspase 9, an important component of the intrinsic apoptotic pathway [26]. Finally, the DNA fragmentation assay clearly evidenced that PPAR $\gamma$  was involved in the apoptotic process triggered by BRL since this effect was completely reversed by GW, while the apoptosis was only partially abolished inhibiting p53 expression by AS/p53, a plasmid encoding for p53 antisense [26]. The reported finding evidenced that the cross talk between PPAR $\gamma$  and p53 is responsible, at least in part, in the BRL-induced apoptosis in MCF7 cells [26] and that alternative signalling cascades may be involved, like the Fas/FasL signalling that triggers the extrinsic apoptosis pathway, as we observed in this study. Interestingly, PPAR $\gamma$ -induced apoptosis through FasL appears to be a general mechanism in breast cancer cells since it occurs in MCF7, MDA and BT20 cells.

In conclusion, we have shown that FasL expression is induced by PPAR $\gamma$  through the binding to the transcription factor Sp1, demonstrating for the first time that PPAR $\gamma$  triggers apoptotic events in breast cancer cells via Fas/FasL signalling pathway. However, the genomic response to PPAR $\gamma$  activation remains complex and the understanding of the interactions between PPAR $\gamma$  and other factors amplifies our knowledge on genes participating in cell-cycle modulation and apoptosis. The data presented place FasL as a novel molecular target to add to the variety of anticancer activities mediated by PPAR $\gamma$  and further candidate PPAR $\gamma$ -ligands for the treatment of patients with ER $\alpha$ + and ER $\alpha$ - breast cancer.

## References

- Francis GA, Fayard E, Picard F, Auwerx J (2003) Nuclear receptors and the control of metabolism. *Ann Rev Physiol* 65:261–311

2. Shearer BG, Hoekstra WJ (2003) Recent advances in peroxisome proliferator-activated receptor science. *Curr Med Chem* 10: 267–280
3. Kota BP, Huang TH, Roufogalis BD (2005) An overview on biological mechanisms of PPARs. *Pharmacol Res* 51:85–94
4. Elstner E, Muller C, Koshizuka K, Williamson EA, Park D, Asou H, Shintaku P, Said JW, Heber D, Koeffler HP (1998) Ligands for peroxisome proliferator-activated receptor gamma and retinoic acid receptor inhibit growth and induce apoptosis of human breast cancer cells in vitro and in BNX mice. *Proc Natl Acad Sci USA* 95:8806–8811
5. Haydon RC, Zhou L, Feng T, Breyer B, Cheng H, Jiang W, Ishikawa A, Peabody T, Montag A, Simon MA, He TC (2002) Nuclear receptor agonists as potential differentiation therapy agents for human osteosarcoma. *Clin Cancer Res* 8:1288–1294
6. Konopleva M, Andreeff M (2002) Role of peroxisome proliferator-activated receptor-gamma in hematologic malignancies. *Curr Opin Hematol* 9:294–302
7. Panigrahy D, Shen LQ, Kieran MW, Kaipainen A (2003) Therapeutic potential of thiazolidinediones as anticancer agents. *Expert Opin Invest Drugs* 12:1925–1937
8. Suzuki T, Hayashi S, Miki Y, Nakamura Y, Moriya T, Sugawara A, Ishida T, Ohuchi N, Sasano H (2006) Peroxisome proliferator-activated receptor gamma in human breast carcinoma: a modulator of estrogenic actions. *Endocr Relat Cancer* 13:233–250
9. Yu J, Qiao L, Zimmermann L, Ebert MP, Zhang H, Lin W, Rocken C, Malferriner P, Farrell GC (2006) Troglitazone inhibits tumor growth in hepatocellular carcinoma in vitro and in vivo. *Hepatology* 43:134–143
10. Kim SH, Yoo CI, Kim HT, Park JY, Kwon CH, Keun Kim Y (2006) Activation of peroxisome proliferator-activated receptor-gamma (PPARGamma) induces cell death through MAPK-dependent mechanism in osteoblastic cells. *Toxicol Appl Pharmacol* 215:198–207
11. Lehrke M, Lazar MA (2005) The many faces of PPARgamma. *Cell* 123:993–999
12. Grommes C, Landreth GE, Heneka MT (2004) Antineoplastic effects of peroxisome proliferator-activated receptor gamma agonists. *Lancet Oncol* 5:419–429
13. Turturro F, Oliver RE III, Friday E, Nissim I, Welbourne TC (2007) Troglitazone and pioglitazone interactions via PPAR{gamma} independent and dependent pathways in regulating physiological responses in renal tubule derived cell lines. *Am J Physiol Cell Physiol* 292:C1137–C1146
14. Green DR (1998) Apoptotic pathways: the roads to ruin. *Cell* 94:695–698
15. Nagata S (1997) Apoptosis by death factor. *Cell* 88:355–365
16. Chinnaiyan AM, Dixit VM (1997) Portrait of an executioner: the molecular mechanism of FAS/APO-1-induced apoptosis. *Semin Immunol* 9:69–76
17. Debatin KM (2004) Apoptosis pathways in cancer, cancer therapy. *Cancer Immunol Immunother* 53:153–159
18. Pinkoski MJ, Green DR (1999) Fas ligand, death gene. *Cell Death Differ* 6:1174–1181
19. Wajant H (2006) CD95L/FasL and TRAIL in tumour surveillance and cancer therapy. *Cancer Treat Res* 130:141–165
20. O’Connell J, O’Sullivan GC, Collins JK, Shanahan F (1996) The Fas counterattack: Fas-mediated T cell killing by colon cancer cells expressing Fas ligand. *J Exp Med* 184:1075–1082
21. Muschen M, Moers C, Warskulat U, Niederacher D, Betz B, Even J, Lim A, Josien R, Beckmann MW, Haussinger D (1999) CD95 ligand expression in dedifferentiated breast cancer. *J Pathol* 189:378–386
22. Reimer T, Herrring C, Koczan D, Richter D, Gerber B, Kabelitz D, Friese K, Thiesen HJ (2000) FasL:Fas ratio—a prognostic factor in breast carcinomas. *Cancer Res* 60:822–828
23. Kasibhatla S, Brunner T, Genestier L, Echeverri F, Mahboubi A, Green DR (1998) DNA damaging agents induce expression of Fas ligand and subsequent apoptosis in T lymphocytes via the activation of NF-kappa B and AP-1. *Mol Cell* 4:543–551
24. Mo YY, Beck WT (1999) DNA damage signals induction of fas ligand in tumor cells. *Mol Pharmacol* 55:216–222
25. Bonfiglioglio D, Gabriele S, Aquila S, Catalano S, Gentile M, Middea E, Giordano F, Andò S (2005) Estrogen receptor alpha binds to peroxisome proliferator-activated receptor (PPAR) response element and negatively interferes with PPAR gamma signalling in breast cancer cells. *Clin Cancer Res* 11:6139–6147
26. Bonfiglioglio D, Aquila S, Catalano S, Gabriele S, Belmonte M, Middea E, Qi H, Morelli C, Gentile M, Maggolini M, Andò S (2006) Peroxisome proliferator-activated receptor-gamma activates p53 gene promoter binding to the nuclear factor-kappaB sequence in human MCF7 breast cancer cells. *Mol Endocrinol* 20:3083–3092
27. Catalano S, Rizza P, Gu G, Barone I, Giordano C, Marsico S, Casaburi I, Middea E, Lanzino M, Pellegrino M, Andò S (2007) Fas ligand expression in TM4 sertoli cells is enhanced by estradiol “in situ” production. *J Cell Physiol* 211:448–456
28. Maggolini M, Donzè O, Picard D (1999) Non-radioactive method for inexpensive quantitative RT-PCR. *Biol Chem* 380:695–697
29. Andrews NC, Faller DV (1991) A rapid micropreparation technique for extraction of DNA-binding proteins from limiting numbers of mammalian cells. *Nucleic Acids Res* 19:2499
30. Beidler DR, Tewari M, Friesen PD, Poirier G, Dixit VM (1995) The baculovirus p35 protein inhibits Fas- and tumor necrosis factor-induced apoptosis. *J Biol Chem* 270:16526–16528
31. Keane MM, Ettenberg SA, Lowrey GA, Russell EK, Lipkowitz S (1996) Fas expression and function in normal and malignant breast cell lines. *Cancer Res* 56:4791–4798
32. Toillon RA, Descamps S, Adriaenssens E, Ricort JM, Bernard D, Boilly B, Le Bourhis X (2002) Normal breast epithelial cells induce apoptosis of breast cancer cells via Fas signaling. *Exp Cell Res* 275:31–43
33. McClure RF, Heppelmann CJ, Paya CV (1999) Constitutive Fas ligand gene transcription in Sertoli cells is regulated by Sp1. *J Biol Chem* 274:7756–7762
34. Philipsen S, Suske G (1999) A tale of three fingers: the family of mammalian Sp/XKLF transcription factors. *Nucleic Acids Res* 27:2991–3000
35. Blume S, Snyder R, Ray R, Thomas S, Koller C, Miller DM (1991) Mithramycin inhibits SP1 binding and selectively inhibits transcriptional activity of the dihydrofolate reductase gene in vitro and in vivo. *J Clin Invest* 88:1613–1621
36. Montague JW, Cidlowski JA (1996) Cellular catabolism in apoptosis: DNA degradation and endonuclease activation. *Experientia* 52:957–962
37. Theocharisa S, Margeli A, Kouraklis G (2003) Peroxisome proliferator-activated receptor-gamma ligands as cell-cycle modulators. *Curr Med Chem Anticancer Agents* 3:239–251
38. Suda T, Takahashi T, Golstein P, Nagata S (1993) Molecular cloning and expression of the FAS Ligand, a novel member of the tumor necrosis factor family. *Cell* 75:1169–1178
39. Nagata S, Golstein P (1995) The fas death factor. *Science* 267:1449–1456
40. Hahne M, Rimoldi D, Schroter M, Romero P, Schreier M, French LE, Schneider P, Bornand T, Fontana A, Lienard D, Cerottini J, Tschopp J (1996) Melanoma cell expression of Fas (Apo-1/CD95) ligand: implications for tumor immune escape. *Science* 274:1363–1366
41. Oshimi Y, Oda S, Honda Y, Nagata S, Miyazaki S (1996) Involvement of Fas Ligand and Fas-mediated pathway in the

- cytotoxicity of human natural killer cells. *J Immunol* 157:2909–2915
42. Mullauer L, Mosberger I, Grusch M, Rudas M, Chott A (2000) Fas ligand is expressed in normal breast epithelial cells and is frequently up-regulated in breast cancer. *J Pathol* 190:20–30
  43. Landowski TH, Gleason-Guzman MC, Dalton WS (1997) Selection for drug resistance results in resistance to Fas-mediated apoptosis. *Blood* 89:1854–1861
  44. Chu K, Lee ST, Koo JS, Jung KH, Kim EH, Sinn DI, Kim JM, Ko SY, Kim SJ, Song EC, Kim M, Roh JK (2006) Peroxisome proliferator-activated receptor-gamma-agonist, rosiglitazone, promotes angiogenesis after focal cerebral ischemia. *Brain Res* 1093:208–218
  45. Cippitelli M, Fionda C, Di Bona D, Lupo A, Piccoli M, Frati L, Santoni A (2003) The cyclopentenone-type prostaglandin 15-deoxy-delta 12,14-prostaglandin J2 inhibits CD95 ligand gene expression in T lymphocytes: interference with promoter activation via peroxisome proliferator-activated receptor-gamma-independent mechanisms. *J Immunol* 170:4578–4592
  46. Chung SW, Kang BY, Kim SH, Pak YK, Cho D (2000) Oxidized low density lipoprotein inhibits interleukin-12 production in lipopolysaccharide-activated mouse macrophages via direct interactions between peroxisome proliferator-activated receptor- and nuclear factor- B. *J Biol Chem* 275:32681–32687
  47. Coutureir C, Brouillet A, Couriaud C, Koumanov K, Bereziat G, Andreani M (1999) Interleukin 1 $\beta$  induces type II-secreted phospholipase A<sub>2</sub> gene in vascular smooth muscle cells by a nuclear factor B and peroxisome proliferator-activated receptor-mediated process. *J Biol Chem* 274:23085–23093
  48. Xiao S, Matsui K, Fine A, Zhu B, Marshak-Rothstein A, Widom RL, Ju S-T (1999) FasL promoter activation by IL-2 through SP1 and NFAT but not Egr-2 and Egr-3. *Eur J Immunol* 29:3456–3465
  49. Rengarajan J, Mittelstadt PR, Mages HW, Gerth AJ, Kroczeck RA, Ashwell JD, Glimcher LH (2000) Sequential involvement of NFAT and Egr transcription factors in FasL regulation. *Immunity* 12:293–300
  50. Black AR, Black JD, Azizkhan-Clifford J (2003) Sp1 and kruppel-like factor family of transcription factors in cell growth regulation and cancer. *J Cell Physiol* 188:143–160
  51. Sugawara A, Uruno A, Kudo M, Ikeda Y, Sato K, Taniyama Y, Ito S, Takeuchi K (2002) Transcription suppression of thromboxane receptor gene by peroxisome proliferator-activated receptor- $\gamma$  via an interaction with Sp1 in vascular smooth muscle cells. *J Biol Chem* 277:9676–9683
  52. Sassa Y, Hata Y, Aiello LP, Taniguchi Y, Kohno K, Ishibashi T (2004) Bifunctional properties of peroxisome proliferator-activated receptor  $\gamma$ 1 in KDR gene regulation mediated via interaction with both Sp1 and Sp3. *Diabetes* 53:1222–1229

# Peroxisome Proliferator-Activated Receptor- $\gamma$ Activates p53 Gene Promoter Binding to the Nuclear Factor- $\kappa$ B Sequence in Human MCF7 Breast Cancer Cells

Daniela Bonofiglio,\* Saveria Aquila,\* Stefania Catalano, Sabrina Gabriele, Maria Belmonte, Emilia Middea, Hongyan Qi, Catia Morelli, Mariaelena Gentile, Marcello Maggiolini, and Sebastiano Andò

Department of Pharmaco-Biology (D.B., S.A., S.C., S.G., M.B., E.M., H.Q., C.M., M.M.), Department of Cellular Biology (M.G., S.A.), Faculty of Pharmacy (S.A.) University of Calabria, 87030 Arcavacata di Rende, (Cosenza) Italy

The aim of the present study was to provide new mechanistic insight into the growth arrest and apoptosis elicited by peroxisome proliferator-activated receptor (PPAR) $\gamma$  in breast cancer cells. We ascertained that PPAR $\gamma$  mediates the inhibition of cycle progression in MCF7 cells exerted by the specific PPAR $\gamma$  agonist rosiglitazone [BRL4653 (BRL)], because this response was no longer notable in the presence of the receptor antagonist GW9662. We also provided evidence that BRL is able to up-regulate mRNA and protein levels of the tumor suppressor gene p53 and its effector p21<sup>WAF1/Cip1</sup> in a time- and dose-dependent manner. Moreover, in transfection experiments with deletion mutants of the p53 gene promoter, we documented that the nuclear factor- $\kappa$ B sequence is required for the transcriptional response to BRL.

Interestingly, EMSA showed that PPAR $\gamma$  binds directly to the nuclear factor- $\kappa$ B site located in the promoter region of p53, and chromatin immunoprecipitation experiments demonstrated that BRL increases the recruitment of PPAR $\gamma$  on the p53 promoter sequence. Next, both PPAR $\gamma$  and p53 were involved in the cleavage of caspases-9 and DNA fragmentation induced by BRL, given that GW9662 and an expression vector for p53 anti-sense blunted these effects. Our findings provide evidence that the PPAR $\gamma$  agonist BRL promotes the growth arrest and apoptosis in MCF7 cells, at least in part, through a cross talk between p53 and PPAR $\gamma$ , which may be considered an additional target for novel therapeutic interventions in breast cancer patients. (*Molecular Endocrinology* 20: 3083–3092, 2006)

**P**EROXISOME PROLIFERATOR-activated receptor  $\gamma$  (PPAR $\gamma$ ) is a prototypical member of the nuclear receptor superfamily and integrates the control of energy, lipid, and glucose homeostasis (1–4). PPAR $\gamma$  regulates differentiation and induces cell growth arrest and apoptosis in a large variety of cells (Ref. 5 and references therein), including both primary and metastatic breast malignancy (6, 7). However, the molecular mechanisms involved in the inhibitory effects mediated by PPAR $\gamma$  remain to be elucidated.

It is well known that the p53 tumor suppressor gene regulates the transcription of effectors that are also responsible for growth arrest and apoptosis (reviewed in Ref. 8). Among the p53 target genes, the p21<sup>WAF1/Cip1</sup> has been recognized to exert an essential role in medi-

ating cell cycle arrest at both G<sub>1</sub> and G<sub>2</sub>-M checkpoints (9–11). p21<sup>WAF1/Cip1</sup> inhibits cyclin D1 or E/cyclin-dependent kinase in G<sub>1</sub> and cyclin B/cdc2 in G<sub>2</sub>-M arrest, eliciting regulatory effects on DNA replication and repair (12). Moreover, it has been reported that p53 is able to promote apoptosis in certain cell types in a transcription-independent manner (13).

The function of p53 as a tumor suppressor is finely tuned through an interaction with other transduction pathways regulating the cell network (14–18). For instance, striking evidence has recently emerged for a cross talk between p53 and relevant transcription factors, such as the glucocorticoid, androgen, and estrogen receptors (19). It was therefore proved that these nuclear receptors are able to induce a cytosolic accumulation of p53, altering its stability and, consequently, its function (19).

In the present study, we provide new insight into the molecular mechanisms by which the specific PPAR $\gamma$  ligand rosiglitazone [BRL4653 (BRL)] induces the growth arrest and apoptosis in MCF7 human breast cancer cells. By performing a panel of different assays, we have demonstrated that the biological effects of BRL are triggered, at least in part, by PPAR $\gamma$  binding to the nuclear factor  $\kappa$ B sequence located within the p53 promoter region. Our findings have provided ev-

First Published Online September 28, 2006

\* D.B. and S.A. contributed equally to this work.

Abbreviations: BRL, Rosiglitazone (BRL4653); ChIP, chromatin immunoprecipitation; GW, GW9662; NF $\kappa$ B, nuclear factor- $\kappa$ B; P, parthenolide; PMSF, phenylmethylsulfonylfluoride; Pol II, polymerase II; PPAR $\gamma$ , peroxisome proliferator-activated receptor- $\gamma$ ; PPRE, PPAR response element; SDS, sodium dodecyl sulfate; SFM, serum-free medium.

*Molecular Endocrinology* is published monthly by The Endocrine Society (<http://www.endo-society.org>), the foremost professional society serving the endocrine community.

idence of a cross talk between p53 and PPAR $\gamma$ , which assumes a biological relevance for possible new pharmacological strategies in breast cancer.

## RESULTS

### BRL Induces G<sub>0</sub>-G<sub>1</sub> Cycle Arrest in MCF7 Cells

On the basis of our (20) and other (21, 22) studies demonstrating the inhibitory effects of the PPAR $\gamma$  agonists on proliferation of breast cancer cells, we first investigated the activity of BRL on MCF7 cell cycle progression. A 48-h exposure to BRL caused the inhibition of G<sub>0</sub>-G<sub>1</sub>→S phase progression in a dose-dependent manner with concomitant decrease in the proportion of cells entering in S phase (Table 1). Of note, this effect was mediated by PPAR $\gamma$ , because it was no longer notable in the presence of the specific antagonist GW9662 (GW).

### BRL Up-Regulates p53 and p21<sup>WAF1/Cip1</sup> Expression in MCF7 Cells

Considering that the tumor suppressor gene p53 is mainly involved in the growth arrest promoted by different factors, we aimed to examine the potential ability of PPAR $\gamma$  to modulate the expression of p53 along with its natural target gene p21<sup>WAF1/CIP1</sup>. The mRNA (Fig. 1) and protein (Fig. 2) levels of both p53 and p21<sup>WAF1/CIP1</sup> were up-regulated in a time- and dose-dependent manner in MCF7 cells treated with BRL. These stimulations were abrogated by GW (Figs. 1 and 2) suggesting a direct involvement of PPAR $\gamma$ .

### BRL Transactivates p53 Gene Promoter

The aforementioned observations prompted us to investigate whether PPAR $\gamma$  is able to transactivate an expression vector encoding p53 promoter gene. Thus, MCF7 cells were transiently transfected with a luciferase reporter construct (named p53-1) containing the upstream region of the p53 gene spanning from –1800 to +12 (Fig. 3A) and treated with increasing concentrations of BRL for 24 h. Interestingly, the dose-dependent activa-

tion of p53–1 by BRL was reversed in the presence of GW, indicating that a PPAR $\gamma$ -mediated mechanism was involved in the transcriptional response to BRL (Fig. 3B).

To identify the region within the p53 promoter responsible for transactivation, we used deletion constructs expressing different binding sites such as CTF-1/YY1, nuclear factor-Y (NF-Y), and NF $\kappa$ B (Fig. 3A). In transfection experiments performed using the mutants p53-6 and p-53-13 encoding the regions from –106 to +12 and from –106 to –40, respectively, the responsiveness to BRL was still observed, whereas using the mutant p53-14 encoding the sequence from –106 to –49 we did not detect an increase in luciferase activity (Fig. 3C). Consequently, the region from –49 to –40, which corresponds to the NF $\kappa$ B site (Fig. 3A), was required for the transactivation of p53 by BRL.

### PPAR $\gamma$ Binds to NF $\kappa$ B Sequence in EMSA

To further evaluate whether the NF $\kappa$ B site is responsible for the action triggered by BRL, we performed EMSA experiments. Using synthetic oligodeoxynucleotides corresponding to the NF $\kappa$ B sequence, we observed the formation of a single band in nuclear extracts from MCF7 cells (Fig. 4A, lane 1), which was abrogated by 100-fold molar excess of unlabeled probe (Fig. 4A, lane 2), demonstrating the specificity of the DNA binding complex. Of note, BRL treatment induced a strong increase in the specific band (Fig. 4A, lane 3), which was immunodepleted and supershifted using anti-PPAR $\gamma$  (Fig. 4A, lane 4) and anti-NF $\kappa$ B (Fig. 4A, lane 5) antibodies. Interestingly, the PPAR $\gamma$  transcribed and translated protein was able to bind to [<sup>32</sup>P]NF $\kappa$ B oligonucleotide (Fig. 4A, lane 6). The specificity of the band was proved by a 100-fold excess of cold probe (Fig. 4A, lane 7) and confirmed by a consensus PPAR response element (PPRE) used as a cold competitor (Fig. 4A, lane 8). In addition, the immunodepleted band obtained using the anti-PPAR $\gamma$  antibody (Fig. 4A, lane 9), but not observed with the anti-NF $\kappa$ B antibody (Fig. 4A, lane 10), confirmed that PPAR $\gamma$  binds in a specific manner to the NF $\kappa$ B site present in the promoter of p53. As next controls, we used NF $\kappa$ B protein alone (Fig. 4B, lane 1) and in com-

**Table 1.** BRL Induces G<sub>0</sub>-G<sub>1</sub> Cycle Arrest in MCF7 Cells

Treatment	$\mu$ M	Cell Cycle Phase		
		G <sub>0</sub> -G <sub>1</sub>	S	G <sub>2</sub> -M
C		53 ± 7.2	30 ± 4.4	17 ± 2.1
BRL	1	67 ± 7.4 <sup>a</sup>	20 ± 3.3 <sup>a</sup>	13 ± 2.2
BRL	10	76 ± 8.1 <sup>a</sup>	14 ± 3.1 <sup>a</sup>	10 ± 2.6 <sup>a</sup>
BRL	50	82 ± 8.3 <sup>b</sup>	10 ± 2.4 <sup>b</sup>	8 ± 1.2 <sup>b</sup>
GW	10	54 ± 6.5	29 ± 3.5	17 ± 2.1
BRL + GW	1 + 10	53 ± 6.1	29 ± 3.2	18 ± 2.3

<sup>a</sup>  $P < 0.05$ , BRL-treated vs. untreated cells.

<sup>b</sup>  $P < 0.01$ , BRL-treated vs. untreated cells.

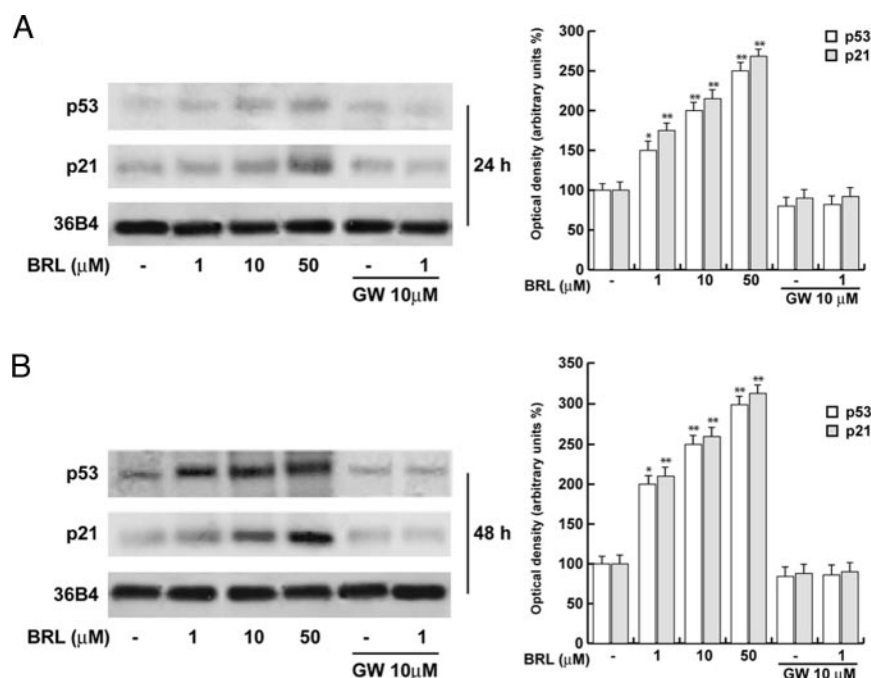


**Fig. 1.** BRL Up-Regulates p53 and p21<sup>WAF1/Cip1</sup> mRNA Expression in MCF7 Cells

Semiquantitative RT-PCR evaluation of p53 and p21<sup>WAF1/Cip1</sup> mRNA expression. MCF7 cells were treated for 24 h (A) and 48 h (B) with increasing concentrations of BRL as indicated and 10  $\mu$ M GW alone or in combination with 1  $\mu$ M BRL. 36B4 mRNA levels were determined as control. The *side panels* show the quantitative representation of data (mean  $\pm$  sd) of three independent experiments after densitometry and correction for 36B4 expression. \*,  $P < 0.05$ ; and \*\*,  $P < 0.01$  BRL-treated vs. untreated cells

ination with either cold competitor (Fig. 4B, lane 2) or the anti-NF $\kappa$ B antibody (Fig. 4B, lane 3).

### Functional Interaction of PPAR $\gamma$ with p53 in Chromatin Immunoprecipitation (ChIP) Assay

The interaction of PPAR $\gamma$  with p53 was further elucidated by ChIP experiments. MCF7 cells were treated with formaldehyde to form DNA-protein cross-links and then sonicated. Thereafter, using anti-PPAR $\gamma$ , anti-NF $\kappa$ B, and anti-RNA polymerase II (Pol II) antibodies, we immunoprecipitated the complexes, and the binding of PPAR $\gamma$ , NF $\kappa$ B, and RNA Pol II, respectively, to the NF $\kappa$ B site within the p53 promoter was revealed by PCR. As shown in panel A of Fig. 5, BRL increased the recruitment of PPAR $\gamma$  to the promoter of p53. The BRL-induced effect was slightly reduced by TGF $\beta$ , but not altered in presence of the specific inhibitor of NF $\kappa$ B parthenolide (P) (23) (Fig. 5A). As it concerns the recruitment of NF $\kappa$ B to p53, evaluated using the anti-NF $\kappa$ B antibody, TGF $\beta$  enhanced such interaction that was abolished by P (Fig. 5A). Moreover, P was able to prevent the binding of RNA Pol II to p53 induced by TGF $\beta$ , but not that determined by BRL (Fig. 5A). These findings confirmed the ability of PPAR $\gamma$  to stimulate the transcription of p53 in a NF $\kappa$ B-independent manner (Fig. 5A). Next, the anti-PPAR $\gamma$  antibody did not immunoprecipitate a region upstream the NF $\kappa$ B site located within the p53 promoter gene (Fig. 5B).

### BRL Induces Caspase-9 Cleavage and DNA Fragmentation in MCF7 Cells

Having demonstrated that PPAR $\gamma$  mediates p53 expression induced by BRL, we investigated the cleavage of caspase 9, which is an important component of the intrinsic apoptotic process (24). Notably, the treatment of MCF7 cells with BRL for 48 h promoted the caspase-9 activation, which was prevented by GW and in presence of an expression vector encoding p53 antisense (AS/p53) (Fig. 6A), which abolished p53 expression (Fig. 6B). On the contrary, the effect of BRL on the cleavage of caspase 9 was still notable using the NF $\kappa$ B inhibitor P (Fig. 6A), which abrogating the NF $\kappa$ B protein levels (Fig. 6C) excluded the contribution of such factor in the action elicited by BRL.

As evidenced in DNA fragmentation assay, PPAR $\gamma$  was also involved in the apoptotic process triggered by BRL because this effect was completely and partially reversed by GW and the AS/p53, respectively (Fig. 6D). Again, P did not modify the activity of BRL (Fig. 6D). Taken together, these results indicate that, at least in part, a cross talk between PPAR $\gamma$  and p53 may be responsible for the growth arrest and apoptosis induced by BRL in MCF7 cells.

### DISCUSSION

In recent years, a great deal of attention focused on the antiproliferative effects of PPAR $\gamma$  in a variety of

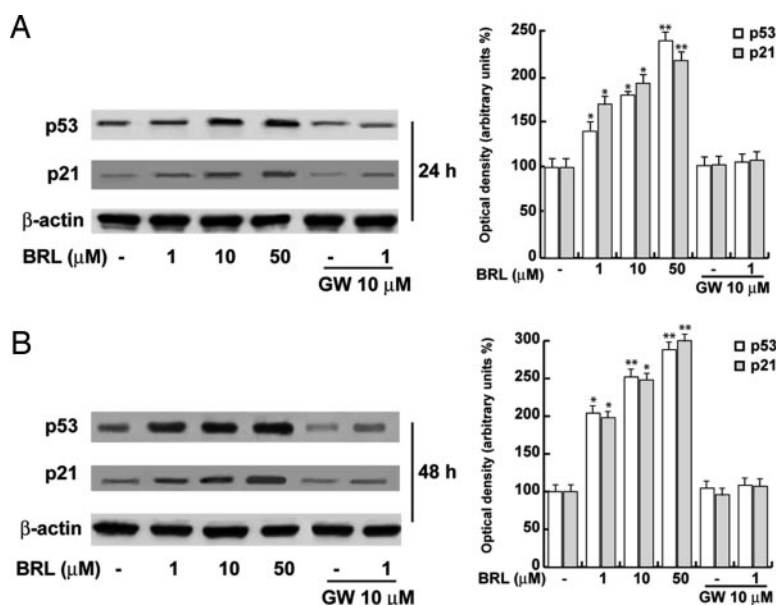


**Fig. 2.** BRL Up-Regulates p53 and p21<sup>WAF1/Cip1</sup> Protein Expression in MCF7 Cells

Immunoblots of p53 and p21<sup>WAF1/Cip1</sup> from MCF7 cells extracts treated for 24 h (A) and 48 h (B) with increasing BRL concentrations, 10  $\mu$ M GW alone or in combination with 1  $\mu$ M BRL.  $\beta$ -Actin was used as loading control. The *side panels* show the quantitative representations of data (mean  $\pm$  SD) of three independent experiments performed for each condition. \*,  $P < 0.05$ ; and \*\*,  $P < 0.01$  BRL-treated vs. untreated cells

cancer cell types. Treatments with PPAR $\gamma$  ligands have been demonstrated to induce cell cycle arrest and apoptosis in different cancer models (6, 7, 25). In addition, an interaction between PPAR $\gamma$  and p53 was hypothesized, but not clarified, at molecular level in cholangiocarcinoma (26), in human gastric cancer cells (27), and even in rat vascular smooth muscle cells (28). In addition, from our and other studies emerged the ability of PPAR $\gamma$  to up-regulate the expression of the tumor suppressor gene phosphatase and tensin analog, which is required for both a negative modulation of phosphatidylinositol 3-kinase/Akt-dependent cell proliferation (20, 29, 30) and a p53-mediated regulation of cell survival and apoptosis (31). Consequently, PPAR $\gamma$  and p53 may converge in a tumor suppressor activity that remains to be further elucidated.

To provide new insight into the inhibitory action exerted by the cognate PPAR $\gamma$ -ligand BRL, we first demonstrated that PPAR $\gamma$  mediates the growth arrest in G<sub>0</sub>-G<sub>1</sub> phase induced by BRL in MCF7 cells. In addition, considering the key role elicited by p53 in the growth inhibition and apoptosis (14, 17), we have evaluated whether PPAR $\gamma$  signaling converges on p53 transduction pathway in MCF7 cells. Of interest, we found that BRL exposure up-regulates both p53 mRNA and protein levels with a concomitant increase of p21<sup>WAF1/Cip1</sup> expression. These effects were abrogated in the presence of the specific antagonist GW, addressing a PPAR $\gamma$ -mediated mechanism. Therefore, investigating the potential ability of BRL to modulate p53 promoter gene, we performed transient transfections in MCF7 cells using diverse deletion mu-

tants of p53 promoter gene (32). The dose-dependent transactivation of p53 by BRL involved PPAR $\gamma$  directly because the transcriptional activity was prevented by GW treatment. Moreover, we documented that the region spanning from -49 to -40, which corresponds to the NF $\kappa$ B site, is required for the responsiveness to BRL.

It deserves to be mentioned that the transcription factor NF $\kappa$ B can regulate both pro- and antiapoptotic signaling pathways depending on cell type, the extent of NF $\kappa$ B activation, and the nature of the apoptotic stimuli (33). NF $\kappa$ B was reported to physically interact with PPAR $\gamma$  (34), which in some circumstances binds to DNA cooperatively with NF $\kappa$ B (35, 36), further enhancing the NF $\kappa$ B-DNA binding (37). Furthermore, PPAR $\gamma$  agonists were able to enhance the binding of NF $\kappa$ B to the upstream  $\kappa$ B regulatory element site of *c-myc* (38). Our EMSA experiments extended the aforementioned observations because nuclear extracts of MCF7 cells treated with BRL showed an increased binding to the NF $\kappa$ B sequence located in the p53 promoter region. Given that the anti-PPAR $\gamma$  and anti-NF $\kappa$ B antibodies were both able to induce shifted bands, we performed an EMSA study using a cell-free system to ascertain the potential direct interaction of PPAR $\gamma$  with the NF $\kappa$ B site. Interestingly, we observed the formation of a single DNA-binding complex, which was again shifted by the anti-PPAR $\gamma$  antibody. These findings were supported by ChIP assay in MCF7 cells demonstrating the ability of BRL to enhance the recruitment of PPAR $\gamma$  and RNA Pol II to the promoter of p53 even in presence of the NF $\kappa$ B inhibitor P. Overall, these data indicate that the

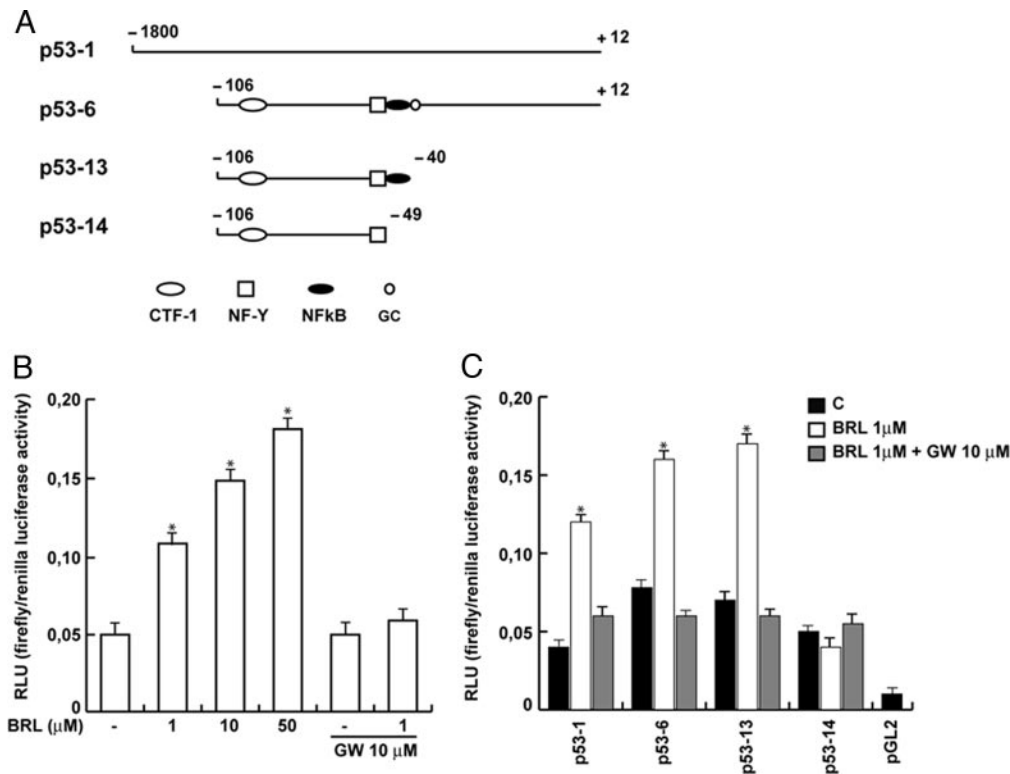


**Fig. 3.** Effects of BRL on p53-Gene Promoter-Luciferase Reporter Constructs in MCF7 Cells

A, Schematic map of the p53 promoter fragments used in this study. B, MCF7 cells were transiently transfected with p53 gene promoter-luciferase reporter construct (p53-1) and treated for 24 h with increasing BRL concentrations, 10  $\mu$ M GW alone or in combination with 1  $\mu$ M BRL. C, MCF7 cells were transiently transfected with p53 gene promoter-luc reporter constructs (p53-1, p53-6, p53-13, p53-14) and treated for 24 h with 1  $\mu$ M BRL and/or 10  $\mu$ M GW. The luciferase activities were normalized to the *Renilla* luciferase as internal transfection control and data were reported as relative light units. Columns are mean  $\pm$  SD of three independent experiments performed in triplicate. \*,  $P < 0.05$  BRL-treated vs. untreated cells. pGL<sub>2</sub>, Basal activity measured in cells transfected with pGL<sub>2</sub> basal vector; RLU, relative light units. CTF-1, CCAAT-binding transcription factor-1; NF-Y, nuclear factor-Y.

PPAR $\gamma$ -mediated growth arrest upon addition of BRL in MCF7 cells involves, at least in part, the direct stimulation of p53 transcription.

p53 acts as a tumor suppressor depending on its physical and functional interaction with diverse cellular proteins (39), like some nuclear receptors that, in turn, exert an inhibitory activity on p53 biological outcomes (19). In the supplemental data, published on The Endocrine Society's Journals online web site at <http://mend.endojournals.org>, we show an evident coimmunoprecipitation and colocalization of PPAR $\gamma$  and p53 after BRL treatment. However, additional experiments are required to better characterize such interaction and its functional consequences.

A large body of evidence has suggested the straightforward role of p53 signaling in the apoptotic cascades that include the activation of caspases, a family of cytoplasmic cysteine proteases (40). The intrinsic apoptotic pathway involves a mitochondria-dependent process, which results in cytochrome c release and, thereafter, activation of caspase-9 (24). Furthermore, apoptosis is characterized by distinct morphological changes including the internucleoso-

mal cleavage of DNA, which is recognized as a DNA ladder (Ref. 24 and references therein). Notably, we evidenced that in a consecutive series of events BRL 1) up-regulates the expression of p53 and 2) its effector p21<sup>WAF1/Cip1</sup>, 3) triggers the cleavage of caspases-9, and 4) induces DNA fragmentation in a PPAR $\gamma$ -mediated manner. Given the ability of AS/p53 to reduce the last two biological effects of BRL, an involvement of p53 in such PPAR $\gamma$ -dependent activity may be argued. On the contrary, the cleavage of caspase-9 and DNA fragmentation observed upon BRL treatment did not show changes suppressing the NF $\kappa$ B at protein level with P, suggesting that this factor is not required for the apoptotic events elicited by BRL.

In the present study we have provided a new insight into the molecular mechanism through which PPAR $\gamma$  mediates the growth arrest and apoptosis induced by BRL in MCF7 cells. Our findings suggest that a cross talk between p53 and PPAR $\gamma$  may assume biological relevance in setting novel therapeutic interventions in breast cancer.



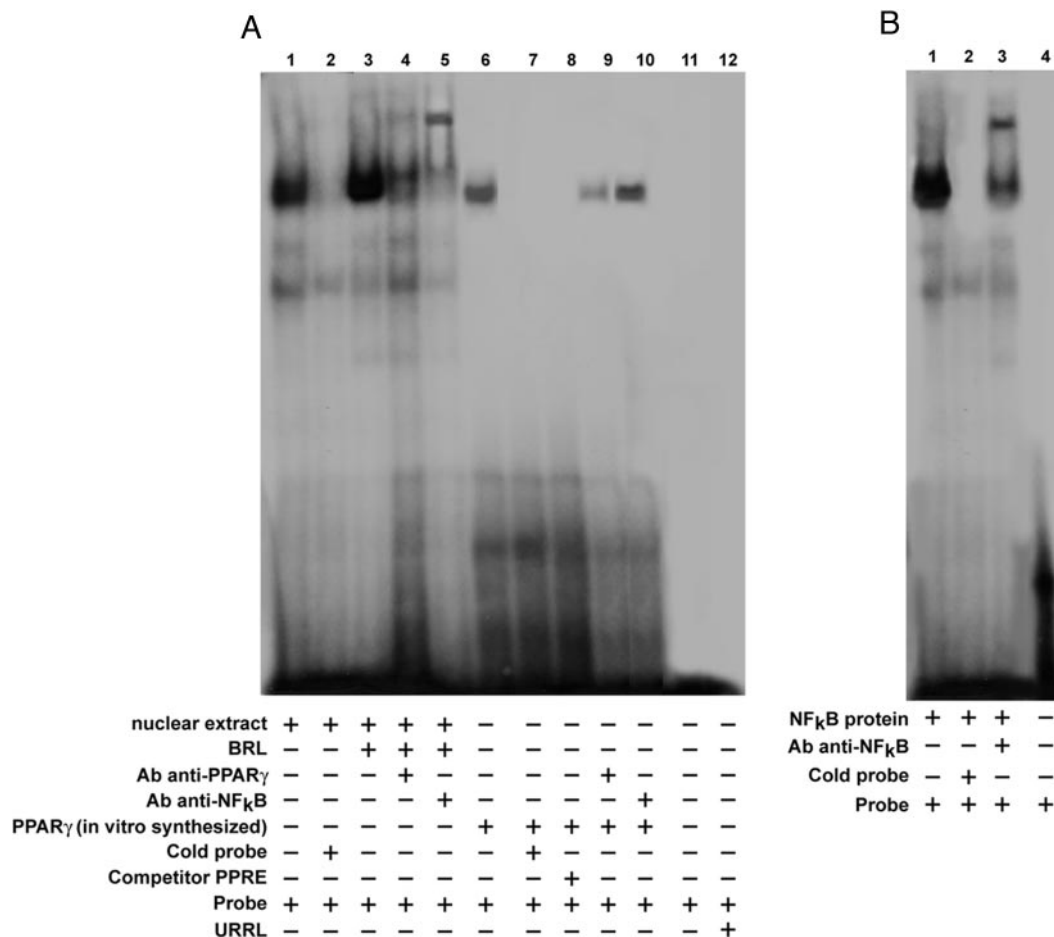


**Fig. 4.** PPAR $\gamma$  Binds to NF $\kappa$ B Site in the p53 Promoter Region in EMSA

A, Nuclear extracts from MCF7 cells (lane 1) or 2  $\mu$ l of PPAR $\gamma$  translated protein (lane 6) were incubated with a double-stranded NF $\kappa$ B sequence probe labeled with [ $\gamma$ <sup>32</sup>P] and subjected to electrophoresis in a 6% polyacrylamide gel. Competition experiments were performed adding as competitor a 100-fold molar excess of unlabeled NF $\kappa$ B probe (lanes 2 and 7) or as cold competitor PPRE (lane 8). In lane 3, nuclear extracts from MCF7 were treated with 10  $\mu$ M BRL. Anti-PPAR $\gamma$  and anti-NF $\kappa$ B Abs were incubated with nuclear extracts from MCF7 cells treated with 10  $\mu$ M BRL (lanes 4 and 5, respectively) or added to PPAR $\gamma$  protein (lanes 9 and 10, respectively). Lane 11 contains probe alone, lane 12 contains 2  $\mu$ l of unprogrammed rabbit reticulocyte lysate incubated with NF $\kappa$ B (URRL). B, NF $\kappa$ B protein (1  $\mu$ l) (lane 1) was incubated with a double-stranded NF $\kappa$ B sequence probe labeled with [ $\gamma$ <sup>32</sup>P] and subjected to electrophoresis in a 6% polyacrylamide gel. A 100-fold molar excess of unlabeled NF $\kappa$ B probe (lanes 2) or anti-NF $\kappa$ B antibody (Ab) (lane 3) was added to NF $\kappa$ B protein.

## MATERIALS AND METHODS

### Reagents

BRL49653 was a gift from GlaxoSmithKline (West Sussex, UK), the irreversible PPAR $\gamma$ -antagonist GW was purchased from Sigma (Milan, Italy), human recombinant TGF $\beta$  was obtained from ICN Biomedicals (DBA, Milan, Italy), and P was purchased from Alexis (San Diego, CA).

### Plasmids

The p53 promoter-luciferase reporters, constructed using pGL2 for cloning of p53-1 and -6, and TpGL2 for p53-13 and -14 were kindly provided by Dr. Stephen H. Safe (Texas A&M University, College Station, TX). The constructs used were generated by Safe (32) from the human p53 gene promoter as follows: p53-1 (containing the -1800 to +12 region), p53-6

(containing the -106 to +12 region), p53-13 (containing the -106 to -40 region) and p53-14 (containing the -106 to -49 region).

As an internal transfection control, we cotransfected the plasmid pRL-CMV (Promega Corp., Milan, Italy) that expresses *Renilla* luciferase enzymatically distinguishable from firefly luciferase by the strong cytomegalovirus enhancer/promoter. The p53 antisense plasmid (AS/p53) and PPAR $\gamma$  expression plasmid were gifts from Dr. Moshe Oren (Weizmann Institute of Science, Rehovot, Israel) and Dr. R. Evans (The Salk Institute, San Diego, CA), respectively.

### Cell Cultures

Wild-type human breast cancer MCF7 cells (a gift from Dr. Ewa Surmacz, Sbarro Institute for Cancer Research and Molecular Medicine, Philadelphia, PA) were grown in DMEM plus glutamax containing 10% fetal calf serum (Invitrogen, Milan, Italy) and 1 mg/ml penicillin-streptomycin.

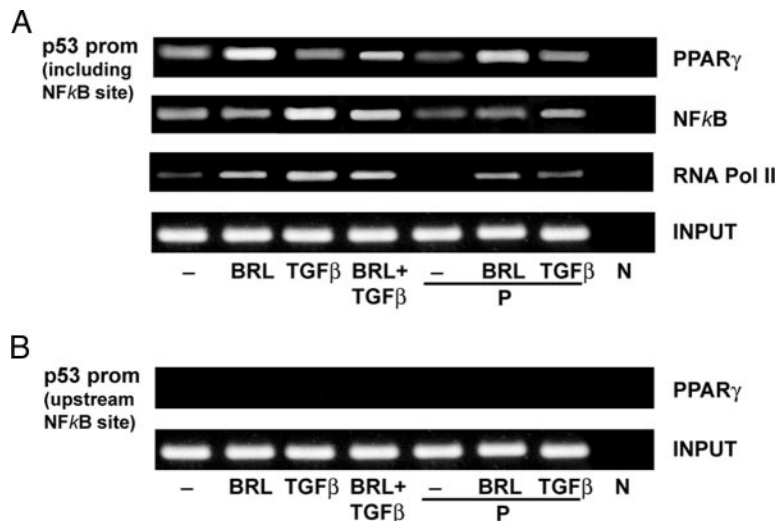


**Fig. 5.** Functional Interaction of PPAR $\gamma$  and p53 in ChIP Assay

MCF7 cells were treated for 1 h with 10  $\mu$ M BRL, 10 ng/ml TGF $\beta$ , 15  $\mu$ M P, as indicated. The soluble chromatin was immunoprecipitated with anti-PPAR $\gamma$ , anti-NF $\kappa$ B and anti-RNA Pol II antibodies. The p53 promoter (prom) sequence including the NF $\kappa$ B site (panel A) and that located upstream the NF $\kappa$ B site (panel B) were detected by PCR with specific primers, as described in *Materials and Methods*. To control input DNA, p53 promoter was amplified from 30  $\mu$ l of initial preparations of soluble chromatin (before immunoprecipitations). Normal rabbit antiserum was used as negative control (N).

#### DNA Flow Cytometry

MCF7 cells at 50–60% confluence were shifted to serum-free medium (SFM) for 24 h and then treatments were added in SFM for 48 h. Thereafter, cells were trypsinized, centrifuged at 1500 rpm for 3 min, washed with PBS, and then treated with 20  $\mu$ g/ml RNase A (Calbiochem, La Jolla, CA). DNA was stained with 100  $\mu$ g/ml propidium iodide for 30 min at 4 C protected from light, and cells were analyzed with the FAC-Scan (Becton Dickinson and Co., Franklin Lakes, NJ).

#### RT-PCR Assay

MCF7 cells were grown in 10-cm dishes to 70–80% confluence and exposed to treatments for 24 and 48 h in SFM. Total cellular RNA was extracted using TRIZOL reagent (Invitrogen) as suggested by the manufacturer. The purity and integrity were checked spectrophotically and by gel electrophoresis before carrying out the analytical procedures. The evaluation of gene expression was performed by a semiquantitative RT-PCR method as previously described (41). For p53, p21<sup>WAF1/Cip1</sup>, and the internal control gene 36B4, the primers were: 5'-GTGGAAGGAAATTTGCGTGT-3' (p53 forward) and 5'-CCAGTGTGATGATGGTGAGG-3' (p53 reverse), 5'-GCTTCATGCCAGCTACTTCC-3' (p21 forward) and 5'-CTGTGCTCACTTCAGGGTCA-3' (p21 reverse), 5'-CTCAACATCTCCCCCTTCTC-3' (36B4 forward) and 5'-CAAATCCCATATCCTCGTCC-3' (36B4 reverse) to yield, respectively, products of 190 bp with 18 cycles, 270 bp with 18 cycles, and 408 bp with 12 cycles. The results obtained as optical density arbitrary values were transformed to percentage of the control (percent control) taking the samples from untreated cells as 100%.

#### Transfection Assay

MCF7 cells were transferred into 24-well plates with 500  $\mu$ l of regular growth medium/well the day before transfection. The medium was replaced with SFM on the day of transfection, which was performed using Fugene 6 reagent as recom-

mended by the manufacturer (Roche Diagnostics, Mannheim, Germany) with a mixture containing 0.5  $\mu$ g of promoter-luc reporter plasmid, 5 ng of pRL-CMV. After transfection for 24 h, treatments were added in SFM as indicated, and cells were incubated for an additional 24 h. Firefly and *Renilla* luciferase activities were measured using the Dual Luciferase Kit (Promega Corp., Madison, WI). The firefly luciferase values of each sample were normalized by *Renilla* luciferase activity, and data were reported as relative light units.

MCF7 cells plated into 10-cm dishes were transfected with 5  $\mu$ g of AS/p53 using Fugene 6 reagent as recommended by the manufacturer (Roche Diagnostics). The activity of AS/p53 was verified using Western blot to detect changes in p53 protein levels. Time course analysis revealed that p53 levels were effectively suppressed at 18 h after transfection (data not shown). Empty vector was used to ensure that DNA concentrations were constant in each transfection.

#### EMSA

Nuclear extracts from MCF7 cells were prepared as previously described for EMSA (42). Briefly, MCF7 cells plated into 10-cm dishes were grown to 70–80% confluence, shifted to SFM for 24 h, and then treated with 10  $\mu$ M BRL for 6 h. Thereafter, cells were scraped into 1.5 ml of cold PBS. Cells were pelleted for 10 sec and resuspended in 400  $\mu$ l cold buffer A [10 mM HEPES-KOH (pH 7.9) at 4 C, 1.5 mM MgCl<sub>2</sub>, 10 mM KCl, 0.5 mM dithiothreitol, 0.2 mM phenylmethylsulfonylfluoride (PMSF), 1 mM leupeptin] by flicking the tube. The cells were allowed to swell on ice for 10 min and then vortexed for 10 sec. Samples were then centrifuged for 10 sec and the supernatant fraction was discarded. The pellet was resuspended in 50  $\mu$ l of cold Buffer B (20 mM HEPES-KOH, pH 7.9; 25% glycerol; 1.5 mM MgCl<sub>2</sub>; 420 mM NaCl; 0.2 mM EDTA; 0.5 mM dithiothreitol; 0.2 mM PMSF; 1 mM leupeptin) and incubated in ice for 20 min for high-salt extraction. Cellular debris was removed by centrifugation for 2 min at 4 C, and the supernatant fraction (containing DNA-binding proteins) was stored at -70 C. *In vitro*-transcribed and translated PPAR $\gamma$  was synthesized using the T7 polymerase in the rabbit reticulocyte lysate system from PPAR $\gamma$  plasmid as

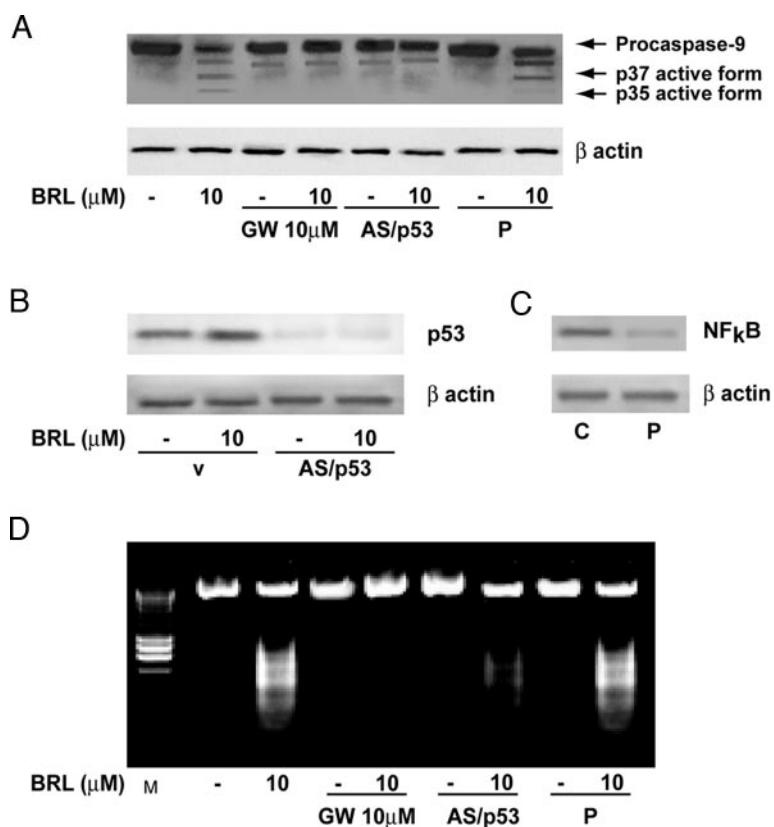


**Fig. 6.** BRL Induces Cleavage of Caspase-9 and DNA Laddering

A, MCF7 cells were treated with BRL alone or in combination with GW or P for 48 h as indicated, or transfected with an expression plasmid encoding for p53 antisense (AS/p53). Positions of procaspase-9 and its cleavage products are indicated by *arrowheads* to the *right*. One of three similar experiments is presented.  $\beta$ -Actin was used as loading control on the same stripped blot. B, p53 protein expression (evaluated by Western blot) in MCF7 cells transfected with an empty vector (v) or a AS/p53 and treated as indicated.  $\beta$ -Actin was used as loading control. C, NF $\kappa$ B expression in MCF7 cells untreated or treated with P as indicated.  $\beta$ -Actin was used as loading control. D, DNA laddering was performed in MCF7 cells treated for 72 h as indicated, or transfected with AS/p53.

directed by the manufacturer (Promega). The probe was generated by annealing single-stranded oligonucleotides and labeled with [ $\gamma$ <sup>32</sup>P]ATP (Amersham Pharmacia, Buckinghamshire, UK) and T4 polynucleotide kinase (Promega) and then purified using Sephadex G50 spin columns (Amersham Pharmacia). The DNA sequence of the NF $\kappa$ B used as probe or as cold competitor is the following: NF $\kappa$ B, 5'-AGT TGA GGG GAC TTT CCC AGG C-3' (Sigma Genosys, Cambridge, UK). As cold competitor we also used PPPE oligonucleotide: 5'-GGGACCAGGACAAAGGTCACGTT-3' (Sigma Genosys). The protein-binding reactions were carried out in 20  $\mu$ l of buffer [20 mM HEPES (pH 8), 1 mM EDTA, 50 mM KCl, 10 mM dithiothreitol, 10% glycerol, 1 mg/ml BSA, 50  $\mu$ g/ml polydeoxyinosinic deoxycytidylic acid] with 50,000 cpm of labeled probe, 5  $\mu$ g of MCF7 nuclear protein, or 2  $\mu$ l of transcribed and translated *in vitro* PPAR $\gamma$  protein, or 1  $\mu$ l of NF $\kappa$ B protein (Promega), and 5  $\mu$ g of polydeoxyinosinic deoxycytidylic acid. The mixtures were incubated at room temperature for 20 min in the presence or absence of unlabeled competitor oligonucleotides. For the experiments involving anti-PPAR $\gamma$  and anti-NF $\kappa$ B antibodies (Santa Cruz Biotechnology, Inc., Santa Cruz, CA), the reaction mixture was incubated with these antibodies at 4 C for 30 min before addition of labeled probe. The entire reaction mixture was electrophoresed through a 6% polyacrylamide gel in 0.25 $\times$  Tris borate-EDTA for 3 h at 150 V. Gel was dried and subjected to autoradiography at -70 C.

#### ChIP

MCF7 cells were grown in 10-cm dishes to 50–60% confluence, shifted to SFM for 24 h, and then treated with 10  $\mu$ M BRL for 1 h. Thereafter, cells were washed twice with PBS and cross-linked with 1% formaldehyde at 37 C for 10 min. Next, cells were washed twice with PBS at 4 C, collected and resuspended in 200  $\mu$ l of lysis buffer (1% SDS; 10 mM EDTA; 50 mM Tris-HCl, pH 8.1), and left on ice for 10 min. Then, cells were sonicated four times for 10 sec at 30% of maximal power (Vibra Cell 500 W; Sonics and Materials, Inc., Newtown, CT) and collected by centrifugation at 4 C for 10 min at 14,000 rpm. The supernatants were diluted in 1.3 ml of immunoprecipitation buffer (0.01% SDS; 1.1% Triton X-100; 1.2 mM EDTA; 16.7 mM Tris-HCl, pH 8.1; 16.7 mM NaCl) followed by immunoclearing with 80  $\mu$ l of sonicated salmon sperm DNA/protein A agarose (DBA Srl, Milan, Italy) for 1 h at 4 C. The precleared chromatin was immunoprecipitated with anti-PPAR $\gamma$ , anti-NF $\kappa$ B, and anti-RNA Pol II antibodies (Santa Cruz Biotechnology). At this point, 60  $\mu$ l salmon sperm DNA/protein A agarose was added, and precipitation was further continued for 2 h at 4 C. After pelleting, precipitates were washed sequentially for 5 min with the following buffers: Wash A [0.1% SDS, 1% Triton X-100, 2 mM EDTA, 20 mM Tris-HCl (pH 8.1), 150 mM NaCl], WA B [0.1% SDS, 1% Triton X-100, 2 mM EDTA, 20 mM Tris-HCl (pH 8.1), 500 mM NaCl],

and Wash C [0.25 M LiCl, 1% Nonidet P-40, 1% sodium deoxycholate, 1 mM EDTA, 10 mM Tris-HCl (pH 8.1)], and then twice with TE buffer (10 mM Tris, 1 mM EDTA). The immunocomplexes were eluted with elution buffer (1% SDS, 0.1 M NaHCO<sub>3</sub>). The eluates were reverse cross-linked by heating at 65 C and digested with proteinase K (0.5 mg/ml) at 45 C for 1 h. DNA was obtained by phenol-chloroform-isoamyl alcohol extraction. Two microliters of 10 mg/ml yeast tRNA (Sigma) was added to each sample, and DNA was precipitated with 70% ethanol for 24 h at –20 C and then washed with 95% ethanol and resuspended in 20  $\mu$ l of TE buffer. A 5  $\mu$ l volume of each sample was used for PCR with primers flanking a sequence present in the p53 promoter: 5'-CT-GAGAGCAAACGCAAAG-3' (forward) and 5'-CAGC-CCGAACGCAAAGTGTC-3' (reverse) containing the  $\kappa$ B site from –254 to –42 region and 5'-GAAAACGTTAGGGT-GTGG-3' (forward) and 5'-GGTGCAGAGTCAGGATTC-3' (reverse) upstream of the  $\kappa$ B site from –528 to –452 region (GenBank accession no. J0423). The PCR conditions for the two p53 promoter fragments were, respectively, 45 sec at 94 C, 40 sec at 57 C, 90 sec at 72 C, 45 sec at 94 C, 40 sec at 55 C, and 90 sec at 72 C. The amplification products obtained in 30 cycles were analyzed in a 2% agarose gel and visualized by ethidium bromide staining. The negative control was provided by PCR amplification without a DNA sample. The specificity of reactions was ensured using normal mouse and rabbit IgG (Santa Cruz Biotechnology).

### Immunoblotting

MCF7 cells were grown in 10-cm dishes to 70–80% confluence and exposed to treatments for 24 and 48 h in SFM as indicated. Cells were then harvested in cold PBS and resuspended in lysis buffer containing 20 mM HEPES (pH 8), 0.1 mM EDTA, 5 mM MgCl<sub>2</sub>, 0.5 M NaCl, 20% glycerol, 1% Nonidet P-40, and inhibitors (0.1 mM Na<sub>3</sub>VO<sub>4</sub>, 1% PMSF, 20 mg/ml aprotinin). Protein concentration was determined by Bio-Rad Protein Assay (Bio-Rad Laboratories, Hercules, CA).

A 50- $\mu$ g portion of protein lysates was used for Western blotting, resolved on a 10% SDS-polyacrylamide gel, transferred to a nitrocellulose membrane, and probed with an antibody directed against the p53, p21<sup>WAF1/Cip1</sup>, caspases-9, and NF $\kappa$ B (Santa Cruz Biotechnology). As internal control, all membranes were subsequently stripped (0.2 M glycine, pH 2.6, for 30 min at room temperature) of the first antibody and reprobed with anti- $\beta$ -actin antibody.

The antigen-antibody complex was detected by incubation of the membranes for 1 h at room temperature with peroxidase-coupled goat antimouse or antirabbit IgG and revealed using the enhanced chemiluminescence system (Amersham Pharmacia). Blots were then exposed to film (Kodak film, Sigma). The intensity of bands representing relevant proteins was measured by Scion Image laser densitometry scanning program.

### DNA Fragmentation

DNA fragmentation was determined by gel electrophoresis. MCF7 cells were grown in 10-cm dishes to 70% confluence and treated with 10  $\mu$ M BRL and/or 10  $\mu$ M GW and/or 15  $\mu$ M P. After 72 h cells were collected and washed with PBS and pelleted at 1800 rpm for 5 min. The samples were resuspended in 0.5 ml of extraction buffer (50 mM Tris-HCl, pH 8; 10 mM EDTA, 0.5% SDS) for 20 min in rotation at 4 C. DNA was extracted with phenol-chloroform three times and once with chloroform. The aqueous phase was used to precipitate acids nucleic with 0.1 vol of or 3 M sodium acetate and 2.5 volumes cold EtOH overnight at –20 C. The DNA pellet was resuspended in 15  $\mu$ l of H<sub>2</sub>O treated with RNase A for 30 min at 37 C. The absorbance of the DNA solution at 260 and 280 nm was determined by spectrophotometry. The extracted DNA (40  $\mu$ g/lane) was subjected to electrophoresis on 1.5%

agarose gels. The gels were stained with ethidium bromide and then photographed.

### Statistical Analysis

Statistical analysis was performed using ANOVA followed by Newman-Keuls testing to determine differences in means.  $P < 0.05$  was considered as statistically significant.

### Acknowledgments

We thank Dr. Stephen H. Safe for providing the human p53 gene promoter and the deletion mutants and Moshe Oren and R.M. Evans for the gifts of the p53 antisense and PPAR $\gamma$  expression plasmid, respectively. We also thank D. Sturino (Faculty of Pharmacy, University of Calabria, Calabria, Italy) for the English review.

Received May 8, 2006. Accepted July 26, 2006.

Address all correspondence and requests for reprints to: Professor Sebastiano Andò, Faculty of Pharmacy-University of Calabria, Arcavacata-Rende (Cosenza) 87036, Italy. E-mail: sebastiano.ando@unical.it or daniela.bonofiglio@tin.it.

This work was supported by Associazione Italiana Ricerca sul Cancro, Ministero dell'Istruzione Università e Ricerca, and Ministero della Salute.

Disclosure Statement: The authors have nothing to disclose.

### REFERENCES

1. Shearer BG, Hoekstra WJ 2003 Recent advances in peroxisome proliferator-activated receptor science. *Curr Med Chem* 10:267–280
2. Francis GA, Fayard E, Picard F, Auwerx J 2003 Nuclear receptors and the control of metabolism. *Annu Rev Physiol* 65:261–311
3. Chawla A, Repa JJ, Evans RM, Mangelsdorf DJ 2001 Nuclear receptors and lipid physiology: opening the X-files. *Science* 294:1866–1870
4. Yamauchi T, Kamon J, Waki H, Murakami K, Motojima K, Komeda K, Ide T, Kubota N, Terauchi Y, Tobe K, Miki H, Tsuchida A, Akanuma Y, Nagai R, Kimura S, Kadowaki T 2001 The mechanisms by which both heterozygous peroxisome proliferator-activated receptor  $\gamma$  (PPAR $\gamma$ ) deficiency and PPAR  $\gamma$  agonist improve insulin resistance. *J Biol Chem* 276:41245–41254
5. Fajas L, Egler V, Reiter R, Miard S, Lefebvre AM, Auwerx J 2003 PPAR  $\gamma$  controls cell proliferation and apoptosis in an RB-dependent manner. *Oncogene* 22:4186–4193
6. Mueller E, Sarraf P, Tontonoz P, Evans RM, Martin KJ, Zhang M, Fletcher C, Singer S, Spiegelman BM 1998 Terminal differentiation of human breast cancer through PPAR  $\gamma$ . *Mol Cell* 1:465–470
7. Elstner E, Muller C, Koshizuka K, Williamson EA, Park D, Asou H, Shintaku P, Said JW, Heber D, Koeffler HP 1998 Ligands for peroxisome proliferator-activated receptor  $\gamma$  and retinoic acid receptor inhibit growth and induce apoptosis of human breast cancer cells in vitro and in BNX mice. *Proc Natl Acad Sci USA* 95:8806–8811
8. Vousden KH, Lu X 2002 Live or let die: the cell's response to p53. *Nat Rev Cancer* 2:594–604
9. Liu G, Lozano G 2005 p21 stability: linking chaperones to a cell cycle checkpoint. *Cancer Cell* 7:113–114
10. el-Deiry WS, Tokino T, Velculescu VE, Levy DB, Parsons R, Trent JM, Lin D, Mercer WE, Kinzler KW, Vogelstein B 1993 WAF1, a potential mediator of p53 tumor suppression. *Cell* 75:817–825

11. Harper JW, Adami GR, Wei N, Keyomarsi K, Elledge SJ 1993 The p21 Cdk-interacting protein Cip1 is a potent inhibitor of G1 cyclin-dependent kinases. *Cell* 75:805–816
12. Tom S, Ranalli TA, Podust VN, Bambara RA 2001 Regulatory roles of p21 and apurinic/apyrimidinic endonuclease 1 in base excision repair. *J Biol Chem* 276:48781–48789
13. Caelles C, Helmlberg A, Karin M 1994 p53-Dependent apoptosis in the absence of transcriptional activation of p53-target genes. *Nature* 370:220–223
14. Yu J, Zhang L 2005 The transcriptional targets of p53 in apoptosis control. *Biochem Biophys Res Commun* 331:851–858
15. O'Brate A, Giannakakou P 2003 The importance of p53 location: nuclear or cytoplasmic zip code? *Drug Resistance Updates* 6:313–322
16. Appella E 2001 Modulation of p53 function in cellular regulation. *Eur J Biochem* 268:2763
17. Haupt S, Berger M, Goldberg Z, Haupt Y 2003 Apoptosis—the p53 network. *J Cell Sci* 116:4077–4085
18. Woods DB, Vousden KH 2001 Regulation of p53 function. *Exp Cell Res* 264:56–66
19. Sengupta S, Wasylyk B 2004 Physiological and pathological consequences of the interactions of the p53 tumor suppressor with the glucocorticoid, androgen, and estrogen receptors. *Ann NY Acad Sci* 1024:54–71
20. Bonofiglio D, Gabriele S, Aquila S, Catalano S, Gentile M, Middea E, Giordano F, Andò S 2005 Estrogen receptor  $\alpha$  binds to peroxisome proliferator-activated receptor (PPAR) response element and negatively interferes with PPAR  $\gamma$  signalling in breast cancer cells. *Clin Cancer Res* 11:6139–6147
21. Patel L, Pass I, Coxon P, Downes CP, Smith SA, Macphee CH 2001 Tumor suppressor and anti-inflammatory actions of PPAR $\gamma$  agonist are mediated via up-regulation of PTEN. *Curr Biol* 11:764–768
22. Clay CE, Namen AM, Atsumi G, Willingham MC, High KP, Kute TE, Trimboli AJ, Fonteh AN, Dawson PA, Chilton FH 1999 Influence of J series prostaglandins on apoptosis and tumorigenesis of breast cancer cells. *Carcinogenesis* 20:1905–1911
23. Hehner SP, Heinrich M, Bork PM, Vogt M, Ratter F, Lehmann V, Schulze-Osthoff K, Droge W, Schmitz ML 1998 Sesquiterpene lactones specifically inhibit activation of NF- $\kappa$  B by preventing the degradation of I $\kappa$ B- $\alpha$  and I $\kappa$ B- $\beta$ . *J Biol Chem* 273:1288–1297
24. Cohen GM 1997 Caspases: the executioners of apoptosis. *Biochem J* 326:1–16
25. Brockman JA, Gupta RA, Dubois RN 1998 Activation of PPAR $\gamma$  leads to inhibition of anchorage-independent growth of human colorectal cancer cells. *Gastroenterology* 115:1049–1055
26. Han C, Demetris AJ, Michalopoulos GK, Zhan Q, Shelhamer JH, Wu T 2003 PPAR $\gamma$  ligands inhibit cholangiocarcinoma cell growth through p53-dependent GADD45 and p21 pathway. *Hepatology* 38:167–177
27. Nagamine M, Okumura T, Tanno S, Sawamukai M, Motomura W, Takahashi N, Kohgo Y 2003 PPAR $\gamma$  ligand-induced apoptosis through a p53-dependent mechanism in human gastric cancer cells. *Cancer Sci* 94:338–343
28. Okura T, Nakamura M, Takata Y, Watanabe S, Kitami Y, Hiwada K 2000 Troglitazone induces apoptosis via the p53 and Gadd45 pathway in vascular smooth muscle cells. *Eur J Pharmacol* 407:227–235
29. Di Cristofano A, Pandolfi PP 2000 The multiple roles of PTEN in tumor suppression. *Cell* 100:387–390
30. Yamada KM, Araki M 2001 Tumor suppressor PTEN: modulator of cell signaling, growth, migration and apoptosis. *J Cell Sci* 114:2375–2382
31. Stambolic V, MacPherson D, Sas D, Lin Y, Snow B, Jang Y, Benchimol S, Mak TW 2001 Regulation of PTEN transcription by p53. *Mol Cell* 8:317–325
32. Qin C, Nguyen T, Stewart J, Samudio I, Burghardt R, Safe S 2002 Estrogen up-regulation of p53 gene expression in MCF-7 breast cancer cells is mediated by calmodulin kinase IV-dependent activation of a nuclear factor  $\kappa$ B/CCAAT-binding transcription factor-1 complex. *Mol Endocrinol* 16:1793–1809
33. Fujioka S, Schmidt C, Sclabas GM, Li Z, Pelicano H, Peng B, Yao A, Niu J, Zhang W, Evans DB, Abbruzzese JL, Huang P, Chiao PJ 2004 Stabilization of p53 is a novel mechanism for proapoptotic function of NF- $\kappa$ B. *J Biol Chem* 279:27549–27559
34. Chung SW, Kang BY, Kim SH, Pak YK, Cho D, Trinchieri G, Kim TS 2000 Oxidized low density lipoprotein inhibits interleukin-12 production in lipopolysaccharide-activated mouse macrophages via direct interactions between peroxisome proliferator-activated receptor- $\gamma$  and nuclear factor- $\kappa$  B. *J Biol Chem* 275:32681–32687
35. Coutureir C, Brouillet A, Couriaud C, Koumanov K, Berezziat G, Andreani M 1999 Interleukin 1 $\beta$  induces type II-secreted phospholipase A $_2$  gene in vascular smooth muscle cells by a nuclear factor  $\kappa$ B and peroxisome proliferator-activated receptor-mediated process. *J Biol Chem* 274:23085–23093
36. Sun YX, Wright HT, Janciasukiene S 2002  $\alpha$ 1-Antichymotrypsin/Alzheimer's peptide A $\beta$  (1–42) complex perturbs lipid metabolism and activates transcription factors PPAR $\gamma$  and NF $\kappa$ B in human neuroblastoma (Kelly) cells. *J Neurosci Res* 67:511–522
37. Ikawa H, Kameda H, Kamitani H, Baek SJ, Nixon JB, Hsi LC, Eling TE 2001 Effect of PPAR activators on cytokine-stimulated cyclooxygenase-2 expression in human colorectal carcinoma cells. *Exp Cell Res* 267:73–80
38. Schlezinger JJ, Jensen BA, Mann KK, Ryu HY, Sherr DH 2002 Peroxisome proliferator-activated receptor  $\gamma$ -mediated NF- $\kappa$ B activation and apoptosis in pre-B cells. *J Immunol* 169:6831–6841
39. Oren M, Damalas A, Gottlieb T, Michael D, Taplick J, Leal JF, Maya R, Moas M, Seger R, Taya Y, Ben-Ze'Ev A 2002 Regulation of p53: intricate loops and delicate balances. *Ann NY Acad Sci* 973:374–383
40. Schuler M, Green DR 2001 Mechanisms of p53-dependent apoptosis. *Biochem Soc Trans* 29:684–688
41. Maggolini M, Donzé O, Picard D 1999 A non-radioactive method for inexpensive quantitative RT-PCR. *Biol Chem* 380:695–697
42. Andrews NC, Faller DV 1991 A rapid micropreparation technique for extraction of DNA-binding proteins from limiting numbers of mammalian cells. *Nucleic Acids Res* 19:2499

**Molecular Endocrinology** is published monthly by The Endocrine Society (<http://www.endo-society.org>), the foremost professional society serving the endocrine community.

*Online Supplement Published by the American Society for Investigative Pathology*

# The American Journal of **PATHOLOGY**

Cellular and Molecular Biology of Disease



**Società Italiana di Patologia XXIX National Congress Abstracts**

**September 2008 Volume 173, Supplement**

software analysis and statistical analysis were performed. Results: A cluster of interesting proteins come up from the statistical analysis, which expression corresponds to a good response to NACT. Among these we found cell growth and maintenance proteins such vimentines, energetic pathway proteins like ALDO-a, lactic-dehydrogenase, phosphoglycerate-kinase and triose-phosphate isomerase. Proteasome regulators, anti-apoptotic 14-3-3 enzymes, apolipoprotein-A and nucleic acids metabolism proteins, such as DJ-1, were also found. Conclusions: The NIF/TIF study seems to be useful for the detection of markers predictive of response to treatment. In this study, the identification of a combination of proteins differentially expressed will probably be more sensitive and specific than a single molecular marker for screening, diagnosis, prognosis, and prediction of therapeutic response. The final aim will be the identification of prognostic and predictive markers in serum.

**NB 11. Molecular and Proteomic Characterization of Primary Cell Cultures from Normal Kidney and Renal Cell Carcinoma**

C. Bianchi<sup>1</sup>, S. Bombelli<sup>1</sup>, L. Invernizzi<sup>2</sup>, C. Chinello<sup>3</sup>, B. Torsello<sup>4</sup>, V. Angeloni<sup>1</sup>, P. Brambilla<sup>1</sup>, F. Raimondo<sup>1</sup>, V. Proserpio<sup>2</sup>, S. Casellato<sup>3</sup>, S. Ferrero<sup>4</sup>, F. Magni<sup>1</sup>, R. Perego<sup>1</sup>

<sup>1</sup>Department of Experimental Medicine, Milano-Bicocca University, Monza, Italy, <sup>2</sup>Department of Laboratory Medicine, Desio Hospital, Desio, Italy, <sup>3</sup>Institute of Urology, IRCCS Policlinico, University of Milano, Milan, Italy, <sup>4</sup>Department of Medicine, Surgery and Dentistry, University of Milan, Milano, Italy.

Renal cell carcinomas (RCCs), 3% of human malignancies, have difficult and late diagnosis and proteomic studies looking for biomarkers are ongoing. To detect RCC biomarkers, overcoming tissue cellular heterogeneity, 39 primary cultures were established from normal and tumor renal tissues. Most of normal cortex and tumor cells expressed proximal and distal tubule markers. 2-DE/MS analysis of cortex and RCC cultures identified 44 differentially expressed proteins. We analyzed, by Real-Time PCR and western blot, the expression of 3 proteins (ANXA3, LASP1 and CTSB) more abundant in RCC cultures, and of non-receptor tyrosine kinase Arg. These proteins are involved either in VHL/HIF-1 angiogenesis or cytoskeleton remodeling pathways. We evidenced a different isoform expression pattern between normal and RCC cultures.

**NB 12. Gamma-Glutamyltransferase-Dependent Resistance of Melanoma Cells to Arsenic Trioxide – The Role of Catalase induction.**

C. Giommarrelli<sup>1</sup>, R. Supino<sup>2</sup>, A. Paolocchi<sup>1</sup>, F. Zunino<sup>2</sup>, A. Pompella<sup>1</sup>, A. Corti<sup>1</sup>

<sup>1</sup>Department of Experimental Pathology, University of Pisa, Pisa, Italy, <sup>2</sup>Istituto Nazionale Tumori, Milano, Italy, <sup>3</sup>Istituto Nazionale Tumori, Milano, Italy.

Our aim was to evaluate if  $\gamma$ -glutamyltransferase (GGT) expression can modulate cell sensitivity to hydrogen peroxide (H<sub>2</sub>O<sub>2</sub>), ascorbic acid (AA) or arsenic trioxide (ATO). GGT-overexpression caused increased resistance against H<sub>2</sub>O<sub>2</sub> and AA, as judged by levels of apoptosis (TUNEL assay), DNA damage response (c-H2AX and p53 phosphorylation) and activation of cell death pathways (cytochrome c release, caspase activation). Accordingly, a higher resistance against ATO or AA+ATO was observed. A twice higher catalase activity was detectable in the GGT rich clone. GGT-overexpression is associated with increased anti-oxidant defenses, but also with higher levels of DNA-damage (Comet assay), likely with the meaning of a factor in neoplastic progression.

The financial support of the Istituto Toscano Tumori (ITT, Firenze) is gratefully acknowledged.

**NB 13. Overexpression of Glutathione-S-Transferases Omega 1 (GSTO1) Enhances the Resistance of HeLa Cells to Cisplatin**

S. Piaggi<sup>1</sup>, A. Corti<sup>1</sup>, A. Pompella<sup>1</sup>, A. Casini<sup>1</sup>

<sup>1</sup>Experimental Pathology, BMIE, University, Pisa, Italy.

Background: GSTO1 may play a role in the acquisition of the chemoresistance to cisplatin. Methods: Immunoblot analysis and RT-PCR studies were performed on HeLa cells seeded at high and low density. Cytotoxicity studies and measurement of glutathione were made on HeLa cells stably transfected with GSTO1. Results and Conclusion: Our results show that cells reaching high degree of confluence overexpressed the GSTO1 either when cells were seeded directly at high density or if they reach the high density after three days of culture. The levels of glutathione were the same in high and low density cells and in stably transfected cells. Cytotoxicity studies on stably transfected cells show an increased resistance to cisplatin.

**NB 14. Exploring Mutant P53 Gain of Functions in Vivo Through Conditional RNA Interference**

G. Bossi<sup>1</sup>, F. Marampon<sup>2</sup>, B. Zan<sup>2</sup>, G. Blandino<sup>2</sup>, A. Sacchi<sup>1</sup>

<sup>1</sup>Experimental Oncology, Regina Elena Cancer Institute, Rome, Italy, <sup>2</sup>University of L'Aquila, L'Aquila, Italy, <sup>3</sup>Rome Oncogenomic Center, Regina Elena Cancer Institute, Rome, Italy, <sup>4</sup>Regina Elena Cancer Institute, Rome, Italy.

Mutant-p53 proteins are thought to have acquired 'gain-of-function' (GOF) activity

that mainly contributes to tumor aggressiveness. In this study, mimicking physiological conditions, we describe the establishment of a lentiviral-based-system for conditional interference with mutant-p53 expression. In vivo studies assessed the efficacy of conditional RNA interference in inhibiting gain-of-function activity of mutant-p53 proteins by reducing tumor growth ability. Moreover by using this system, microarray data were validated in vitro and in vivo and putative mutant-p53 target genes that may contribute to its gain-of-function effects in cancer were identified. Results are confirmatory that depletion of mutant-p53 protein impacts on tumor malignancy and validated the inducible lentiviral-based system as an efficient tool to study the gain-of-function activity of human tumor derived p53 mutants.

**NB 15. Imatinib Mesylate Resistance by T315I Mutation and its Prevalence in Indian Chronic Myeloid Leukemia Patients (First Study from India)**

A.B. R. Mir<sup>1</sup>, S. Sazawal<sup>1</sup>, B. Bohra<sup>1</sup>, R. Chobey<sup>1</sup>, R. Saxena<sup>1</sup>

<sup>1</sup>Department of Hematology, All India Institute of Medical Sciences, Department of Hematology, All India Institute of Medical Sciences, NEW DELHI, India.

Aim: a) To detect T315I mutation and study its role in Imatinib mesylate resistance. b) To study prevalence of T315I mutation in relapsed CML patients. Methodology: 200 CML patients diagnosed by RT-PCR and treated with Imatinib (400mg to 600mg/day). ASO-PCR was done for T315I mutation. Results: 45/200 developed hematological and molecular resistance, 10/200 were in AP/Bc CML. ASO-PCR was done for T315I. 37/45 and 8/10 were positive for T315I mutation. T315I positive cases showed poor prognosis. T315I was detected in 80% to 85% of our relapsed cases. Survival and time-to-progression curves were obtained from Kaplan-Meier method. Conclusion: The early detection of T315I mutation proved to be helpful in therapeutic decisions in CML patients. ASO-PCR based detection of T315I proved to be economical, sensitive and rapid.

**NB 16. Idiotype-Specific Peptides as Tools for the Specific Delivery of Therapeutic Compounds into Tumors**

E. Iaccino<sup>1</sup>, C. Falcone<sup>1</sup>, F.M. Tuccillo<sup>2</sup>, M. Schiavone<sup>3</sup>, S. Cariglino<sup>4</sup>, A. De Franco<sup>4</sup>, I. Quinto<sup>1</sup>, C. Palmieri<sup>1</sup>, G. Scala<sup>1</sup>

<sup>1</sup>University of Catanzaro, Catanzaro, Italy, <sup>2</sup>Fondazione G.Pascale, Naples, Italy, <sup>3</sup>Department of Biochemistry and Medical Biotechnology, University of Naples 'Federico II', Naples, Italy, <sup>4</sup>Biotechnology Research Center (Italsistemi), Crotona, Italy.

B-cell lymphomas are characterized by clonal expansion of tumor cells expressing a B Cell Receptor (BCR) that include idiotypic immunoglobulin (Id). Id is determined by rearrangements of the immunoglobulin V regions that are unique for each clonal B-cell population and functions as a tumor-specific marker. Random peptide libraries (RPL) are important tools to define the antigen specificity and the characterization of Id ligands for tumor B cells. We evaluated the ability of Id-specific peptide (Id-peptides) for B-lymphoma cells selected by screening RPLs as a tool for the specific delivery of a therapeutic cargo into tumor cell. Results can be summarized as follows: a) 3 phage clones selected screening RPLs with immunoglobulins purified from A20 B-lymphoma cells b) Synthetic peptides, corresponding to the insert of phage clones, maintained their antigenic properties c) Id-peptides targeted specifically tumor cells in vivo d) Id-peptides were internalized into target tumor cells e) Id-peptides were able to deliver a cargo fluorophore (FITC) or a protein (GFP) into target tumor cells. This evidence shows that Id-peptides are powerful candidates for specific delivery of therapeutic drugs into tumors.

**NUTRITION AND CANCER**

**NC 01. The Apoptotic Effects of Rosiglitazone and 9 Cis Retinoic Acid at Low Dose on Human Breast Carcinoma Cells as Markers of Benefit in Neoadjuvant Therapy of Mammary Cancer.**

D. Bonfiglioli<sup>1</sup>, E. Cione<sup>1</sup>, H. Qi<sup>1</sup>, A. Pingitore<sup>1</sup>, M. Perri<sup>1</sup>, S. Catalano<sup>1</sup>, M. Panno<sup>1</sup>, G. Genchi<sup>1</sup>, S. Andò<sup>1</sup>

<sup>1</sup>University of Calabria, Arcavacata di Rende, Cosenza, Italy.

Activation of PPARgamma and RXR heterodimer elicits antineoplastic effects on breast carcinoma. We evaluated the anti-tumor efficacy of combining low doses of the PPARgamma agonist rosiglitazone (BRL) and RXR agonist 9 cis retinoic acid (9cisRA) on normal and four malignant breast cell lines. The combined treatment of BRL 100nM and 9cisRA 50nM reduced the vitality only in cancer cells. Functional experiments indicated that NFkB binding site in p53 promoter is the effector of BRL and 9 cis-RA signalling in cancer cells. Both ligands activated intrinsic apoptotic pathway in malignant but not in normal breast cells. These data address how combined low dose of PPARgamma and RXR agonists may elicit chemopreventive effect in the treatment of breast cancer.

of Btk, "IBtk" = Inhibitor of Bruton Tyrosine Kinase (Liu et al., Nat. Immunol., 2001). Here, we have investigated the fate of IBtk upon B cell receptor (BCR) stimulation. We show that IBtk is transiently phosphorylated by kinases of PKC family which leads to its dissociation from Btk. Mapping of PKC phosphorylation sites in IBtk identified the critical serine residue as S90. IBtk mutated in S90 constitutively bound to Btk and efficiently inhibited calcium mobilization and NF $\kappa$ B activation upon BCR triggering in B cells, thus preventing activation of primary B lymphocytes and proliferation of B lymphomas.

**ST 43. First Evidence of Non-Genomic Estradiol induced Up-Regulation of Aromatase Enzymatic Activity in MCF-7 Breast Cancer Cells.**

S. Catalano<sup>1</sup>, I. Barone<sup>1</sup>, C. Giordano<sup>1</sup>, P. Rizza<sup>1</sup>, H. Qi<sup>1</sup>, G. Gu<sup>1</sup>, D. Bonofiglio<sup>1</sup>, S. Andò<sup>1</sup>

<sup>1</sup>University of Calabria, Arcavacata di Rende, Cosenza, Italy.

In situ estrogen production plays an important role in breast tumor promotion. We demonstrated, in MCF-7 cells, that 17- $\beta$ -estradiol rapidly enhances aromatase activity in the presence of unmodified enzyme expression. Aromatase kinetics studies showed, upon increasing dose of 17- $\beta$ -estradiol, decreased Km and unchanged Vmax. 17- $\beta$ -estradiol phosphorylates in vivo aromatase protein and site-directed mutagenesis experiments revealed that 361 tyrosine residue phosphorylation is crucial in estradiol up-regulation of aromatase activity. We evidenced the involvement of the tyrosine-kinase Src since inhibition of its signalling abrogated the up-regulatory effects induced by 17- $\beta$ -estradiol on aromatase activity and phosphorylation of aromatase protein. These findings indicate a short non-genomic autocrine loop between 17- $\beta$ -estradiol and aromatase emphasizing the role of local estrogen production in promoting breast cancer growth.

**ST 44. Androgen Receptor (AR) Inhibits Cyclin D1 Promoter Activity. May AR be Considered as an Oncosuppressor in Breast Cancer?**

M. Lanzino<sup>1</sup>, D. Sisci<sup>1</sup>, C. Garofalo<sup>1</sup>, C. Morelli<sup>1</sup>, S. Catalano<sup>1</sup>, I. Casaburi<sup>1</sup>, S. Andò<sup>1</sup>

<sup>1</sup>University of Calabria, Arcavacata di Rende, Cosenza, Italy.

In the breast, androgens counterbalance positive serum- and estrogen-induced growth stimuli, which are intimately linked to breast tumorigenesis. We demonstrate that in MCF-7 cells, non-aromatizable 5- $\alpha$ -dihydrotestosterone decreases serum- as well as estradiol-induced cyclin D1 expression through inhibition of cyclin D1 promoter transcriptional activity. Mutagenesis, DAPA, EMSA and ChIP analysis indicated that this inhibitory effect is mediated by direct binding of AR to a putative AR response sequence, whose identification allows to define cyclin D1 as an androgen target gene in breast. Moreover AR negatively modulates ER-mediated signalling through competition for AIB1, crucial in the functional coupling of ER with the cyclin D1 promoter, further evidencing AR inhibitory effects and raising a role for AR as a new oncosuppressor in breast.

**ST 45. Effects of Selective Cyclooxygenase-2 Inhibitors Etoricoxib and Celecoxib on Colorectal Cancer Cell Lines**

M. T. Rotelli<sup>1</sup>, D. Boccale<sup>1</sup>, M. Rinaldi<sup>1</sup>, M. Notarnicola<sup>2</sup>, M. G. Caruso<sup>2</sup>, D. F. Altomare<sup>1</sup>, V. Memeo<sup>1</sup>

<sup>1</sup>University of Bari, Bari, Italy, <sup>2</sup>IRCCS 'De Bellis', Castellana Grotte, Italy.

Background: Cyclooxygenase-2 (COX-2) plays a role in colorectal cancer development by inhibiting apoptosis and increasing angiogenesis. Methods: Cytotoxicity (MTT test) and effects on COX-2 and VEGF expression (Real Time-PCR, ELISA) of two selective COX-2 inhibitors, etoricoxib and celecoxib were studied on colorectal cancer cell-lines (CaCo2, HT29, SW480, SW620) at different concentrations. Results: Cytotoxicity and VEGF and COX-2 expression were dependent on drug type (celecoxib > etoricoxib), concentration, cell lines. SW480 and its metastatic counterpart (SW620) from the same patient showed different response. Conclusions: Many potential factors might be involved in biological activity of coxibs. Even if celecoxib appears to be a more potent agent than etoricoxib, therapeutic use of coxibs on colorectal cancer depends on full comprehension of tumor's biology.

**ST 46. Insulin Receptor Substrate 1 Modulates the Transcriptional Activity and the Stability of Androgen Receptor in Breast Cancer Cells.**

D. Sisci<sup>1</sup>, M. Lanzino<sup>1</sup>, C. Garofalo<sup>1</sup>, C. Morelli<sup>1</sup>, I. Casaburi<sup>1</sup>, S. Andò<sup>1</sup>

<sup>1</sup>Farmacobiologico, Università della Calabria, Arcavacata di Rende, Cosenza, Italy.

Although the majority of human breast cancers expresses androgen receptor (AR), its role in breast tumorigenesis remains largely unexplored. Here we demonstrate that 5- $\alpha$ -dihydrotestosterone inhibits MCF-7 cell growth induced by IGF-I. Immunoprecipitation, transient transfection and ChIP assays demonstrate that, upon 5- $\alpha$ -

dihydrotestosterone stimulation, IRS-1, the major IGF-1R substrate, interacts and translocates into the nucleus with AR and is recruited to the androgen responsive region of target gene promoters where participates to sustain AR-mediated transcription. Moreover, siIRS-1 suggests that IRS-1/AR interaction decreases the ubiquitin/proteasome-dependent degradation of AR, increasing its stability. Therefore, IRS-1 appears to be a novel AR regulator required to sustain AR activity suggesting the existence of a functional interplay between the IGF system and AR in breast cancer.

**ST 47. Different Biological Effects of Chenodeoxycholic Acid (CDCA) in Endometrial Cancer Cells.**

I. Casaburi<sup>1</sup>, M. Lanzino<sup>1</sup>, S. Catalano<sup>1</sup>, S. Aquila<sup>1</sup>, A. Vivacqua<sup>1</sup>, P. Avena<sup>1</sup>, M. Maggiolini<sup>1</sup>, S. Andò<sup>1</sup>, D. Sisci<sup>1</sup>

<sup>1</sup>University of Calabria, Arcavacata di Rende, Cosenza, Italy.

CDCA acts as a tumor promoter in animal models and enhances cell transformation and apoptosis in several tumor cell lines. Here we investigated the biological effects of different concentrations of CDCA on human endometrial cancer Ishikawa cells. [3H]Thymidine incorporation suggests that Ishikawa cell growth was stimulated by CDCA at low concentrations (<30 $\mu$ M) and suppressed at higher (>50 $\mu$ M). Worthily, in all circumstances ERK activation occurred while p38-MAPK was activated only at higher concentrations concomitantly with the cleavage of poly(ADP-ribose)-polymerase, DNA fragmentation, Cyclin D1 down-regulation and p21WAF1/CIP1 up-regulation. Indeed, the crucial role of p38 MAPK pathway, in the above mentioned apoptotic events, is abrogated in the presence of its specific inhibitor, SB203580. All these findings address how CDCA may be perspective implemented in the novel therapeutic strategies for endometrial cancer treatment.

**ST 48. Increased Expression of Dystroglycan Inhibits Growth and Tumorigenicity of Human Prostate Cancer Cells By Sequestering Components of the ERK-MAP Kinase Cascade**

B. De Paola<sup>1</sup>, M. Goracci<sup>2</sup>, F. Rafanelli<sup>2</sup>, A. Galiano<sup>2</sup>, C. Graziani<sup>2</sup>, A. Cittadini<sup>2</sup>, A. Sgambato<sup>1</sup>

<sup>1</sup>Università Cattolica del Sacro Cuore, Roma, Italy, <sup>2</sup>Catholic University, Roma, Italy.

Dystroglycan (DG), a cell adhesion receptor, is a complex composed of two subunits,  $\alpha$  and  $\beta$ , linking laminin in the extracellular matrix to the cytoskeleton. We and other demonstrated that DG expression, and mainly the extracellular  $\alpha$ -DG, is reduced or lost in a variety of human cancers, including prostate cancer. Overexpression of an exogenous DG cDNA in LNCaP prostate cancer cells was not able to restore  $\alpha$ -DG detection although expression of the  $\beta$ -DG was significantly increased. These cells also displayed an induced cell adhesion while cell growth and tumorigenicity were reduced. To investigate the mechanisms underlying these effects, we analyzed the expression of the  $\alpha$ -DG core protein in the DG-overexpressing cells and found that its expression is increased confirming that the lack of the  $\alpha$ -DG detection is due to post-transductional events. We also analyzed the interaction between  $\beta$ -DG and components of the ERK-MAP kinase cascade including MEK and ERK and found an increased interaction of  $\beta$ -DG with both pERK and pMEK. Interaction with Grb2 was also affected by DG overexpression. We are currently analyzing how these events affect the activity of MAP kinase cascade. Taken together, these findings support the hypothesis that DG might interfere with the Ras/MAPK signaling cascade by sequestering important players of the pathway and might help to understand the significance of the loss of DG expression in cancer cells.

**ST 49. Breast Cancer Cells Expressing the K303R Estrogen Receptor (ER)- $\alpha$  Mutant are Resistant to an Aromatase Inhibitor.**

I. Barone<sup>1</sup>, Y. Cui<sup>1</sup>, S. Ando<sup>2</sup>, S. A. W. Fuqua<sup>1</sup>

<sup>1</sup>Breast Center, Baylor College of Medicine, Houston, TX, United States of America.

<sup>2</sup>Centro Sanitario, Cell Biology Department, University of Calabria, Arcavacata di Rende, Cosenza, Italy.

Despite the success of hormonal therapy with aromatase inhibitors (AIs), many patients exhibit de novo resistance. We identified a lysine to arginine transition at residue 303 (K303R) of ER $\alpha$  in invasive breast cancers, which confers estrogen hypersensitivity. We hypothesize that the mutant provides a continuous mitogenic stimulus to the breast even during menopause, thus affording a proliferative advantage during treatment with AIs. To test whether the mutation is resistant to AIs, we utilized MCF-7 parental and MCF-7-K303R-overexpressing cells stably transfected with an aromatase expression vector. Cells were stimulated with the aromatase substrate, androstenedione (AD), with or without the AI anastrozole (AN). We found that AN decreased AD-stimulated growth of WT cells, using MTT and soft agar assays, but AN had no effect on K303R cells. Aromatase activity was reduced by AN, thus resistance cannot be explained by an insensitivity of the aromatase



**FASEB SUMMER RESEARCH CONFERENCES**

**Retinoids**

**June 15 – 20, 2008  
New Haven, Connecticut**

**ORGANIZERS**

**Susan M Smith, PhD  
Noy Noy, PhD**

**The Federation gratefully acknowledges the following  
educational grants for the**



**FASEB Summer Research  
Conferences**

*<http://www.faseb.org>*

9650 Rockville Pike • Bethesda, Maryland 20814

## Poster 19B

### **Activated pathway through which Rosiglitazone and 9 cis Retinoic Acid, when combined at low doses, induce apoptosis in human breast cancer cells.**

**E. Cione, D. Bonofiglio, H. Qi, M. Perri, A. Pingitore, S. Catalano, M.L. Panno, G. Genchi and S. Andò**

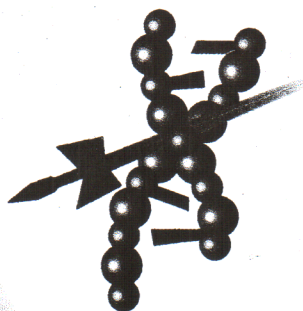
**Department of Pharmaco-Biology and Department of Cell Biology-University of Calabria, Italy**

Ligand activation of the nuclear receptor PPAR $\gamma$  induces cell death in many types of cancer cell lines. RXR is able to form heterodimers with PPAR $\gamma$ , LXR, FXR, PXR, and others nuclear receptors. It has been largely reported that RXR ligands exert antitumoral effects through activation of different transduction pathways. In our study, we evaluated the ability of PPAR $\gamma$  ligand Rosiglitazone (BRL), in combination with RXR ligand 9 *cis* retinoic acid (9RA), both at nanomolar levels, to promote PPARE-mediated gene transcription in breast cancer cells. MTT assay was performed to test BRL and 9RA influence on cell viability alone and in combination. About 50% decrement of cell viability was detected only when both ligands were present in four malignant breast cell lines: MCF-7, MCF-7TR, SKBR-3 and T-47D. Normal breast epithelial MCF-10 cells did not suffer any reduction in vitality with the same treatment. Using MCF-7 breast cancer cell line, we investigated the potential pathways through which cell death was being induced. Performing transient transfection with p53 promoter gene, we demonstrated that BRL 100 nM plus 9 *cis* RA 50 nM, only in combination, transactivated p53 promoter and such activity was absent in its deleted construct in NF $\kappa$ -B domain. In addition, EMSA and ChIP assays demonstrated how these compounds alone were not able to recruit PPAR $\gamma$  to p53 promoter sequence, while they appeared to have that capability in the presence of BRL plus 9RA. As a consequence, we found that the combination of these agents increased mRNA and protein level of p53 and its target gene p21. Nevertheless the role of PPAR $\gamma$ -RXR heterodimer for p53 gene regulation has never been studied so far at such low physiological, versus pharmacological, doses. The attention was focused on the intrinsic apoptotic mechanisms: MCF-7 cells treated with BRL plus 9RA, highlighted how the ordained sequence of apoptotic events occurs with a release of cytochrome *c* after 24 h, a strong caspase 9 activation after 48 h and, finally, DNA laddering after 50 h treatment. Moreover, there was no change in the caspase 8 activation, involved in the extrinsic pathway of apoptosis. In order to clarify the role of p53 in these conditions, we inhibited p53 expression transfecting antisense p53 oligodeoxynucleotides in MCF-7 cells *in vitro* and we did not observe DNA ladders. Thus, the effect of both ligands enhances 9RA and BRL's own anti-tumorigenic activity reducing the doses at which the combination is efficacious. Hence our data lay the fundamentals of a promising therapy with great therapeutic benefits, and may specifically induce the regression of breast tumors due to its apoptosis-promoting effects.

BIT Life Sciences' 1<sup>st</sup> Annual **WORLD**



Shanghai City Flower



# Cancer

## CONGRESS-2008

Theme: From Basic Research  
to Therapeutics

Time: June 12-15, 2008

Place: Everbright Convention & Exhibition Center, Shanghai, China

# 2008中国上海癌症大会

## 主题：从基础研究到治疗

时间：2008年6月12-15日

地点：中国·上海光大会展中心国际大酒店

### Hosting Organization

主办单位



中国医药生物技术协会

### Operating Organization

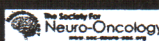
承办单位



BIT Life Sciences  
World Leader of Intelligence  
Exchanges in Life Sciences

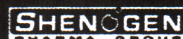
### Supporting Organizations

协办单位



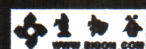
### Event Sponsors

赞助单位



### Media Partners

媒体支持单位



<http://www.bitlifesciences.com/cancer2008/>

Title: Evidences that BRL in combination with 9 cis RA at low doses inhibits cell growth and induces apoptosis in MCF-7 human breast cancer cells.

Dr. Hongyan Qi, Daniela Bonofiglio, Erika Cione, Attilio Pingitore, Mariarita Perri, Stefania Catalano, Maria Luisa Pannofino, Francesca Giordano, Giuseppe Genchi and Sebastino Ando

Abstract:

The activation of Peroxisome Proliferator-Activated Receptor gamma (PPAR $\gamma$ ) that forms heterodimers with Retinoid X Receptor (RXR) elicits an antineoplastic effect on several cancer cell lines, including breast carcinoma. In the present investigation, we evaluated the effect of low doses of PPAR $\gamma$  and RXR ligands, rosiglitazone (BRL) and 9 cis retinoic acid (9 cis RA) respectively, on MCF-7 cell growth and apoptosis. After 48 hours of treatment with BRL 100 nM and 9 cis RA 50 nM we observed a 50% decrease on cell viability only when these agents were given in combination. Taking into account that mitogen-activated protein kinase (MAPK) signal is essential for growth of human breast cancer cell lines, we explored the action of combined treatment in MCF-7 cells. We observed a strong inhibition of ERK1/ERK2 pathway and a significant reduction of p38 MAPK, suggesting a downregulatory effect on survival and proliferation cell signalling. Reporter assays indicated that BRL plus 9 cis RA were able to induce the transcriptional activity of the Peroxisome Proliferator-Responsive Element in a PPAR $\gamma$ -dependent manner and they, also, stimulated the transactivation of the p53 gene promoter. Site-directed mutagenesis studies performed with p53 deleted constructs showed that the NF $\kappa$ B binding site is required for the transcriptional response to low doses of BRL plus 9 cis RA in MCF-7 cells. Furthermore, ChIP assay demonstrated that these agents only when in combination appeared to be effective in the recruitment of PPAR $\gamma$  on the p53 promoter sequence. In addition, both ligands upregulated mRNA and protein expression of p53 and its target gene p21. To evaluate the activation of the intrinsic apoptotic pathway, pro-caspase 9 cleavage and DNA fragmentation were assessed, demonstrating that BRL and 9 cis RA given in combination produced apoptosis respect to either single agent in MCF-7 breast cancer cells. These findings indicate that association of low doses of PPAR $\gamma$  and RXR ligands could be a promising therapy for breast cancer patients.

Biography

During completion of her doctorate in oncology at the University of Calabria, Italy, started in 2005, Dr. Hongyan Qi has been working in basic cancer research in the laboratory of General Pathology directed by Prof. Sebastiano Ando. In the recent years, together with Dr. Daniela Bonofiglio, she has investigated different molecular mechanisms through which Peroxisome Proliferator-Activated Receptor gamma (PPAR $\gamma$ ) ligand rosiglitazone (BRL) induces antiproliferative effect, cell cycle arrest and apoptosis in human breast cancer cells. Recently, she has explored the involvement of the p53 (Bonofiglio et al., Mol Endo 2006) and Fas/FasL (Bonofiglio et al., Breast Cancer Res Treat 2008) pathways in the PPAR $\gamma$ -mediated apoptosis of breast cancer cells.

In the last year, Dr. Qi has investigated the molecular mechanism underlying BRL antiproliferative effects in follicular and anaplastic human thyroid carcinoma cells. Functional studies evidenced a direct interaction between PPAR $\gamma$  and Sp1 able to activate p21Cip1/WAF1 promoter and consequently to inhibit thyroid tumor cell growth (Bonofiglio and Qi, Endocr Related Cancer 2008).

Altogether these results candidate PPAR $\gamma$  ligands as potential agents for the treatment of patients affected by breast and thyroid cancer.

Dr. Hongyan Qi  
Department of Pharmaco-Biology  
University of Calabria  
Italy  
E-mail: qi\_hongyan555@yahoo.it



*J. Ren*

2006

UN SECOLO DI NOBEL



Università degli Studi  
di Pavia



Società Italiana  
di Patologia

**XXVIII Congresso Nazionale  
SIP 2006  
Società Italiana di Patologia**

**Pavia, 19 - 22 Settembre 2006**

Università degli Studi di Pavia  
Corso Strada Nuova, 65

**FAS LIGAND PROMOTER ACTIVATION BY PEROXISOME  
PROLIFERATOR ACTIVATED RECEPTOR GAMMA AGONIST  
ROSIGLITAZONE OCCURS THROUGH SP1 SITE IN MCF7 BREAST  
CANCER CELLS**

**<sup>1</sup>Gabriele S., <sup>1</sup>Bonofiglio D., <sup>1</sup>Belmonte M., <sup>1</sup>Qi H., <sup>1</sup>Catalano S., <sup>1</sup>Aquila S., <sup>2</sup>Andò S.**

*<sup>1</sup>Dipartimento Farmaco-Biologico, <sup>1</sup>Dipartimento di Biologia Cellulare, Università della Calabria, Arcavacata di Rende (CS) - 87036 - Italy*

Fas ligand (FASL) is a trans-membrane protein that belongs to the tumor necrosis factor family of cytokines and induces apoptosis by crosslinking with the FAS receptor.

In the current study, we explored a possibile link between FASL and Peroxisome Proliferator-Activated Receptor gamma (PPAR $\gamma$ ), a member of ligand-dependent transcriptional factor, implicated in growth inhibition and apoptosis of several tumors.

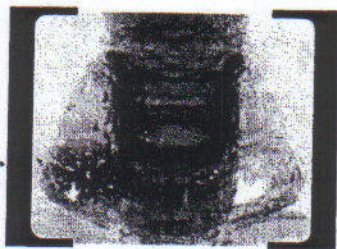
Using MCF7 breast cancer cells, we investigated by reverse transcription-polymerase chain reaction (RT-PCR) and <sup>32</sup>P-Western Blotting the ability of PPAR $\gamma$  agonist rosiglitazone (BRL) to regulate FASL expression.

Our data showed an upregulation of mRNA and protein expression of FASL in MCF7 cells treated for 24 hours with increasing BRL concentrations, which was abrogated by a specific PPAR $\gamma$  antagonist GW9662. These results were supported by transient transfection assays revealing that BRL transactivated human FASL promoter gene in a PPAR $\gamma$ -dependent manner. In MCF7 cells transfected with deleted constructs of FASL promoter, we found that the Sp1/NFAT/NFkB site is required for this transactivation.

Next, Electrophoretic Mobility Shift Assay demonstrated that BRL increased the binding of nuclear extracts to Sp1 region in the FASL gene promoter, suggesting the key role of this site for BRL-responsiveness in MCF7 cells. Upon BRL treatment we observed how the enhanced expression of FASL was concomitantly with the cleavage of the caspase-8, featuring the induction of extrinsic apoptotic process.

In conclusion, these data evidence the capability of BRL to induce FASL expression through Sp1 together with caspase-8 cleavage in breast cancer cells, thus address PPAR $\gamma$  as a potential target for anticancer therapy.

CONGRESSO NAZIONALE



## **CARCINOMI TIROIDEI**

*dal laboratorio al letto del malato e ritorno*

Assisi

---

2-4 Febbraio 2006

ABSTRACT

**The peroxisome proliferator-activated receptor  
gamma ligand rosiglitazone up-regulates  
p21 gene expression in human thyroid carcinoma cells**

*D. Bonofiglio\*, S. Catalano\*, S. Gabriele\*, M. Belmonte\*, H. Qi\*, M. Maggiolini\* and S. Andò\*\*.*  
*\*Dept. Pharmaco-Biology, \*\*Dept. Cellular Biology, University of Calabria*  
*87030 Arcavacata di Rende (CS) Italy.*

The Peroxisome Proliferator-Activated Receptor gamma (PPARgamma), a member of the nuclear receptor superfamily of ligand-dependent transcriptional factors, has been implicated in the growth inhibition and apoptosis of diverse cancer cells. However, the exact mechanisms by which PPARgamma exerts these activities remain to be elucidated.

We have explored the role of PPARgamma ligand named rosiglitazone (BRL) on the expression of the cyclin-dependent kinase inhibitor p21 in human follicular and anaplastic thyroid carcinoma cells, WRO and FRO, respectively. BRL exposure inhibited in a dose-dependent manner the proliferation of both thyroid tumor cells. Interestingly, BRL treatments up-regulated p21 mRNA and protein levels and inhibited cyclin D1 expression, whereas did not modify p53 protein content. Besides, in transient transfection assays performed in both thyroid cancer cells BRL triggered the transcriptional activity of an expression vector encoding p21 gene promoter. Next, in electrophoresis mobility shift experiments BRL elicited an increase of the nuclear protein binding activity of Sp1 that presents conspicuous responsive elements within the p21 gene promoter.

Our results indicate that the p21 upregulation by PPARgamma ligand BRL may be mediated through an increased Sp1 binding to p21 promoter gene. Further studies are required to evaluate the effectiveness of BRL as a potential agent able to inhibit thyroid cancer progression.



FONDAZIONE GIOVANNI LORENZINI MILAN, ITALY  GIOVANNI LORENZINI MEDICAL FOUNDATION HOUSTON, USA

3<sup>rd</sup> International Symposium on  
**PPARS**  
**PPARS**  
**EFFICACY AND SAFETY**  
From Basic Science to Clinical Applications  
**2005**

Monte Carlo (Monaco) - March 19-23, 2005

**ABSTRACT BOOK**



INTERNATIONAL  
ATHEROSCLEROSIS  
SOCIETY



National Heart,  
Lung, and Blood Institute  
NIH, USA

#### UP-REGULATION OF P53 GENE EXPRESSION BY PPAR $\gamma$ IN HUMAN MCF-7 BREAST CANCER CELLS.

Bonofiglio Daniela<sup>1</sup>, Aquila Saveria<sup>1</sup>, Gabriele Sabrina<sup>1</sup>, Gentile Mariacelena<sup>2</sup>, Belmonte Maria<sup>1</sup>, Morelli Catia<sup>1</sup>, Qi Hongyan<sup>1</sup>, Fusaro Serafina<sup>1</sup> and Andò Sebastiano<sup>2,3</sup>  
<sup>1</sup>Dept. Pharmaco-Biology, <sup>2</sup> Dept. Cellular Biology, <sup>3</sup>Faculty of Pharmacy University of Calabria 87030 Arcavacata di Rende (CS) Italy.

p53 tumor suppressor gene functions in both cell cycle arrest and apoptosis. Stemming from the broadened evidence that PPAR $\gamma$  inhibits cell proliferation and induces apoptosis in a variety of cell types, it becomes intriguing to investigate a possible link between PPAR $\gamma$  and p53 signalling in breast cancer cells.

In this aim, we treated MCF-7 breast cancer cells with or without a synthetic PPAR $\gamma$  ligand, rosiglitazone (BRL) for 7 days. After treatment, cell proliferation was significantly reduced in a dose-dependent manner and the effect was reversed by a PPAR $\gamma$  antagonist like GW demonstrating that it is specifically mediated by PPAR $\gamma$ . The antiproliferative effects of BRL, after 48 hours of treatment were correlated to a G0/G1 arrest in MCF-7 cells cycle progression. Concomitantly, we observed an up-regulation of p53 and p21 expression at both protein and mRNA levels and in a dose-dependent manner. Upon BRL treatment p21 is located prevalently in the nucleus, while p53 appears also present in the cytoplasm, where it colocalizes with PPAR $\gamma$  as confirmed by immunofluorescence assay. The physical interaction between these last two proteins that is enhanced by BRL emerges by the coimmunoprecipitation studies. An enhanced p53 cytosol compartmentalization, produced by BRL treatment, well fits with the simultaneous cleavage of caspase 9 and it addresses how PPAR $\gamma$  is involved in p53-mediated intrinsic apoptosis. Besides, functional studies demonstrated that PPAR $\gamma$  was able to activate p53 promoter, an effect specifically reversed by GW. Our studies attempting to identify the functional elements located in the regulatory region of p53 promoter and effectors of PPAR $\gamma$  responsiveness, are still in progress.

#### ROLE OF THE OLEIC ACID AND PPAR $\beta/\delta$ IN NEURONAL DIFFERENTIATION

Elisabetta Benedetti<sup>1</sup>, Barbara D'Angelo<sup>1</sup>, MariaAngela D'Amico<sup>1</sup>, Silvia Di Loreto<sup>2</sup>, AnnaMaria Cimini<sup>1</sup>. <sup>1</sup>Basic Applied Biol., Univ. of L'Aquila, Italy; <sup>2</sup>I.T.O.I., Natl. Council of Res., L'Aquila, Italy.

The neuronal differentiation is a complex process which requires a sequential expression of distinct factors, as lipidic molecules. The oleic acid induces in neurons, neurite outgrowth, neuronal clustering and increased expression of the growth axonal protein (GAP43). (1) It is well known the strong involvement of the peroxisomal proliferator activated receptor (PPARs) in the pathway of lipidic molecules. Recently we demonstrated the presence of the three isoforms of PPARs,  $\alpha$ ,  $\beta/\delta$  and  $\gamma$  in the cortical neurons. Moreover, we reported that the expression of all isoforms was differentially modulated during neuronal maturation. In particular it was been suggested a pivotal role of PPAR $\beta$  during the developmental stages, as the increased expression of these receptor is correlated to the expression of its target gene, the long-chain acyl-CoA synthetases (ACS2), important enzyme for neuronal functions. (2) Here we compare the effects of oleic acid with those of GW610742X, a synthetic and specific ligand of PPAR $\beta$ , on cortical neuronal cultures. A pronounced neuronal clusterig was observed after 96h of treatments. In addition we observed different immunolocalization of GAP43 in the treated cultures respect to the control ones. GAP43 positive neurites were detected already at 24h and the axonal cone immunolocalization of GAP43 was showed after 96h of treatment. Furthermore, after 24 h of treatment an increased expression and activation of PPAR $\beta$ , joined to an increased level of the protein were demonstrated. These results suggest that PPAR $\beta$  is involved in neuronal maturation. Particularly, we hypothesize that oleic acid might be a natural ligand of PPAR $\beta$ .

Citations: 1) Tabernero A, et al., 2001. J Neurochem. 79:606-616

2) Cimini A, et al, Neuroscience (in press).

#### PPAR $\alpha$ PROTECTS AGAINST ALCOHOL-INDUCED LIVER DAMAGE

N. Tanaka\*, Y. Kamijo\*, E. Sugiyama\*, J.M. Peters\*\*, Gonzalez\*\*\*, and T. Aoyama\*

\*Dept. of Metabolic Regulation, Institute on Aging Adaptation, Shinshu University Graduate School of Medicine, Matsumoto, Japan. \*\*Dept. of Veterinary Science, Center for Molecular Toxicology and Carcinogenesis, Pennsylvania State University, Univ. Park, PA, USA. \*\*\*Laboratory of Metabolism, National Cancer Institute, NIH, Bethesda, MD, USA.

To investigate the roles of PPAR $\alpha$  in alcoholic liver injury, wild-type and PPAR $\alpha$ -null mice were continuously fed a diet containing 4% ethanol, and liver injury was analyzed. PPAR $\alpha$ -null mice fed ethanol exhibited marked hepatic steatosis, hepatomegaly, hepatic inflammation, cell toxicity, fibrosis, apoptosis, and mitochondrial swelling. Some of these hepatic abnormalities were consistent with those of patients with alcoholic liver injury and were not found in wild-type mice. To elucidate the molecular mechanisms of ethanol-induced liver injury, PPAR $\alpha$ -null mice were investigated, and changes related to ethanol and acetaldehyde metabolism, oxidative stress, inflammation, hepatocyte proliferation, fibrosis, and mitochondrial permeability transition activation occurred specifically in PPAR $\alpha$ -null mice as compared with wild-type mice. In conclusion, these studies suggest a protective role of PPAR $\alpha$  in alcoholic liver disease. Humans may be more susceptible to liver toxicity induced by ethanol as PPAR $\alpha$  expression in human liver is considerably lower compared to that of rodents.

#### A PAN-PPAR LIGAND INHIBITS PROLIFERATION OF CANCER CELLS AND INDUCES APOPTOSIS VIA PPAR-DEPENDENT AND PPAR-INDEPENDENT MECHANISMS.

K. Berge, K.J. Tronstad, T. Røst, R.K. Berge  
Institute of Medicine, Section of Medical Biochemistry, Haukeland University Hospital, N-5021 Bergen, Norway.

Peroxisome proliferator-activated receptors (PPARs) are transcription factors which regulate transcription of genes involved in fatty acid metabolism and energy homeostasis. In addition, these transcription factors have been shown to play crucial roles in the control of cell growth and differentiation. Recently, several reports have documented the antiproliferative effect of PPAR agonists in several cancer models. In this study, we investigated the growth-limiting properties of a new bioactive fatty acid analogue, TTA, which has been shown to be a ligand for all three isoforms of PPAR. We investigated the effects of TTA-administration on cell proliferation in glioma, breast and colon cancer cells. The growth of all cell lines was inhibited after TTA administration. TTA also reduced growth of glioma tumours implanted in rats. Administration of the PPAR-selective antagonist GW9662 abolished the growth inhibition induced by the PPAR $\gamma$ -specific ligand BRL49653, but only marginally reduced the effect of TTA in the glioma cell line. Thus, TTA seems to inhibit proliferation of glioma cancer cells through both PPAR-dependent and PPAR-independent pathways, of which the latter appears to predominate. Moreover, we have documented that TTA induces apoptosis via direct interactions with the mitochondria. In order to try to explain the underlying effects we performed a microarray study using the colon cancer cell line. Approximately 2000 interesting genes were then chosen to be measured by RT-PCR in a three cancer cell lines. In conclusion we have identified both PPAR target genes and genes regulated by other transcription factors that might be important in the growth inhibitory effect of TTA in cancer cells.